

MULTI STOREY BUILDINGS |

THREE-DIMENSIONAL ANALYSIS OF  
SHEAR WALL MULTI STOREY BUILDINGS

by

JAYANTA K. BISWAS M. Eng.

A Thesis

Submitted to the Faculty of Graduate Studies  
in Partial Fulfilment of the Requirements

for the Degree  
Doctor of Philosophy

McMaster University

September 1974

DOCTOR OF PHILOSOPHY (1974)

McMASTER UNIVERSITY  
Hamilton, Ontario.

TITLE: Three Dimensional Analysis of  
Shear Wall Multi Storey Buildings

AUTHOR: JAYANTA K. BISWAS, M. Eng.

SUPERVISOR: Dr. W. K. Tso

NUMBER OF PAGES: vi, 256

SCOPE AND CONTENTS:

The thesis studies the importance of torsion in multi storey buildings having asymmetric layout of shear walls. A method of three dimensional analysis based on the continuous approach has been developed. The problem of torsion in a two wall core structure has been examined in detail including a test on a plexiglas model. The method of analysis presented in this thesis is general enough to deal with buildings with a large number of shear walls in plan and allows variation of structural properties along the height of the building. A number of representative examples are worked out to demonstrate applicability. The use of the method in studying the dynamic properties of multi storey buildings is shown. The response of a torsionally unbalanced building due to the application of a bidirectional earthquake is examined. Based on these results, recommendations are made on the structural behaviour of such buildings.

### ACKNOWLEDGEMENTS

I wish to express my profound gratitude to Dr. W. K. Tso for his continued guidance and encouragement in carrying out this thesis.

I am also grateful to the Department of Civil Engineering and Engineering Mechanics, McMaster University for making me available the research and teaching assistantship. This investigation was made possible through the financial assistance of the National Research Council of Canada, to whom I extend my sincere thanks.

I also thank the staffs of the Applied Dynamics Laboratory, and many others for their co-operation in carrying out this investigation.

TABLE OF CONTENTS

<u>Chapter</u>		<u>Page</u>
1	<u>INTRODUCTION</u>	
	1.1 High-Rise Buildings and the Use of Shear Walls.....	1
	1.2 Review of Past Works.....	6
2	<u>TORSIONAL ANALYSIS OF TWO WALL CORE STRUCTURES</u>	
	2.1 Introduction.....	17
	2.2 Notations Used.....	20
	2.3 Statement of the Problem.....	22
	2.4.1 Equilibrium Conditions.....	24
	2.4.2 Compatibility Conditions.....	27
	2.4.3 Final Equation and Solution.....	30
	2.5.1 Example.....	34
	2.5.2 Comparison of Other Methods.....	35
	2.6.1 Experiment.....	39
	2.6.2 Results and Discussions.....	42
	2.7 Design Curves.....	44
	2.8 Conclusions.....	47

3	<u>THREE-DIMENSIONAL ANALYSIS OF UNIFORM SHEAR WALL STRUCTURES</u>	
3.1	Introduction.....	72
3.2	Notations.....	75
3.3	Statement of the Problem.....	80
3.4.1	Equilibrium Conditions.....	84
3.4.2	Compatibility Conditions.....	93
3.5	Reduction of Governing Equations and Solutions.....	96
3.6	Example and Discussion of Results.....	106
3.7	Stiffness Representation of the Floor Slab.....	111
3.8	Conclusions.....	113

4	<u>THREE-DIMENSIONAL ANALYSIS OF NON-UNIFORM SHEAR WALL STRUCTURES</u>	
4.1	Introduction.....	133
4.2	Notations.....	136
4.3	Statement of the Problem.....	139
4.4.1	Differential Equation for Segment i....	141
4.4.2	Transfer Matrix Method.....	144
4.5	Example and Discussion of Results.....	155
4.6	Conclusions.....	157

5	<u>DYNAMIC ANALYSIS OF SHEAR WALL BUILDINGS</u>	
	5.1 Introduction.....	167
	5.2 Notations.....	170
	5.3 Statement of the Problem.....	171
	5.4 Equations of Motion.....	172
	5.4 Solution.....	177
	5.5 Example and Discussion of Results.....	180
	5.6 Conclusions.....	190

6	<u>CONCLUSIONS AND RECOMMENDATIONS</u>	
	6.1 Conclusions.....	214
	6.2 Recommendations.....	216

APPENDIX

A	Vlasov's Theory of Thin Walled Beams.....	219
B	Experimental Data.....	224
C	Elements of Matrix [A].....	228
D	Shear Walls Connected by Two Rows of Connecting Beams.....	230
E	Solution for Non-uniform Shear Wall Structures.....	237
F	Elements of Matrix [K] and [M].....	242
G	List of Computer Programs.....	244

	BIBLIOGRAPHY.....	245
--	-------------------	-----

## CHAPTER I

### INTRODUCTION

#### 1.1 High-Rise Buildings and the Use of Shear Walls

Many high-rise buildings have been constructed in different cities of the world. The trend of construction of high-rise buildings for both office and residential purposes is rapidly increasing. The main reasons for this trend are the increase in population densities due to urbanization, the growth of population and the high cost of land in urban areas. The economic prosperity and the technological advancement are also partly responsible for the evolution of tall buildings. In many cases, tall buildings evolve as prestige symbols for commercial enterprises and organisations.

Although the construction of high-rise buildings has solved the problem of usable space in urban areas, it has caused many environmental, psychological and social problems. The construction of tall buildings in the neighbourhood of low-rise dwellings may spoil the existing urban aesthetics. It can also aggravate traffic problems if the location does not fit into the existing planning of



the city. Closely spaced high-rise buildings may also cause pollution problems and obstruct sunlight to the adjacent properties. A child brought up in high-rise buildings has less chance to explore and manipulate the environment. This may adversely affect the psychological development of the child in future years. The inhabitants of high-rise buildings often exhibit greater feeling of indifference and withdrawal towards neighbours. This is in contrast to the dwellers of low-rise houses<sup>(10)</sup>. The crime rate in high-rise buildings is higher compared to relatively low-rise buildings<sup>(13)</sup>. These are some of the problems for which the tall buildings are criticised in the recent times.

The extent to which tall buildings are responsible for all these problems is a debatable question. However, it is recognised that the construction of more high-rise buildings is a feasible solution to the housing problem in the near future. Therefore, to make this an acceptable solution, a joint effort of city planners, architects, engineers and social scientists is necessary to eliminate or minimise these problems. Not only each group of specialists should provide<sup>a</sup> solution to the problem facing them, but also should be aware of the problems facing the other groups.

In addition to these environmental, psychological and social problems, there remain many engineering and technical problems associated with tall buildings construction. To provide efficient elevating devices for the users, the operation of heating and cooling systems, the supply of water and electricity, to provide telephone and other communication, throughout the building, to provide safety against fire hazards, to provide structural safety to withstand wind and earthquake effects, to devise new construction materials and improve construction techniques are some of these problems. This thesis deals with one aspect of these problems associated with tall buildings, namely, the study of <sup>the</sup> deformation behaviour of high-rise buildings of shear wall construction subjected to lateral loading such as wind loads and loads caused by earthquakes.

Structural components such as walls, beams, columns and floor slabs form an integrated structural system of a building. The structure and its components support the vertical and lateral loads applied to the building. The vertical load arises due to the self weight of the components, the occupants and other objects broadly classified as live loads. The lateral loads arise due to the action of wind, earthquake or blast

effect. Different structural loads to be considered in the design of buildings are given in the National Building code of Canada<sup>(49)</sup> and SEAOC Recommendations<sup>(60)</sup>. To design a structurally safe building, it is necessary to find the load taken by each component, so that each component can be designed accordingly. For that reason a structural analysis is needed. The next step is to proportion the components such that the criteria for stresses and deflections are satisfied. The Canadian Structural Design Manual<sup>(8)</sup> provides guidance in the design of structural components with steel, reinforced concrete, prestressed concrete and other materials.

In high-rise buildings, the consideration of deflection due to lateral loads becomes particularly important. For that reason it is necessary to provide adequate lateral stiffness to the structure. This lateral stiffness can be provided by using various specially designed structural systems. The response of various structural systems due to lateral loads has been compiled in the ACI Committee Report<sup>(1)</sup>. Among these systems, the use of reinforced concrete shear wall as vertical and lateral stiffening elements has become very common. In such a system, the high in-plane stiffness of the shear walls is employed to resist the lateral loads. The floor

slabs which are very stiff in their own planes distribute the lateral loads among the walls. The complex interaction of the stiff floors with the walls increases the lateral stiffness of the structure. Besides acting as load bearing walls, these shear walls act as internal partitions, acoustic barriers and provide fire divisions within the building. The arrangement of shear walls in a typical apartment building is shown in Figure (1.1). The shear walls are mainly located on both sides of the corridor. The elevator shaft and stair well is also enclosed by shear walls. In an office building, the arrangement of shear walls is different. The shear walls are located at the center of the building mainly to form a service core for the staircases and elevators. The central core is surrounded by columns which are interconnected to form different structural frames. The arrangement of shear walls in a typical office building is shown in Figure (1.2). The present thesis is a study of these types of structures and their structural behaviour when subjected to lateral loadings.

1.2 Review of Past Works

When the shear walls are arranged in a symmetric manner in the plan of the building, wind and seismic loads will cause translational displacements only. In these cases, the deformation of the building is confined to a plane and the load-displacement behaviour of the structure can be described by a two-dimensional analysis. The common examples of symmetric buildings are the apartment buildings with two-parallel sets of regularly spaced shear walls. In such cases, the behaviour of the whole building can be studied from the two-dimensional behaviour of a typical pair of shear walls. The shear walls may be coupled either through the floor slabs or floor beams or both. This class of problem is generally known as the plane coupled shear walls problem. The analysis of uniform plane coupled shear walls subjected to static loading has been presented by Chitty<sup>(11)</sup>, Beck<sup>(2)</sup>, Eriksson<sup>(27)</sup> and Rosman<sup>(54, 55)</sup>. Sets of design curves for a few common loading cases are presented by Coull and Choudhury<sup>(17,18)</sup>. Extensions to cover the cases with non-uniform shear walls are reported by Burns<sup>(6)</sup>, Coull and Puri<sup>(19, 20)</sup>, Traum<sup>(71)</sup>, Rosman<sup>(56)</sup> and Tso and Chan<sup>(79)</sup>. The effect of the flexibility of foundation on the coupled shear walls is included

in studies by Coull<sup>(22, 23)</sup>, Tso<sup>(72)</sup> and Tso and Chan<sup>(79)</sup>. The inelastic behaviour of the plane coupled shear walls has been studied by Winokur and Gluck<sup>(84)</sup> and Paulay<sup>(52)</sup>. The dynamic properties of the coupled shear wall has been studied by Tso and Chan<sup>(78)</sup>, Jennings and Skattum<sup>(41)</sup>. An approximate seismic analysis based on the response spectrum technique is presented by Tso and Biswas<sup>(73, 75)</sup>. The multiple bay planar shear wall has been treated by Hussein<sup>(36)</sup>, Elkholy and Robinson<sup>(26)</sup> and Coull and Subedi<sup>(24)</sup>. The methods of analysis mentioned above employed the continuous approach which replaces the connecting beams between the walls by a continuous distribution of laminae of equivalent stiffness. Coupled shear walls can also be analysed as equivalent frames using standard matrix structural analysis techniques. The typical examples of this approach are the works of Candy<sup>(9)</sup>, McLeod<sup>(43)</sup>, Schwaighofer and Microys<sup>(61)</sup> and Stafford Smith<sup>(63)</sup>. The finite width of the shear wall is accounted for by assuming sets of infinitely rigid beams connected to the column of the equivalent frame. The length of the rigid beam is taken from the centerline to the edge of the shear wall. The finite element idealisation has been proposed by MacLeod<sup>(44)</sup> and Butlin and McMillan<sup>(7)</sup>. A solution of coupled shear walls by the continuous approach, the equivalent frame method and the

finite element method has been compared by Choudhury<sup>(12)</sup>. Essentially, the three approaches give the same results for the cases studied.

When symmetry does not exist in the plan of the building, the lateral loads will cause twisting of the building in addition to translation. Out-of-plane displacement exists in this case. A two-dimensional approximation becomes inadequate in determining the structural behaviour of the building and a three-dimensional analysis will be necessary. A review of the methods of three-dimensional analysis of tall buildings is presented by Stafford Smith<sup>(64)</sup> and Stamato<sup>(67)</sup>.

Treating the structure as a collection of rectangular space frames with floor slabs idealised as infinitely rigid diaphragms, Weaver and Nelson<sup>(82)</sup> developed a three-dimensional analysis of multi-storey buildings composed of frames. Neglecting the transverse stiffness of the floor slabs Winokur and Gluck<sup>(84)</sup> presented a method of three-dimensional analysis of asymmetric multi storey buildings. The stiffness matrix of the structure was determined from the stiffness of the individual elements and the rigid in-plane diaphragm action of the floor slabs. Using the stiffness matrix approach, Heidebrecht and Swift<sup>(32)</sup> presented a method where the coupling action of the floor slab was

considered by assuming equivalent beams connecting the shear walls. Based on Vlasov's theory<sup>(81)</sup>, an additional degree of freedom was introduced to consider the warping deformation of the shear walls having thin-walled open sections. A similar approach with a finite element idealization for the transverse stiffness of the floor slab was used by Taranath<sup>(70)</sup>. An approximate method of analysis of building structures consisting of parallel system of shear walls and box cores was presented by Coull and Irwin<sup>(21)</sup>. The continuous approach has been used to determine the flexibility of the wall units. The analysis of the complete structure is then performed by combining the stiffnesses of different portion of the building. Another approximate method for buildings consisting of two-dimensional panels was presented by Stamato and Stafford Smith<sup>(66)</sup>. The vertical interaction between the panels were considered and the flexibility matrix formulation was used. A similar method using the stiffness approach but neglecting the vertical interaction between different units was reported by Ghali and Neville<sup>(28)</sup>. Majid and Croxton<sup>(45)</sup> proposed a wind analysis of building structures consisting of skeleton frames and a collage of shear walls and floor slab. In this method, the influence coefficients of the components were determined independently and then the equilibrium and



compatibility were satisfied. This method took into account the in-plane bending of the floor slabs. The in-plane deformation of the floor slab was also considered by Zienkiewicz, Parekh and Teply<sup>(87)</sup>. A finite element idealisation of the shear walls and the connecting floors slabs has been used in the analysis. Gluck<sup>(29)</sup> presented a three-dimensional analysis of asymmetric structures using the continuous approach. The differential equations in displacement variables were obtained and the axial deformations of the shear walls were neglected for simplification. Using a similar approach, but considering the axial deformation of the shear walls, a method was proposed by Rosman<sup>(59)</sup>. In the formulation, the axial force in the shear walls is used as variables. Similar treatments using the distributed shear in the connecting beam as unknown variables in the problem was reported by Gluck and Gellert<sup>(30, 31)</sup>. Jaeger, Mufti and Mamet<sup>(38)</sup> developed a method of analysis of two and three walled coupled units arranged in a symmetric manner. Differential equations were set up using bending moments as the variables.

Box-type cores formed from groups of shear walls surrounding<sup>a</sup> lift shaft and stair well are also very efficient in providing lateral stiffness. In office buildings, such cores are surrounded by columns to provide

large office spaces. In many cases the contribution of the columns in providing lateral stiffness may be neglected. If the core is located centrally, lateral loads applied to the building will induce only flexural deformation of the core structure. Osawa<sup>(51)</sup> and Tani<sup>(69)</sup> studied the flexural behaviour of such core structures. However, when the core is located eccentrically, the lateral loads will induce torsion in addition to flexure of the core structure. The complementary energy principle has been used by Jenkins and Harrison<sup>(39)</sup> for the torsion analysis of core wall structures. The continuous approach has been used by Michael<sup>(41)</sup> Rosman<sup>(57, 58)</sup> and Tso and Biswas<sup>(75, 76)</sup> to study the torsional behaviour of core structure consisting of channel shaped shear walls constrained by two rows of connecting beams. Using the same approach, Heidebrecht and Stafford Smith<sup>(33)</sup> have presented an approximate torsion analysis of open-section cores constrained by one row of connecting beams. A finite element idealisation has been used by Stafford Smith and Taranath<sup>(65)</sup> in treating the floor slabs surrounding open-section core structures.

The various methods used for the analysis of shear wall buildings can be classified into two basic approaches. They are the discrete approach and the continuous approach. In the discrete approach, the behaviour of the building is described by displacements or forces at a discrete number

of points in the structure. The methods based on the discrete approach usually lead to a system of algebraic equations. The solution then gives the forces or displacements at the discrete points of the structure. In the discrete approach, the matrix techniques of structural analysis<sup>(42)</sup> can be used to the best advantage. In the continuous approach the horizontal stiffening elements connecting the vertical elements are replaced by a medium of equivalent stiffness continuously distributed along the height of the building. This approach usually leads to a system of differential equations. Solutions of these equations give the displacement and internal forces at every point of the structure.

The discrete approach is more versatile as it can deal with buildings having change of cross-section of the shear walls or variation of structural components along the height. However, due to the large number of variables and parameters necessary to define the problem, the effect of the different parameters are not easily visualised. Therefore, this approach provides less physical insight into the behaviour of the structure under different conditions of loading. In the continuous approach, the overall behaviour of the structure is described by a small number of functions and parameters. Therefore, the effect of these

parameters on the results can be visualised readily. However, this approach is not particularly suitable for dealing with building having change of cross-section of the shear walls or other structural components along the height of the structure. It may also be pointed out that the errors found in the continuous approach becomes smaller as the number of storeys of the building increases. On the other hand, in the methods based on the discrete approach, the round off errors are greater when the number of storeys and hence, unknowns become very large.

In the present research work, the behaviour of multi storey shear wall structures is studied. An approximate method to analyse the three-dimensional deformation of the structure is presented. The continuous approach is used in the analysis. The vertical interaction between the shear walls due to the coupling action of the floor slabs and/or beams and the axial deformation of the shear walls have been considered.

The following problems are studied in particular. The torsional behaviour of core wall structures is studied in Chapter 2. The problem of asymmetric shear wall structures is treated in Chapter 3. The effect of change of floor plans with respect to height of the structure is studied in Chapter 4. The behaviour of asymmetric shear

Wall structures subjected to dynamic load is studied in Chapter 4. It is hoped that the present research work will provide a means of analysing high-rise buildings of shear wall construction and also provide some insight to the three-dimensional behaviour of this type of structures under lateral loading.

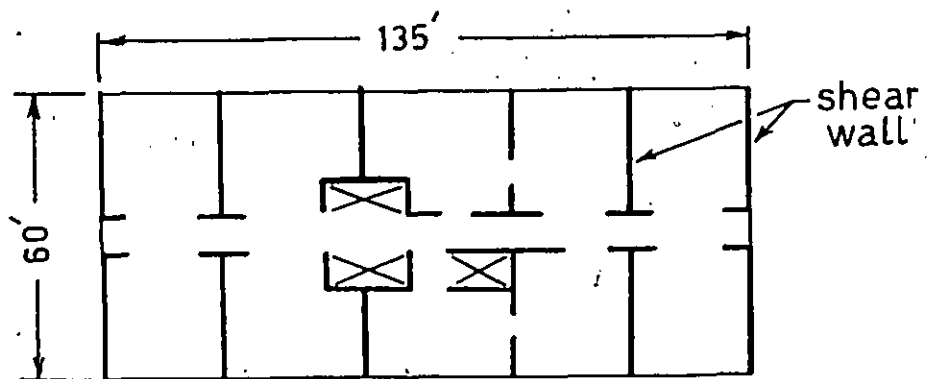
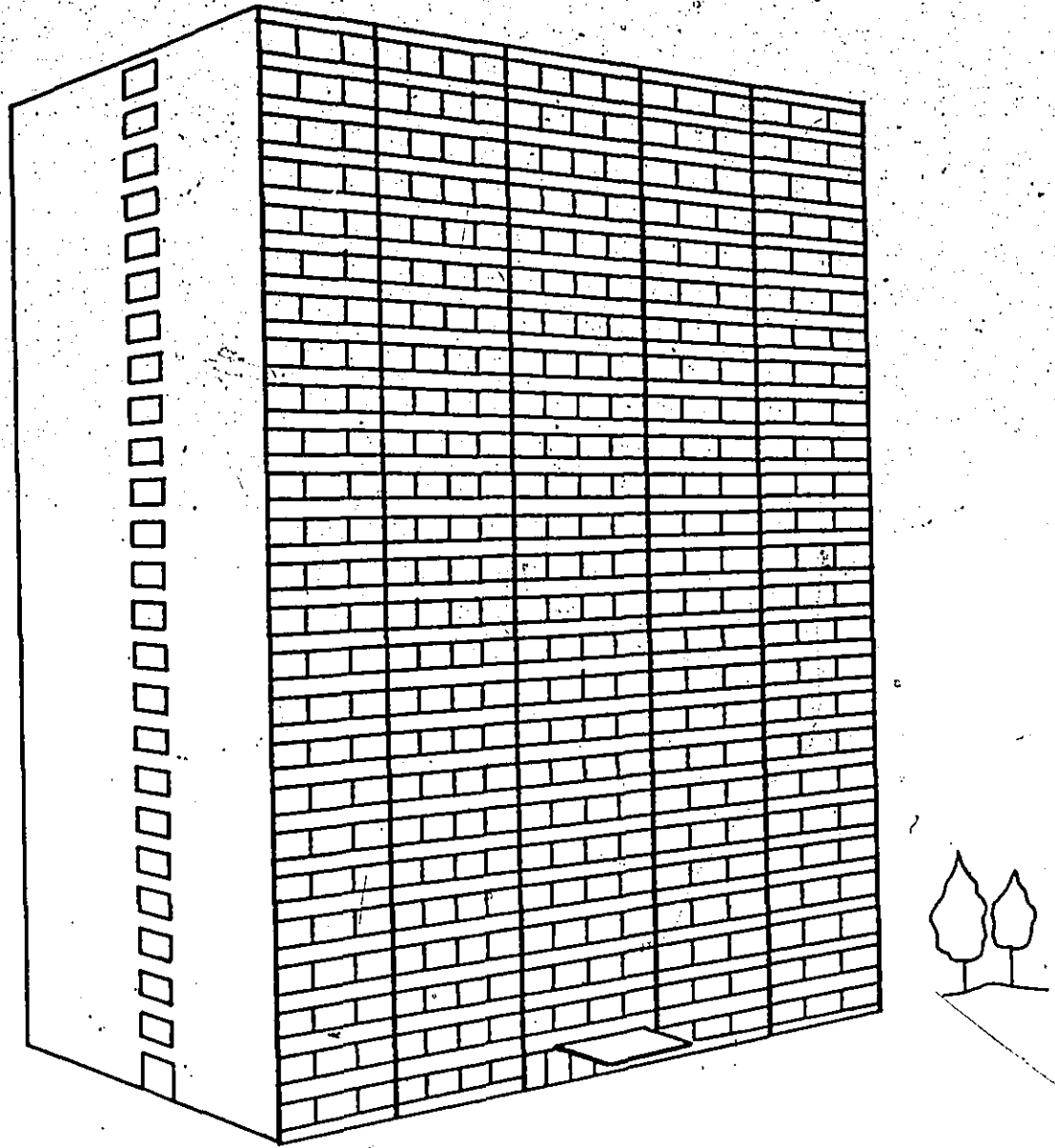


FIG. 1.1 A TYPICAL APARTMENT BUILDING

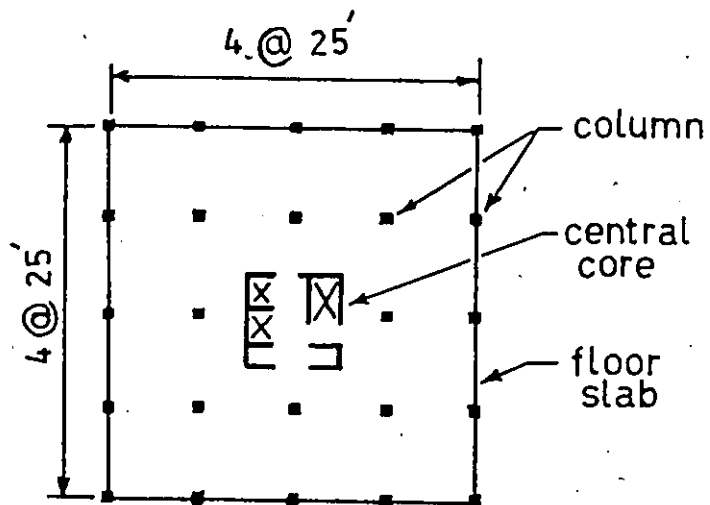
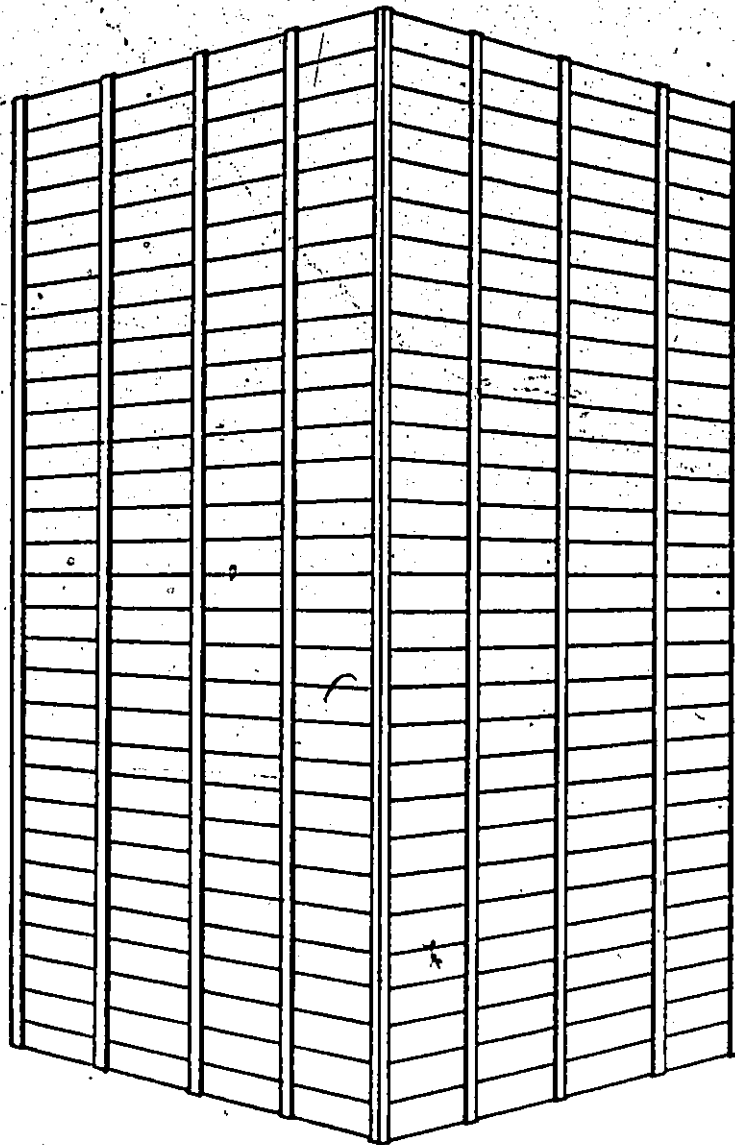


FIG. 1.2 A TYPICAL OFFICE BUILDING

## CHAPTER II

### TORSIONAL ANALYSIS OF SYMMETRIC TWO WALL CORE STRUCTURE

#### 2.1 Introduction

In high-rise buildings, the resistance to lateral load is often provided by core structures alone. These core structures are formed by an assembly of reinforced concrete shear walls running along the height of the building. These shear walls are interconnected at every floor level through beams or floor slabs. The elevators, staircases and service ducts for the building are normally housed in this concrete core structure. The core structure is usually surrounded by columns. The core and columns are interconnected by structural framing. Figure (1.2) shows a typical structural arrangement in an office building where a concrete core is used. The stiffness of the columns is much less than the core structure. In most cases the contribution of the columns to the lateral stiffness of the building is small compared with that of the core and it can be assumed that the lateral load is resisted by the core alone. The action of wind or earthquake induces lateral loading as shown in Figure (2.1). When the



core is located at the center, these lateral forces will produce translations of the building with no rotation. When the core is not located at the center or other asymmetry exists in the building, it will undergo rotation in addition to translation as shown in Figure (2.1). Even in a symmetric building, the National Building Code of Canada 1970<sup>(49)</sup> requires some accidental torque to be considered in lateral loading calculations. Most of the studies on core wall structures are related to the flexural behaviour of core walls subjected to lateral loading<sup>(51, 69)</sup>. However, the torsional behaviour of core structures has received very little attention until recently. Michael<sup>(48)</sup> analysed a symmetric core consisting of two equal channel shaped shear walls subjected to applied torques. The continuous method was used. However, the torque contribution due to the bimoments on the walls were not accounted for in the analysis. Consequently, the results tended to underestimate the torsional stiffness of the structure and overestimate the warping stresses. Rosman<sup>(57, 58)</sup> presented a torsional analysis of core structures. Using the complementary energy principle, the differential equations were derived in terms of the axial forces in the shear walls. Such equations are convenient for static load analysis. However, it is difficult to incorporate the dynamic effect directly

in the analysis.

In this chapter, the problem of a core structure subjected to applied torques is studied. The rotational deformation of the structure is taken as the unknown variable of the problem. Differential equations are derived from first principles. Explicit solutions are obtained for the rotation, stresses and other design parameters. An example is worked out to show the significance of the warping stresses. The importance of the different structural parameters is then discussed. An experiment is then performed to show the accuracy of the theoretical calculation. Finally, design curves are presented to provide a rapid calculation of the design parameters. The use of these design curves is illustrated by an example.

## 2.2 Notations

The following notations will be used in this Chapter.

$A_D^*$	Equivalent area of connecting beam for shear deformation.
$E, G$	Modulus of elasticity and shear modulus of material.
$H$	Total height of structure.
$I_b$	Moment of inertia of connecting beam.
$I_x$	Moment of inertia of one wall about x axis.
$I_w$	Sectorial inertia of one wall.
$J$	St. Venant's torsion factor for one wall.
$P$	Concentrated torque at top.
$a, b$	Dimensions of the core.
$x_c$	Distance from the centre of the core to the shear centre of the wall.
$x_e$	Distance from the centre of the core to the centroid of the wall.
$h$	Storey height.
$l$	Clear span of connecting beam.
$p$	Uniformly distributed torque.
$\rho$	Triangularly distributed torque (top intensity).
$q_j$	Distributed shear in connecting beam $j$ .
$r$	Enclosed area of the core = $ab$ .
$\gamma$	Beam stiffness factor.

- $\xi, \eta, \theta$  Deflection in x direction, y direction and rotation of centre of core respectively.
- $\sigma$  Warping stress.
- $\Omega, S_{\Omega}$  Sectorial properties of the core.
- $\omega$  Sectorial area of the wall at the mid point of the laminae.
- $(\ )'$  Prime denotes differentiation with respect to z co-ordinate.

### 2.3 Statement of the Problem

The plan view of the core structure to be analysed is shown in Figure (2.2). The core consists of two identical shear walls in the shape of channel sections connected either by floor slabs or by beams at every floor level. The effect of the floor slabs can be represented by connecting beams of equivalent stiffnesses. The cross section of the shear walls and the stiffness property of the beams are taken to be constant throughout the height of the structure. The floor height of the structure is also assumed to be constant.

The following assumptions are used to formulate the mathematical model for the core structure.

1. The floor slabs in the building act as rigid diaphragms so that no cross-sectional deformation of the core structure is possible.
2. The individual walls can be treated as open thin-walled beams and Vlasov's theory of thin-walled beams holds (81).
3. The out-of-plane stiffness effect of floor slabs can be represented by equivalent connecting beams.
4. The connecting beams at each floor are further replaced by a uniform distribution of independently

acting laminae with equivalent stiffness properties throughout the height of the structure.

5. The mid-points of the connecting beams are assumed to be points of contraflexure.
6. The walls and the beams are assumed to be linearly elastic.

Point O is the reference point and the geometric center of the structure. Co-ordinate axes  $x$  and  $y$  are parallel and perpendicular to the connecting beams.  $z$  is the vertical axis along the height of the building.  $G_j$  and  $S_j$  denote the centroid and shear center of wall  $j$  ( $j = 1, 2$ ) respectively. The distance of the centroid and the shear center from O is denoted by  $x_e$  and  $x_c$  respectively. Let the horizontal displacements of point O in  $x$  and  $y$  direction be  $\xi$  and  $\eta$  respectively and the rotation of the section be  $\theta$ . The core is subjected to a distribution of applied torque along the height of the structure.

Using assumption (4) the core structure with beams connected at discrete points is converted into a mathematical model which can be described by continuous functions. This mathematical model consists of the two shear walls connected by two rows of laminae with equivalent stiffness properties distributed throughout the height. The action of the floor

slabs as rigid diaphragms in their own plane do not allow any deformation of the core section. Therefore, the behaviour of such a structure is governed by the deflections and rotation of any reference point of the section. In this case, the governing variables are  $\xi(z)$ ,  $\eta(z)$  and  $\theta(z)$ . However, for the symmetric core subjected to applied torque only, the structure will undergo rotation  $\theta(z)$  about the center point and no lateral deflections will result.

Since the center points of each row of laminae are considered the points of contraflexure, there are no bending moments at these points. If an imaginary cut is made through the center points of one row of laminae and another cut through the center points of the other row of laminae, distributed shear  $q_1(z)$  and  $q_2(z)$  will then be exposed as shown in Figure (2.4). These are the two unknowns in addition to  $\theta(z)$  to be considered in the analysis.

#### 2.4.1 Equilibrium Conditions

When the structure deforms, internal torque is developed to balance the external torque  $Q_t$ . This internal torque consists of two parts. The first part is the torque derived from the individual walls. From the theory of thin-walled beams, the shear forces and torques as a

result of deformations from each wall are shown in Figure (2.3). Therefore, the torque due to the forces in the walls about point O is given by:

$$Q_w = -EI_w(\theta_1''' + \theta_2''') + GJ(\theta_1' + \theta_2') + EI_x x_c(\eta_1''' - \eta_2''') \quad (2.1)$$

Where  $\xi_j$ ,  $\eta_j$  and  $\theta_j$  are the displacements and rotation of the shear center of the  $j^{\text{th}}$  wall. Based on the assumptions that ~~for~~ floor slabs act as rigid diaphragms,  $\xi_j$ ,  $\eta_j$  and  $\theta_j$  can be expressed in terms of  $\xi$ ,  $\eta$  and  $\theta$  as follows:

$$\xi_1 = \xi_2 = \xi \quad (2.2a)$$

$$\theta_1 = \theta_2 = \theta \quad (2.2b)$$

$$\eta_1 = \eta - x_c \theta, \quad \eta_2 = \eta + x_c \theta \quad (2.2c)$$

Using equation (2.2), there is obtained

$$Q_w = -2EI_w^* \theta''' + 2GJ\theta' \quad (2.3)$$

where  $I_w^* = I_w + I_x x_c^2$  (2.3a)

In addition, the two rows of laminae offer additional torque  $Q_b$  to balance the applied torque  $Q_t$ . Consider a free body diagram of a length of the wall  $dz$  as shown in



Figure (2.4). Additional shear forces  $Q_{xj}$ ,  $Q_{yj}$  and torques  $Q_{tj}$  ( $j = 1, 2$ ) develop in the sections due to the existence of the distributed shears  $q_1$  and  $q_2$ . From consideration of the equilibrium of each wall about  $y$  and  $x$  axes, there is obtained:

$$Q_{x1} = Q_{x2} = (q_1 + q_2)X_c \quad (2.4a)$$

$$Q_{y1} = Q_{y2} = (q_1 - q_2) \frac{b}{2} \quad (2.4b)$$

The distributed shear forces  $q_1$  and  $q_2$  acting along the mid points of the rows laminae produces a bimoment on the walls. Bimoment is a generalized force quantity considered in the theory of thin-walled beams. A detailed treatment of bimoment is included in Appendix A. The bimoment produced in this case is equal to the shear force times the sectorial area  $\omega$  at the point of application. As a result, additional flexural twists  $Q_{t1}$  and  $Q_{t2}$  develop and are given by:

$$Q_{t1} = Q_{t2} = (q_1 - q_2)\omega \quad (2.5)$$

The resultant torque  $Q_b$  due to these forces and torques about the point  $O$  becomes

$$\begin{aligned}
 Q_b &= Q_{t1} + Q_{t2} + (Q_{y1} + Q_{y2}) x_c & (2.6) \\
 &= r (q_1 - q_2)
 \end{aligned}$$

Where  $r$  is the enclosed area of the core ( $r = ab$ ).

The torque equilibrium equation can be obtained by equating the internal torque due to the shear walls and the rows of laminae to the applied torque. Using equations (2.3) and (2.6) there is obtained:

$$-2EI_\omega \theta''' + 2GJ\theta' + r(q_1 - q_2) = Q_t \quad (2.7)$$

#### 2.4.2. Compatibility Conditions

There is only one condition of equilibrium of torque available and there are three variables  $\theta$ ,  $q_1$  and  $q_2$  to be determined. Therefore, the system is statically indeterminate of the order two and two additional conditions are necessary. These two conditions are obtained from the compatibility of deformation at the points of cut of the two rows of laminae.

When two imaginary cuts are made along the mid-points of the two rows of laminae and the structure is

allowed to deform, the points to the left and to the right of the cut of each laminae suffer relative displacements. Let the relative displacement for the laminae in row 1 due to the lateral deflections and rotation of the shear walls be  $\delta_1(1)$ . (Using the theory of thin walled beams (Appendix A),  $\delta_1(1)$  is found to be:

$$\delta_1(1) = (\xi_2' + \xi_1') X_c + (\eta_2' - \eta_1') \frac{b}{2} + (\theta_2' + \theta_1') \omega \quad (2.8)$$

In addition, the bending and shear deformations of the laminae due to  $q_1$  produce a displacement  $\delta_2(1)$ . It can be expressed as

$$\delta_2(1) = \frac{q_1}{E\gamma} \quad (2.9)$$

where  $\gamma = \frac{12I_b}{t^3 h (1 + 12EI_b / (G A_b^* t^2))}$  (2.9a)

Also, the distributed shear  $q_1$  produces axial compressive force on one shear wall and tensile force on the other wall. This axial force  $T$  can be expressed as:

$$T = \int_z^H (q_1(\bar{z}) + q_2(\bar{z})) d\bar{z} \quad (2.10)$$

The axial deformation of the wall due to this axial force  $T$  will induce a relative displacement  $\delta_3(1)$  at the imaginary cut. This displacement can be expressed as:

$$\delta_3(1) = \int_0^z \frac{2T(\bar{z})}{EA} d\bar{z} \quad (2.11)$$

The relative displacements  $\delta_1(1)$ ,  $\delta_2(1)$  and  $\delta_3(1)$  are graphically illustrated in Figure (2.5).

The condition of compatibility requires that:

$$\delta_1(1) = \delta_2(1) + \delta_3(1) \quad (2.12)$$

Using the geometric relations from equation (2.2), the compatibility conditions for the 1st row of laminae becomes:

$$2X_e \xi' + r\theta' = \int_0^z \frac{2T(\bar{z})}{AE} d\bar{z} + \frac{q_1}{E\gamma} \quad (2.13)$$

In a similar way, the compatibility condition for the second row of laminae can be obtained as:

$$2X_e \xi' - r\theta' = \int_0^z \frac{2T(\bar{z})}{AE} d\bar{z} + \frac{q_2}{E\gamma} \quad (2.14)$$

Subtracting equation (2.14) from equation (2.13), the following expression is obtained.

$$2E\gamma r\theta = (q_1 - q_2) \tag{2.15}$$

2.4.3 Final Equation and Solution

Combining equation (2.7) and (2.15) the final equation is obtained as:

$$2EI_{\omega} \theta''' + 2EI_{x_c} x_c^2 \theta''' - 2E\gamma r^2 \theta' - 2GJ\theta' = -Q_t \tag{2.16}$$

The first term in this equation represents the warping resistance due to each individual channel shaped shear wall. The second term is the warping term caused by the diaphragm action of the floor slabs. The third and fourth terms represent the effect of the connecting beams and the St. Venant's torsional stiffness of the core walls, respectively.

For computational purposes, it is convenient to write equation (2.16) in the following form.

$$\theta''' - \lambda^2 \theta' = -\beta Q_t \tag{2.17}$$

where  $\lambda^2 = (E\gamma r^2 + GJ) / (EI_{\omega}^*) \tag{2.17a}$

$$\beta = 1 / (2EI_{\omega}^*) \tag{2.17b}$$

At the base there is no rotation and warping is prevented by the rigid base. The top of the building is free so that there is no bimoment. Mathematically these boundary conditions can be written as:

$$\theta(0) = 0 \quad (2.18a)$$

$$\theta'(0) = 0 \quad (2.18b)$$

$$\theta''(H) = 0 \quad (2.18c)$$

The problem of torsional analysis of a symmetric twin core structure subjected to applied torques reduces to the solution of equation (2.17) subjected to the boundary conditions (2.18a, b, c).

Due to the symmetry of the problem, there is no lateral deflection of the structure when subjected to applied torque.

$$\text{Therefore: } \xi = \eta = 0 \quad (2.19)$$

Also in this case, it follows from equations (2.13) and (2.14) that:

$$q_1 = -q_2 \quad (2.20a)$$

and

$$T = 0 \quad (2.20b)$$

The equation (2.17) is a third order linear differential equation with constant coefficients. Solving this equation with the appropriate boundary conditions, the value of  $\theta(z)$  can be obtained. Knowing  $\theta(z)$ , the distributed shear in the laminae can be obtained from equation (2.15).

Therefore:

$$q_1 = -q_2 = EYr\theta' \quad (2.21)$$

Finally, the warping stress in the shear walls can be obtained from the thin-walled beam theory as:

$$\sigma = E\Omega\theta'' \quad (2.22)$$

Where  $\Omega$  represents the distribution of the warping stress across the section. For the symmetric core,  $\Omega$  is graphically shown in Figure (2.6).

Wind forces acting on buildings are often approximated as trapezoidally distributed along the height. A trapezoidal distribution can be analysed as a superposition of a uniform and a triangular distribution. In pseudo-dynamic analysis, the action of the earthquake is represented by a concentrated force at the top and a triangularly distributed force along the height. Therefore, in torsion

analysis of buildings, the loading cases of interest are

- (i) a concentrated torque applied at the top of the structure;
- (ii) a distributed torque of uniform intensity; and (iii) a triangularly distributed torque with maximum intensity at the top.

The explicit solutions for these three cases of loading are given as follows:

Due to a concentrated torque  $P$  at the top

$$\theta = \frac{\beta P}{\lambda^3} \left[ -\text{Sinh}(\lambda z) + \text{Tanh}(\lambda H) \{ \text{Cosh}(\lambda z) - 1 \} + \lambda z \right] \quad (2.23)$$

Due to a uniformly distributed torque of intensity  $p$

$$\theta = \frac{\beta p H}{\lambda^3} \left[ (-\text{Sinh}(\lambda z) + \{ \text{Tanh}(\lambda H) + \text{Sech}(\lambda H) / (\lambda H) \} \{ \text{Cosh}(\lambda z) - 1 \} + \lambda z - \lambda z^2 / 2H) \right] \quad (2.24)$$

Due to a triangularly distributed torque of top intensity  $\bar{p}$

$$\theta = \frac{\beta \bar{p} H}{\lambda^3} \left[ -\alpha \text{Sinh}(\lambda z) + \{ \alpha \text{Tanh}(\lambda H) + \text{Sech}(\lambda H) / (\lambda H) \} \{ \text{Cosh}(\lambda z) - 1 \} + \alpha \lambda z - (\lambda z^3) / (6H^2) \right]$$

Where:  $\alpha = \frac{1}{2} - 1/(\lambda H)^2$  (2.25)



### 2.5.1 Example

An example is worked out to show the importance of the warping stresses due to torsional deformation. A twenty storey building with a plan dimension 100 ft x 100 ft will be considered. The concrete core is assumed to be located eccentrically with an eccentricity of 5 ft. The core structure dimensions are taken to be  $a = 30$  ft long by  $b = 15$  ft wide with an opening width  $c = 6$  ft. The wall thickness is taken to be 8 in, floor thickness 6 in and storey height 10 ft. The modulus of elasticity  $E$  used is  $5.8 \times 10^5$  Ksf and Poisson's ratio used is 0.15. It is assumed that at each floor level, a 3 ft width of slab acts as an equivalent beam connecting the shear walls. The design eccentricity for the example calculated according to clause no. (4.17) of the National Building Code of Canada 1970<sup>(49)</sup> is 12.5 ft. A concentrated load of 100 kip acting at the design eccentricity of 12.5 ft is considered to act at the top of the structure as shown in Figure (2.7). Due to this load, the structure undergoes bending about the  $y$  axis and torsion about the  $z$  axis. The flexural stresses due to the 100 kip load acting through  $O$  can be computed using methods of plane coupled shear wall analysis<sup>(17)</sup>. The warping stresses due to a torque of 1250 kip.ft is

then computed using equation (2.22). The flexural and warping stresses thus obtained are plotted in Figure (2.7). It is seen from the plot that the warping stresses are as high as 40% of the flexural stresses at the critical areas. This shows that the warping stresses due to torsion is of significant importance in the design of core structures.

#### 2.5.2 Comparison with other methods

It is desirable to compare the theoretical results with other analytical methods often used to estimate the torsional stiffness of core structures. These methods are based on simplified assumptions. The differential equations for these methods can be obtained by modifying equation (2.16). The following cases will be considered for comparisons.

1. The floor slab has infinite in-plane rigidity but completely flexible out-of-plane. Therefore, the connecting beams representing the out-of-plane stiffness of the slabs will have zero stiffness. The differential equation for this case can be obtained by substituting  $\gamma = 0$  in equation (2.16). The equation obtained in this way is:

$$2EI_{\omega} \theta''' - 2GJ \theta' = -Q_t \quad (2.26)$$

2. The rigid diaphragm action of the floor slabs is completely neglected. The torsional stiffness of the core in this case is taken to be the sum of the warping stiffness of the two channel shaped shear walls. The differential equation for this case is:

$$2EI_{\omega} \theta''' - 2GJ \theta' = -Q_t \quad (2.27)$$

3. The local torsional properties of the individual shear walls are neglected. The differential equation therefore contains terms from rigid diaphragm action of the floor slabs and the stiffness of the connecting beams as follows:

$$2EI_x x_c^2 \theta''' - 2E\gamma r^2 \theta' = -Q_t \quad (2.28)$$

4. The St. Venant's torsional stiffness of the core is neglected. Neglecting the last term of the equation (2.16), the differential equation for this case is obtained as:

$$2EI_{\omega} \theta''' - 2E\gamma r^2 \theta' = -Q_t \quad (2.29)$$

5. In the torsion analysis of a core structure by Michael<sup>(48)</sup>, the torque contribution  $Q_{t1}$  and  $Q_{t2}$  due to bimoment from the shear force in the rows of the connecting of laminae was not taken into account. The theory can be reduced to the following differential equation:

$$2EI_{\omega} \theta''' - 2E_{\gamma} R \theta' = -Q_t \quad (2.30)$$

$$\text{Where: } R = b^2 a(a+2X_c)/4 \quad (2.30a)$$

It can be shown that for the core structure considered,  $R$  is always less than  $r^2$ .

6. The structure is assumed to be a closed box of the same overall dimension as the core. The differential equation for this case is:

$$GI_p \theta' = Q_t \quad (2.31)$$

Where:  $I_p$  is the polar moment of inertia of the box section.

To compare the different methods, the core structure used in the example with a concentrated torque of 1250 kip.ft acting at the top is considered. This structure has been analysed using different methods and the

rotation at the top and warping stresses at the base are computed. The relative torsional stiffness  $S_n/S_o$  and the relative warping stress at A  $\sigma_n/\sigma_o$  provide a good comparison of the various approaches.  $S_o$  and  $\sigma_o$  are the torsional stiffness at the top and warping stress at point A at the base of the structure according to equation (2.16).  $S_n$  and  $\sigma_n$  are the same parameters obtained using method n.

The results are tabulated in Table 2.1.

TABLE 2.1.

	M E T H O D					
	1	2	3	4	5	6
Torsional Stiffness ratio $S_n/S_o$	.585	.565	.961	.980	.750	244
Warping Stress ratio $\sigma_n/\sigma_o$	5.41	5.50	1.04	1.01	1.23	-

The closed box approximation (Method 6) results in an extremely high estimation of the torsional stiffness. It is also seen that rigid diaphragm action of the floor slab and the connecting beam stiffness is quite important in providing strength and reducing the stress level of the structure. Neglecting these actions will reduce strength by about 40% and increase stresses by about 5 times.

(Method 1 and 2). On the other hand, the results obtained using these two terms alone (Method 3) are within 4% from the correct values. The contribution of St. Venant's torsional stiffness is also very small (Method 4). Neglecting this effect will cause a difference of only 2%. Therefore, it is seen that the results are insensitive to the local torsional properties of the shear walls. Michael's<sup>(48)</sup> analysis always under-estimates the torsional stiffness and over-estimates the stresses (Method 5). In this case the difference is of the order of 24%.

#### 2.6.1 Experiment

An experiment is undertaken to verify the theoretical results. Static load tests are carried out on a 20 storey plexiglass model. The model dimensions are taken roughly as a 1/40th of the full scale structure. The core dimensions are:  $a = 6.5$  in,  $b = 5$  in,  $l = 1.5$  in,  $t = 0.244$  in. The storey height is 2.45 in and the connecting beams are 3/8 in deep and 0.244 in width. The model is built by assembling four plexiglas sheets. Rectangular holes are milled at regular intervals on two plexiglas sheets. Chloroform is used to fuse together the components so as to have monolithic connection at the joints. The construc-

tion of the model is shown in Figure (2.8). Diagonal braces made of plexiglas are used at every fourth storey level to provide the rigid diaphragm action of the floor slabs. These diagonal braces will restrict any deformation of the cross section of the core. The base of the model is made of 3/4 in plexiglas plate. The test rig consists of a thick base plate connected to two heavy I sections. The model base is bolted to the base plate to provide the fixed end conditions. The experimental set-up is shown in Figure (2.9).

The model is subjected to two cases of loading. In the first case, a concentrated load is applied at the top of the model through point O in the X direction. Due to this loading, the model under-went bending in the xz plane without any torsion. The results of this test was compared with the well established theory for the analysis plane coupled shear walls<sup>(17)</sup>. This served as a check on how well the model is constructed.

In the second case, a concentrated torque is applied at the top of the model by hanging weights through an arrangement of pulleys as shown in Figure (2.9). Electric resistance strain gauges are attached at different points of the model as shown in Figure (2.10). Lead wires from the strain gauges are hooked up to a strain indicator

through switch boxes. Strain readings at every increment of loading are taken. To compensate for the effect of temperature change during <sup>The</sup> experiment on the strain results, a dummy gauge fixed on a piece of plexiglas is used in the bridge arm of the strain indicator. Deflections of the structure are measured from the readings of dial gauges mounted at different points of the model. To reduce the effect of creep of plexiglas, sustained loading was avoided and the test was performed as quickly as possible. The strain gauge and dial gauge readings taken at every load interval during loading and unloading phase are tabulated in Appendix B. From these readings, the deflection, rotation and strain at different points of the model are calculated.

The following is a list of equipment and material used in the experiment.

A. Model Material: Plexiglas

Elastic Properties:  $E = 4.3 \times 10^5$  psi,  $G = 1.6 \times 10^5$  psi.

B. Electric Resistance Strain Gauges.

Make: Micro Measurement

Type: EA-41-250 B.G.-120.

Resistance:  $120\Omega \pm 0.15\%$

Gauge Factor:  $2.01 \pm 0.5\%$

Gauge Length: 0.25 in.



C. Dial Gauges

Make: Baty

Reading: .001 in sensitivity.

D. Strain Indicator

Make: Budd Corporation

Reading: Directly calibrated to strain in  $\mu$  in/in.

Range:  $\pm 40,000 \mu$  in/in.

### 2.6.2 Results and Discussions

For the lateral load test on the model, the deflections and distributed shear in the connecting beams are plotted in Figure (2.11) and axial strains in the core walls at two levels are plotted in Figure (2.12). The theoretical results are calculated according to the well established plane coupled shear wall theory<sup>(17)</sup>. Measurements<sup>g</sup> of deflection and distributed shears at two opposite faces of the structure show that the model is fairly symmetrical in construction. For the torsional load test, the rotation and distributed beam shear are plotted in Figure (2.13) and strains on the core walls at two levels are plotted in Figure (2.14). The results from the theoretical analysis is also shown in these figures. Theoretical values based on Michael's<sup>(48)</sup> analysis is also presented.

The experimental deflections and strains for the lateral loading case are in good agreement with the theory. This checks the construction of the model and the value of the elastic modulus used in the analysis. The slight over-estimate of the axial strains and under-estimate of the deflection may be caused by the flexibility of the fixed support. The theoretical calculation over-estimates the beam shear by about 15%. This may be caused by the rounded corner of the openings making the connecting beam more stiff than assumed. Some error in the measurement of strains is also anticipated because the length of the gauge (.25 in), which is comparable to the length of the connecting beam (1.5 in).

For the case of torsional loading, the rotations and strains are in good agreement with the theory. The over-estimation of the theoretical distributed shear is also indicated in this case. Michael's analysis for the torsion of core structures did not consider the torque contributions  $Q_{t1}$  and  $Q_{t2}$ . Due to this omission, the theory under-estimates the torsional stiffness and over-estimates the warping stresses. In this case the difference is of the order of 45% as seen from Figures (2.13) and (2.14).

## 2.7 Design Curves

Design curves are commonly used for the rapid determination of different parameters. Design curves for the core structure subjected to three common torque distributions are presented in Figures (2.15) to (2.23). In order to use the curves it is necessary to know the geometric and elastic properties of the shear walls and connecting beams forming the core. The value of  $\lambda$  is then computed using equation (2.17a). The quantity  $\lambda H$  is then calculated. The non-dimensional parameter  $K$  at a desired level ( $z/H$ ) is then determined from the curves. To distinguish the values of  $K$  for different design parameters and load distributions, two sets of subscripts are used. The first subscript can be 1, 2 or 3, denoting the quantity is for the calculation of the rotation, distributed shear or warping stress respectively. The second subscript can be C, U or T depending on whether a concentrated torque applied to the top, a uniformly distributed torque or a triangularly distributed torque is being applied. In this way  $K_{3u}$  is the parameter for warping stresses calculation due to an uniformly distributed torque. The design parameters  $\theta$ ,  $q_1$  and  $\sigma$  is computed from the following relations.

For a concentrated torque  $P$  at the top

$$\theta = \frac{PH^3}{6EI_{\omega}^*} K_{1C} \quad (2.32a)$$

$$\varphi_1 = \frac{P\gamma r H^2}{4I_{\omega}^*} K_{2C}$$

$$\sigma = \frac{PH\Omega}{2I_{\omega}^*} K_{3C} \quad (2.32c)$$

For a uniformly distributed torque of intensity  $p$ .

$$\theta = \frac{pH^4}{16EI_{\omega}^*} K_{1U} \quad (2.33a)$$

$$\varphi_1 = \frac{pH^3 \gamma r}{12I_{\omega}^*} K_{2U} \quad (2.33b)$$

$$\sigma = \frac{pH^2 \Omega}{4I_{\omega}^*} K_{3U} \quad (2.33c)$$

For a triangularly distributed torque of top intensity  $\bar{p}$

$$\theta = \frac{11\bar{p}H^4}{240EI_{\omega}^*} K_{1T} \quad (2.34a)$$

$$\varphi_1 = \frac{\bar{p}\gamma r H^3}{16I_{\omega}^*} K_{2T} \quad (2.34b)$$

$$\sigma = \frac{\bar{p}H^2 \Omega}{6I_{\omega}^*} K_{3T} \quad (2.34c)$$

### 2.7.1 Example

The use of the design curves is demonstrated by solving an example. Let us choose a 30'x15' concrete core the dimensions of which are shown in Figure (2.7). Let us determine the rotation at the top, distributed shear at the mid-height and the maximum warping stress at the base. It is assumed that the design wind loading on the face of the building produces a uniformly distributed torque of intensity 5 kip.ft/ft.

The geometric properties of the core are calculated as follows:

$$I_{\omega} = 1.64 \times 10^4 \text{ ft}^6$$

$$I_x = 1.09 \times 10^3 \text{ ft}^4$$

$$X_c = 20 \text{ ft.}$$

$$\gamma = 2.27 \times 10^4$$

$$r = 450 \text{ ft}^2$$

$$J = 120 \text{ ft}^4$$

$$I_{\omega}^* = 4.49 \times 10^5 \text{ ft}^6$$

$$H = 200 \text{ ft.}$$

The modulus of elasticity on Poisson's ratio for concrete are taken to be  $5.8 \times 10^5$  ksf and 0.15 respectively. The shear modulus of concrete is calculated as  $2.5 \times 10^5$  ksf. The value of  $\lambda H$  computed using equation (2.17a) is 2.06.

To obtain the rotation at the top, the value of  $K_{1U}$  is needed. The value of  $K_{1U}$  corresponding to  $\lambda H = 2.06$  and  $z/H = 1$  as read from Figure (2.17) is 0.4. The rotation  $\theta$  is calculated from equation (2.33a) is  $7.66 \times 10^{-4}$  radians.

To obtain the distributed shear at the mid-height, the value of  $K_{2U}$  corresponding to  $\lambda H = 2.06$  and  $z/H = 0.5$  as read from Figure (2.18) is 0.36. The distributed beam shear  $q_1$  using equation (2.33b) is 0.272 K/ft.

To obtain the maximum warping stress at the base, the value of  $K_{3U}$  corresponding to  $\lambda H = 2.06$  and  $z/H = 0$  as read from Figure (2.19) is 0.6. It is seen from Figure (2.5) that the maximum warping stress occurs at the end of the flange. The value of the stress distribution factor  $\Omega$  at that point is  $203 \text{ ft}^2$ . Therefore, the warping stress calculated using equation (2.33c) is 13.5 ksf or 94 psi.

## 2.8 Conclusion

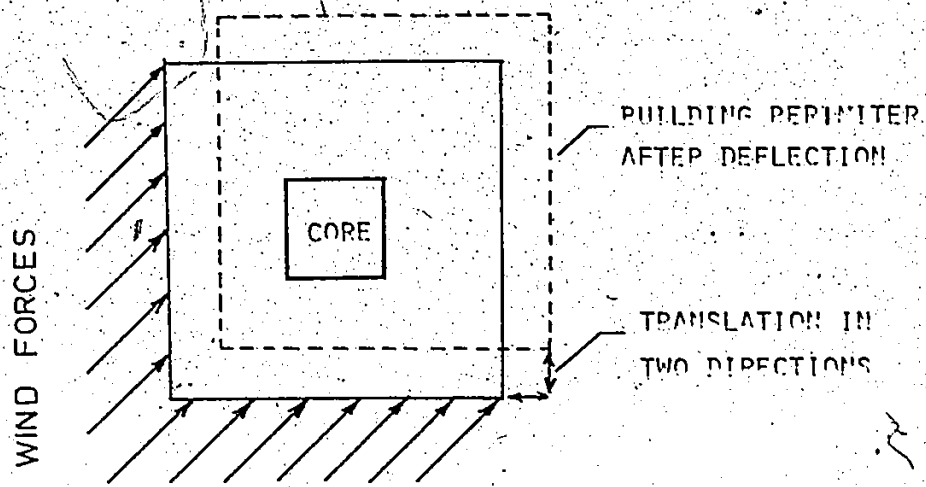
An approximate theory to analyse symmetrical core wall structures subjected to applied torques is presented. The theory is sufficiently simple that explicit solution can be obtained for any given load distribution. The

accuracy of the theory is demonstrated by tests on a model core structure of plexiglas material. The importance of torsional analysis in the design of core walls is shown by means of an example. It is shown that the warping stress constitutes a significant portion of the direct stress even for a building with small eccentricity. The significance of the rigid diaphragm action of the floor slabs and the stiffness of the connecting beam, in providing torsional stiffness is also demonstrated. It is seen that the results are insensitive to the local torsional properties of the shear walls. Therefore, for practical purpose they can be neglected. Finally, design curves are presented for three common load distributions. These curves can be used to determine very quickly the parameters of interest in designing the structure. In the analysis, shear walls in the shape of channels are treated. With minor modifications, the theory can be applied for cases with shear walls having different shapes as long as the symmetry of the core is maintained.

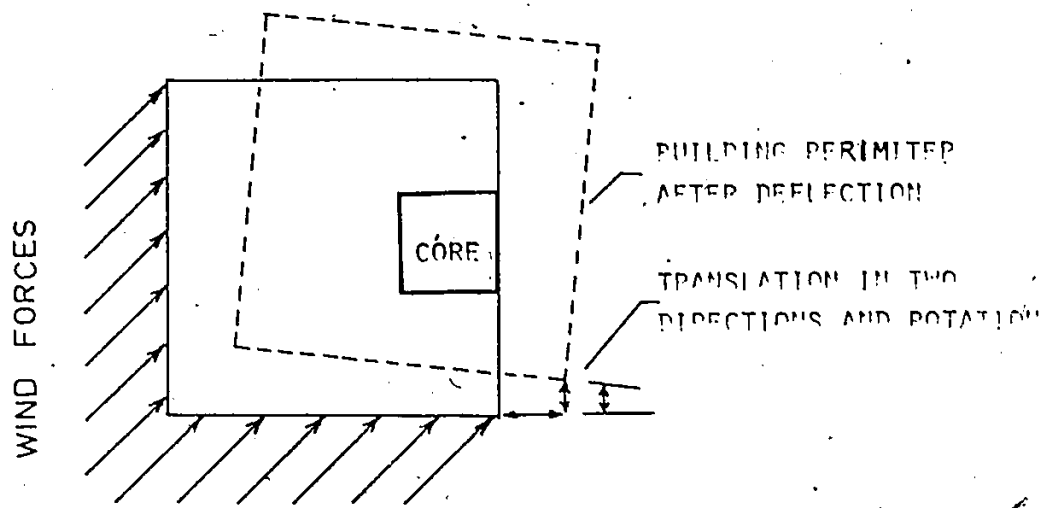
Compared with the formulation of the problem using complementary energy approach (57, 58), the present approach to the problem offers the following advantages. Firstly, using displacement as the unknown variable to the problem, the equations presented can readily be extended to study

the dynamic behaviour of such structures subjected to time dependent applied torques. The dynamic effect on the structure can be included as inertial torque loading. Secondly, formulating the problem in this manner gives a better physical interpretation of how the torque is being resisted by different structural actions.





(A) SYMMETRIC BUILDING



(B) ASYMMETRIC BUILDING

FIG. 2.1

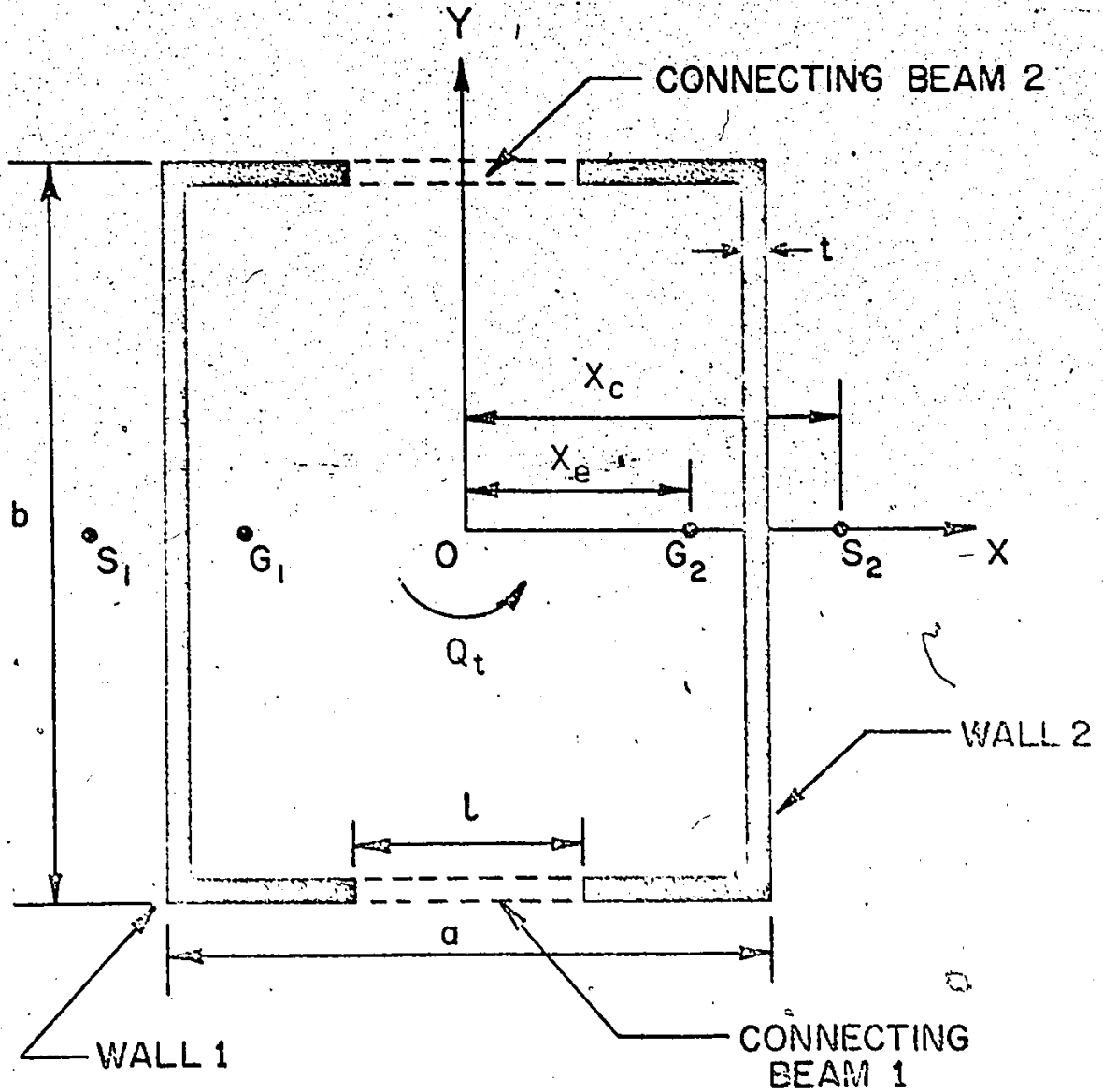


FIG. 2.2 PLAN OF TWO WALL CORE STRUCTURE

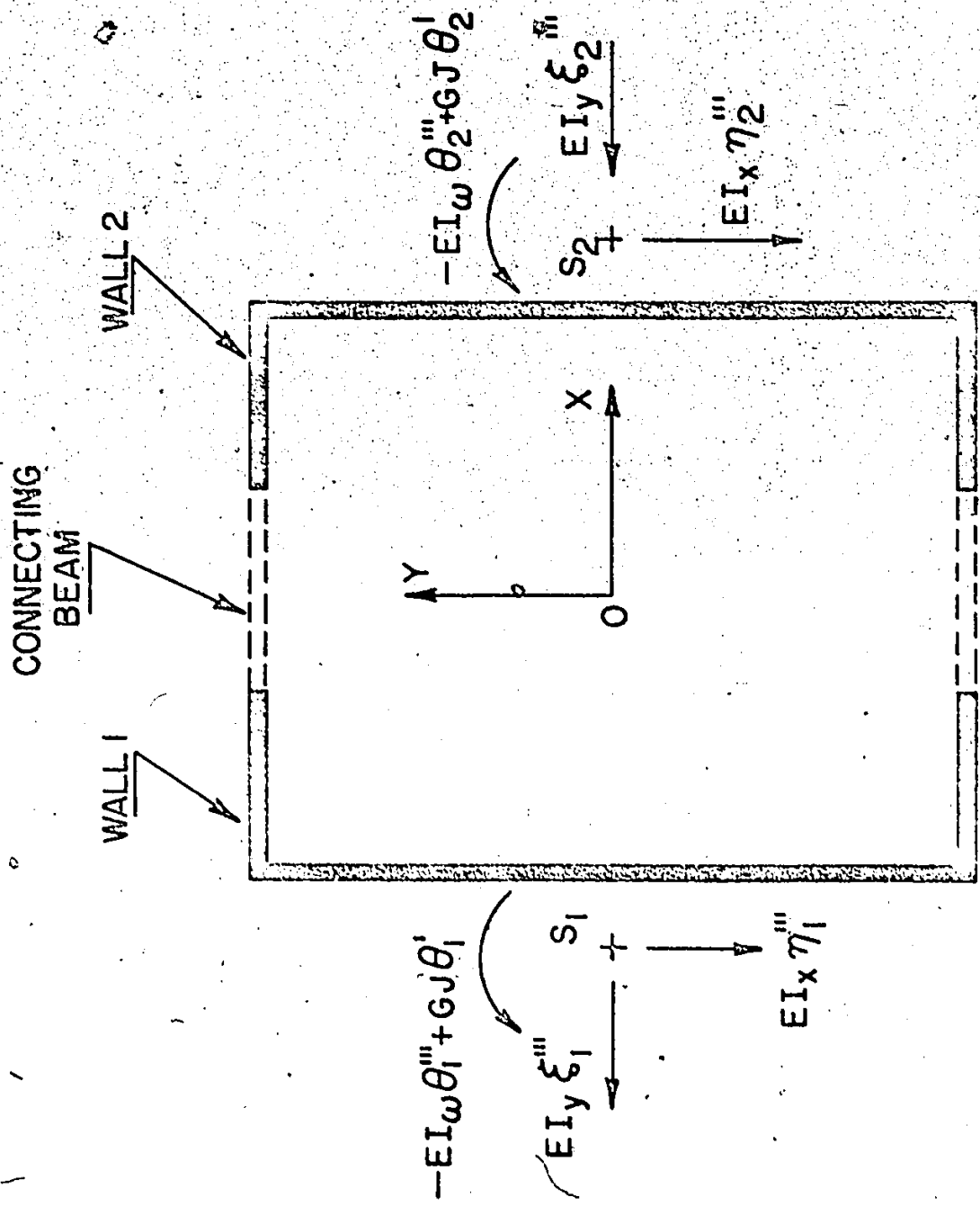


FIG. 2.3 SHEAR FORCES AND TORQUES FROM INDIVIDUAL WALL

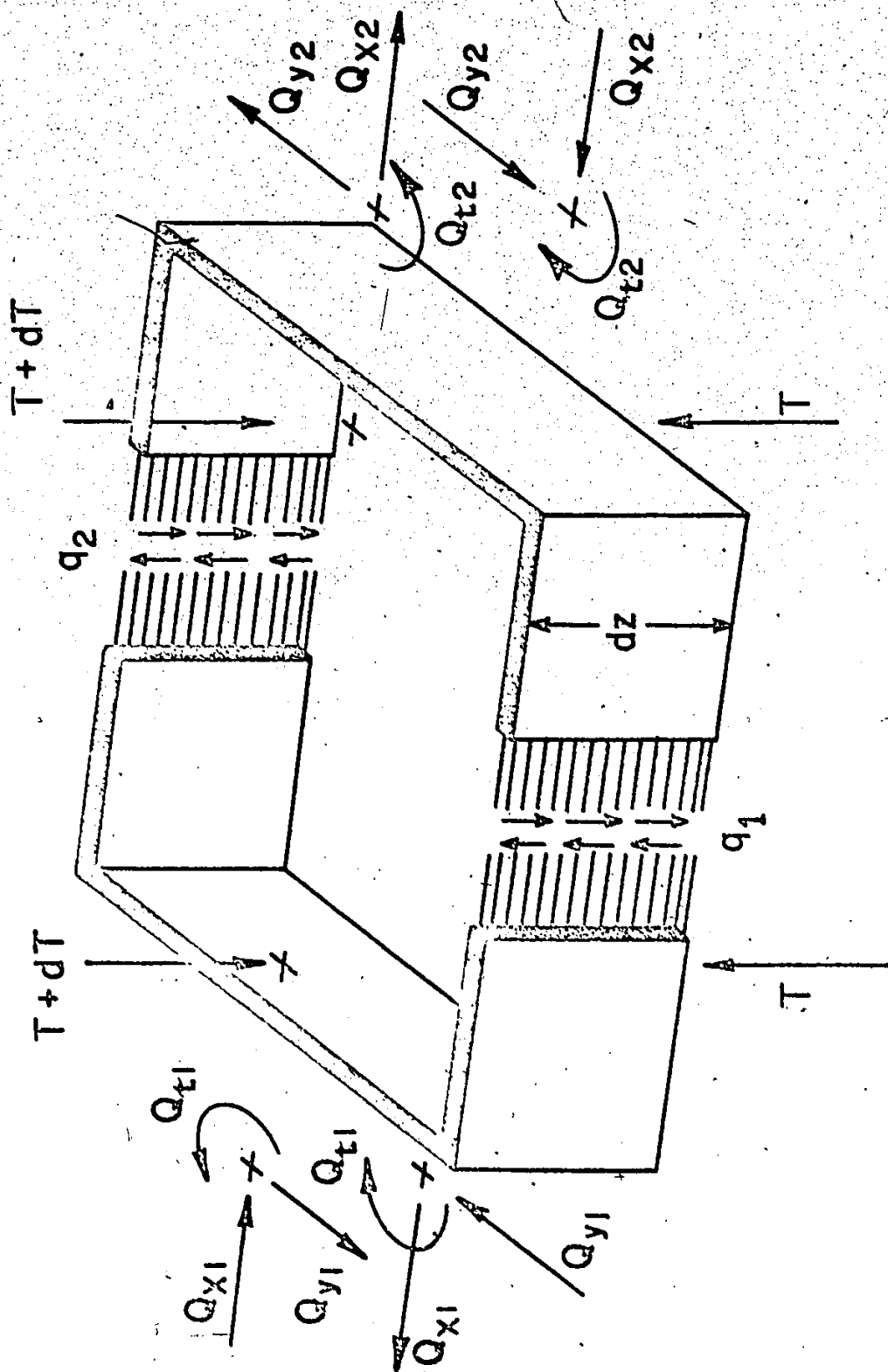
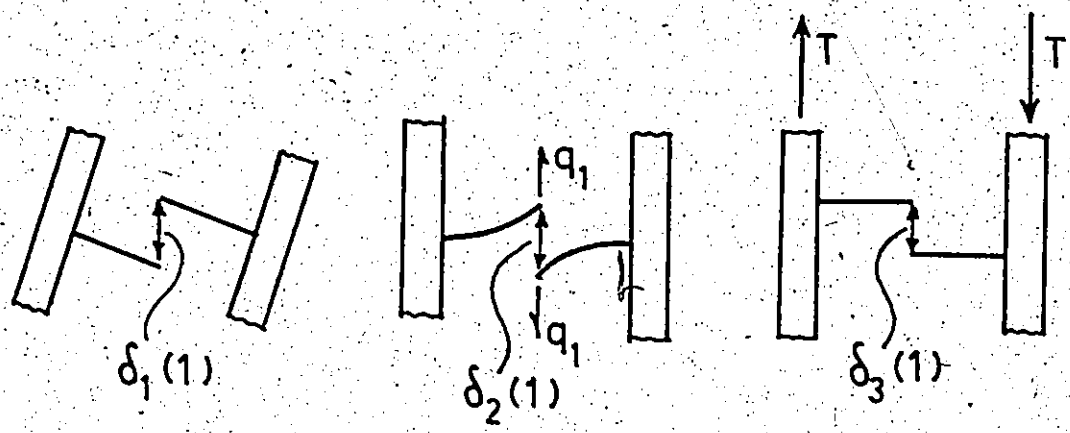


FIG. 2.4 SHEAR FORCES AND TORQUES DUE TO DISTRIBUTED SHEAR



(a) DUE TO LATERAL DISPLACEMENT OF THE SHEAR WALLS  $\delta_1(1)$   
 (b) DUE TO DEFORMATION OF THE LAMINAE  $q_1$   $\delta_2(1)$   
 (c) DUE TO AXIAL DEFORMATION OF THE SHEAR WALLS  $T$   $\delta_3(1)$

FIG. 2.5 RELATIVE DISPLACEMENTS AT THE CENTER OF CONNECTING LAMINAE 1

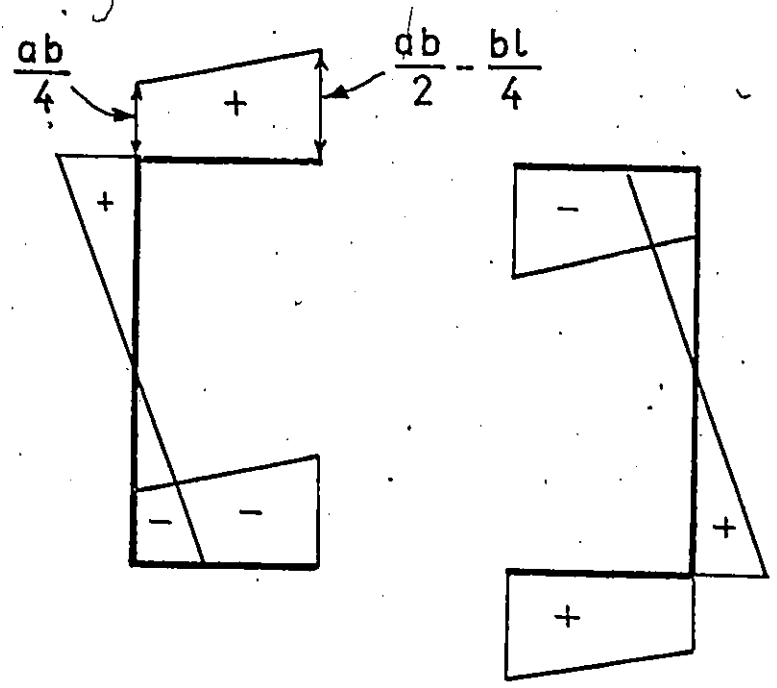


FIG. 2.6 WARPING STRESS DISTRIBUTION

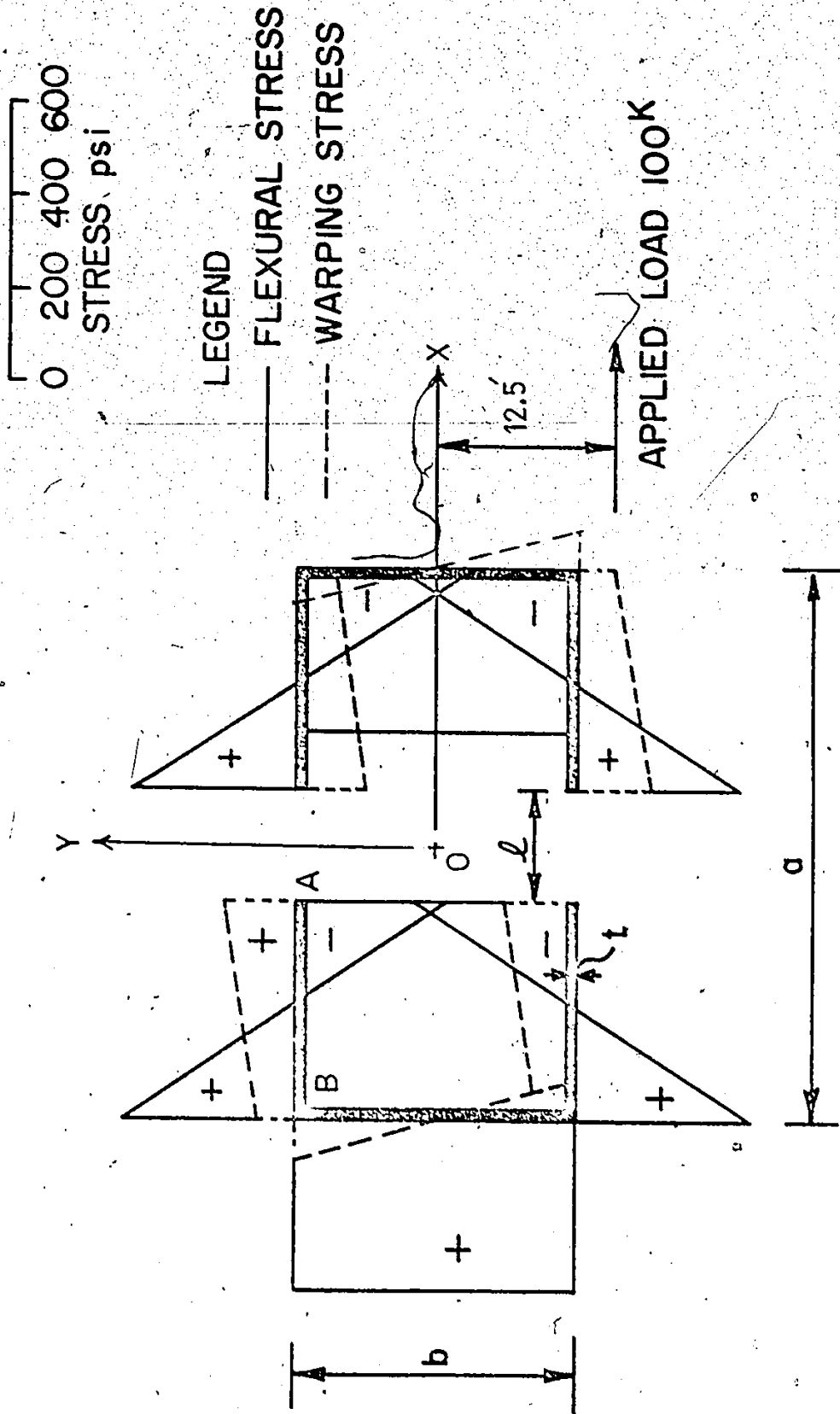


FIG. 2.7 COMPARISON OF STRESSES IN THE EXAMPLE CORE

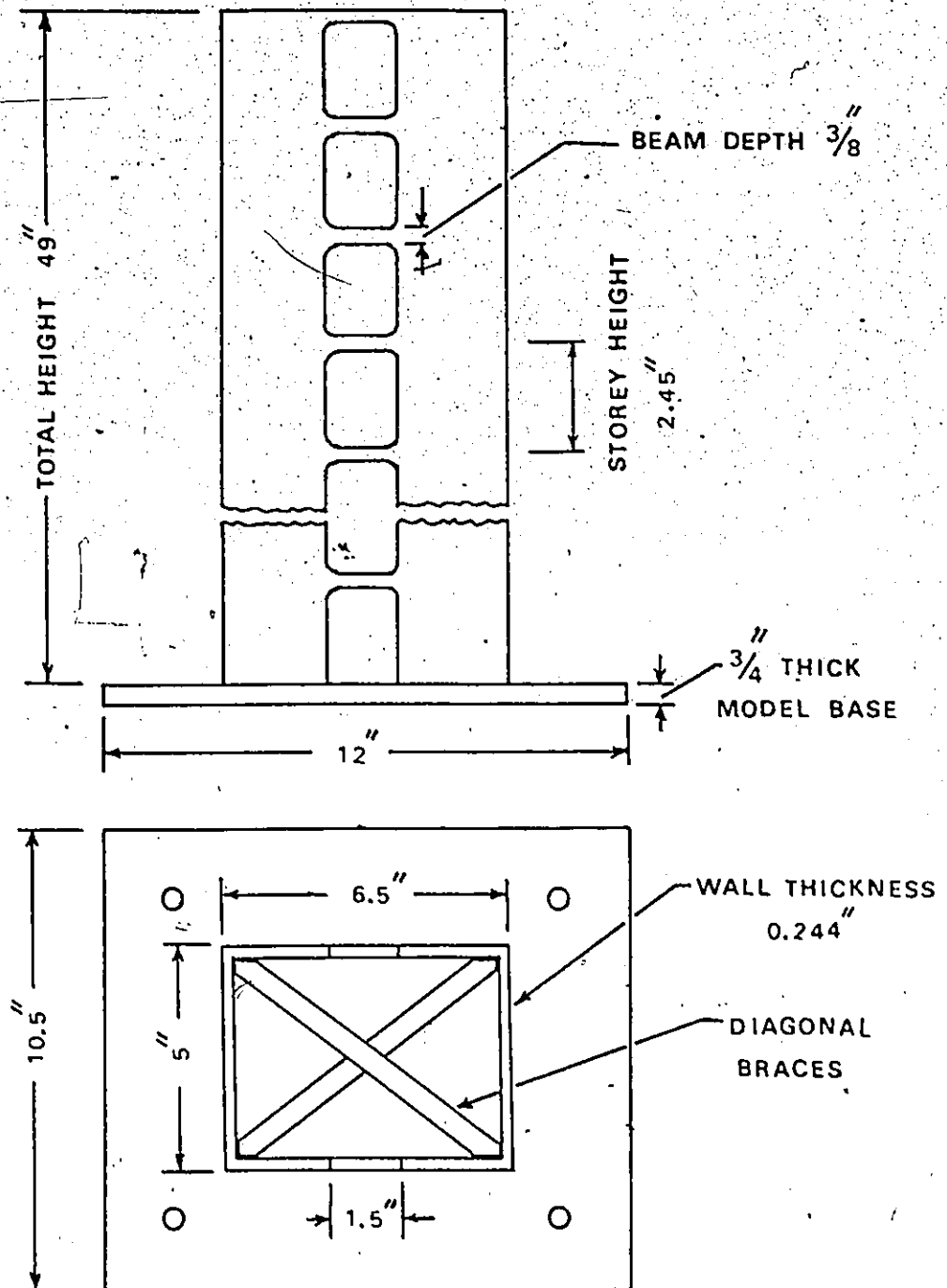


FIG. 2.8 EXPERIMENTAL MODEL

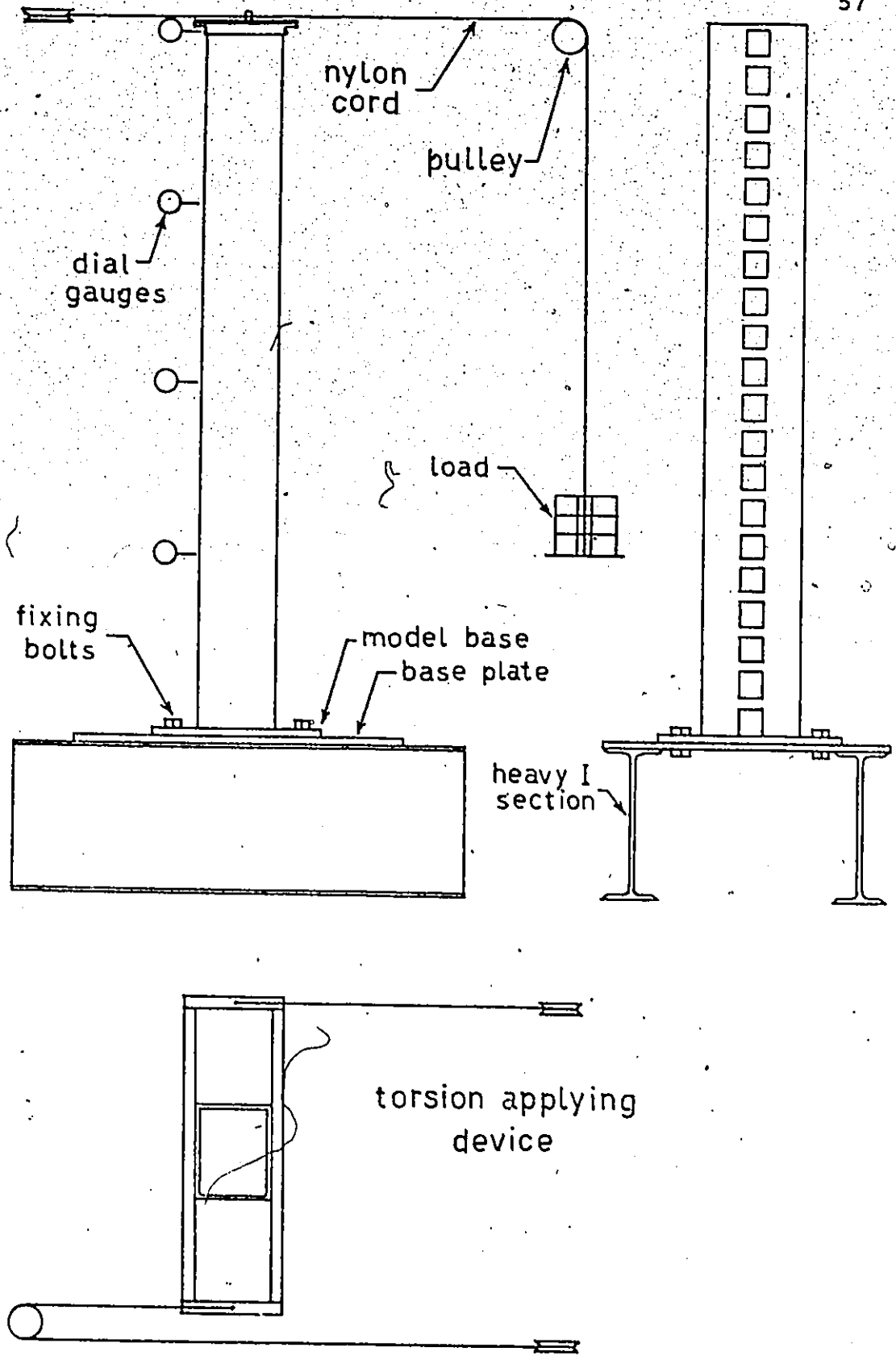
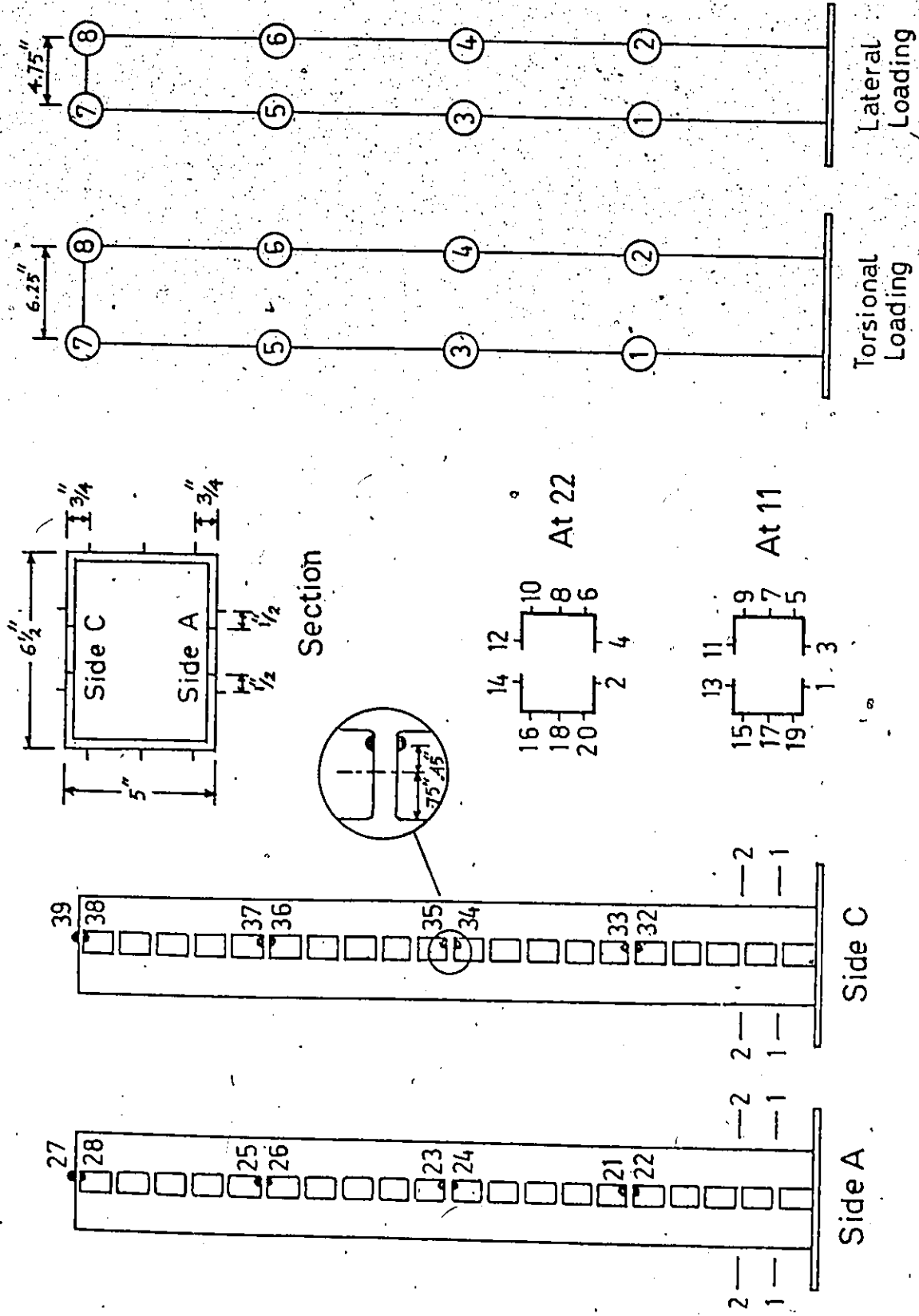


FIG. 2.9. EXPERIMENTAL SET UP

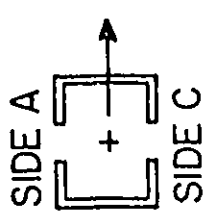
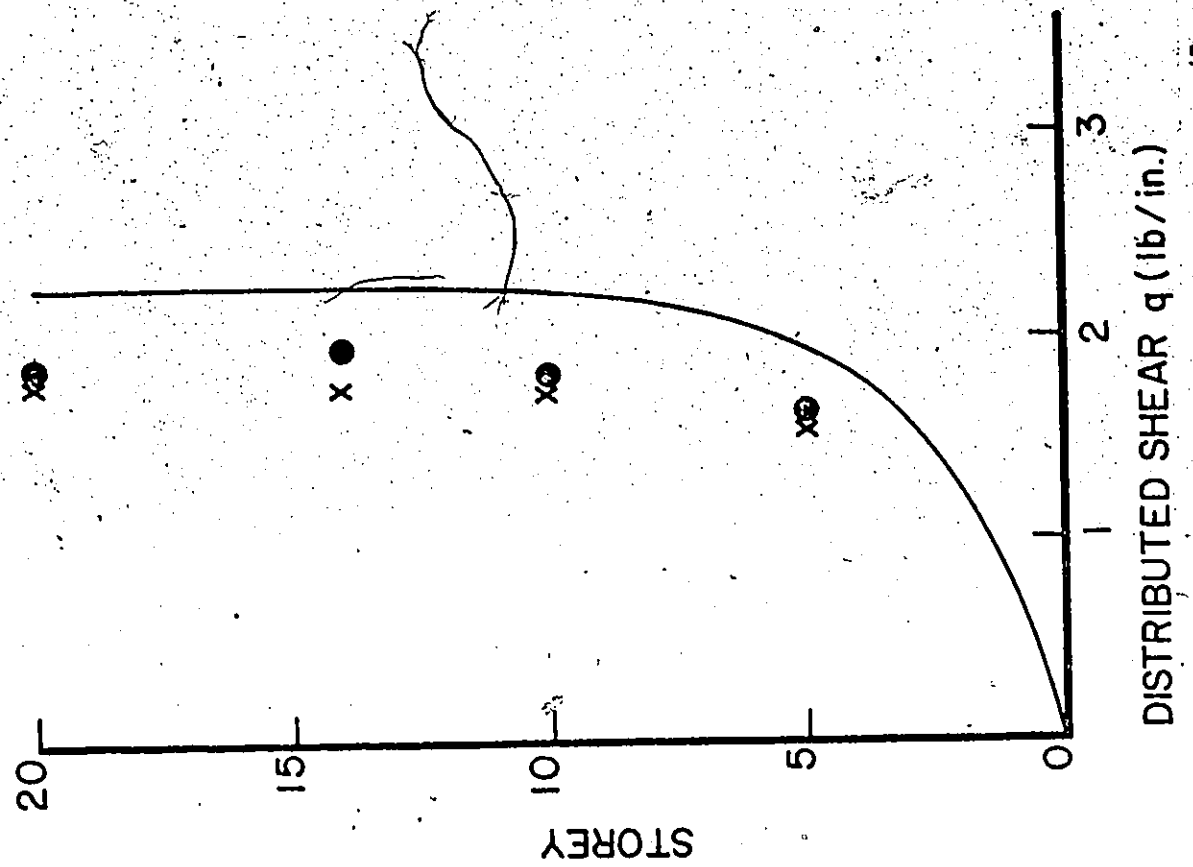




(a) STRAIN GAUGE POSITIONS

(b) DIAL GAUGE POSITIONS

FIG. 2.10



25 lb LOAD AT TOP

EXPERIMENT  
 ○ - SIDE A  
 x - SIDE C

THEORY

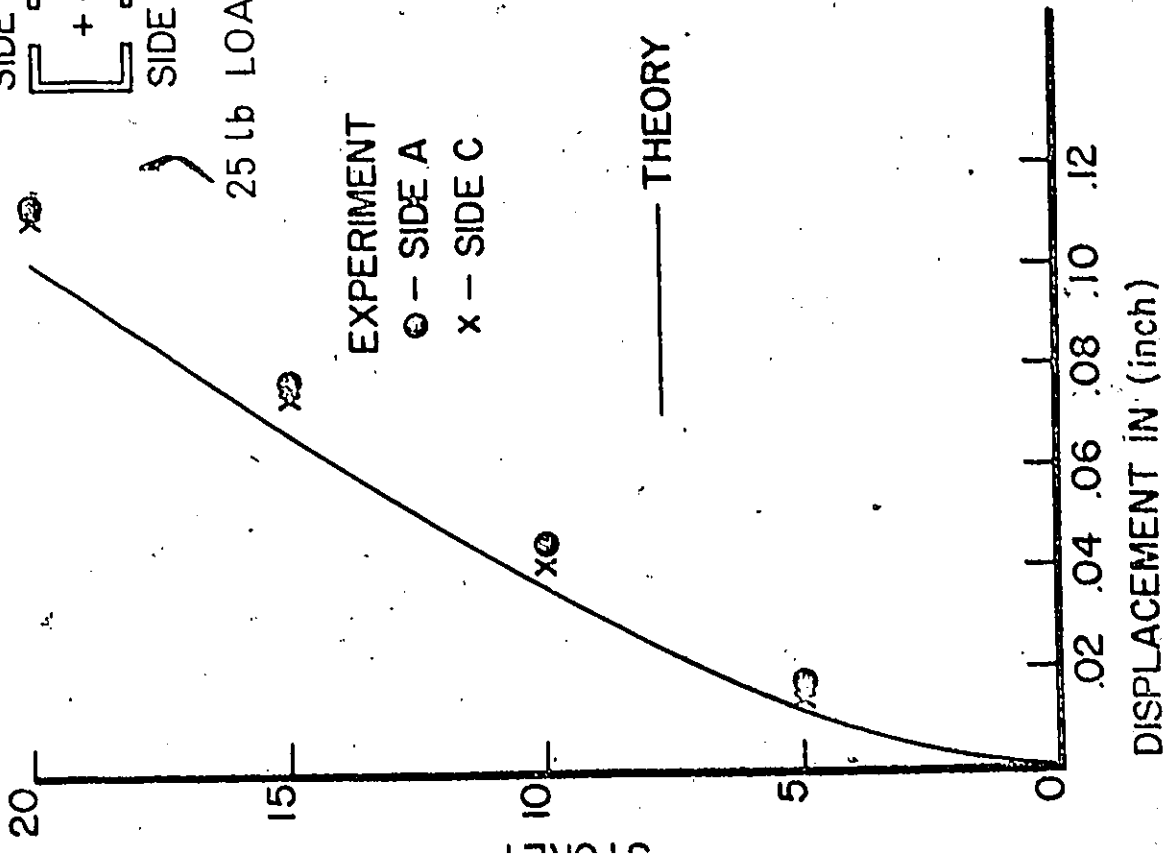


FIG. 2.11 LOAD TEST RESULTS

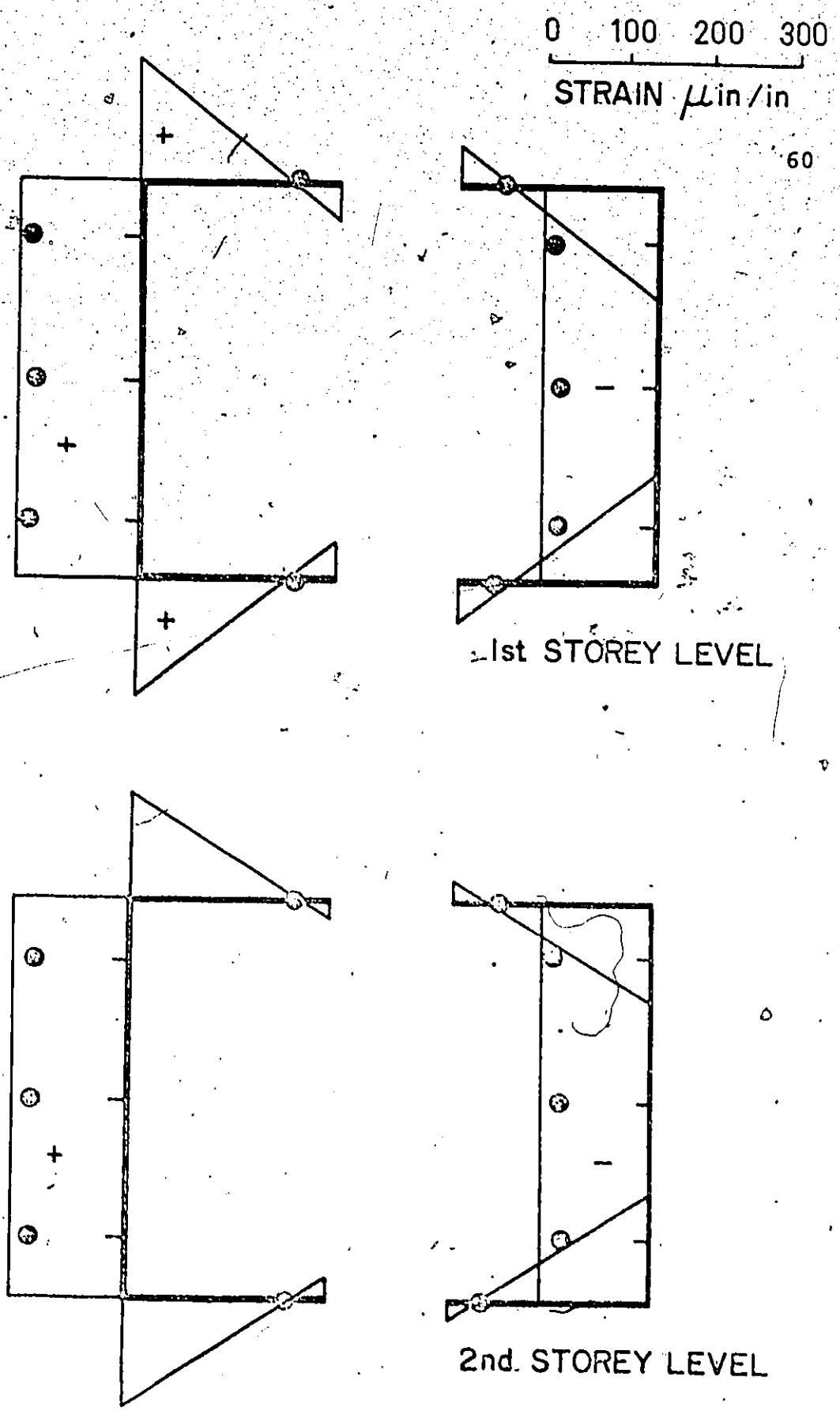


FIG. 2.12 AXIAL STRAIN DUE TO 251b LOAD

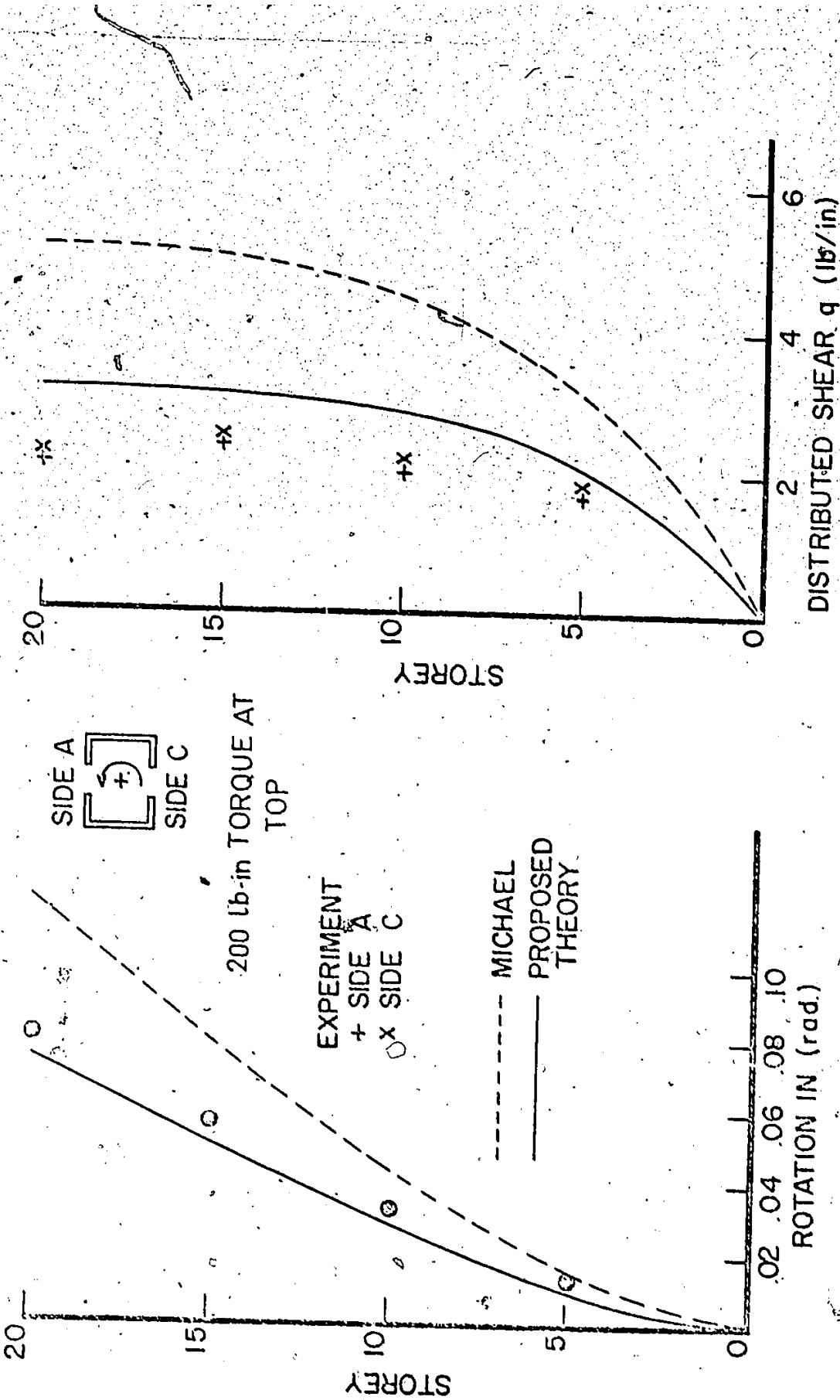
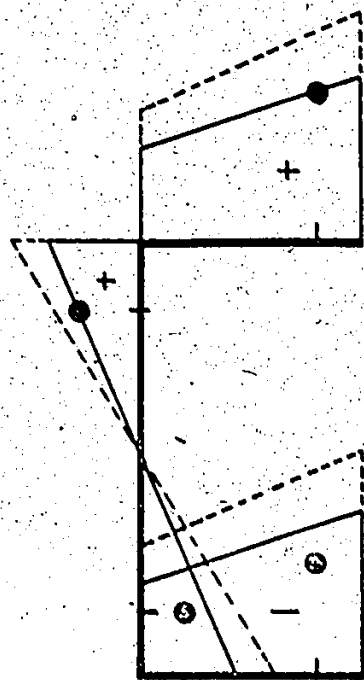
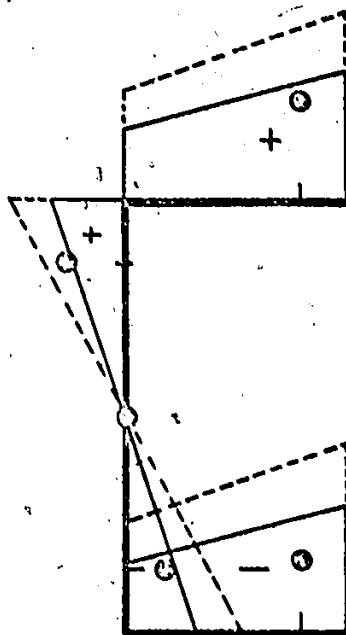


FIG. 213 LOAD TEST RESULTS

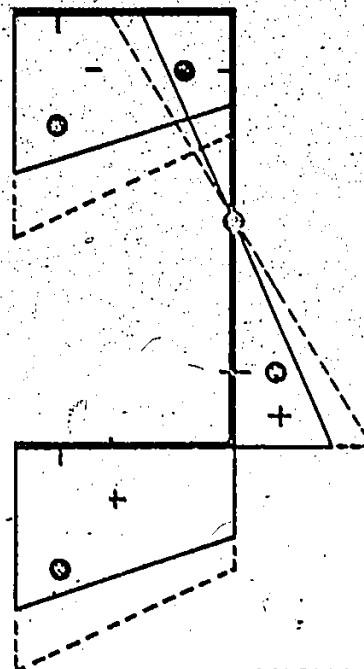


1st STOREY LEVEL



2nd STOREY LEVEL

0 100 200 300 62  
STRAIN  $\mu$  in/in



--- MICHAEL PROPOSED  
— PROPOSED

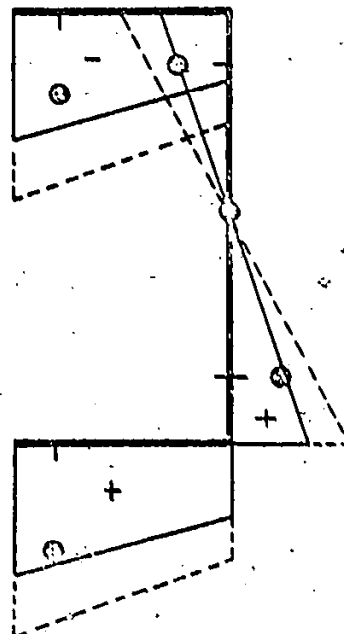


FIG. 2.14 AXIAL STRAIN DUE TO 200 lb-in TORQUE

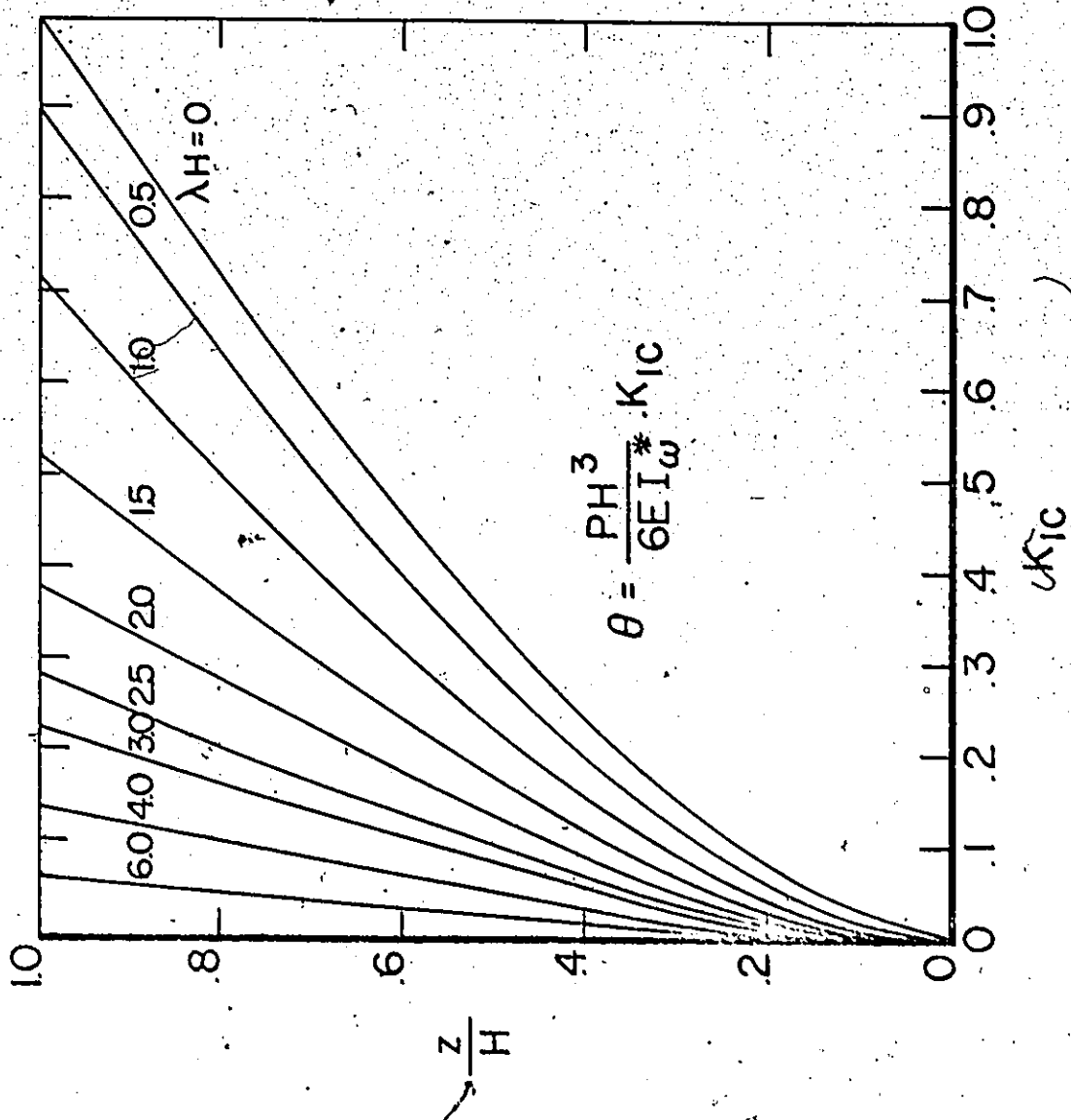


FIG. 2.15

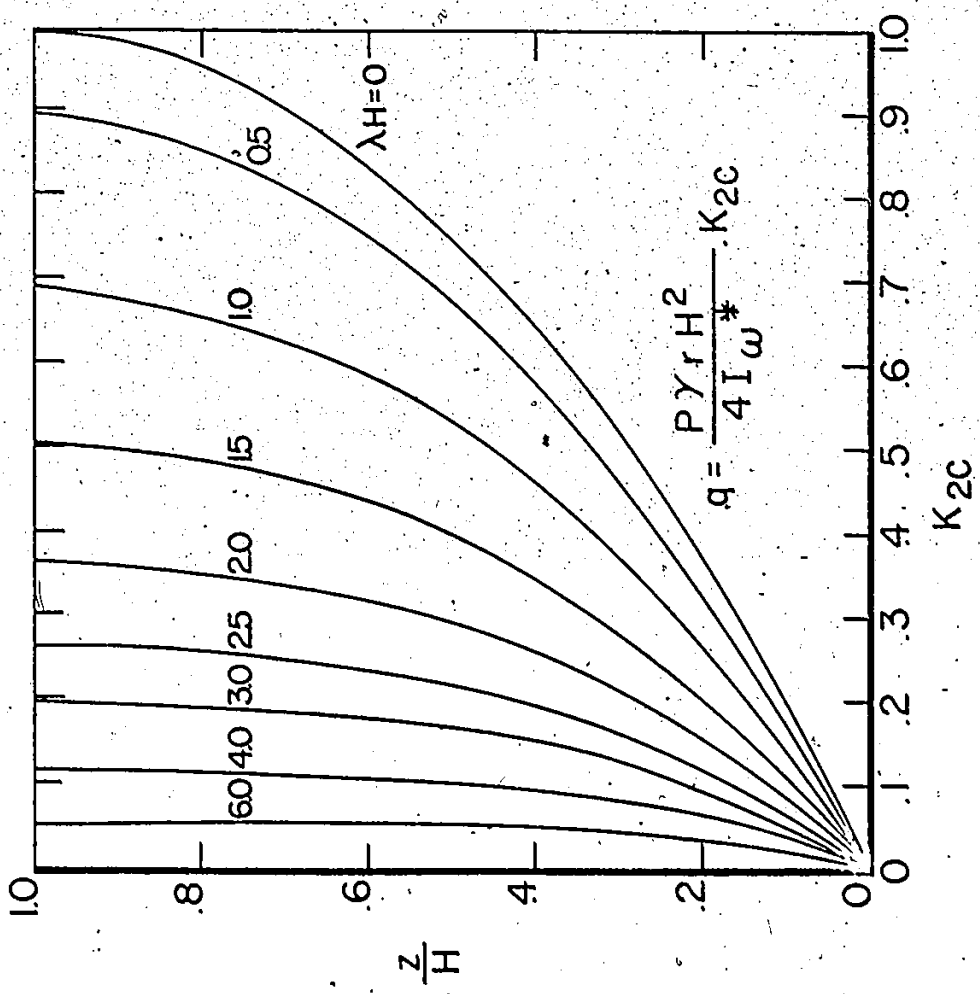


FIG. 2.16

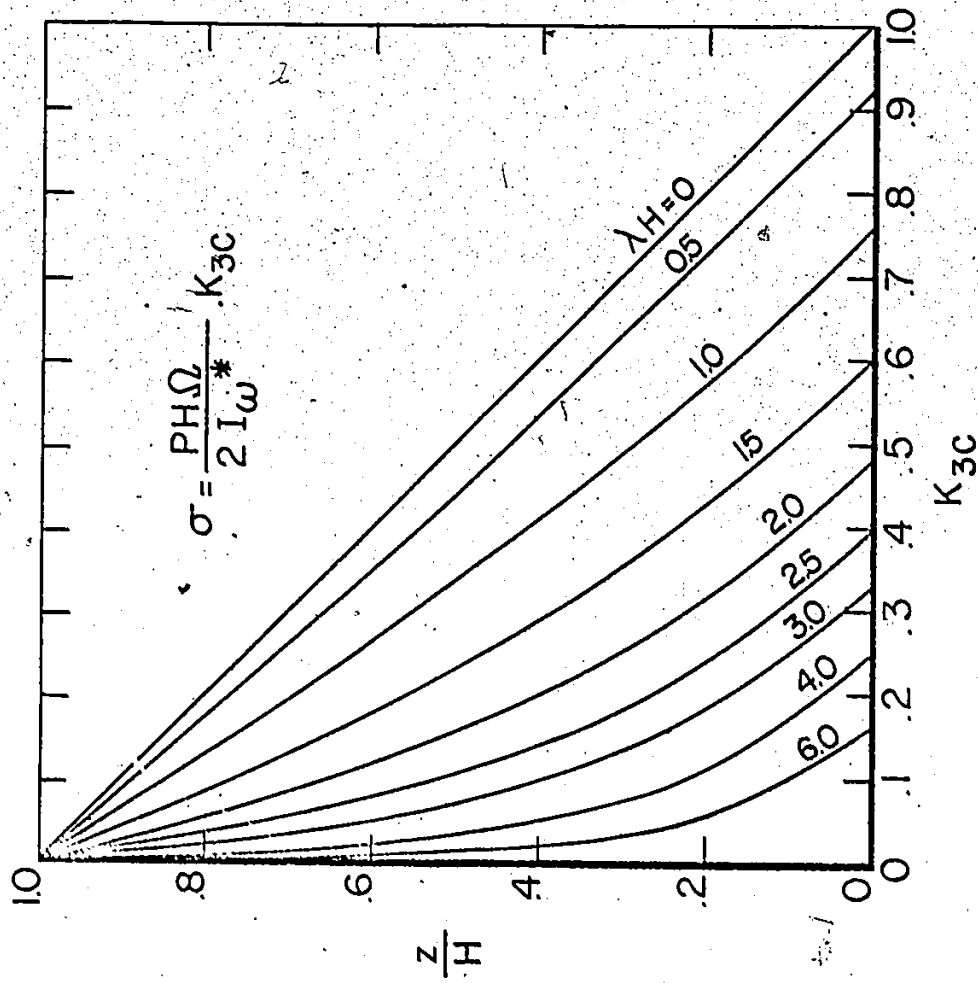


FIG. 2.17



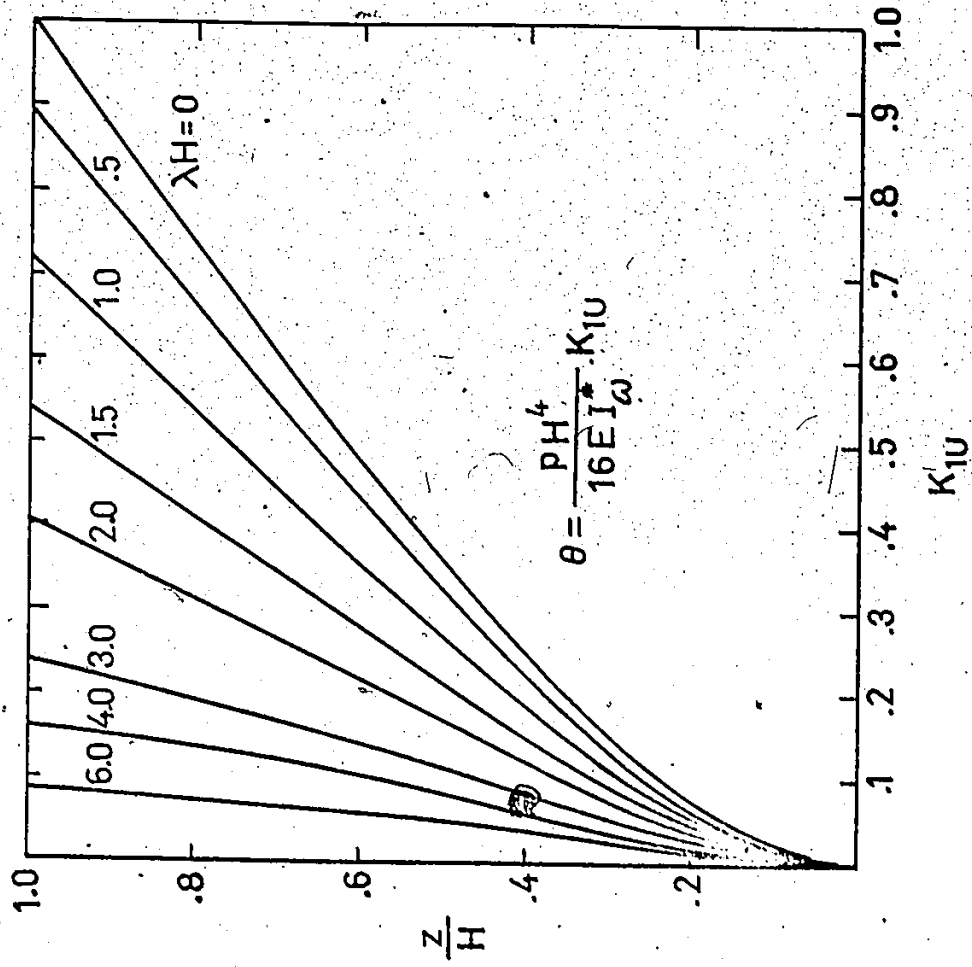


FIG. 2.18

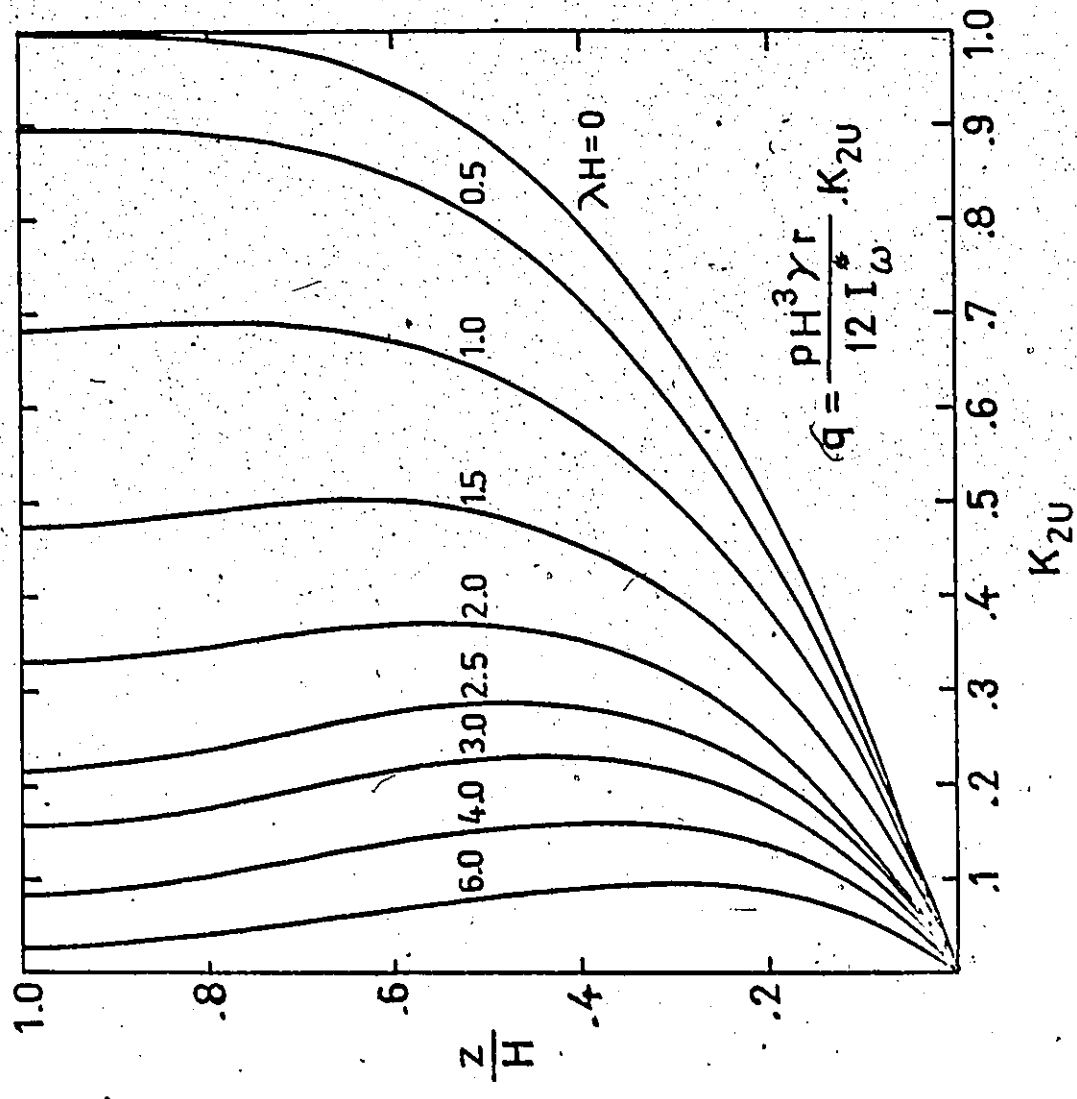


FIG. 2.19

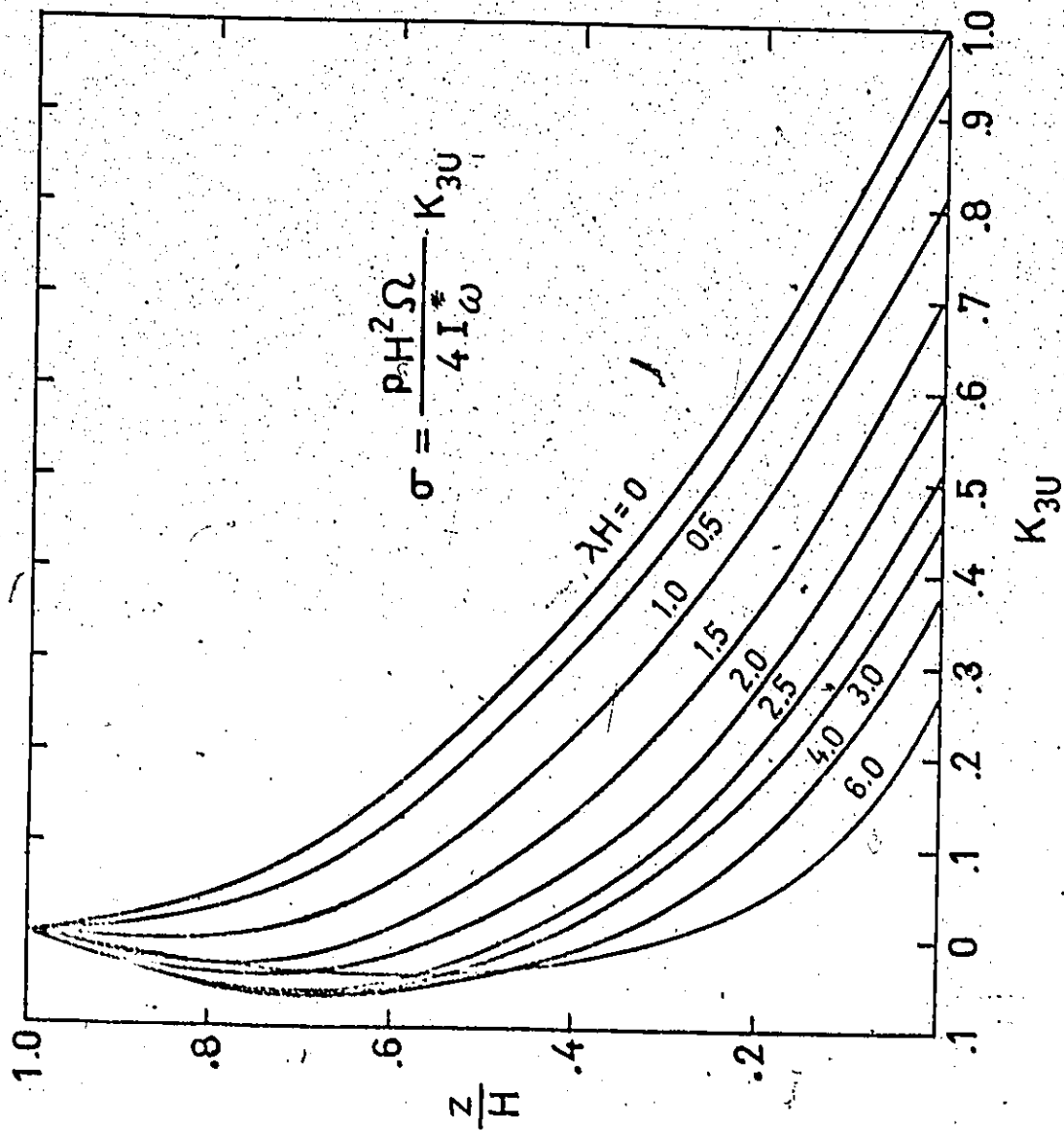


FIG. 2.20

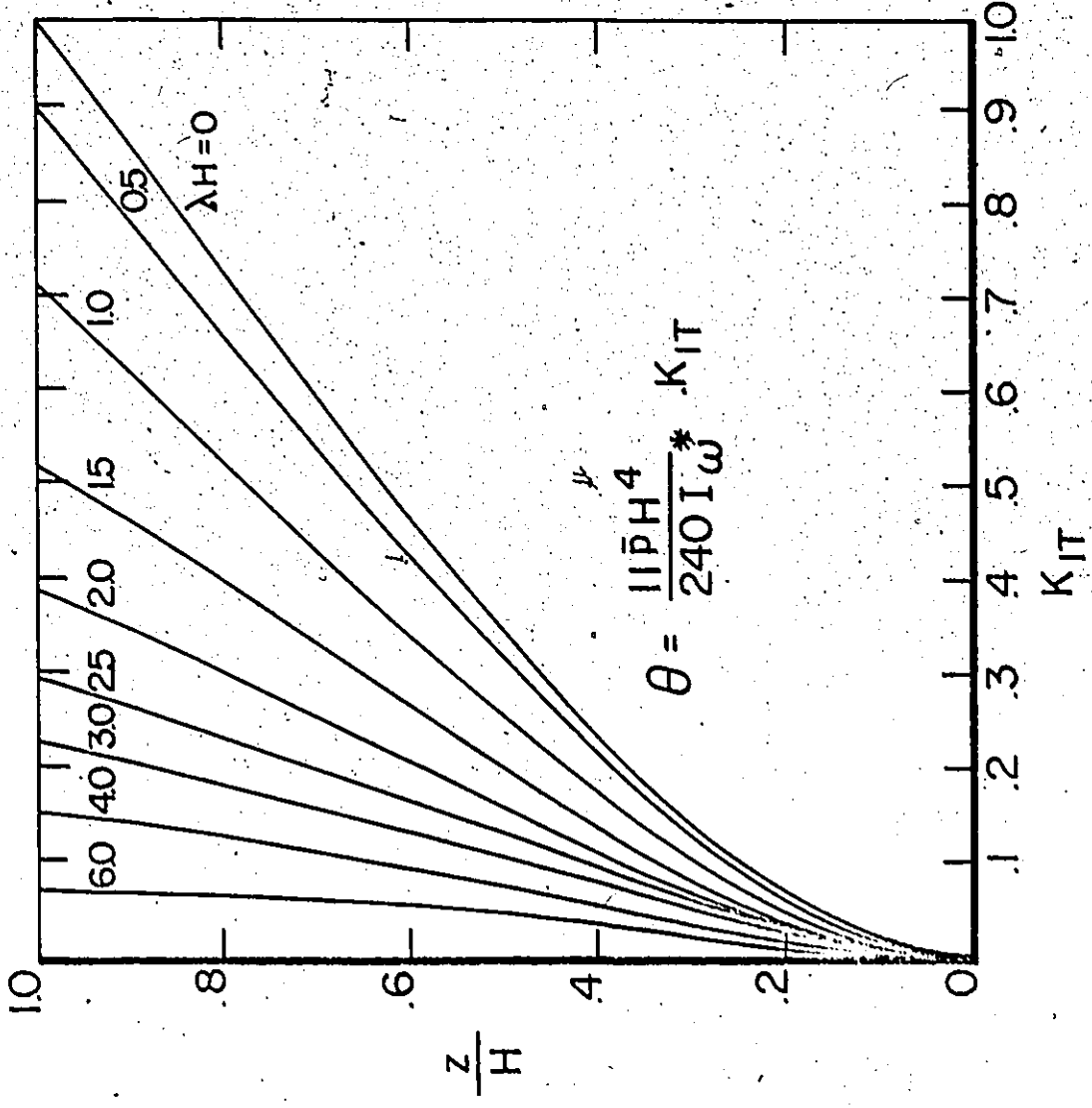


FIG. 2.21

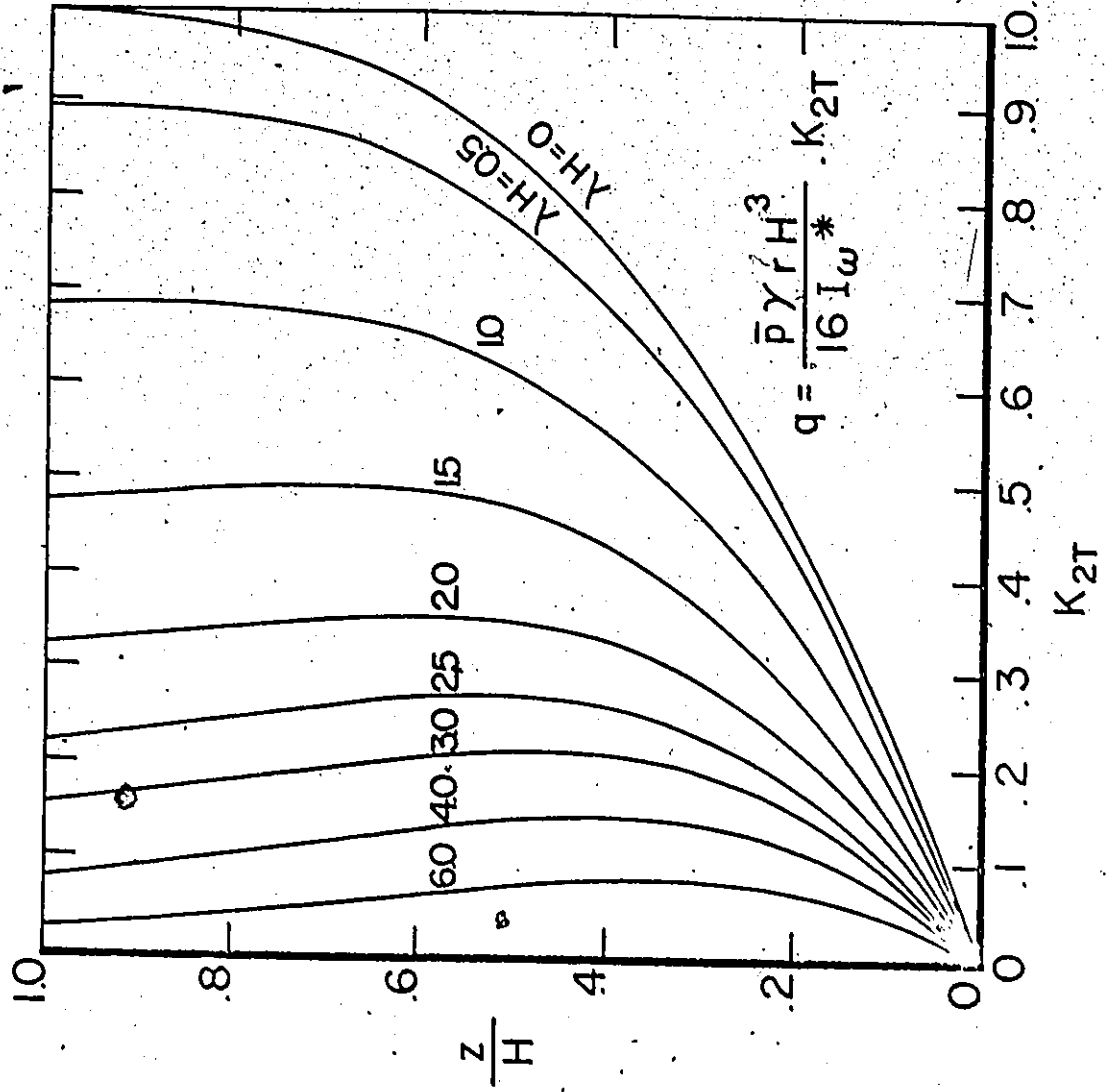


FIG. 2.22

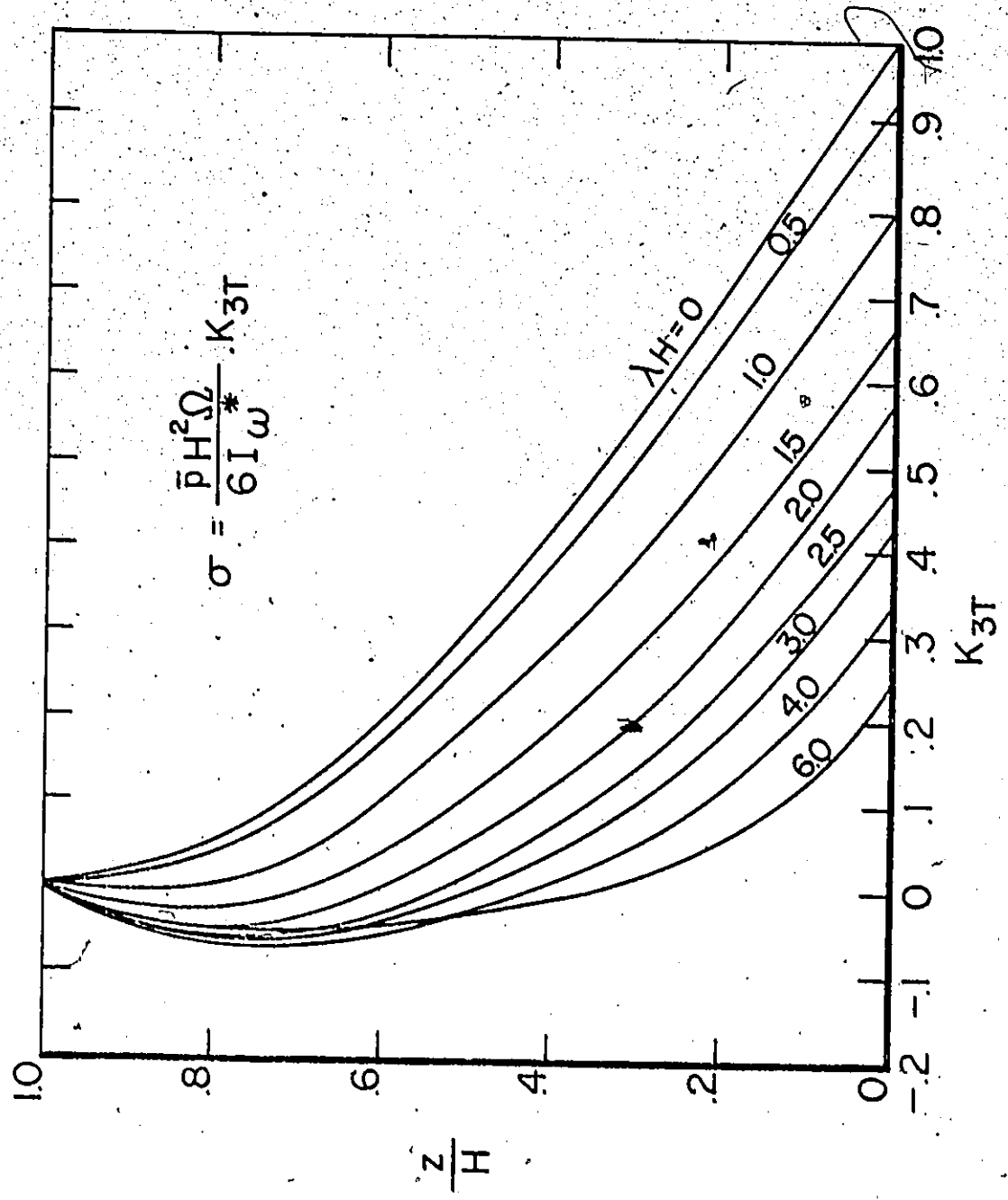


FIG. 2.23

## CHAPTER III

### THREE-DIMENSIONAL ANALYSIS OF UNIFORM SHEAR WALL STRUCTURES

#### 3.1 Introduction

Multi storey buildings often have floor plans with asymmetric layout of shear walls. In such cases the lateral load applied to the building will cause twisting in addition to translational deflection of the building. In such cases, a three-dimensional analysis of the structure will be necessary. The importance of the interaction of the shear walls with the floor slabs to resist lateral load has generally been recognised. Various approximations to take into account this interaction have been suggested by different investigators. In general the floor slabs are treated as rigid diaphragms with very high in-plane-stiffness. The out-of-plane stiffness of the floor slabs is neglected by Winokur and Gluck<sup>(83)</sup>. The floor slab is replaced by a number of connecting beams spanning between the shear walls by Gluck<sup>(29)</sup>, Coull and Irwin<sup>(21)</sup>, Heidebrecht and Swift<sup>(32)</sup> and many other researchers. A detailed study of the action of the floor slab is reported by Choudhury<sup>(12)</sup> and Taranath<sup>(70)</sup>

using the finite element formulation. Considerable computational effort is required in this approach which in turn would restrict its applications to relatively simple layout of building plan. It appears therefore, that a practical way to approximate the out-of-plane stiffness of the floor slab is to replace the floor slab with connecting beams with appropriate stiffnesses and at proper locations. Other than a few simple configurations of shear wall arrangement like cross wall structures<sup>(53)</sup> and core structures<sup>(48, 57)</sup>, very little study has been made to provide guidelines to determine the appropriate locations and the proper stiffness of the connecting beams. Recently, Rosman<sup>(59)</sup> and Gluck and Gellert<sup>(30)</sup> have presented formulations for a three-dimensional analysis of shear wall structures. Using the planar shear walls as basic elements, Rosman described the solution in terms of  $n$  force functions where  $n$  represents the total number of bands of connecting beams and the number of wall joints. Gluck and Gellert presented the problem in terms of  $m$  force functions where  $m$  indicates the number of bands of connecting beams. In both aforementioned cases, coupled differential equations in terms of the force functions are obtained. It is felt however that such formulations are inconvenient for general use since the number of unknown variables are dependent on the wall arrangement and connect-



ing beam pattern considered.

In this chapter, the general problem of three-dimensional analysis of shear wall structures is presented in terms of three displacement functions of the structure, namely, the horizontal displacements in two perpendicular directions and the rotation of the structure about a vertical axis. The theory of thin-walled beams of open section is used to describe the behaviour of the shear walls. The out-of-plane stiffness of the floor slab is approximated by connecting beams. No restrictions are placed on the shapes and number of the shear walls in the structure. Also, the locations of the connecting beams can be specified arbitrarily. A computer program based on the formulation is prepared. Two examples are solved and the results are compared with other existing methods of analysis. Based on the examples, some guidelines are given for choosing the locations and stiffnesses of the connecting beams to represent the out-of-plane stiffness of the floor slabs.

### 3.2 Notations

The following notations will be used in this chapter.

- |                              |  |
|------------------------------|--|
| $A_{bk}$                     | = Area of $k^{\text{th}}$ connecting beam of type 1.                                   |
| $A_{bi}$                     | = Area of $i^{\text{th}}$ connecting beam of type 2.                                   |
| $A_m$                        | = Cross-sectional area of wall $m$ .   |
| $[A]$                        | = Axial deformation matrix (Appendix C).   |
| $[B]$                        | = 3x3 Coefficient matrix of load vector.   |
| $E, G$                       | = Young's modulus and shear modulus of material respectively.                          |
| $h$                          | = Floor height.  |
| $H$                          | = Total height of structure.   |
| $I$                          | = No. of connecting beams of type 2.   |
| $I_{bk}$                     | = Moment of inertia of $k^{\text{th}}$ connecting beam of type 1.                      |
| $I_{bi}$                     | = Moment of inertia of $i^{\text{th}}$ connecting beam of type 2.                      |
| $\bar{I}_{xm}, \bar{I}_{ym}$ | = Principal moments of inertia of wall $m$ about $\bar{x}_m$ and $\bar{y}_m$ axes.     |
| $I_{xm}, I_{ym}, I_{xym}$    | = Moment of inertia and product of inertia of wall $m$ referred to global $X, Y$ axes. |
| $I_{xcm}, I_{ycm}$           | = Modified inertias of wall $m$ .  |
| $I_{\omega m}$               | = Sectorial inertia of wall $m$ .  |

$$I_{yy}^* = \sum_{m=1}^M I_{ym}.$$

$$I_{xx}^* = \sum_{m=1}^M I_{xm}.$$

$$I_{xy}^* = \sum_{m=1}^M I_{xym}.$$

$$I_{yc}^* = \sum_{m=1}^M I_{ycm}.$$

$$I_{xc}^* = \sum_{m=1}^M I_{xcm}.$$

$$I^* = \sum_{m=1}^M (I_{wm} + x_{cm}^2 I_{xm} + y_{cm}^2 I_{ym} - 2x_{cm} y_{cm} I_{xym})$$

$J_m$  = St. Venant's torsional stiffness of wall m.

$$J^* = \sum_{m=1}^M J_m$$

$K$  = No. of type 1 beams considered.

$[K_0]$  = Stiffness matrix of individual wall.

$[K_1]$  = Stiffness matrix for the contribution of the connecting beams.

$[K_2]$  = St. Venant's stiffness of individual shear walls.

$L_k$  = Clear span of  $k^{\text{th}}$  connecting beam of type 1.

$L_i$  = Clear span of  $i^{\text{th}}$  connecting beam of type 2.

- $(L)$  = Applied load vector =  $(-V_x, -V_y, -Q_t)$  col.
- $M$  = No. of shear walls.
- $M_{x0}$  = Component of overturning moment about x.
- $M_{y0}$  = Component of overturning moment about y.
- $(P_x, P_y, P_t)$  col. = Concentrated load vector acting at the top.
- $(\bar{P}_x, \bar{P}_y, \bar{P}_t)$  col. = Uniformly distributed load vector acting throughout the height
- $(\bar{\bar{P}}_x, \bar{\bar{P}}_y, \bar{\bar{P}}_t)$  col. = Triangularly distributed load vector having apex at the bottom.
- $Q_t$  = Applied torque.
- $q_k(z)$  = Distributed shear along  $k^{\text{th}}$  row of type 1 laminae.
- $\bar{q}_i(z)$  = Distributed shear along  $i^{\text{th}}$  row of type 2 laminae.
- $(q)$  =  $(q_1(z), q_2(z), \dots, q_k(z))$  col.
- $(\bar{q})$  =  $(\bar{q}_1(z), \bar{q}_2(z), \dots, \bar{q}_I(z))$  col.
- $r_{xk}, r_{yk}$  = Distance between the shear centers of walls connected by  $k^{\text{th}}$  beam in the X, Y direction respectively.
- $r_{ok}$  = Effective sectorial ordinate at the center of  $k^{\text{th}}$  beam.

- $[R]$  = Kx3 Lateral deformation matrix.  
 $T_m(z)$  = Axial force in wall m.  
 $V_x, V_y$  = Applied shear force in X and Y direction.  
 $\bar{X}_m, \bar{Y}_m$  = Direction of principal axes of wall m.  
 $X_{cm}, Y_{cm}$  = Co-ordinates of shear center of wall m.  
 $X_{em}, Y_{em}$  = Co-ordinates of centroid of wall m.  
 $\bar{X}_{cm}, \bar{Y}_{cm}$  = Distance of shear center of wall m from origin measured along  $\bar{X}_m$  and  $\bar{Y}_m$  directions.  
 $X_{bk}^y, Y_{bk}$  = Co-ordinate of center of  $k^{th}$  beam.  
 $\gamma_K$  = Stiffness of  $k^{th}$  row of type 1 laminae (equation 3.26a).  
 $\bar{\gamma}_j$  = Stiffness of  $j^{th}$  row of type 2 laminae (equation 3.28a).  
 $[r]$  = Diagonal flexibility matrix for type 1 laminae size KxK (equation 3.30a).  
 $[r]$  = Diagonal flexibility matrix for type 2 laminae size IxI (equation 3.31a).  
 $\{\Delta\}$  = Generalised displacement vector  
 $= \{\xi(z), \eta(z), \theta(z)\}_{col.}$   
 $\xi(z), \eta(z), \theta(z)$  = Horizontal displacement of the referred point in X and Y directions and rotation about oz axis.

$\epsilon_m, \eta_m, \theta_m$ 

= Horizontal displacement of the shear center of wall  $m$  in  $\bar{X}_m$  and  $\bar{Y}_m$  directions and rotation.

 $\phi_m$ 

= Angle between global axes  $X, Y$  and principal axes  $\bar{X}_m, \bar{Y}_m$  of wall  $m$ .

 $( )'$ 

= Derivative with respect to  $z$ .

### 3.3 Statement of the Problem

Let us consider a shear wall structure consisting of  $M$  shear walls resting on a rigid foundation. At every floor level, these shear walls are either connected by floor slabs and sometimes by beams. For flat slab constructions the effect of the floor slabs are represented by appropriately placed connecting beams of equivalent stiffness. In cases where the slabs are supported by beams, the effect of the slabs can be included in the beam stiffness by considering the beams as T shape or L shape beams. Let  $N$  be the number of connecting beams used to represent the slab in each floor. The beams can connect two different shear walls or two points of the same shear walls. A beam will be referred to as type 1 beam if it connects two different shear walls, and type 2 beam if it connects two points of the same shear wall. This distinction is necessary because of the difference in actions provided by these two types of beams. Of the total  $N$  beams considered, it is assumed that  $K$  beams are type 1 beams and  $I$  beams are type 2 beams so that  $N = K + I$ . The shear walls can have any open cross-sectional shapes. The locations and orientations of the shear walls and the connecting beams can be arbitrarily specified in plan. The structure with uniform stiffness

properties will be treated in this chapter. This implies the uniformity of the shear walls, even spacing of floors and constant beam stiffness and span length throughout the height of the structure.

The analysis is based on the following assumptions:

1. The rigid diaphragm action of the floors is assumed so that the whole structural assembly moves as a rigid body in the horizontal directions.
2. The proportion of the shear walls are such that the individual walls can be treated as thin-walled beams of open sections (81).
3. The out-of-plane stiffness of the floor slab is approximated by connecting beams of appropriate stiffness.
4. The discrete connecting beams are further replaced by a uniform distribution of independently acting laminae with equivalent stiffness properties throughout the height of the structure.
5. The mid-points of the connecting laminae are assumed to be points of contraflexure.
6. The walls and the beams are assumed to be linearly elastic.

Due to the diaphragm action provided by the floors, the structure has only three degrees of freedom in horizontal



movements. Referring to an arbitrary located global axes system  $O X Y Z$ , these degrees of freedom may be denoted as  $\xi(z)$ ,  $\eta(z)$  which are the displacements of point  $O$  in the  $X$  and  $Y$  directions, and a rotation of the structure  $\theta(z)$  about the  $OZ$  axis.  $\xi(z)$ ,  $\eta(z)$  and  $\theta(z)$  will be taken as the generalized displacement functions of the problem defining the deformation of the structure.

The figure (3.1) illustrates the geometry of a typical pair of shear walls with a row of type 1 connecting beams. The  $m^{\text{th}}$  and  $n^{\text{th}}$  wall ( $m < n$ ) are connected by the  $k^{\text{th}}$  row of type 1 connecting beams.

Referring to the global axes, the co-ordinates of the centroid  $G_m$  and the shear center  $S_m$  of the  $m^{\text{th}}$  wall are denoted by  $(X_{om}, Y_{om})$  and  $(X_{cm}, Y_{cm})$  respectively. The co-ordinate of the center of the  $k^{\text{th}}$  row of connecting beams are denoted by  $(X_{bk}, Y_{bk})$ . The principal directions of wall  $m$  make an angle  $\phi_m$  with the global axes. The geometry of a typical shear wall with a type 2 beam is illustrated in Figure (3.2). The  $i^{\text{th}}$  row of type 2 connecting beams is connected between points  $a$  and  $b$  of the  $j^{\text{th}}$  shear wall.

Before getting into the details of the mathematical development, it is useful to have an overall view of the method of attack. If imaginary cuts are made along the mid-points of each band of connecting laminae, the internal

shear forces at the mid-point will be exposed. Since there are  $N$  rows of connecting laminae,  $N$  force functions  $q_1(z) \dots \dots q_N(z)$  for the type 1 beams and  $\bar{q}_1(z) \dots \dots \bar{q}_N(z)$  for the type 2 beams are required to describe these shear forces. In addition, it is convenient to introduce  $M$  force functions  $T_1(z) \dots \dots T_M(z)$  to describe the axial forces in the  $M$  shear walls of the structure. Together with the three generalised displacement variables  $\xi(z)$ ,  $\eta(z)$  and  $\theta(z)$ , there are in general  $M+N+3$  unknown functions to be determined. The necessary equations for the determination of these unknown functions can be obtained from the following considerations.

(a) There are three overall equations of equilibrium corresponding to the force equilibrium in the two horizontal directions and a torque equilibrium equation about the vertical axis. (b) A relation can be obtained between the axial force functions  $T_j(z)$  and the distributed shear force functions  $q_i(z)$  by vertical equilibrium consideration of each individual shear wall. (c) Finally, a compatibility equation can be written for each band of connecting beams to ensure the deformations to either side of the imaginary cut are compatible. Therefore, one can obtain  $M+N+3$  equations for the determination of the unknowns. Subsequently, it is possible to eliminate the axial force functions and shear force functions and obtain differential equations in

the displacement variables. The detailed development of these equations are shown in the next section.

### 3.4.1 Equilibrium Conditions

The contribution of the  $m^{\text{th}}$  wall to the moment equilibrium condition in the Y direction consists of the bending moments in the two principal directions plus the axial force in the wall  $T_m$  acting along the line of centroids as shown in Figure (3.3). Resolving in the OY direction, the contribution of the  $m^{\text{th}}$  wall can be written as:

$$E\bar{I}_{ym} \cos\phi_m \xi_m'' - E\bar{I}_{xm} \sin\phi_m \eta_m'' - T_m X_{cm} \quad (3.1)$$

Where  $\bar{I}_{xm}$  and  $\bar{I}_{ym}$  are the principal moments of wall  $m$ . Based on the rigid diaphragm action of the floor slab the horizontal displacements and rotation along the principal directions of wall  $m$  are related to the global displacement functions by:

$$\begin{Bmatrix} \xi_m \\ \eta_m \\ \theta_m \end{Bmatrix} = \begin{bmatrix} \cos\phi_m & \sin\phi_m & -\bar{Y}_{cm} \\ -\sin\phi_m & \cos\phi_m & \bar{X}_{cm} \\ 0 & 0 & 1 \end{bmatrix} \begin{Bmatrix} \xi \\ \eta \\ \theta \end{Bmatrix} \quad (3.2)$$

Using the geometric relation in equation (3.2), the moment contribution of the  $m^{\text{th}}$  wall can be expressed as:

$$EI_{ym} \xi'' + EI_{xym} \eta'' - EI_{ycm} \theta'' - T_m X_{cm} \quad (3.3)$$

where  $I_{ym}$ ,  $I_{xm}$  and  $I_{xym}$  are moments of inertia and product of inertia of wall  $m$  in the global directions.  $I_{ycm}$  is defined by:

$$I_{ycm} = Y_{cm} I_{ym} - X_{cm} I_{xym} \quad (3.3a)$$

Prime denotes differentiation with respect to the  $z$  coordinate. Summing up all the contributions from the  $M$  shear walls, the moment equilibrium equation in the  $Y$  direction can be written as:

$$EI_{yy}^* \xi'' + EI_{xy}^* \eta'' - EI_{yc}^* \theta'' - \sum_{m=1}^M T_m X_{cm} = M_{y0} \quad (3.4)$$

where the superscript  $*$  denotes the summation of the respective quantities over all the shear walls.  $M_{y0}$  denotes the component of the applied overturning moment about the  $Y$  direction.

Similar consideration in the  $X$  direction leads to another moment equilibrium equation.

$$EI_{xy}^* \xi'' + EI_{xx}^* \eta'' + EI_{x0}^* \theta'' - \sum_{m=1}^M T_m Y_{cm} = M_{x0} \quad (3.5)$$

where  $M_{x0}$  denotes the component of the applied over turning moment about the X direction.  $I_{xcm}$  is defined as:

$$I_{xcm} = X_{cm} I_{xm} - Y_{cm} I_{xym} \quad (3.5a)$$

The internal torque offered by the structure consists of two parts. The first part arises due to the contribution from the shear walls. The second part comes from the contribution due to the bands of connecting laminae. The contribution of wall m to the torque is shown in Figure (3.4). The torque about an axis through O due to the shearing forces and individual torque acting on the wall m is given by:

$$- E\bar{I}_{\omega m} \theta_m'''' + E\bar{I}_{ym} \bar{Y}_{cm} \xi_m'''' - E\bar{I}_{xm} \bar{X}_{cm} \eta_m'''' \quad (3.6)$$

where  $\bar{I}_{\omega m}$  is the principal sectorial inertia of wall m and  $\bar{X}_{cm}$ ,  $\bar{Y}_{cm}$  are the distances of the shear center of wall m from O measured in the direction of its principal axes.

$\bar{X}_{cm}$  and  $\bar{Y}_{cm}$  can be expressed in terms of  $X_{cm}$  and  $Y_{cm}$  by the following rotation transformation.

$$\begin{Bmatrix} \bar{X}_{cm} \\ \bar{Y}_{cm} \end{Bmatrix} = \begin{bmatrix} \cos\phi_m & \sin\phi_m \\ -\sin\phi_m & \cos\phi_m \end{bmatrix} \begin{Bmatrix} X_{cm} \\ Y_{cm} \end{Bmatrix} \quad (3.7)$$

Using the geometric relations in equation (3.2, 3.7) the torque contribution from the wall  $m$  can be expressed as:

$$-EI_{\omega m} \theta'''' + EI_{y_{cm}} \xi'''' - EI_{x_{cm}} \eta'''' \quad (3.8)$$

where

$$I_{\omega m} = \bar{I}_{\omega m} + I_{x_{cm}} (X_{cm})^2 + I_{y_{cm}} (Y_{cm})^2 - 2I_{x_{cm}y_{cm}} (X_{cm})(Y_{cm}) \quad (3.8a)$$

In addition, the contribution of the St. Venant's torsional stiffness of the wall  $m$  is:

$$GJ_m \theta' \quad (3.9)$$

Therefore, the total torque from all the shear walls about  $O$  is given by:

$$Q_{tw} = EI_{y_{cm}}^* \xi'''' - EI_{x_{cm}}^* \eta'''' - EI_w^* \theta'''' + GJ^* \theta' \quad (3.10)$$

The torque contribution due to the rows of connecting laminae will resist a part of the applied torque. For that

reason let us consider the  $k^{\text{th}}$  row of type 1 connecting laminae. If an imaginary cut is made along the mid-points of this row of connecting laminae, a distribution of shear forces  $q_k(z)$  will be exposed. The convention of the sign of the distributed shear is such that  $q_k$  is positive if it acts upwards on wall  $m$  and downwards on wall  $n$  assuming  $m < n$ . No moment is acting along the imaginary cut since the cut is made to pass through points of contraflexure of the laminae. Shear forces and torques are developed on the  $m^{\text{th}}$  wall and  $n^{\text{th}}$  wall due to  $q_k(z)$ . The relation between the induced shear forces and torques in the walls and  $q_k$  can be obtained by the equilibrium consideration of an elemental section of the walls  $dz$  in height, as shown in Figure (3.5). Considering the equilibrium of moments in wall  $m$  in the  $\bar{X}_m$  and  $\bar{Y}_m$  directions, there is obtained:

$$Q_{xkm} = q_k \left[ (X_{bk} - X_{om}) \cos \phi_m + (Y_{bk} - Y_{om}) \sin \phi_m \right] \quad (3.11a)$$

$$Q_{ykm} = q_k \left[ -(X_{bk} - X_{om}) \sin \phi_m + (Y_{bk} - Y_{om}) \cos \phi_m \right] \quad (3.11b)$$

Similar considerations applied to wall  $n$  will give:

$$Q_{xkn} = -q_k \left[ (X_{bk} - X_{on}) \cos \phi_n + (Y_{bk} - Y_{on}) \sin \phi_n \right] \quad (3.12a)$$

$$Q_{ykn} = -q_k \left[ -(X_{bk} - X_{en}) \sin \phi_n + (Y_{bk} - Y_{en}) \cos \phi_n \right] \quad (3.12b)$$

In addition, the distributed shear  $q_k$  causes bimoments on walls  $m$  and  $n$ . The rate of change of these bimoments gives rise to flexural twists  $Q_{tkm}$  and  $Q_{tkn}$ .

$$Q_{tkm} = q_k \omega_{km} \quad (3.13a)$$

$$Q_{tkn} = -q_k \omega_{kn} \quad (3.13b)$$

Where  $\omega_{km}$  and  $\omega_{kn}$  are sectorial co-ordinates at the mid-point of the connecting laminae  $k$  calculated treating wall  $m$  and wall  $n$  as thin-walled sections respectively. The resultant torque due to these forces about the origin  $O$  is given by:

$$Q_{tbk} = r_{\theta k} q_k \quad (3.14)$$

where

$$\begin{aligned} r_{\theta k} = & X_{cm} (Y_{bk} - Y_{en}) - Y_{cm} (X_{bk} - X_{en}) \\ & - X_{cn} (Y_{bk} - Y_{en}) + Y_{cn} (X_{bk} - X_{en}) \\ & + \omega_{km} - \omega_{kn} \end{aligned} \quad (3.14a)$$



Special treatment is necessary for the type 2 connecting laminae since they connect points in the same shear wall. Let us consider the  $i^{\text{th}}$  row of type 2 connecting laminae as shown in Figure (3.2). If an imaginary cut is made along the mid-point of this row of laminae, a distribution of shear forces  $\bar{q}_i(z)$  will be exposed. Proceeding as before, the torque contribution due to the  $i^{\text{th}}$  row of laminae can be expressed as:

$$Q_{tsi} = \bar{r}_{\theta i} \bar{q}_i \quad (3.15)$$

$$\text{where: } \bar{r}_{\theta i} = \omega_{ia} - \omega_{ib} \quad (3.15a)$$

Therefore, the total contribution to the internal torque  $Q_{tb}$  due to  $K$  rows of type 1 and  $I$  rows of type 2 connecting laminae is obtained by the summation of terms in equation (3.14, 3.15). Therefore:

$$Q_{tb} = \sum_{k=1}^K r_{\theta k} q_k + \sum_{i=1}^I \bar{r}_{\theta i} \bar{q}_i$$

The torque equilibrium of the overall structure requires the internal torque due to the shear walls and the rows of connecting laminae equal to the externally applied torque  $Q_t$ . Therefore:

$$\begin{aligned}
 EI_{yC}^* \xi'''' - EI_{xC}^* \eta'''' - EI_{\omega}^* \theta'''' + GJ^* \theta' \\
 + \sum_{i=1}^I \bar{r}_{\theta i} \bar{q}_i + \sum_{k=1}^K r_{\theta k} q_k = Q_t
 \end{aligned}
 \tag{3.17}$$

Equations (3.4, 3.5 and 3.17) are the three overall equations of lateral equilibrium.

The vertical force in the individual wall can be related to the shear forces  $q_k(z)$ . From a consideration of the vertical equilibrium of each individual wall, it can be shown that:

$$T_m(z) = \sum_k^{C_m} S_k \int_z^H q_k(s) ds
 \tag{3.18}$$

$$(m = 1, 2, \dots, M)$$

where:  $\sum_k^{C_m}$  indicates the summation on  $k$  is taken over all laminae that are connected to the wall  $m$ . The sign convention for  $T_m$  is such that it is positive when it produces tension on wall  $m$ . Therefore, the value  $S_k$  is +1 when  $q_k$  produces tension on wall  $m$  and -1 when it produces compression.

Using equation (3.18) it can be shown that the following relationships hold.

$$\sum_{m=1}^M T_m X_{em} = - \sum_{k=1}^K r_{xk} \int_z^H q_k(s) ds \quad (3.19)$$

$$\sum_{m=1}^M T_m Y_{em} = - \sum_{k=1}^K r_{yk} \int_z^H q_k(s) ds \quad (3.20)$$

Eliminating  $T_m$  by equations (3.19 and 3.20) and differentiating equations (3.4 and 3.5) there is obtained:

$$\begin{aligned} EI_{yy}^* \xi'''' + EI_{xy}^* \eta'''' - EI_{yc}^* \theta'''' - \sum_{k=1}^K r_{xk} q_k \\ = -V_x \end{aligned} \quad (3.21)$$

$$\begin{aligned} EI_{xy}^* \xi'''' + EI_{xx}^* \eta'''' + EI_{xc}^* \theta'''' - \sum_{k=1}^K r_{yk} q_k \\ = -V_y \end{aligned} \quad (3.22)$$

where  $V_x$  and  $V_y$  are applied shear forces in the global X and Y directions, and  $r_{xk} \equiv X_{en} - X_{em}$  = distance between the shear centers of walls m and n in the X direction and  $r_{yk} \equiv Y_{en} - Y_{em}$  = distance between the shear centers in the Y direction.

### 3.4.2 Compatibility Conditions

Equations (3.17, 3.21 and 3.22) provides three equations of equilibrium. The total number of unknowns to be evaluated is  $N+3$ . Therefore, the structural system is statically indeterminate of the order  $N$ .  $N$  additional conditions are obtained from the compatibility of deformations along the imaginary cuts.

In the study of equilibrium conditions, imaginary cuts are made along the mid-points of the rows of connecting laminae, exposing the distributed shears. It is necessary to ensure that in any band of laminae, the displacement of the laminae on both sides of the cut are compatible. There are three contributions to the displacement of the laminae at the cut. First, the relative displacement to the left and the right of the cut exists due to the deflections and rotations of the walls to which the laminae are connected.

Considering the typical  $k^{\text{th}}$  row of type 1 connecting laminae connected to the  $m^{\text{th}}$  and  $n^{\text{th}}$  wall, this relative displacement at the cut can be found using Vlasov's thin-walled beam theory. Expressing it in terms of the generalized displacement functions,

$$(\delta_1)_k = r_{xk} \xi' + r_{yk} \eta' + r_{\theta k} \theta' \quad (3.23)$$

The second source contributing to the relative displacement is due to the axial deformation of the walls. This can be written as:

$$(\delta_2)_k = \int_0^z \frac{T_m(s)}{EA_m} ds - \int_0^z \frac{T_n(s)}{EA_n} ds \quad (3.24)$$

Finally, relative displacement exists due to the deformation of the laminae. This can be written as:

$$(\delta_3)_k = \frac{q_k}{E\gamma_k} \quad (3.25)$$

where 
$$\gamma_k = \frac{12I_{bk}}{hl_k^3 \left(1 + \frac{12EI_{bk}}{l_k^2 G A_{bk}}\right)} \quad (3.26)$$

= equivalent stiffness of the  $k^{\text{th}}$  row of type 1 connecting laminae.

Compatibility condition requires:

$$(\delta_1)_k - (\delta_2)_k - (\delta_3)_k = 0$$

Therefore, the compatibility conditions for the type 1 laminae can be expressed as:

$$r_{xk} \xi' + r_{yk} \eta' + r_{\theta k} \theta' - \int_0^z \frac{T_m(s)}{EA_m} ds - \quad (3.27)$$

$$- \int_0^z \frac{T_n(s)}{EA_n} ds - \frac{q_k}{EY_k} = 0 \quad (k = 1, 2, \dots, K)$$

The compatibility conditions for the type 2 connecting laminae will now be considered. Let us consider a typical  $i^{\text{th}}$  row of type 2 connecting laminae. These laminae are connected between points in the same shear wall. Therefore, the distributed shear forces in type 2 laminae do not induce any axial force in the shear walls. Also, these laminae provide restraint to the rotation of the shear wall only. Therefore, the compatibility conditions for these laminae do not contain any terms resulting from the axial deformation nor the lateral deflection of the shear wall. Proceeding in the same manner as the type 1 connecting laminae, the compatibility conditions for the type 2 connecting laminae can be expressed as:

$$\bar{r}_{\theta i} \theta' - \frac{\bar{q}_i}{E\bar{Y}_i} = 0 \quad (i = 1, 2, \dots, I) \quad (3.28)$$

$$\text{Where: } \bar{Y}_i = \frac{12\bar{I}_{bi}}{h\ell_i^3 (1 + 12E\bar{I}_{bi}/\ell_i^2 GA_{bi})} \quad (3.28a)$$

= Equivalent stiffness of the  $i^{\text{th}}$  row of type 2 connecting laminae.

The equations (3.27 and 3.28) represent a set of  $N$  compatibility conditions. Together with the equilibrium conditions (3.17, 3.21 and 3.22) there are  $N+3$  equations for the unknowns  $\xi(z)$ ,  $\eta(z)$ ,  $\theta(z)$ ,  $q_k(z)$  ( $k=1,2,\dots,K$ ) and  $\bar{q}_1(z)$  ( $i=1,2,\dots,I$ ).

### 3.5 Reduction of Governing Equations and Solution

The governing equations (3.17, 3.21, 3.22, 3.27 and 3.28) can be further simplified to a set of three differential equations in terms of the generalised displacement variables  $\xi(z)$ ,  $\eta(z)$  and  $\theta(z)$ . For that reason, it is convenient to write the equations in matrix form. The equilibrium equations (3.17, 3.21 and 3.22) can be written in the following matrix form.

$$[K_0]\{\Delta\}'''' - [K_S]\{\Delta\}' - [R]^T\{q\} - [\bar{R}]^T\{\bar{q}\} = \{L\} \quad (3.29)$$

where

$$[K_0] = E \begin{bmatrix} I_{yy}^* & I_{xy}^* & -I_{yc}^* \\ & I_{xx}^* & I_{xc}^* \\ \text{(Symmetric)} & & I_{\omega}^* \end{bmatrix} \quad (3.29a)$$

$$[K_s] = E \begin{bmatrix} 0 & 0 & 0 \\ 0 & 0 & 0 \\ 0 & 0 & J^* \end{bmatrix} \quad (3.29b)$$

$$[R]^T = \begin{bmatrix} r_{x1} & r_{x2} & \dots & r_{xk} \\ r_{y1} & r_{y2} & \dots & r_{yk} \\ r_{\theta 1} & r_{\theta 2} & \dots & r_{\theta k} \end{bmatrix} \quad (3.29c)$$

$$[\bar{R}]^T = \begin{bmatrix} 0 & 0 & \dots & 0 \\ 0 & 0 & \dots & 0 \\ \bar{r}_{\theta 1} & \bar{r}_{\theta 2} & \dots & \bar{r}_{\theta I} \end{bmatrix} \quad (3.29d)$$

$$\{L\} = \text{loading vector} = \{-V_x, -V_y, -Q_t\} \text{ col.} \quad (3.29e)$$

\(\Delta\) = Generalised displacement vector

$$= \{\xi(z), \eta(z), \theta(z)\} \text{ col.} \quad (3.29f)$$

$$\{q\} = \{q_1(z), q_2(z), \dots, q_k(z)\} \text{ col.} \quad (3.29g)$$

$$\{\bar{q}\} = \{\bar{q}_1(z), \bar{q}_2(z), \dots, \bar{q}_I(z)\} \text{ col.} \quad (3.29h)$$

$V_x$  and  $V_y$  are the applied shear forces in the global X and Y directions respectively and  $Q_t$  is the applied torque.

Eliminating  $T_m$  using equation (3.18), the compatibility conditions (3.27 and 3.28) can be written in the following form.



$$[R]\{\Delta\}'''' + [A]\{q\} - [r]\{q\}'' = 0 \quad (3.30)$$

$$[\bar{R}]\{\Delta\}' - [r]\{\bar{q}\} = 0 \quad (3.31)$$

where

$$[r] = \frac{1}{E} \begin{bmatrix} 1/\gamma_1 & & 0 \\ & 1/\gamma_2 & \\ & 0 & 1/\gamma_K \end{bmatrix} \quad (3.30a)$$

$$[\bar{r}] = \frac{1}{E} \begin{bmatrix} 1/\bar{\gamma}_1 & & 0 \\ & 1/\bar{\gamma}_2 & \\ & 0 & 1/\bar{\gamma}_I \end{bmatrix} \quad (3.31a)$$

$[A]$  is a symmetrical matrix. The element  $a_{ij}$  in matrix  $[A]$  expresses the contribution to the relative deflection of the laminae along the  $i^{\text{th}}$  cut due to the influence of distributed shear  $q_j$ . Therefore, the matrix  $[A]$  depends on the connecting pattern of the beams to the walls. The rule to obtain elements in matrix  $[A]$  is given in Appendix C.

Eliminating  $\{\bar{q}\}$  from equation (3.29) with the help of equation (3.31) there is obtained:

$$[K_0] \{\Delta\}'''' - [\bar{K}_s] \{\Delta\}' - [R]^T \{q\} = \{L\} \quad (3.32)$$

where: 
$$[\bar{K}_s] = [K_s + \bar{R} \Gamma^{-1} \bar{R}] \quad (3.32a)$$

The elimination of  $\{q\}$  between equations (3.30) and (3.32) is difficult because  $[R]^T$  is a rectangular matrix. To overcome this difficulty, a new vector  $\{e\}$  of size  $2 \times 1$  is defined by the following relation.

$$\{q\} = [\Gamma]^{-1} [R] \{e\} \quad (3.33)$$

The equation (3.32) then becomes:

$$\begin{aligned} \{e\} &= [R^T \Gamma^{-1} R]^{-1} [K_0] \{\Delta\}'''' - [R^T \Gamma^{-1} R]^{-1} [\bar{K}_s] \{\Delta\}' \\ &\quad - [R^T \Gamma^{-1} R]^{-1} \{L\} \end{aligned} \quad (3.34)$$

The equation (3.30) is converted to:

$$[R] \{e\}'' = [A \Gamma^{-1} R] \{e\} + [R] \{\Delta\}'' \quad (3.35)$$

Elimination of  $\{e\}$  between equations (3.34) and (3.35) results in

$$[K_0] \{\Delta\}'''' - [K_1] \{\Delta\}'''' + [K_2] \{\Delta\}' = \{L\}'' - [B] \{L\} \quad (3.36)$$

where:

$$[K_1] = [R]^T [\Gamma]^{-1} [A\Gamma^{-1}R] [R^T\Gamma^{-1}R]^{-1} [K_0] + [R]^T [\Gamma]^{-1} [R] \quad (3.36a)$$

$$[K_2] = [R]^T [\Gamma]^{-1} [A\Gamma^{-1}R] [R^T\Gamma^{-1}R]^{-1} [\bar{K}_B] \quad (3.36b)$$

$$[B] = [R]^T [\Gamma]^{-1} [A\Gamma^{-1}R] [R^T\Gamma^{-1}R]^{-1} \quad (3.36c)$$

It should be pointed out that the elimination scheme as outlined is possible for structures having three or more rows of type 1 beams (i.e.,  $K > 3$ ). The scheme does not work when the structure has two or one row of connecting beams of type 1 because the matrix  $[R^T\Gamma^{-1}R]$  becomes singular. Physically, if a structure has two or one row of connecting laminae, two or one function would be sufficient to describe the behaviour of the structure. Therefore, using three displacement functions to describe the structural system as in equation (3.36) becomes redundant. For a structure having two rows of connecting beams of type 1, the differential equations can be reduced into two equations. A derivation of the equations and solution for such cases is included in Appendix D. For structure with one row of connecting beam only, the problem further reduces to the case of a nonplanar coupled shear wall system<sup>(74, 4)</sup>.

Normally the elements of the matrix  $[K_2]$  are small compared with that of other matrices. Their contribution to the final results is insignificant and these terms can be neglected. The equation (3.36) then becomes:

$$[K_0]\{\Delta\}^V - [K_1]\{\Delta\}'''' = \{L\}'' - [B]\{L\} \quad (3.37)$$

Equation (3.37) is a 3 by 3 matrix equation with constant co-efficients. The solution of this equation consists of a homogeneous solution  $\{\Delta_H\}$  and a particular solution  $\{\Delta_P\}$ . The homogeneous solution can be written as:

$$\{\Delta_H\} = \sum_{j=1}^3 [C_j \cdot \text{Cosh} \lambda_j z \{U_j\} + S_j \cdot \text{Sinh} \lambda_j z \{U_j\}] - \begin{bmatrix} d_{11} & d_{12} & d_{13} \\ d_{21} & d_{22} & d_{23} \\ d_{31} & d_{32} & d_{33} \end{bmatrix} \begin{Bmatrix} 1 \\ z \\ z^2 \end{Bmatrix} \quad (3.38)$$

Where:  $C_j, S_j$  ( $j=1,2,3$ ) and the elements  $d_{ij}$  ( $i=1,\dots,3, j=1,\dots,3$ ) are fifteen arbitrary constants to be determined from the boundary conditions.  $\lambda_j^2$  ( $j=1,2,3$ ) are the eigen-values of the characteristic equation

$$|\lambda^2 I - K_0^{-1} K_1| = 0 \quad (3.39)$$

In this case,  $\lambda_j^2$  ( $j=1,2,3$ ) are all positive and  $\lambda_j$  is taken as the positive root of  $\lambda_j^2$ .  $U_j$  ( $j=1,2,3$ ) is the eigenvector associated with the eigen-value  $\lambda_j$ .

The common loading cases in design consideration are (i) a concentrated load at the top, (ii) a uniformly distributed load and (iii) a triangularly distributed load. For these loading cases, the particular solution can be written in the following form:

$$\{\Delta_p\} = [P] \begin{Bmatrix} z^3 \\ z^4 \\ z^5 \end{Bmatrix} \quad (3.40)$$

where  $[P]$  is a 3 by 3 matrix and its elements depend on the applied loading. The elements of the matrix  $[P]$  for a combined action of a concentrated load, a uniformly distributed load and a triangularly distributed load are as follows:

$$[P] = [P_1 \mid P_2 \mid P_3] \quad (3.40a)$$

$$\{P_3\} = [K_1]^{-1} [B] \begin{Bmatrix} \bar{p}_x \\ \bar{p}_y \\ \bar{p}_t \end{Bmatrix} \frac{1}{120H} \quad (3.40b)$$

$$\{P_2\} = [K_1]^{-1} [B] \begin{Bmatrix} p_x \\ p_y \\ p_t \end{Bmatrix} \frac{1}{24} \quad (3.40c)$$

$$\{P_1\} = [K_1]^{-1} [K_0] \{P_3\} 20 - \frac{1}{6} \begin{Bmatrix} \bar{p}_x \\ \bar{p}_y \\ \bar{p}_t \end{Bmatrix} \frac{1}{H} - \frac{1}{6} [B] \begin{Bmatrix} P_x + p_x H + \bar{p}_x H/2 \\ P_y + p_y H + \bar{p}_y H/2 \\ P_t + p_t H + \bar{p}_t H/2 \end{Bmatrix} \quad (3.40d)$$

Where  $P_x$ ,  $P_y$  and  $P_t$  are the concentrated load in the X and Y directions and torque applied at the top respectively.

$p_x$ ,  $p_y$  and  $p_t$  are the intensities of the uniformly distributed load in the X and Y directions and torque respectively.

$\bar{p}_x$ ,  $\bar{p}_y$  and  $\bar{p}_t$  are the top intensities of the triangularly distributed load in the X and Y directions and torque respectively.

The complete solution of the differential equation (3.37) is given by:

$$\{\Delta\} = \{\Delta_H\} + \{\Delta_p\} \quad (3.41)$$

The constants of integration are determined from the boundary conditions. For a building resting on a rigid foundation, the following boundary conditions apply:

- (a) There is no displacement at the base.

$$\{\Delta\} = 0 \quad \text{at} \quad z = 0 \quad (3.42a)$$

- (b) There is no slope and warping is not permitted at the base.

$$\{\Delta\}' = 0 \quad \text{at} \quad z = 0 \quad (3.42b)$$

- (c) There is no moment, bimoment and axial force at the top.

$$\{\Delta\}'' = 0 \quad \text{at} \quad z = H \quad (3.42c)$$

- (d) The distributed shear forces in the connecting laminae vanishes at the base according to equations (3.27, and 3.28). This condition when substituted in equation (3.29) yields:

$$[K_0] \{\Delta\}''' = \{L\} \quad \text{at} \quad z = 0 \quad (3.42d)$$

- (e) The first derivative of the distributed shear forces in the connecting laminae vanishes at the top. This is obtained by differentiating equations (3.27 and 3.28) and substituting  $z = H$ . The above condition when substituted in the differentiated form of equation (3.29) yields the following relation.

$$[K_0] \{\Delta\}^{iv} = \{L\}' \quad \text{at} \quad z = H \quad (3.42e)$$

After determining the generalised displacement vector  $\{\Delta\}$ , the necessary force functions are determined from substitution. The distributed shear forces in the connecting laminae can be determined from the following relations:

$$\begin{aligned} \{q\} = & [\Gamma]^{-1} [R] [R^T \Gamma^{-1} R]^{-1} [K_O] \{\Delta\} \\ & - [\Gamma]^{-1} [R] [R^T \Gamma^{-1} R]^{-1} [\bar{K}_S] \{\Delta\} \\ & - [\Gamma]^{-1} [R] [R^T \Gamma^{-1} R] \{L\} \end{aligned} \quad (3.43)$$

$$\{\bar{q}\} = [\bar{\Gamma}]^{-1} [\bar{R}] \{\Delta\} \quad (3.44)$$

The axial forces in the shear walls can be determined using the following relation:

$$T_m(z) = \sum_k^{C_m} S_k \int_z^H q_k(s) ds \quad (3.18)$$

The displacements  $\xi_m$ ,  $\eta_m$  and  $\theta_m$  at the shear center of the  $m^{\text{th}}$  shear walls are determined using equation (3.2). Then the axial stress at any point in the  $m^{\text{th}}$  shear wall can be determined from the relation:

$$\sigma = \frac{T_m}{A_m} - E(\xi_m'' \bar{X} + \eta_m'' \bar{Y} + \theta_m'' \bar{\omega}) \quad (3.45)$$



Where  $\bar{X}$  and  $\bar{Y}$  are the co-ordinates of the particular point with respect to the principal axes of the  $m^{\text{th}}$  shear wall and  $\bar{\omega}$  is the sectorial co-ordinate of the particular point.

A computer programme based on the above formulation is prepared. This programme can be used to determine the distributed shear forces in the connecting beams, the axial forces, the normal stress distribution and the displacements of the shear walls due to the three cases of applied loadings.

### 3.6 Examples and Discussion of Results

Two examples are worked out using the proposed method of analysis. The first example is a fifteen storey perspex structure which has been analysed by Taranath<sup>(70)</sup> using a different method of analysis. The reason for taking this example is to test the accuracy of the proposed method by comparing the results obtained by both methods. The second example is a thirty storey cross-shaped building with a centrally located core formed by concrete shear walls. The shear walls are interconnected by means of connecting beams. The purpose for taking this example is to demonstrate the applicability of the proposed method in studying

the structural behaviour of a realistic structure.

Example 1:

Let us consider a fifteen storey model structure consisting of a core surrounded by walls which are connected by slabs at every floor level. The floor height is 4 in, slab thickness is  $3/8$  in and wall thickness is  $1/4$  in. The structure is made of perspex having a modulus of elasticity  $E = 4.25 \times 10^5$  lb/in<sup>2</sup> and Poisson's ratio of 0.35. The floor plan and appropriate dimensions are shown in Figure (3.6). Taranath<sup>(70)</sup> has worked out the same example, using the finite element technique to take into account the transverse stiffness of the floor slab.

In the present analysis, each floor slab is replaced by eight connecting beams. The location of the connecting beams are shown by dashed lines in Figure (3.6). The stiffness of the beams are based on the effective width concept. The effective width of all the beams are taken to be 2 in. The structure is subjected to a concentrated torque of 1 lb.in at the top and the displacements of point O is determined using the theory in section (3.5). The displacements  $\xi$ ,  $\eta$  and  $\theta$  are plotted in Figure (3.7). The results obtained by Taranath<sup>(70)</sup> using a finite element

idealisation of the floor slab are also plotted in the same figure. It can be seen that the results from the two approaches compare very well. In addition, the displacements are also calculated assuming the floor slab to be completely flexible in the out-of-plane direction. A comparison of the deflection curves shows that the floor slab stiffness increases the overall stiffness of the structure by a factor of about three in this particular example. The necessity to include the out-of-plane stiffness of the floor slabs becomes evident.

Example 2:

Let us consider a thirty storey cross-shaped building as shown in Figure (3.8). The lateral stiffness in the building is provided by shear walls forming a core which houses the elevator, stair and the mechanical devices. The shear walls are interconnected by beams and floor slabs at every floor level. The storey height is 11'-6", the slab thickness is taken to be 8 in and wall thickness is taken to be 10 in. The core is made of concrete having modulus of elasticity  $E = 4.32 \times 10^5$  ksf and Poisson's ratio = 0.15. The plan and the detailed dimensions of the core are shown in Figure (3.9). Let the building be subjected

to wind forces which produces a pressure of  $25 \text{ lb/ft}^2$  on the side of the building. The lateral load acting on the core is estimated to be  $7.5 \text{ k/ft}$  acting uniformly throughout the height.

To study the effect of connecting beam patterns four cases with different beam configurations as shown in Figure (3.10) are considered. In case I, three beams at the periphery of the core are taken. In case II, five beams at the periphery of the core are considered. In case III, three additional beams located at the inside of the core are taken into account. Case IV considers 10 beams of which two beams are connected to two points in the same shear wall. In other words, beams 9 and 10 are type 2 connecting beams as previously defined. In calculating the stiffness of the beams a 24 in width of slab is included to act as the flange of the T sections. The shear deformation of the beams are neglected.

The displacements  $\xi$ ,  $\eta$  and  $\theta$  of the reference point O for the different beam configurations are plotted in Figure (3.11). The results of case III are very close to case IV indicating there is only a small contribution from beam 9 and 10. The rotation curves for Case II, III and IV are very close to each other. This shows that as long as all the beams at the outer periphery of the structure

are considered, a good estimate of the torsional stiffness can be obtained. Consideration of additional beams at the inside will affect the results by a small amount only. The distributed shear in beams 1, 2 and 3 and the axial stress distribution at the base is shown in Figure (3.12) and (3.13) respectively. The coupled translation and rotation of the top of the building is shown in Figure (3.14). Due to the loading considered, the lower right corner of the building suffers the maximum translational displacement of 0.88 ft. Considerable rotation of the section is also noticed in the diagram. The effect of neglecting the stiffness of the beams is demonstrated in Figure (3.15). The curves corresponding to zero beam stiffness is essentially the same as suggested by Blume, Newmark and Corning<sup>(5)</sup> in treatment of torsion in tall buildings. In this particular case, such an approximation will result in an under-estimation of the stiffness by a factor of more than 10. Another approximation frequently made is neglecting the axial deformation of the shear walls<sup>(29)</sup>. The effect of such an approximation on the displacement and axial stress distribution is shown in Figures (3.16) and (3.17). It is seen from the figures that neglecting the axial deformation of the shear walls increases the lateral stiffness by a factor of about 2 in this case. The torsional

stiffness is increased about 10% by making this assumption. It is also noticed that such an assumption lead to an under-estimation of the axial stresses by as much as 30%.

### 3.7 Stiffness Representation of the Floor Slab

In the present analysis, the effect of the floor slab is represented by a number of connecting beams. If the floor slab is supported on a set of distinct beams monolithically casted with the slab, certain width of the slab may be assumed to act as the flange of the beam forming a T or L section. In the case where the slab is used alone, the location and the stiffness (effective width) of the connecting beam have to be properly chosen. The following is a guide in making the selection of connecting beam patterns.

1. When the ends of the shear walls are facing at each other, a beam should be considered joining the ends. As in Figure (3.18a) beams in location a, b and c should be considered. The bending stiffness of the beams are inversly proportional to the cube of span length. Therefore, the effectiveness of the beam b will be much smaller than that of beam a. The beam

c is connected to the two ends of the same shear wall. This beam is effective in restraining the torsion of the section only.

2. When the ends of the shear walls are not facing each other as shown in Figure (3.18b), the effectiveness of the beams d and e will be reduced due to the bending deformation of the walls. The same situation has been discussed by Swift<sup>(82)</sup>. In such cases, the effective stiffness of the slabs is greatly reduced and no connecting beam between their points needs to be considered.
3. To obtain the stiffness of the connecting beam, it is necessary to find the effective width of the slab (Figure 3.18c). The effective width of the slab will depend on the thickness and the plan arrangement of the shear walls. Qadeer<sup>(53)</sup> has given a set of curves for the effective width of slab in case of regularly placed cross wall structures. In case of other arrangements, Qadeer curves may be used as a first approximation.
4. As suggested by Michael<sup>(47)</sup>, the effective span of the beams may be used to take into account the local wall deformation at the joint (Figure 3.18d). The effective span may be taken as the clear span plus

the depth of the beam.

### 3.8 CONCLUSIONS

An approach to perform a three-dimensional analysis of uniform shear wall structures with asymmetric floor plan subjected to lateral load is presented. From the study of Taranath's example it is found that the floor slab stiffness can be represented by appropriately placed connecting beams. The other example of a representative shear wall core structure is worked out to show the importance of structural actions of the floor slabs in resisting lateral loads. It has been shown that the stiffness of the connecting beams contributes substantially to the overall stiffness of the structure and should be taken into account. It is also shown that the neglect of the axial deformation of the shear walls results in gross over-estimate of the lateral stiffness. Therefore the axial deformation of the shear walls should be considered in the analysis.

The special features of the proposed method are as follows:

- (a) By using the continuum method of shear wall analysis, the requirement in computational capacity becomes



independent of the number of storeys in the structure. This allows the capacity of the computer to be used to deal with the complexity of the floor plan arrangement.

- (b) The stiffening effect of the floor slabs is replaced by connected beams at appropriate locations. The problem is formulated in terms of three generalised displacement functions so that the number of equivalent connecting beams can be specified arbitrarily and changed without requiring extensive reformulation of the problem. Therefore, the present approach is particularly useful when it is not clear the appropriate number and/or location of the connecting beams that should be used in representing the floor slab stiffness.

- (c) Since displacement variables are used as unknowns, the analysis can readily be extended into a dynamic analysis. The dynamic effect of the structure can be taken into account by including appropriate inertial forces into the equations of equilibrium.

Since there are no restrictions placed on the number, shape, location and orientation of the shear walls, it is believed that the proposed method is useful to study the flexural and torsional behaviour of high-rise shear wall buildings with complex asymmetrical floor plans.

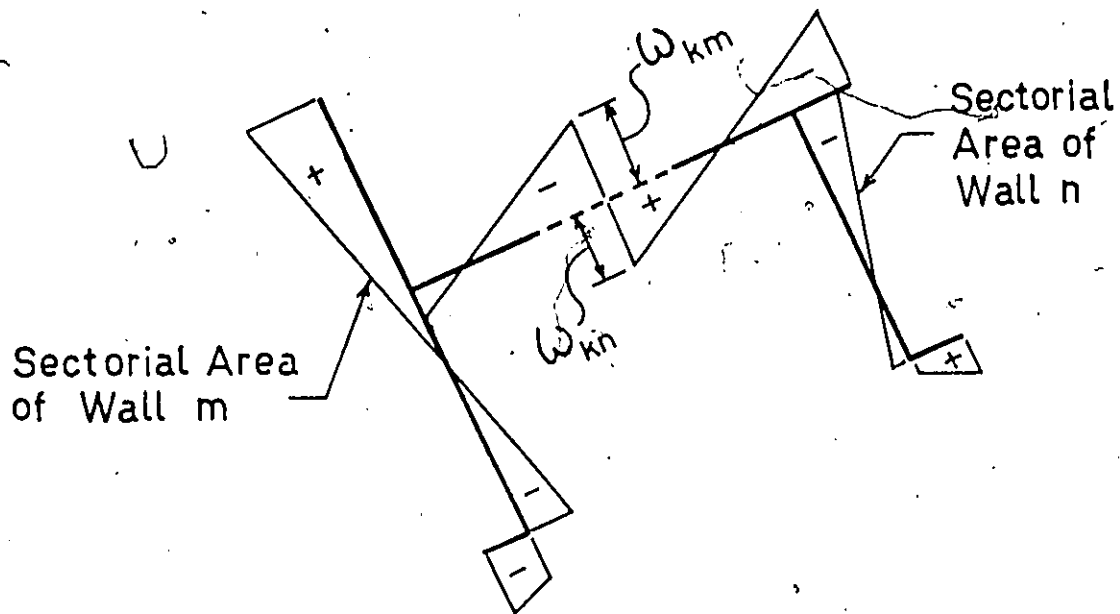
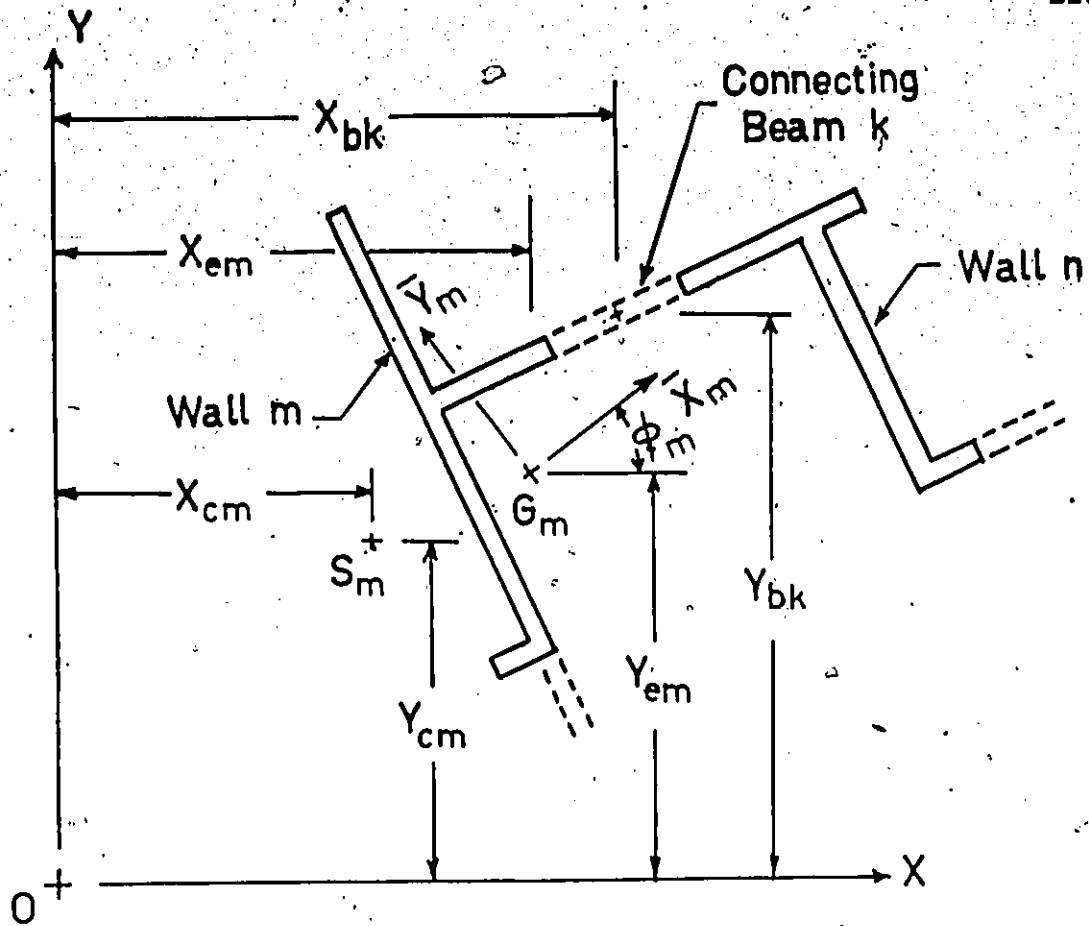


FIG. 3.1 GEOMETRY OF SHEAR WALLS WITH TYPE 1 CONNECTING BEAM

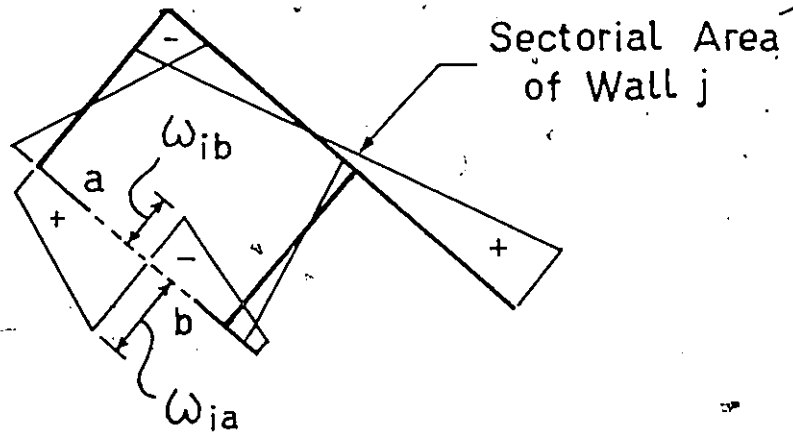
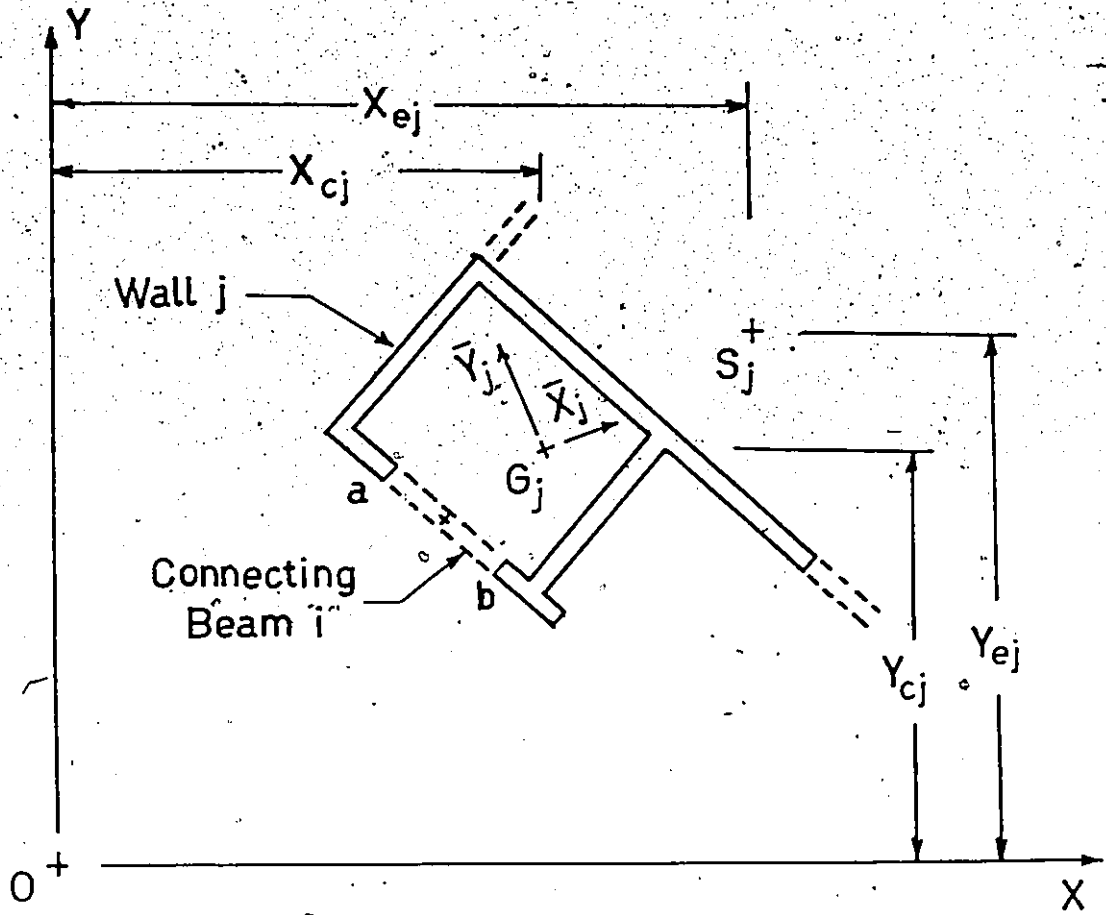


FIG. 3.2 GEOMETRY OF SHEAR WALLS WITH TYPE 2 CONNECTING BEAM

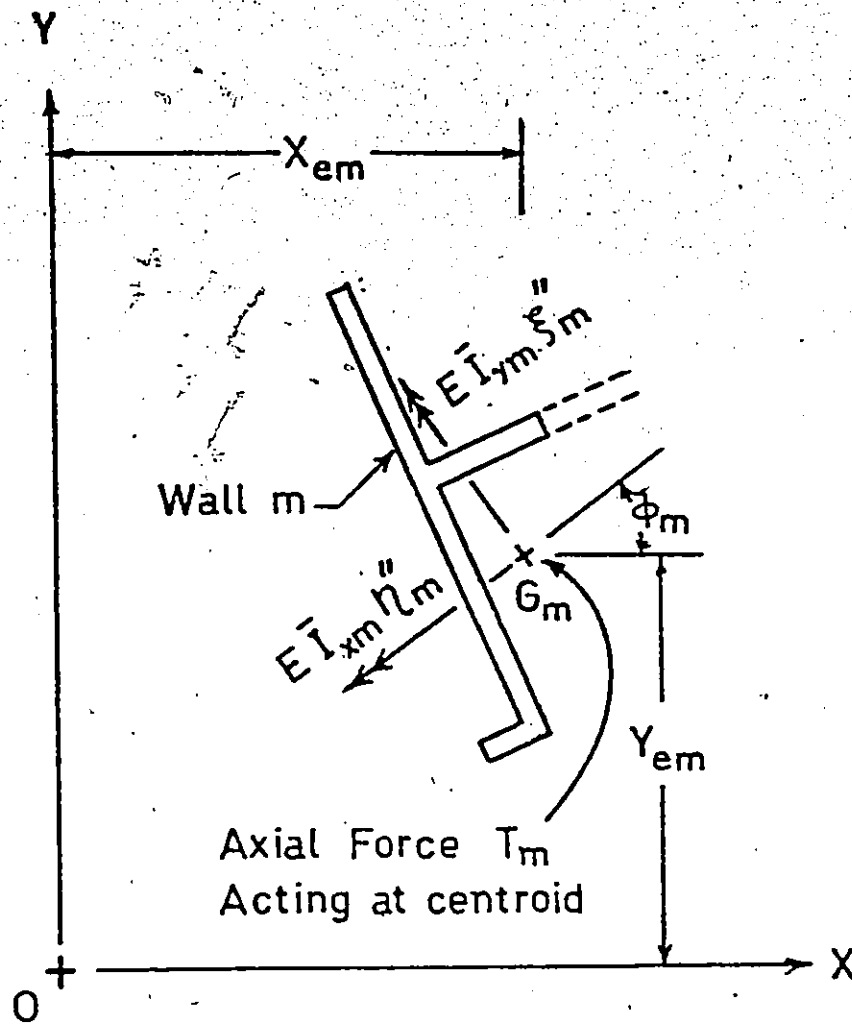


FIG. 3.3 MOMENT CONTRIBUTION FROM WALL  $m$

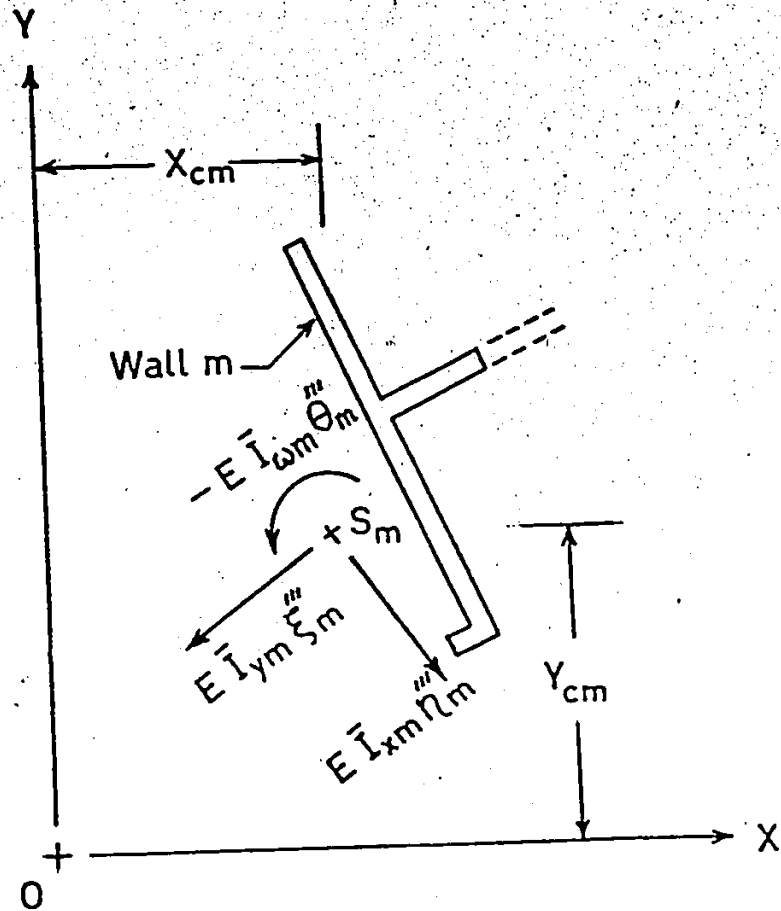


FIG. 3.4 SHEAR FORCE AND TORQUE CONTRIBUTION FROM WALL  $m$

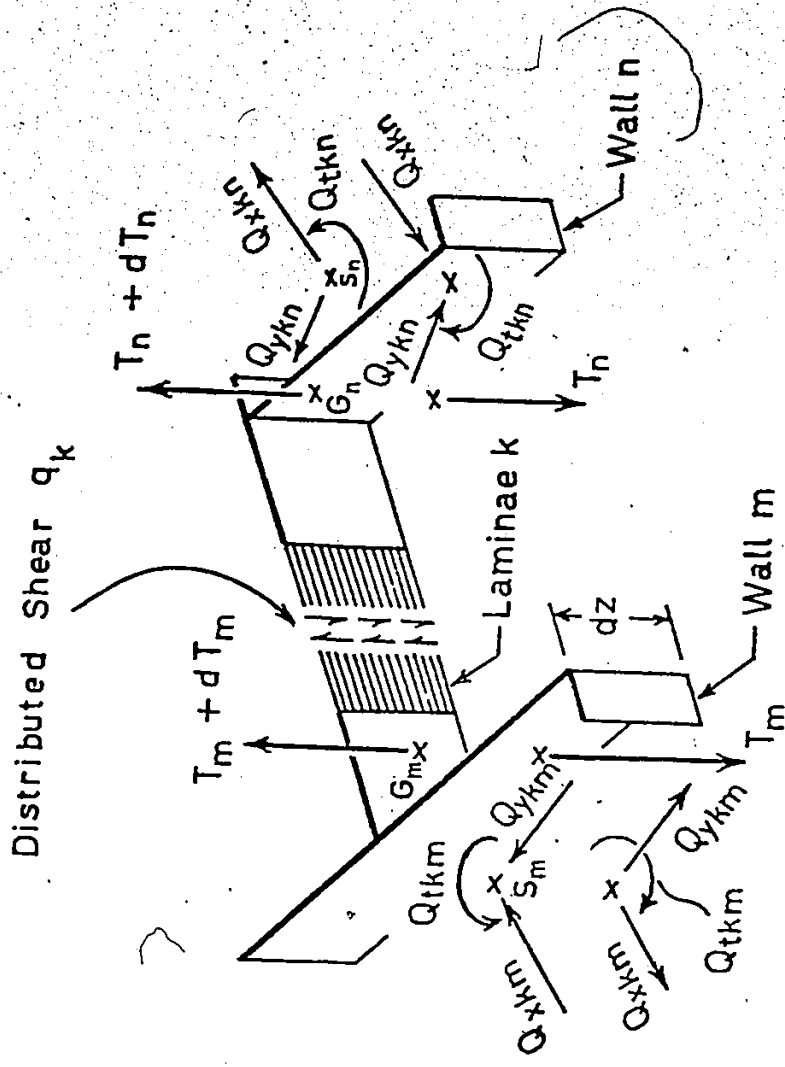
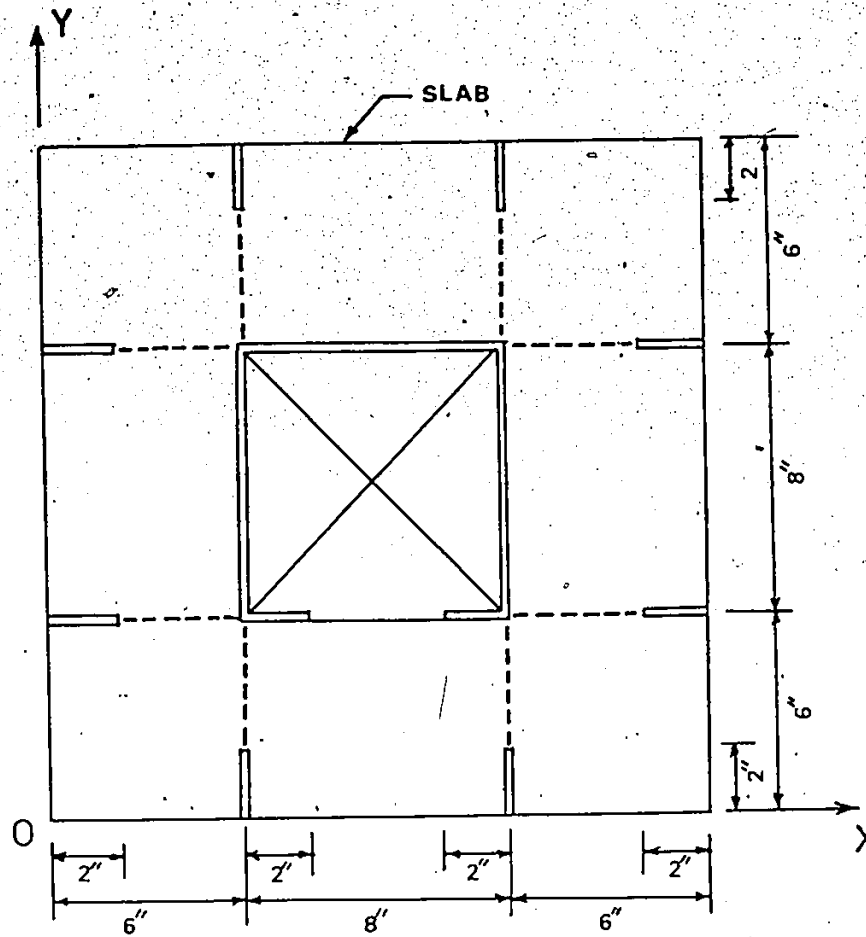


FIG. 3.5 FORCE COMPONENTS ON  $m$ th &  $n$ th WALLS DUE TO DISTRIBUTED SHEAR  $q_k$



----- Connecting Beam Location

Storey Height 4 in

No. of Storeys 15

Wall Thickness 1/4 in

Slab Thickness 3/8 in

Modulus of Elasticity  $4.25 \times 10^5$  psi

Poisson's Ratio 0.35

FIG. 3.6 CORE SURROUNDED BY WALLS

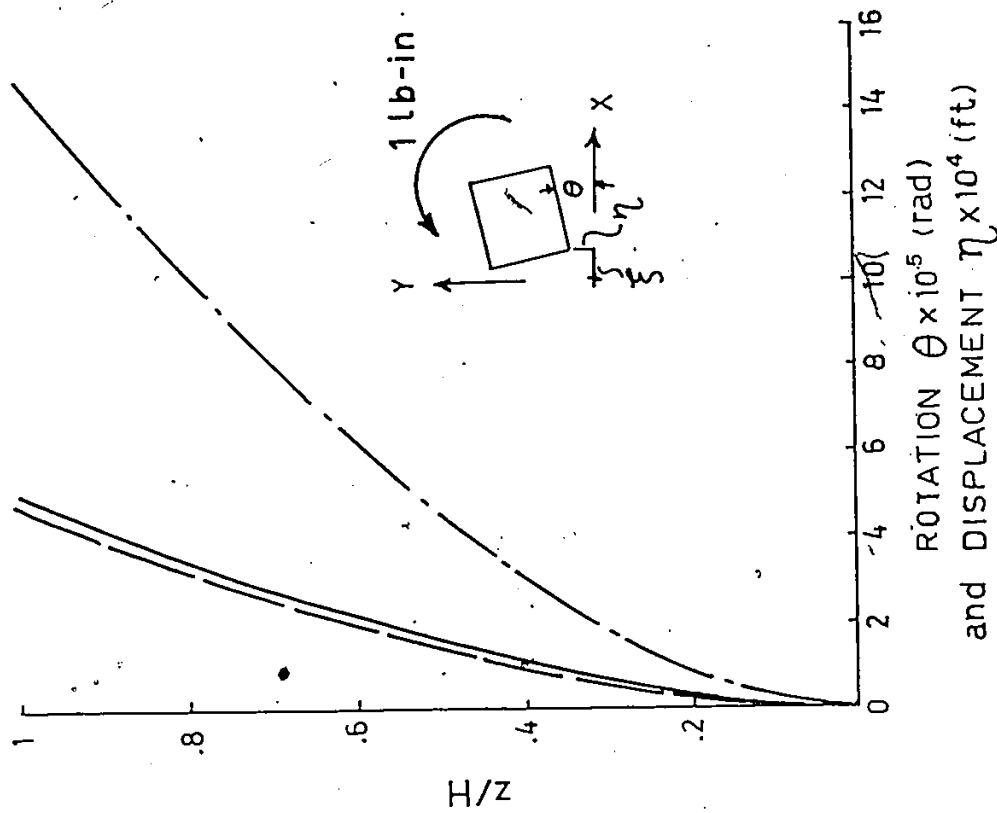
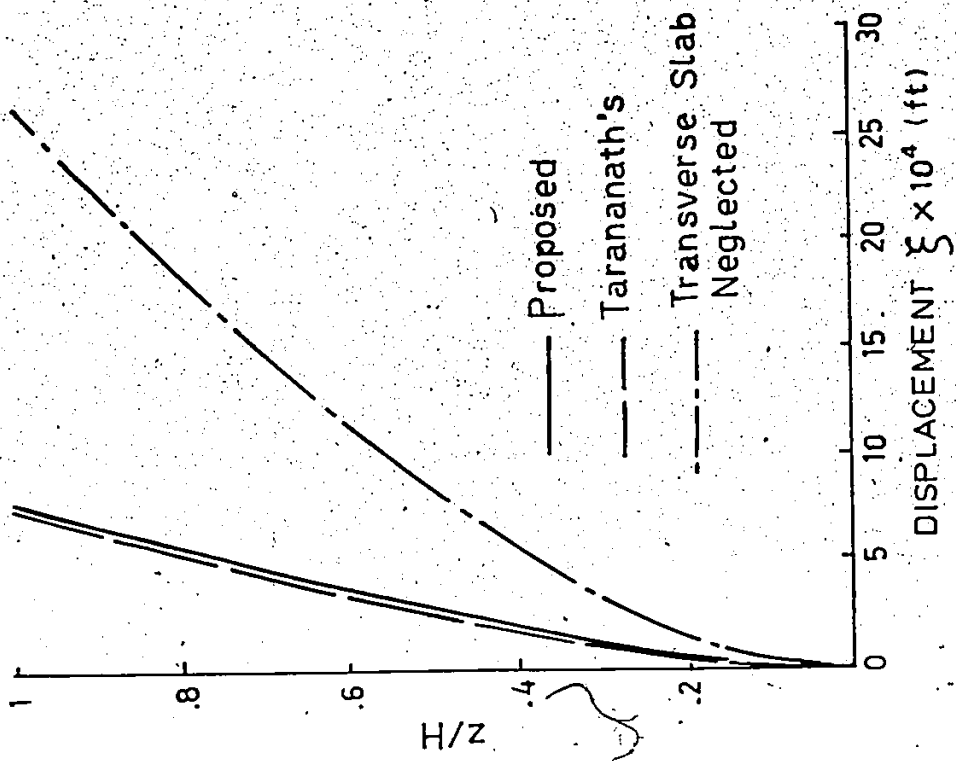


FIG. 3.7 CORE SURROUNDED BY WALLS : 1 LB-IN TORQUE AT TOP



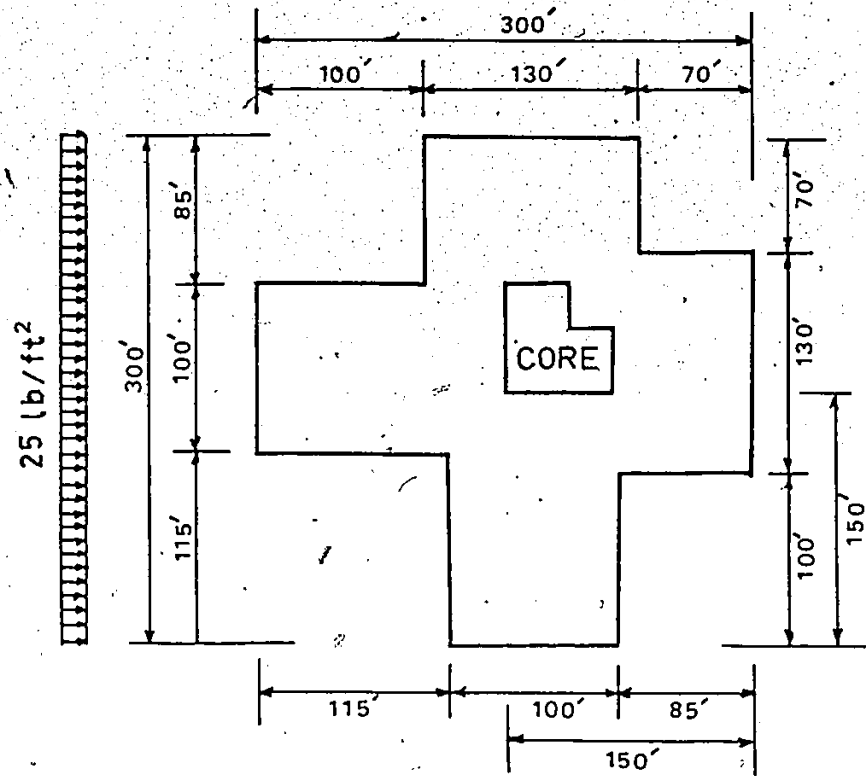
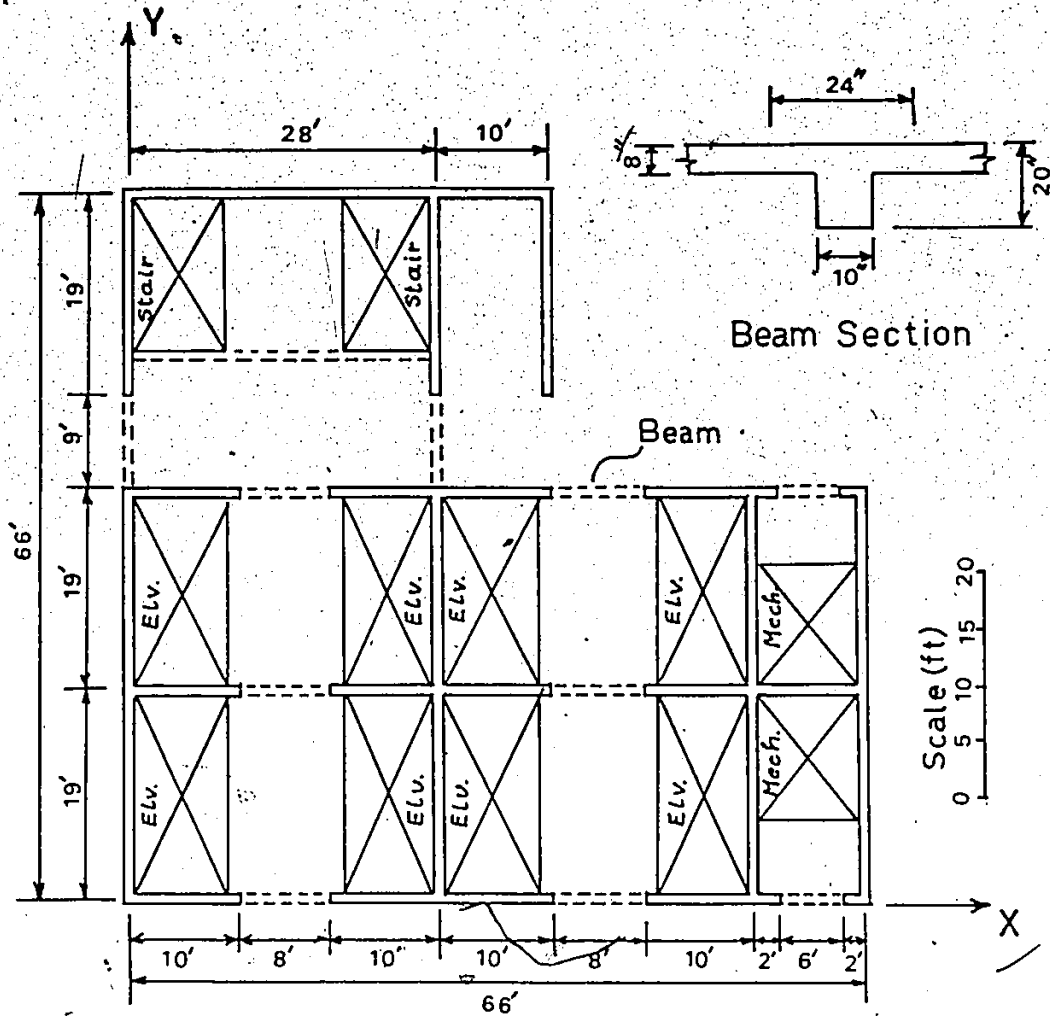
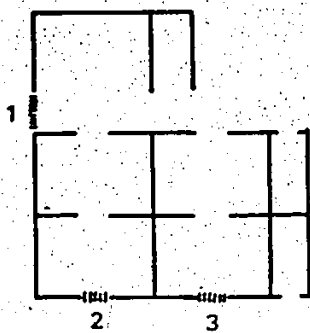


FIG. 3.8 PLAN OF A CROSS-SHAPED BUILDING

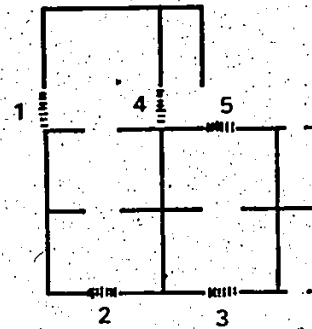


Storey Height 11'-6"  
 No. of Storeys 30  
 Wall Thickness 10"  
 Slab Thickness 8"  
 Modulus of Elasticity  $4.32 \times 10^5$  k.s.f.  
 Poisson's Ratio 0.15

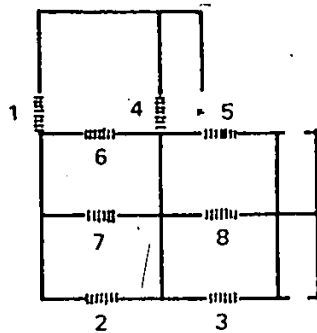
FIG. 3.9 CORE OF THE CROSS-SHAPED BUILDING



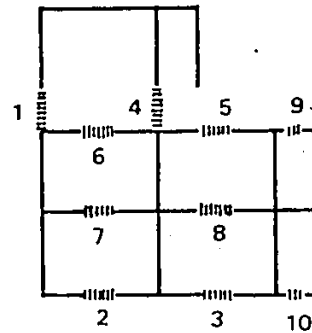
3 Beam Configuration  
Case I



5 Beam Configuration  
Case II



8 Beam Configuration  
Case III



10 Beam Configuration  
Case IV

FIG. 3.10 BEAM CONFIGURATIONS OF THE CORE

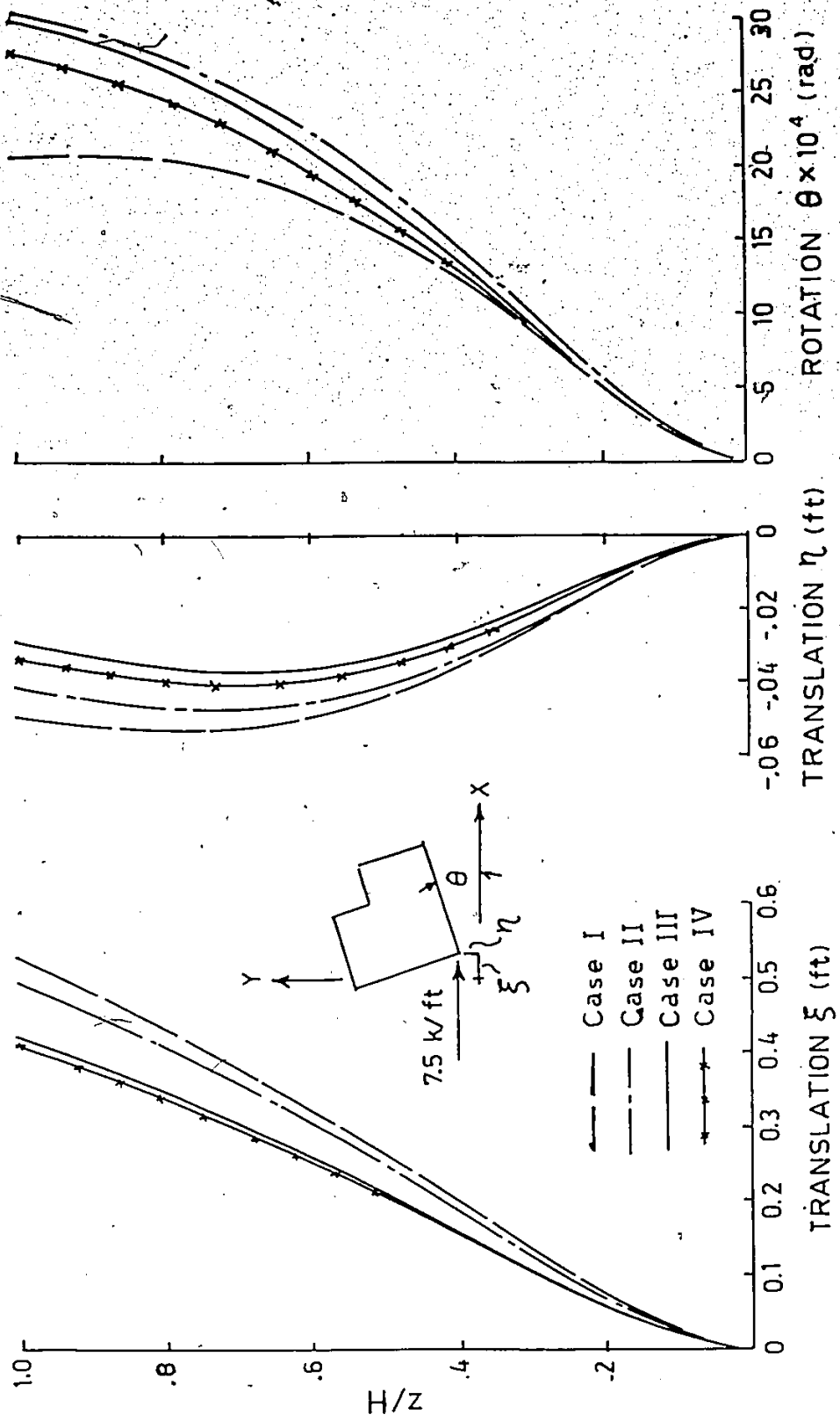


FIG. 3.11 CORE OF THE CROSS-SHAPED BUILDING : DISPLACEMENTS 5

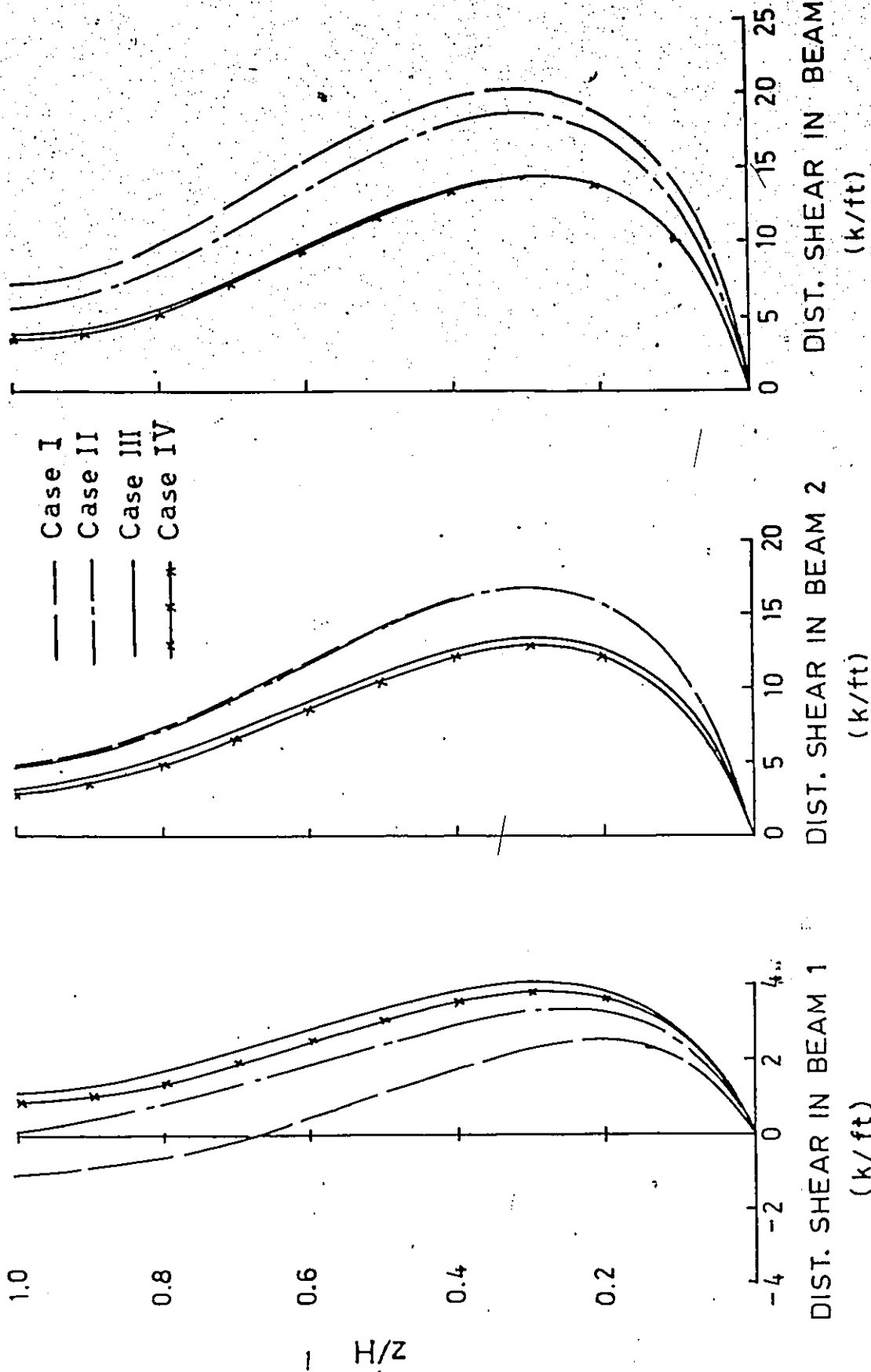


FIG. 3.12 CORE OF THE CROSS SHPED BUILDING : DISTRIBUTED SHEAR IN BEAM 1, 2, 3  
CONNECTING BEAMS

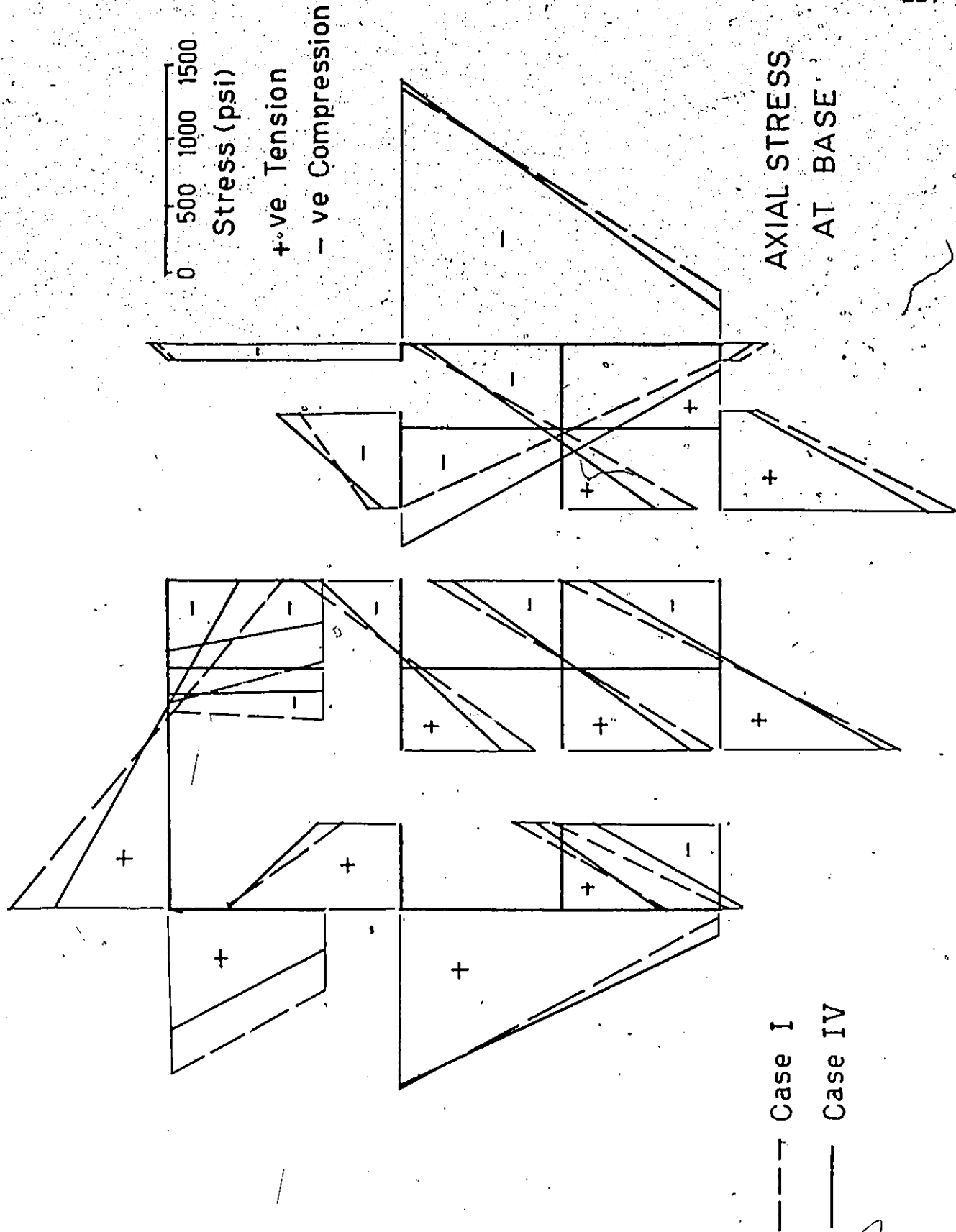


FIG. 3.13 CORE OF THE CROSS-SHAPED BUILDING

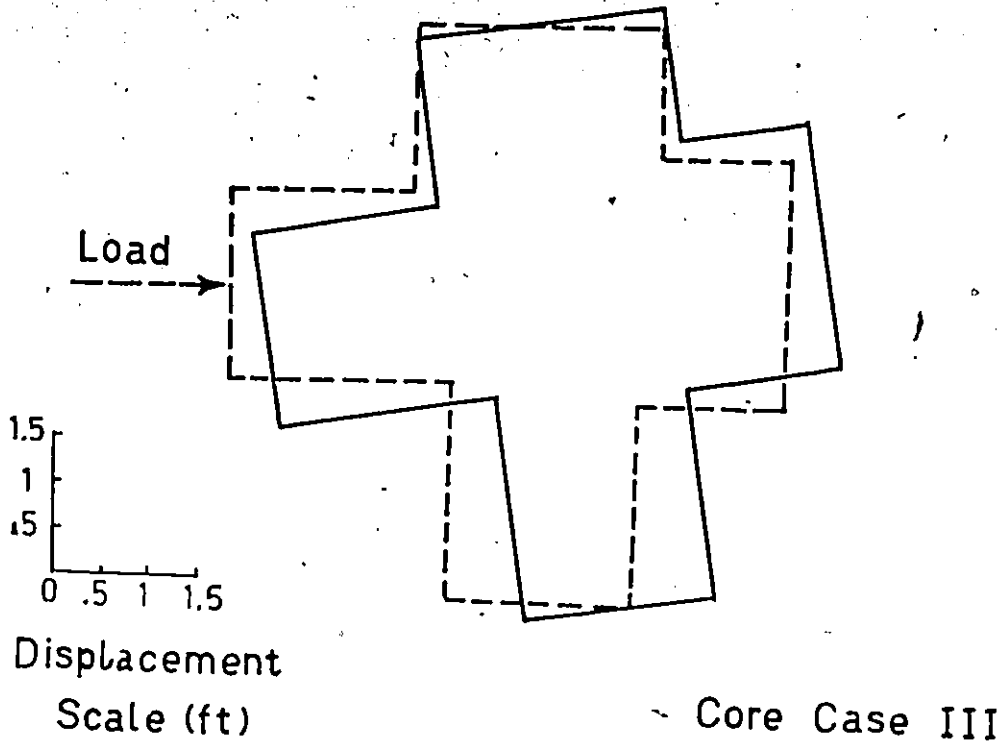


FIG. 3.14 COUPLED TRANSLATION AND ROTATION OF THE CROSS SHAPED BUILDING

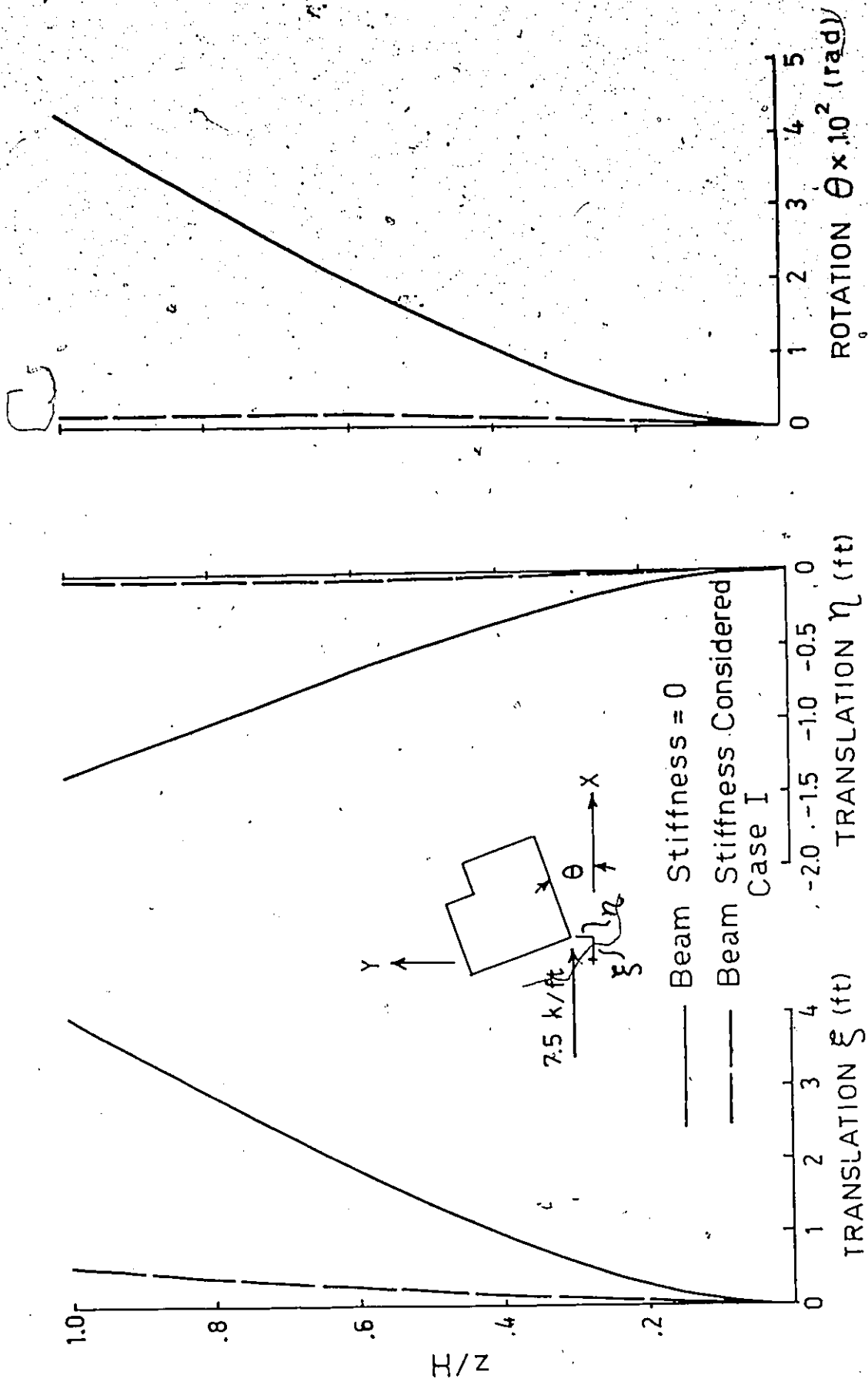


FIG. 3.15 CORE OF THE CROSS-SHAPED BUILDING : THE EFFECT OF NEGLECTING BEAM STIFFNESS 129



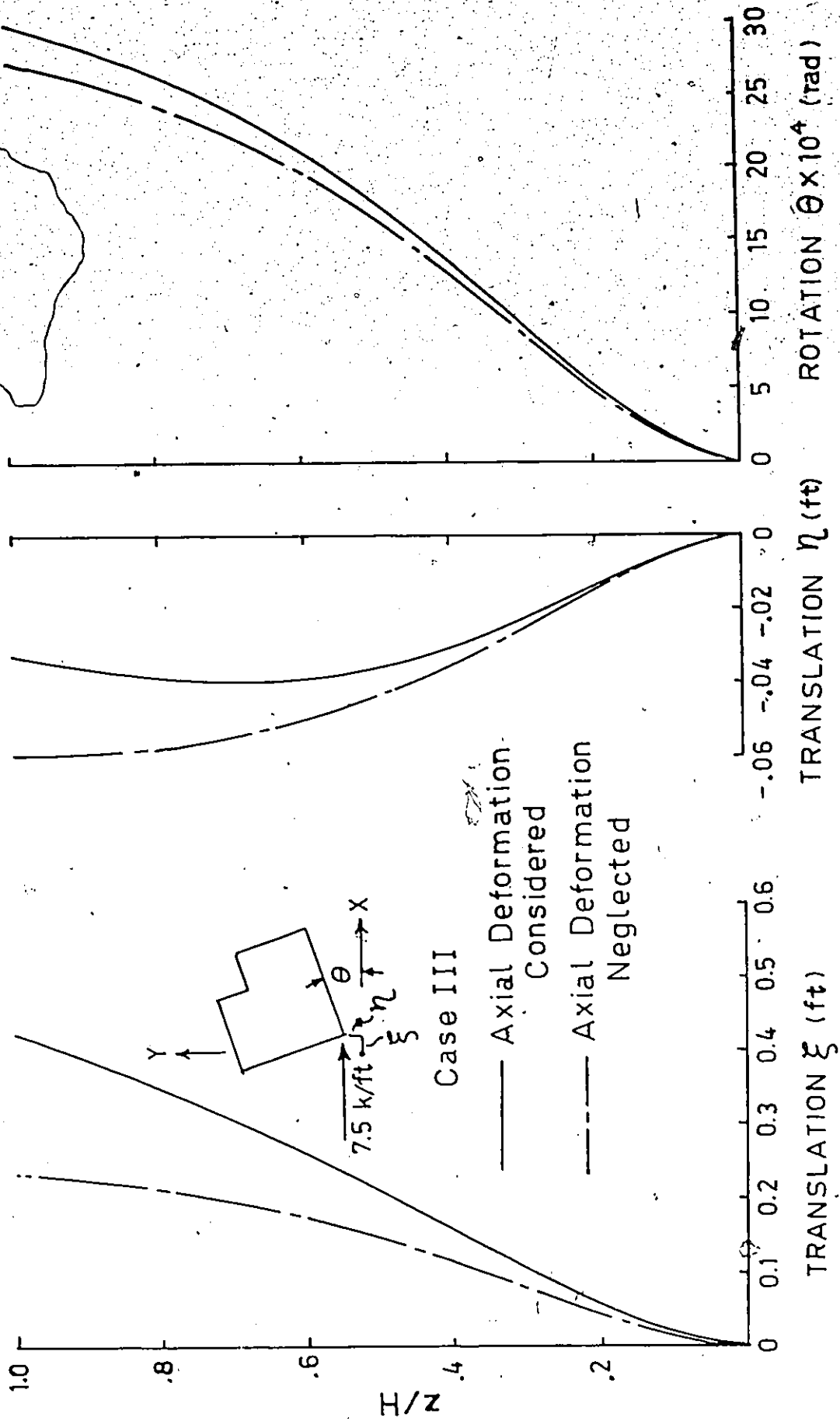


FIG. 3.16 CORE OF THE CROSS SHAPED BUILDING THE EFFECT OF AXIAL DEFORMATION OF SHEAR WALLS

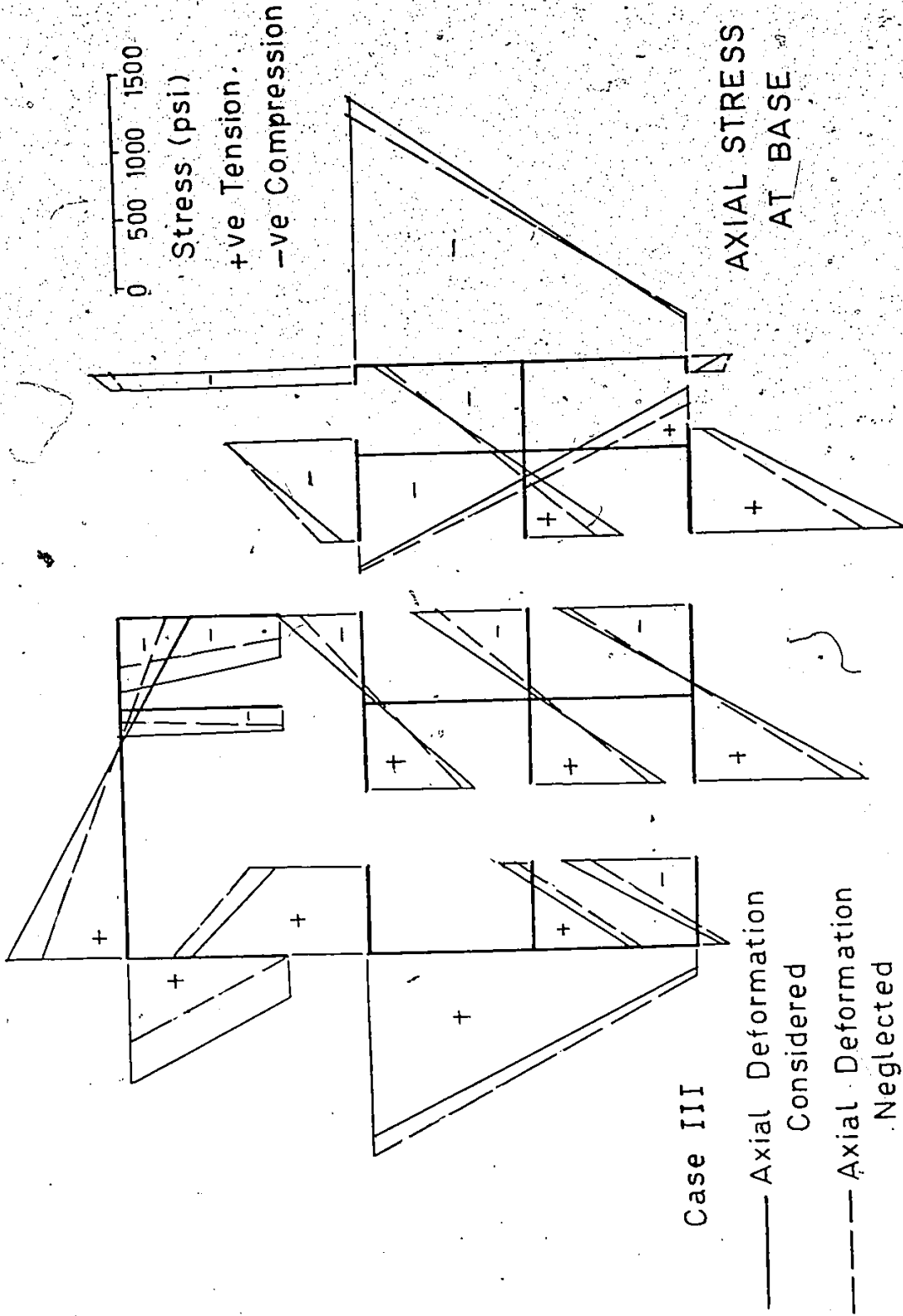
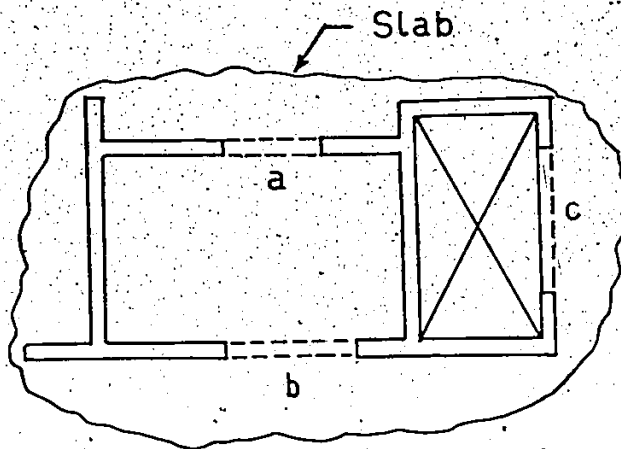
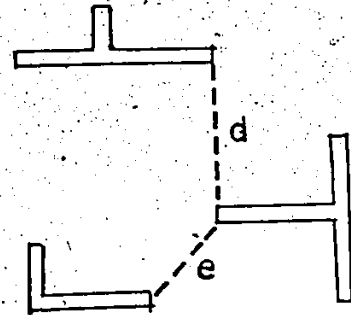


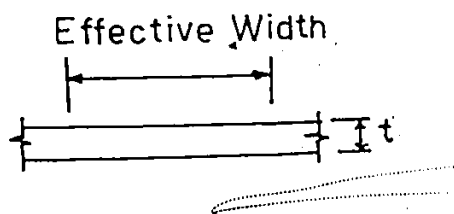
FIG. 3.17 CORE OF THE CROSS-SHAPED BUILDING



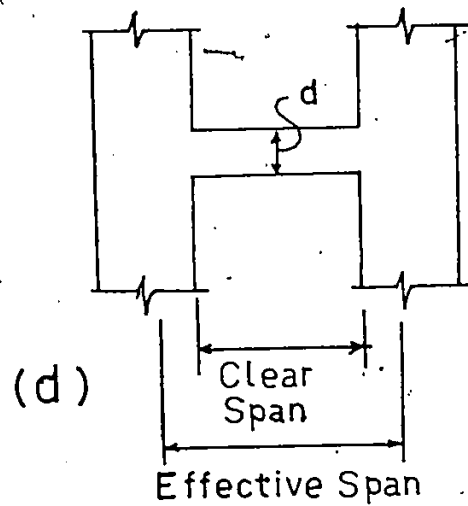
(a)



(b)



(c)



(d)

FIG. 3.18 STIFFNESS OF THE FLOOR SLAB

## CHAPTER IV

### THREE-DIMENSIONAL ANALYSIS OF NON-UNIFORM SHEAR WALL STRUCTURES

#### 4.1 Introduction

Most high-rise buildings have structural property variation along the height of the building. The top parts of the building have to resist smaller shear forces and moments than the lower parts. Therefore, it is justified to decrease the thickness of the shear walls in the upper floors. Sometimes the floor height and the dimensions of the beams have to change for architectural and other reasons. In such cases, it is desirable and may be necessary to take into account the non-uniformity of structural properties along the height in the analysis.

The continuous approach (2, 17, 48) has been widely used for the analysis of shear wall structures. In this approach, however, an assumption is made regarding the uniformity of the structural properties along the height. Therefore, this approach without modification lacks the flexibility to be adopted for the analysis of non-uniform structures. However, it is possible to divide a non-uniform

structure into a number of uniform segments. Each of these segments can be analysed using the continuous approach and the boundary conditions at the common levels between segments can be matched. In such an approach, it becomes necessary to deal with a large number of unknown quantities at a time. The number of these unknown quantities also increases with the increase of the number of uniform segments to be considered. However, this process can be simplified by the use of the matrix transfer method. This method uses successive elimination of the deflection and force quantities to reduce the number of unknowns involved. Such a procedure is followed by Tso and Chan<sup>(80)</sup> for the structural analysis of planar coupled shear wall having stepped variation of cross section. Heidebrecht and Stafford Smith<sup>(33)</sup> have used the matrix transfer method for dealing with the torsional analysis of open section core structures.

The present chapter deals with a study of the three-dimensional behaviour of non-uniform shear wall structures. The plan of the structure can have an asymmetric layout with beams connecting the shear walls at every floor level. The thickness of the shear walls, the stiffness of the connecting beams and the storey height may change at discrete levels along the height of the structure. A combination of the continuous approach and the matrix transfer method is used

in the analysis. A computer programme based on the theoretical formulation has been prepared. An example of a representative building is worked out to demonstrate the applicability of the method of analysis in studying the structural behaviour for such buildings.

## 4.2 Notations

The following notations will be used in this chapter.

$[A^i]$	= Axial deformation matrix for segment $i$ (Appendix C)
$[B^i]$	= 3x3 co-efficient matrix of load vector (Equation 4.12a)
$E, G$	= Modulus of elasticity and shear modulus of material respectively.
$H_i$	= Height of segment $i$ .
$H$	= Total height of structure.
$I$	= No. of type 2 beams considered.
$J$	= No. of uniform segments.
$K$	= No. of type 1 beams considered.
$[K_o^i]$	= 3x3 stiffness matrix of individual wall for segment $i$ (Equation 3.29a).
$[K_l^i]$	= 3x3 stiffness matrix for the contribution of the connecting beams for segment $i$ (Equation 4.12b).
$[K_s^i]$	= 3x3 St. Venant's stiffness of individual wall for segment $i$ (Equation 3.29b).
$\{L_i\}$	= Equivalent load vector for section $i$ , size 20.
$M_{YA}^i, M_{XA}^i$	= Bending moments at the top of station $i$ .
$M_{YB}^i, M_{XB}^i$	= Bending moments at the bottom of section $i$ .
$\{P_i\}$	= Applied load vector at station $i$ = $\{P_{xi}, P_{yi}, P_{ti}\}$ col.

- $Q_{tA}^i$  = Internal torque at the top of station i.
- $Q_{tB}^i$  = Internal torque at the bottom of station i.
- $\{q^i\}, \{\bar{q}^i\}$  = Distributed shear vector in segment i for the type 1 and type 2 beams respectively.
- $\{q_A^i\}, \{\bar{q}_A^i\}$  = Distributed shear vector at the top of station A.
- $\{q_B^i\}, \{\bar{q}_B^i\}$  = Distributed shear vector at the bottom of station B.
- $[R], [\bar{R}]$  = Lateral deformation matrix for the type 1 and type 2 beams respectively (Equations 3.29c, 3.29d).
- $[S_g^i]$  = Segment transfer matrix at  $i^{\text{th}}$  segment.
- $[S_t^i]$  = Station transfer matrix at  $i^{\text{th}}$  station.
- $T_m^i(\hat{z})$  = Axial force in wall m in segment i.
- $T_m^{*i}$  = Axial force at  $m^{\text{th}}$  wall at the top of segment i.
- $T_{mA}^i$  = Axial force in wall m at the top of station i.
- $T_{mB}^i$  = Axial force in wall m at the bottom of station i.
- $t_i$  = Relative thickness of the shear walls at segment i.
- $V_{xA}^i, V_{yA}^i$  = Internal shear force at the top of station i.
- $V_{xB}^i, V_{yB}^i$  = Internal shear force at the bottom of station i.



- $\{v_A^i\} \equiv \{v_{xA}^i, v_{yA}^i, Q_{tB}^i\} \text{ col.}$   
 $\{v_B^i\} = \{v_{xB}^i, v_{yB}^i, Q_{tB}^i\} \text{ col.}$   
 $\gamma_k^i =$  Flexibility of  $k^{\text{th}}$  type 1 beam at segment  $i$  (Equation 3.26a).  
 $\gamma_j^i =$  Flexibility of  $j^{\text{th}}$  type 2 beam at segment  $i$ . (Equation 3.28a).  
 $[\Gamma^i] =$  Diagonal Flexibility matrix for type 1 beams at segment  $i$ , size  $K \times K$ . (Equation 3.30a)  
 $[\bar{\Gamma}^i] =$  Diagonal flexibility matrix for type 2 beams at segment  $i$ , size  $I \times I$ . (Equation 3.31a)  
 $\{\Delta^i\} =$  Generalised displacement vector at segment  $i$ .  
 $\equiv \{\xi^i(z), \eta^i(z), \theta^i(z)\} \text{ col.}$   
 $\{\Delta_A^i\} =$  Generalised displacement vector at the top of station  $i$ .  
 $\{\Delta_B^i\} =$  Generalised displacement vector at the bottom of station  $i$ .  
 $\{\psi_A^i\} =$  State vector at the top of station  $i$ . (Equation 4.13)  
 $\{\psi_B^i\} =$  State vector at the bottom of station  $i$ .  
 $[\kappa^i(z)] =$  A  $20 \times 20$  matrix explained in Appendix D.  
 $\epsilon_k^i =$  The relative vertical displacement of the centroids of the shear walls connecting  $k^{\text{th}}$  beam at the base of segment  $i$ .

### 4.3 Statement of the Problem

Let us consider a shear wall structure of total height  $H$ . It is assumed that the structural properties change at a number of discrete points along the height as shown in Figure (4.1). These structural properties variations include the thickness of the shear walls, the storey height and the stiffness of the connecting beams.

A station is a point where either the structural properties change or where concentrated loads and torques are being applied. For the sake of reference, the stations are numbered consecutively from the base. The base is taken to be station zero, the location for the first change of structural properties or where the first concentrated load acts is denoted as station 1, and so on. Between each pair of stations, the structural properties are uniform and the part of the structure is referred to as a segment. Thus the first segment lies between the station zero and station 1, the second segment lies between the station 1 and station 2, and so on as shown in Figure (4.1). Let there be  $J$  segments to be considered. The height of the  $i^{\text{th}}$  segment is denoted by  $H_i$  ( $i = 1, 2, \dots, J$ ). One limitation of the present theory is that the shear centers and centroids of each shear wall in all segments must lie on the same vertical line.

Therefore, the overall layout of the shear walls and connecting beams at every segment is assumed to be similar.

Free body diagrams for the stations and segments are obtained by cutting the structure by imaginary planes just above and below the station levels. The internal shear forces, moments and torques acting above and below the  $i^{\text{th}}$  station and  $i^{\text{th}}$  segment are shown in the freebody diagram in Figure (4.2).  $V_{xB}^i$  and  $V_{yB}^i$  are the internal shear forces acting in the X and Y directions respectively and  $Q_{tB}^i$  is the internal torque acting at the top of the  $i^{\text{th}}$  segment.  $M_{xB}^i$  and  $M_{yB}^i$  are the internal moments acting in the X and Y directions respectively acting at the same point. The internal shear forces, torques and moments acting at the bottom of the  $i^{\text{th}}$  station are of <sup>the</sup> same magnitude as that acting at the top of the  $i^{\text{th}}$  segment but in the opposite directions.  $V_{xA}^i$  and  $V_{yA}^i$  are the internal shear forces acting in the X and Y directions respectively and  $Q_{tA}^i$  is the internal torque acting at the top of the  $i^{\text{th}}$  station.  $M_{xA}^i$  and  $M_{yA}^i$  are the internal moments acting in the X and Y directions respectively acting at the same point.  $P_{xi}$  and  $P_{yi}$  are the concentrated loads acting in the X and Y directions respectively and  $P_{ti}$  is the applied torque at the  $i^{\text{th}}$  station.  $\xi_B^i$ ,  $\eta_B^i$  and  $\theta_B^i$  are the generalised displacement variables at the bottom of the  $i^{\text{th}}$  station or at the top of the  $i^{\text{th}}$  segment.  $\xi_A^i$ ,  $\eta_A^i$  and  $\theta_A^i$  are the generalised displacement variables at the top of the  $i^{\text{th}}$  station.

#### 4.4.1 Differential Equation for Segment i

Since each segment has uniform properties, they can be treated by the continuous approach as developed in Chapter III. For completeness, it is of use to include a number of governing equations which are derived in Chapter III but find use in the present analysis.

Referring to equation (3.45) the equation of equilibrium for the  $i^{\text{th}}$  segment can be written in the following form:

$$\begin{aligned} \left[ K_O^i \right] \{ \Delta^i \} & - \left[ K_S^i \right] \{ \Delta^i \} - [R]^T \{ q^i \} - [\bar{R}]^T \{ \bar{q}^i \} \\ & = -\{ V_B^i \} \end{aligned} \quad (4.1)$$

The superscript  $i$  indicates the quantities for the  $i^{\text{th}}$  segment. Matrices  $[R]$  and  $[\bar{R}]$  are identical in all the segments. This is because the overall layout of the shear walls and connecting beams at all segments are the same throughout the building.

The compatibility condition for the  $k^{\text{th}}$  type 1 beam in the  $i^{\text{th}}$  segment becomes as follows (ref. equation 3.27):

$$r_{xk} \xi' + r_{yk} \eta' + r_{\theta k} \theta' - \int_0^z \frac{T_m^i(s)}{EA_m^i} ds - \int_0^z \frac{T_n^i(s)}{EA_n^i} ds$$

$$-\epsilon_k^i - \frac{\gamma_k^{i_i} q_k^i}{E} = 0 \quad (4.2)$$

The additional term  $\epsilon_k^i$  is the relative vertical displacement of the centroids of the  $m^{\text{th}}$  and  $n^{\text{th}}$  wall as shown in Figure (4.3). The axial forces in the shear walls are obtained as:

$$T_m^i(z) = T_m^{*i} + \sum_k^{C_m} \int_z^H q_k^i(s) ds \quad (4.3)$$

where  $\sum_k^{C_m}$  indicates the summation on  $k$  is taken over all rows of laminae that are connected to wall  $m$ .  $T_m^{*i}$  is the axial force at the top of  $i^{\text{th}}$  segment for wall  $m$ . The action of  $T_m^{*i}$  is illustrated in Figure (4.3). The compatibility conditions for the type 2 beams is of the same form as in equation (3.28). For the  $j^{\text{th}}$  beam the equation is as follows:

$$\bar{r}_{\theta j} \theta' - \frac{\gamma_j^{i_i} q_j^i}{E} = 0 \quad (4.4)$$

Eliminating  $T_m^j$  using equation (4.3), the resulting compatibility equation (4.2 and 4.4) can be written in the following matrix form:

$$[R]\{\Delta^i\}' + [A^i]\{q^i\} - [r^i]\{q^i\}' = 0 \quad (4.5)$$

$$[\bar{R}]\{\Delta^i\}' - [\bar{F}^i]\{\bar{q}^i\} = 0 \quad (4.6)$$

Eliminating  $\bar{q}^i$  using equation (4.6), equation (4.1) becomes:

$$[K_O^i]\{\Delta^i\}'''' - [\bar{K}_S^i]\{\Delta^i\}' - [R]^T\{q^i\} = -\{V_B^i\} \quad (4.7)$$

where  $[\bar{K}_S^i] = [K_S^i + \bar{R}^T \Gamma^{i-1} \bar{R}]$  (4.7a)

Differentiating equation (4.7) once there is obtained:

$$[K_O^i]\{\Delta^i\}^{iv} - [\bar{K}_S^i]\{\Delta^i\}''' - [R]^T\{q^i\}' = 0 \quad (4.8)$$

To eliminate  $\{q^i\}$ , it is necessary to define a new vector  $\{e^i\}$  by the relation

$$\{q^i\} = [\Gamma^i]^{-1} [R]\{e^i\} \quad (4.9)$$

The equation (4.7) then becomes:

$$\begin{aligned} \{e^i\} = & [R^T \Gamma^{i-1} R]^{-1} [K_O^i]\{\Delta^i\}'''' - [R^T \Gamma^{i-1} R]^{-1} [\bar{K}_S^i]\{\Delta^i\}' \\ & + [R^T \Gamma^{i-1} R]^{-1} \{V_B^i\} \end{aligned} \quad (4.10)$$

The equation (4.5) is then converted to:

$$[R]\{e^i\}' = [A^i \Gamma^i]^{-1} R^i \{e^i\} + [R]\{\Delta^i\}' \quad (4.11)$$

Eliminating  $\{e^i\}$  between equations (4.7) and (4.11) and neglecting the co-efficient of  $\{\Delta^i\}'$ , the differential equation for the  $i^{\text{th}}$  segment is obtained as follows:

$$\begin{bmatrix} K_O^i \\ 0 \end{bmatrix} \{\Delta^i\}^V - \begin{bmatrix} K_1^i \end{bmatrix} \{\Delta^i\}' = \begin{bmatrix} B^i \end{bmatrix} \{V_B^i\} \quad (4.12)$$

where  $\begin{bmatrix} B^i \end{bmatrix} = [R]^T [\Gamma^i]^{-1} [A^i \Gamma^i]^{-1} R [R^T \Gamma^i]^{-1} R$  (4.12a)

$$\begin{bmatrix} K_1^i \end{bmatrix} = \begin{bmatrix} B^i \end{bmatrix} \begin{bmatrix} K_O^i \end{bmatrix} + [R]^T [\Gamma^i]^{-1} [R] \quad (4.12b)$$

#### 4.4.2 Transfer Matrix Method

In transfer matrix method, it is necessary to define a state vector. The state vector is a vector consisting of quantities which will completely define the state at a particular location. The state vector at the top of the  $i^{\text{th}}$  station is denoted by  $\{\psi_A^i\}$  and at the bottom is denoted by  $\{\psi_B^i\}$ . It follows that the state vector at the top of the  $i^{\text{th}}$  segment is  $\{\psi_B^i\}$  and at its bottom is  $\{\psi_A^{i-1}\}$ . In this

case the state vector is of order 20 and consists of the following terms:

$$\begin{aligned} \{\psi_A^i\} = & \{\xi_A^i, \eta_A^i, \theta_A^i, \xi_A^{i'}, \eta_A^{i'}, \theta_A^{i'}, \xi_A^{i''}, \eta_A^{i''}, \theta_A^{i''}, \\ & \xi_A^{i'''}, \eta_A^{i'''}, \theta_A^{i'''}, \xi_A^{iiv}, \eta_A^{iiv}, \theta_A^{iiv}, \\ & M_{yA}^i, M_{xA}^i, V_{xA}^i, V_{yA}^i, Q_{tA}^i\} \end{aligned} \quad (4.13)$$

The segment transfer matrix  $[S_g^i]$  is a 20x20 matrix and relates the state vectors at the ends of the  $i^{\text{th}}$  segment.

Thus:

$$\{\psi_B^i\} = [S_g^i] \{\psi_A^{i-1}\} \quad (4.14)$$

From the solution of the differential equation (4.12),  $[S_g^i]$  is obtained as follows.

$$[S_g^i] = [\kappa^i(H_i)] [\kappa^i(0)]^{-1} \quad (4.15)$$

where  $[\kappa(z)]$  is a 20x20 matrix. The development of equation (4.15) and the elements of  $[\kappa(z)]$  are given in Appendix E.

The station transfer matrix  $[S_t^i]$  is a 20x20 matrix



and is defined by the following relation.

$$\{\psi_A^i\} = \begin{bmatrix} S_t^i \end{bmatrix} \{\psi_B^i\} + \{L_i\} \quad (4.16)$$

The applied loading at the  $i^{\text{th}}$  station  $\{P_i\}$  is included in the equivalent load vector  $\{L_i\}$ . The elements of  $\begin{bmatrix} S_t^i \end{bmatrix}$  and  $\{L_i\}$  is determined from the consideration of continuity and equilibrium at the  $i^{\text{th}}$  station. The lateral displacement at points above and below the  $i^{\text{th}}$  station must have the same value.

$$\therefore \{\Delta_A^i\} = \{\Delta_B^i\} \quad (4.17)$$

The consideration of the vertical displacement above and below the  $i^{\text{th}}$  station gives:

$$\{\Delta_A^i\}' = \{\Delta_B^i\}' \quad (4.18)$$

The equilibrium of moment and axial forces in the shear walls at the  $i^{\text{th}}$  station gives:

$$\begin{Bmatrix} M_{YA}^i \\ M_{XA}^i \end{Bmatrix} = \begin{Bmatrix} M_{YB}^i \\ M_{XB}^i \end{Bmatrix} \quad (4.19)$$

$$\text{and } T_{mB}^i = T_{mA}^i \quad (m=1,2,\dots,M) \quad (4.20)$$

It can be shown that when equations (4.19) and (4.20) is valid, the following relation for the curvature also holds.

$$\{\Delta_A^i\} = [C_1] \{\Delta_B^i\} \quad (4.21)$$

$$\text{where: } [C_1] = \begin{bmatrix} t_i/t_{i+1} & 0 & 0 \\ 0 & t_i/t_{i+1} & 0 \\ 0 & 0 & t_i/t_{i+1} \end{bmatrix} \quad (4.21)$$

$t_i$  is the relative thickness of the shear walls at the  $i^{\text{th}}$  segment.

In deriving the compatibility equations (4.2 and 4.4), cuts are made along the center of the connecting beams. The consideration of compatibility at points above and below the  $i^{\text{th}}$  station yields the following relations for the distributed shear in connecting beams.

$$q_{kA}^i = q_{kB}^i \left( \frac{\gamma_k^i}{\gamma_k} \right) \quad (k=1,2,\dots,N) \quad (4.22)$$

and

$$q_{jA}^{-i} = q_{jB}^{-i} \left( \frac{\bar{\gamma}_j^{-i}}{\gamma_j} \right) \quad (j=1,2,\dots,I) \quad (4.23)$$

where  $\gamma_k^i$  and  $\bar{\gamma}_j^i$  is the flexibility of the type 1 and type 2 connecting beams respectively.

It will be more convenient to express the equation (4.22) in the following matrix form.

$$\{q_A^i\} = [\Gamma^{i+1}]^{-1} [\Gamma^i] \{q_B^i\} \quad (4.24)$$

where  $[\Gamma^i]$  is the flexibility matrix for the type 1 beams at the  $i^{\text{th}}$  segment as explained in equation (3.30a).

The consideration of equilibrium of the shear forces and torques at the  $i^{\text{th}}$  station gives:

$$\{V_A^i\} = \{V_B^i\} - \{P_i\} \quad (2.25)$$

It is necessary to relate the third derivative of the displacements above and below the  $i^{\text{th}}$  station. For that reason the equation (4.7) is applied at points above and below the  $i^{\text{th}}$  station. Eliminating  $\{q_B^i\}$  and  $\{q_A^i\}$  using equation (4.24) and simplifying the resulting equation, there is obtained:

$$\begin{aligned} \{\Delta_A^i\}'''' &= [C_2] \{\Delta_B^i\}'''' + [C_3] \{\Delta_B^i\}' \\ &\quad - [C_4] \{V_B^i\} + \{C_7\} \end{aligned} \quad (4.26)$$

$$\text{where } [C_2] = [K_O^{i+1}]^{-1} [R]^T [\Gamma^{i+1}]^{-1} [R] [R^T \Gamma^{i-1} R] [K_O^i] \quad (4.26a)$$

$$[C_3] = [K_O^{i+1}]^{-1} [K_S^{i+1}] - [K_O^{i+1}]^{-1} [R]^T [\Gamma^{i+1}]^{-1} [R] [R^T \Gamma^{i-1} R]^{-1} [K_S^i] \quad (4.26b)$$

$$[C_4] = [K_O^{i+1}]^{-1} [J] - [K_O^{i+1}]^{-1} [R]^T [\Gamma^{i+1}]^{-1} [R] [R^T \Gamma^{i-1} R]^{-1} \quad (4.26c)$$

$$\{C_7\} = [K_O^{i+1}]^{-1} \{P_i\} \quad (4.26d)$$

A relation between  $\{q_A^i\}'$  and  $\{q_B^i\}'$  is obtained as follows:

$$\begin{aligned} \{q_A^i\}' &= [\Gamma^{i+1}]^{-1} [R] \{\Delta_A^i\}' - \left(\frac{t_i}{t_{i+1}}\right) [\Gamma^{i+1}]^{-1} [R] \{\Delta_B^i\}' \\ &+ \left(\frac{t_i}{t_{i+1}}\right) [\Gamma^{i+1}]^{-1} [\Gamma^i] \{q_B^i\}' \end{aligned} \quad (4.27)$$

The above equation is obtained from the consideration of the derivative of the compatibility equation (4.2) above and below the  $i^{\text{th}}$  station and the equation (4.20). It is also necessary to relate the fourth derivatives of dis-

placements above and below the station  $i$ . For that reason the equation (4.8) is applied at points above and below the  $i^{\text{th}}$  station. Eliminating  $\{q_A^i\}'$  and  $\{q_B^i\}'$  using equations (4.27 and 4.21) and simplifying, the resulting equation becomes:

$$\{\Delta_A^i\}^{iv} = [C_5] \{\Delta_B^i\}^{iv} + [C_6] \{\Delta_B^i\}' \quad (4.28)$$

$$\text{where } [C_5] = \left(\frac{t_i}{t_{i+1}}\right) [K_O^{i+1}]^{-1} [R]^T [\Gamma^{i+1}]^{-1} [R] [R^T \Gamma^{i-1} R]^{-1} [K_O^i] \quad (4.28a)$$

$$[C_6] = \left(\frac{t_i}{t_{i+1}}\right) [K_O^{i+1}]^{-1} [\bar{K}_S^{i+1}] - \left(\frac{t_i}{t_{i+1}}\right) [K_O^{i+1}]^{-1} [R]^T [\Gamma^{i+1}]^{-1} [R] [R^T \Gamma^{i-1} R]^{-1} [\bar{K}_S^i] \quad (4.28b)$$

The equations (4.17 to 4.28) can be used to define the elements of the matrix  $[S_t^i]$  and  $\{L_i\}$ . Elements of these matrices are shown in Appendix E. It should be noted that  $[S_t^i]$  becomes an identity matrix if the  $i$  and  $(i+1)^{\text{th}}$  segment have the same structural properties.

By application of equations (4.14) and (4.16) to each segment and station of the structure, in turn, the following equations are obtained.

$$\{\psi^0\} = [S_g^1] \{\psi_B^1\}$$

$$\{\psi_B^1\} = [S_t^1] \{\psi_A^1\} + \{L_1\}$$

$$\{\psi_A^1\} = [S_g^2] \{\psi_B^2\}$$

$$\{\psi_B^2\} = [S_t^2] \{\psi_A^2\} + \{L_2\}$$

---



---


$$\{\psi_A^{J-1}\} = [S_g^J] \{\psi_B^J\}$$

$$\{\psi_B^J\} = [S_t^J] \{\psi_A^J\} + \{L_J\} \quad (4.29)$$

The station J need not be considered in the computation if the loading at the top  $\{P_J\}$  is considered as one of the end conditions. Through successive substitution of the above equations, the relationship between the base of the structure  $\{\psi_A^0\}$  and the top of the structure  $\{\psi_B^J\}$  can be obtained as follows:

$$\{\psi_A^0\} = [S_s] \{\psi_B^J\} + \{\bar{L}\} \quad (4.30)$$

where  $[S_s]$  is the transfer matrix of the structure and  $\{\bar{L}\}$  is the combined load vector as defined below.

$$[S_s] = \prod_{i=1}^J [S_g^i] [S_t^i] \quad (4.30a)$$

With  $[S_t^J] = [I]$  = Identity matrix

$$\{\bar{L}\} = [S_g^1] \{L_1\} + \sum_{i=2}^{J-1} \prod_{n=1}^{i-1} [S_g^n] [S_t^n] [S_g^i] \{L_i\} \quad (4.30b)$$

To determine the state vector at the base and top of the structure from equation (4.30), it is necessary to consider the boundary conditions. For a building resting on a rigid foundation, the boundary conditions can be expressed as follows.

There is no displacement or slope at the base.

Therefore:

$$\{\Delta_A^0\} = 0 \quad (4.31a)$$

$$\{\Delta_A^0\}' = 0 \quad (4.31b)$$

The distributed shear in the connecting beams vanishes at the base. Therefore:

$$\{\Delta_A^0\}'''' = -[K_O^1]^{-1} \{V_A^0\} \quad (4.31c)$$

There is no moment or bimoment at the top. Therefore:

$$\{\Delta_B^J\}'' = 0 \quad (4.31d)$$

$$\begin{Bmatrix} M_{YB}^J \\ M_{XB}^J \end{Bmatrix} = \begin{Bmatrix} 0 \\ 0 \end{Bmatrix} \quad (4.31e)$$

The first derivative of the distributed shear in the connecting beams vanishes at the top. Therefore:

$$\{\Delta_B^J\}^{iv} = 0 \quad (4.31f)$$

The internal forces acting at the top is the applied loading at that point. Therefore:

$$\{V_B^J\} = \{P_J\} \quad (4.31g)$$

The equation (4.31e) and (4.31g) together with the overall equilibrium condition of the structure gives:

$$\{V_A^0\} = \sum_{i=1}^J \{P_i\} \quad (4.31e)$$



$$\begin{Bmatrix} M_{YB}^O \\ M_{XA}^O \end{Bmatrix} = \sum_{i=1}^J \left\{ \begin{matrix} P_{xi} \\ P_{yi} \end{matrix} \right\} \left( \sum_{n=1}^i H_n \right) \quad (4.31f)$$

When the boundary conditions in equation (4.31a-f) are substituted in the matrix-equation (4.30), and the terms are rearranged, a set of six linear simultaneous equations are obtained. From the solution of this set of equations, the state vectors  $\{\psi_A^O\}$  and  $\{\psi_B^J\}$  can be determined. The state vector at the intermediate stations can then be determined from back substitution into equation (4.29). The distributed shear vector  $\{q^i\}$  can be determined by the use of equations (4.9 and 4.10). The distributed shear vector  $\{\bar{q}^i\}$  can be determined by the use of equation (4.4). The axial force in the shear walls can also be determined from equation (4.3). A computer programme based on the above theory has been prepared. This computer programme can be used to determine the displacement, the distributed shear in the connecting beams, the axial forces and the distribution of longitudinal stresses in the shear walls for non-uniform shear wall structures subjected to lateral loading. It is felt that, in high-rise buildings, there can be a few changes of structural properties along the height. Consideration of five changes seems to be adequate to cover most cases of actual buildings. Therefore, the present

programme is made to handle a maximum of five changes. In this programme, the concentrated load and torque acting at every storey level has been considered. Therefore any distribution of lateral loading can be approximated by a number of concentrated loads and torques acting at the storey levels.

#### 4.5 Example and Discussion of Results

An example is worked out to demonstrate the applicability of the theory and to study the structural behaviour of a non-uniform structure. For that reason a concrete structure as shown in Figure (4.4) is considered. The layout of the shear walls and beams is shown in Figure (4.5). The load resisting behaviour of a structure with a similar layout plan and having uniform properties throughout the height has been studied in Chapter III. In the present example, the wall thickness of the shear wall changes along the height of the building. In the lower 115 feet, the wall thickness is 12 inches, in the middle 115 feet, the thickness is 10 inches and in the upper 115 feet, the thickness is 8 inches. The stiffness of the connecting beams is the same throughout the height. In the present

study, two different cases are considered. In the first case, all the thirty storeys have a constant storey height of 11'-6". In the second case, in the lower part of the core there are two storeys with an increased storey height of 17'-3". All the other storeys have a constant storey height of 11'-6". It is estimated that the core is subjected to a lateral wind force of 7.5 k/ft. acting through 0 in the X direction. This load is approximated by a set of concentrated loads acting at the floor levels. A shear wall connecting beam configuration with 8 beams is used for the theoretical calculation. The modulus of elasticity of concrete is taken to be  $4.32 \times 10^5$  ksf and Poisson's ratio is 0.15. Results are also compared with the core having a uniform shear wall thickness of 10 inches which has been solved in Chapter III. It is noted that the volume of concrete necessary for the construction of the core is approximately same in all the above cases.

The displacements of the reference point 0, the distributed shear in connecting beams and the axial stress distribution at the base due to the applied loading is plotted in Figures (4.6, 4.7 and 4.8). It is found that the change of storey height at the lower part of the core affect the lateral displacements and axial stress distribution by a negligible amount. It is observed from Figure

(4.7) that the distributed shear in the connecting beams are affected locally at the region of change of storey height. From the study of Figures (4.6 and 4.8) it is seen that the non-uniform structure although uses the same amount of concrete as the uniform structure is stiffer than the uniform structure and have lower stress levels. In this case, the lateral displacement is reduced about 10% and the maximum stress at base is reduced about 20%.

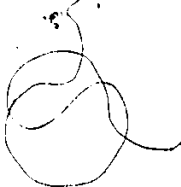
#### 4.6 Conclusions

A method of three-dimensional analysis of non-uniform shear wall structures has been presented. The present method combines the convenience of the continuous approach and the versatility of the matrix transfer method. An example building with a typical layout is worked out using the proposed method of analysis. It is found that by reducing the thickness of the shear walls at the upper storeys, considerable economy of material can be achieved.

The special features of the proposed theory are as follows:

- (a) The non-uniformity of the structural properties is handled by dividing the structure into a number of

segments having uniform properties within each segment. Therefore, any variation of shear wall thickness, cross section of the connecting beams and storey height of the building can be accommodated easily.

- (b) Because of the use of the continuous approach, the requirements of computational capacity becomes independent of the number of storeys. The matrix transfer method also involves manipulation of matrices of size  $20 \times 20$ . The size of these matrices is independent to the number of segments to be considered. For that reason, the present method requires considerably less storage spaces in computer than the available discrete methods for solving a problem of the same complexity.
- (c) In the present method, concentrated load and torque applied at every floor level is considered. Therefore, any arbitrary lateral loading can be approximated by a number of concentrated loads and torques acting at each floor level. In addition, by applying successively a number of unit loads at different points, it is possible to find out the flexibility matrix of the structure. This flexibility matrix can be used for performing a dynamic analysis necessary for finding the responses due to dynamic loads.
- 

It is believed that the proposed method will be useful in studying the flexural torsional behaviour of high-rise shear wall buildings having complex asymmetric floor plan together with changes of structural properties along the height.

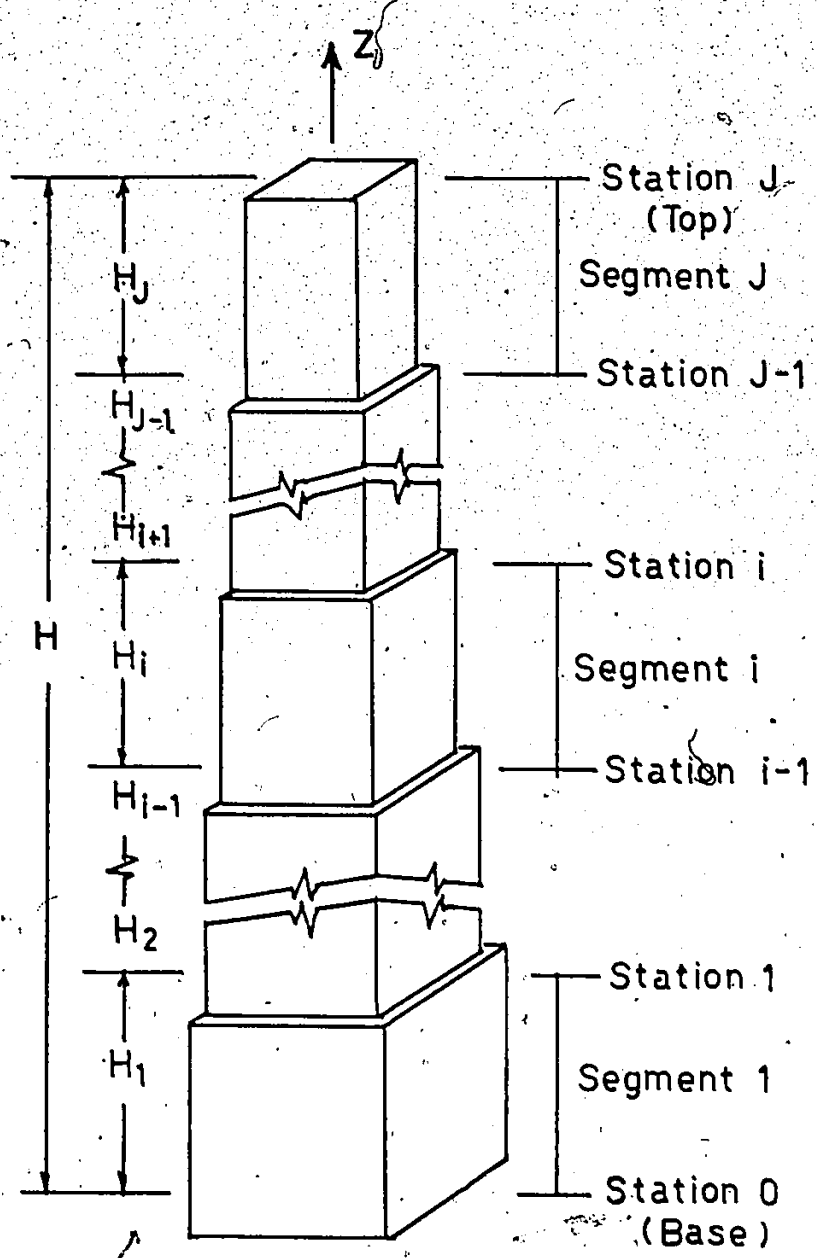


FIG. 4.1 GEOMETRY OF NON UNIFORM SHEAR WALL STRUCTURES

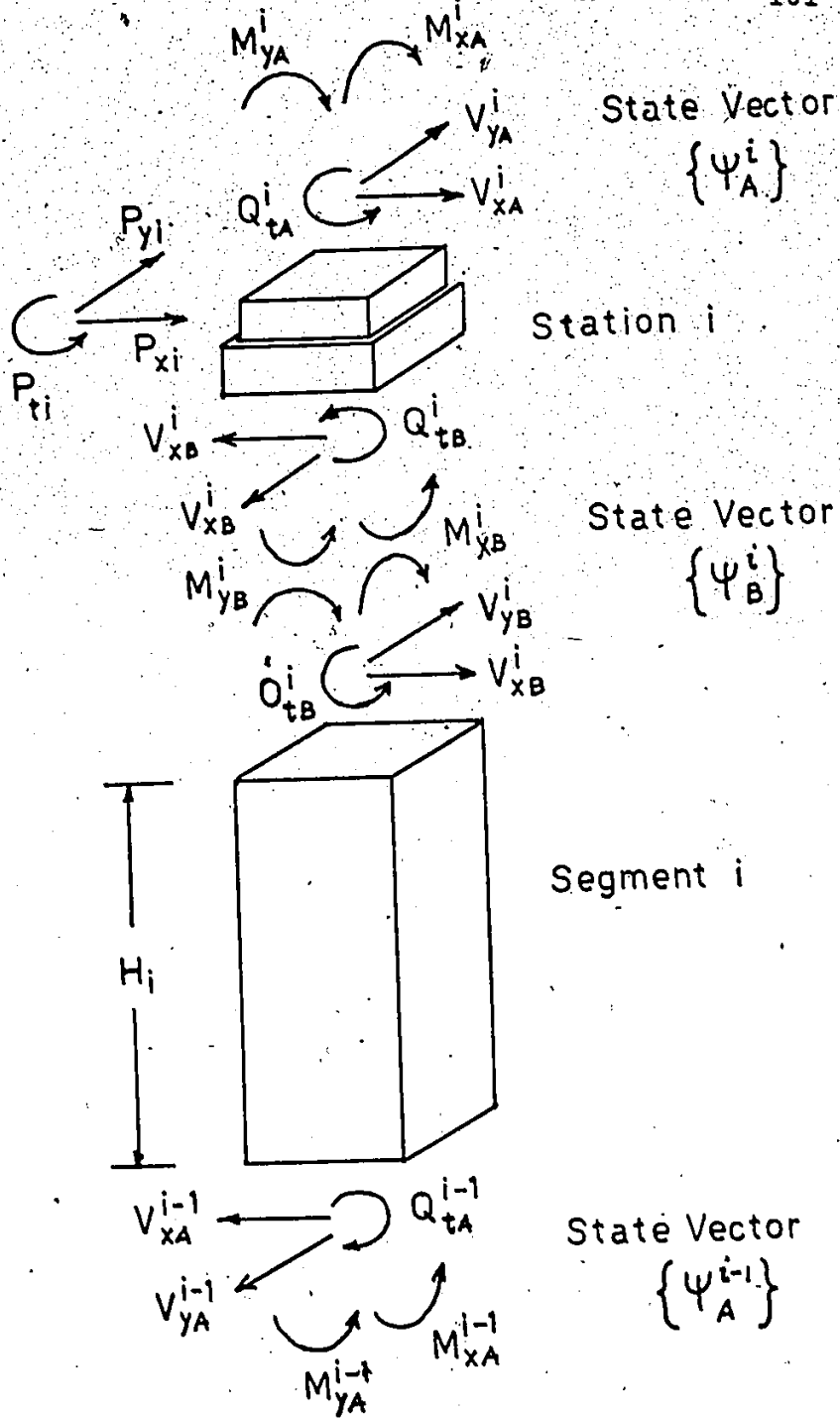


FIG. 4.2 FREE BODY DIAGRAM OF STATION  $i$  AND SEGMENT  $i$



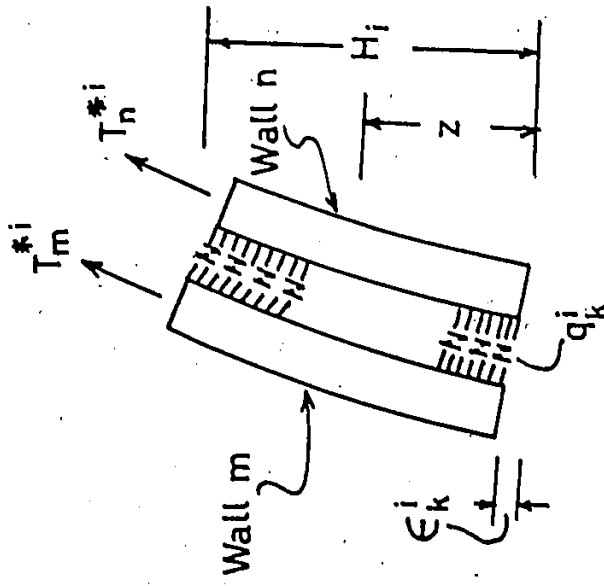
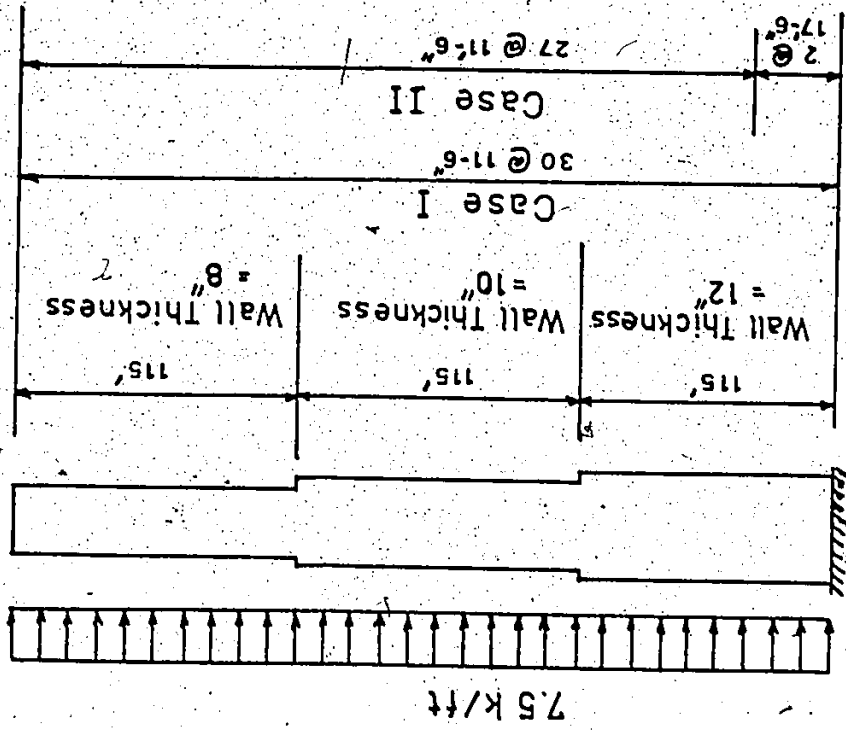
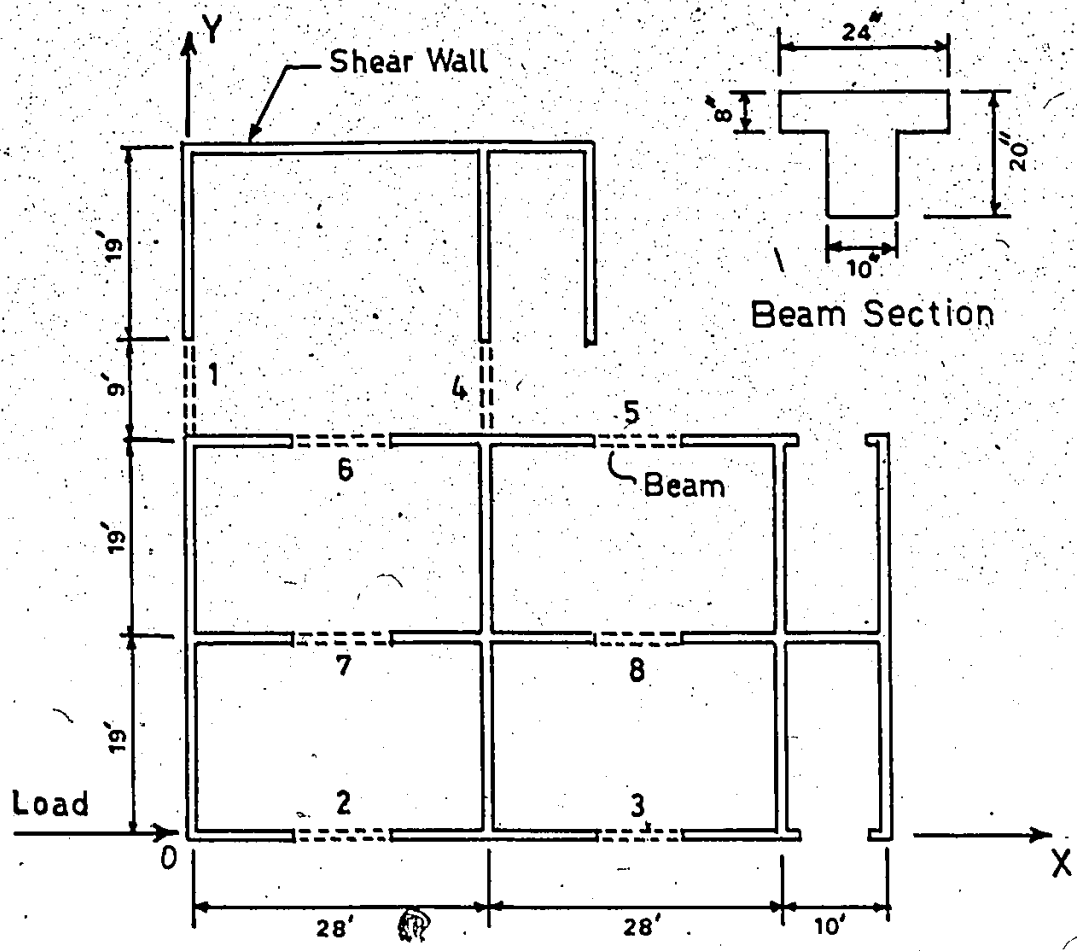


FIG. 4.3

FIG. 4.4 EXAMPLE NON UNIFORM CORE



Slab Thickness 8"  
Modulus of Elasticity  $4.32 \times 10^5$  ksf  
Poisson's Ratio 0.15

FIG. 4.5 LAY OUT OF SHEAR WALLS AND  
CONNECTING BEAMS

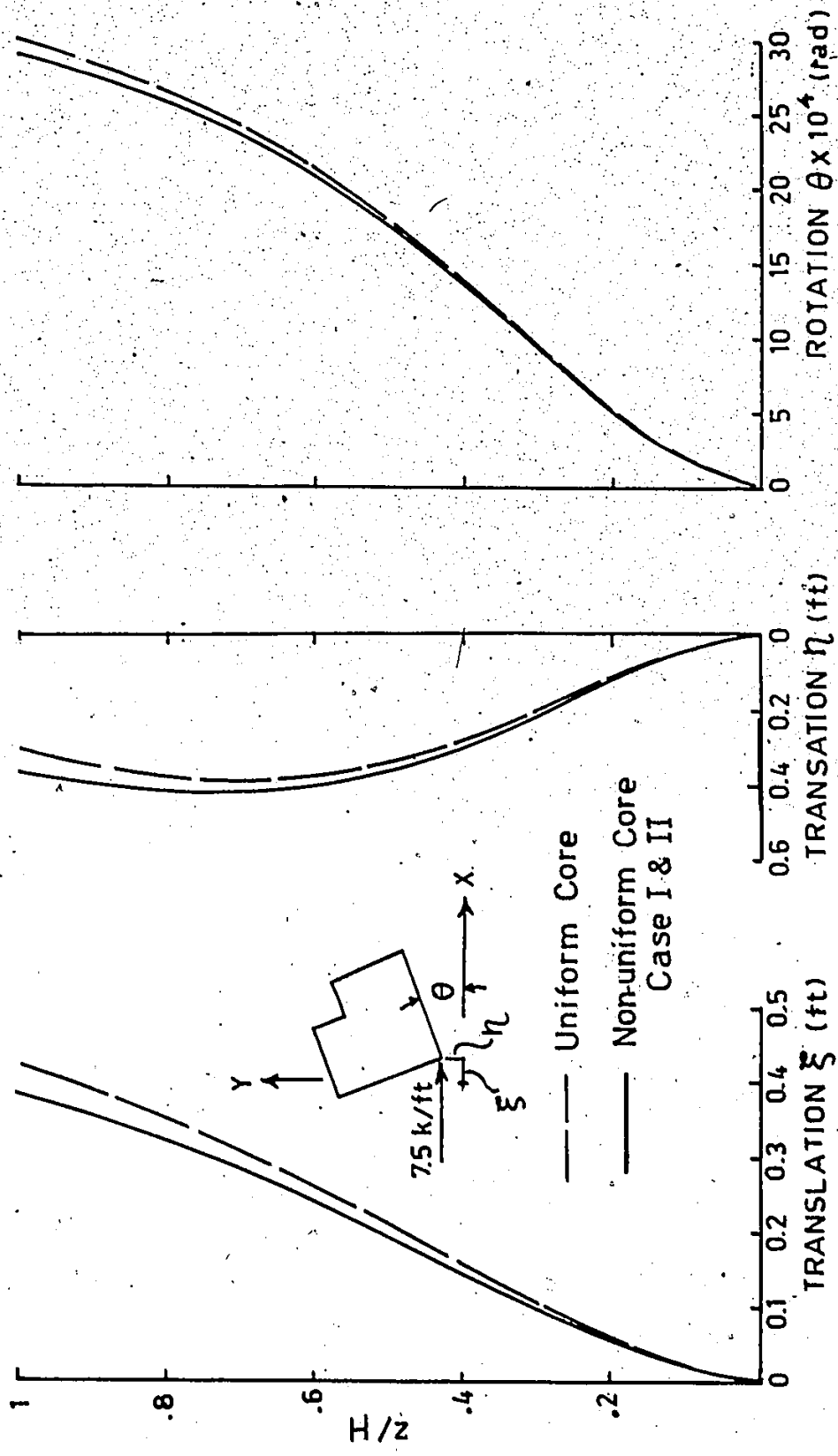
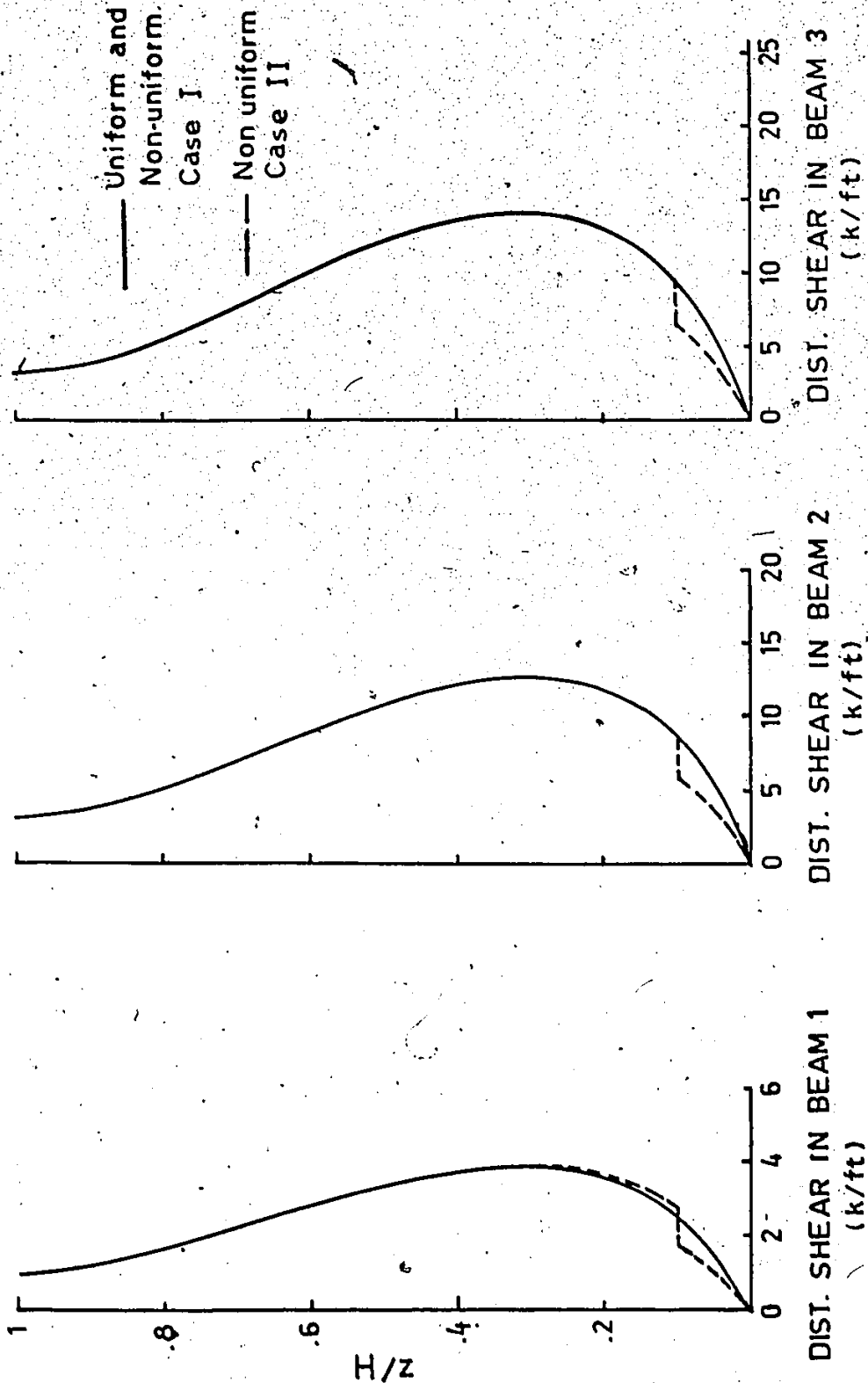


FIG. 4.6 EXAMPLE NON UNIFORM CORE : DISPLACEMENTS



DIST. SHEAR IN BEAM 1      DIST. SHEAR IN BEAM 2      DIST. SHEAR IN BEAM 3  
 (k/ft)                              (k/ft)                              (k/ft)

**FIG. 4.7 EXAMPLE NON UNIFORM CORE : DISTRIBUTED SHEAR IN CONNECTING BEAMS**

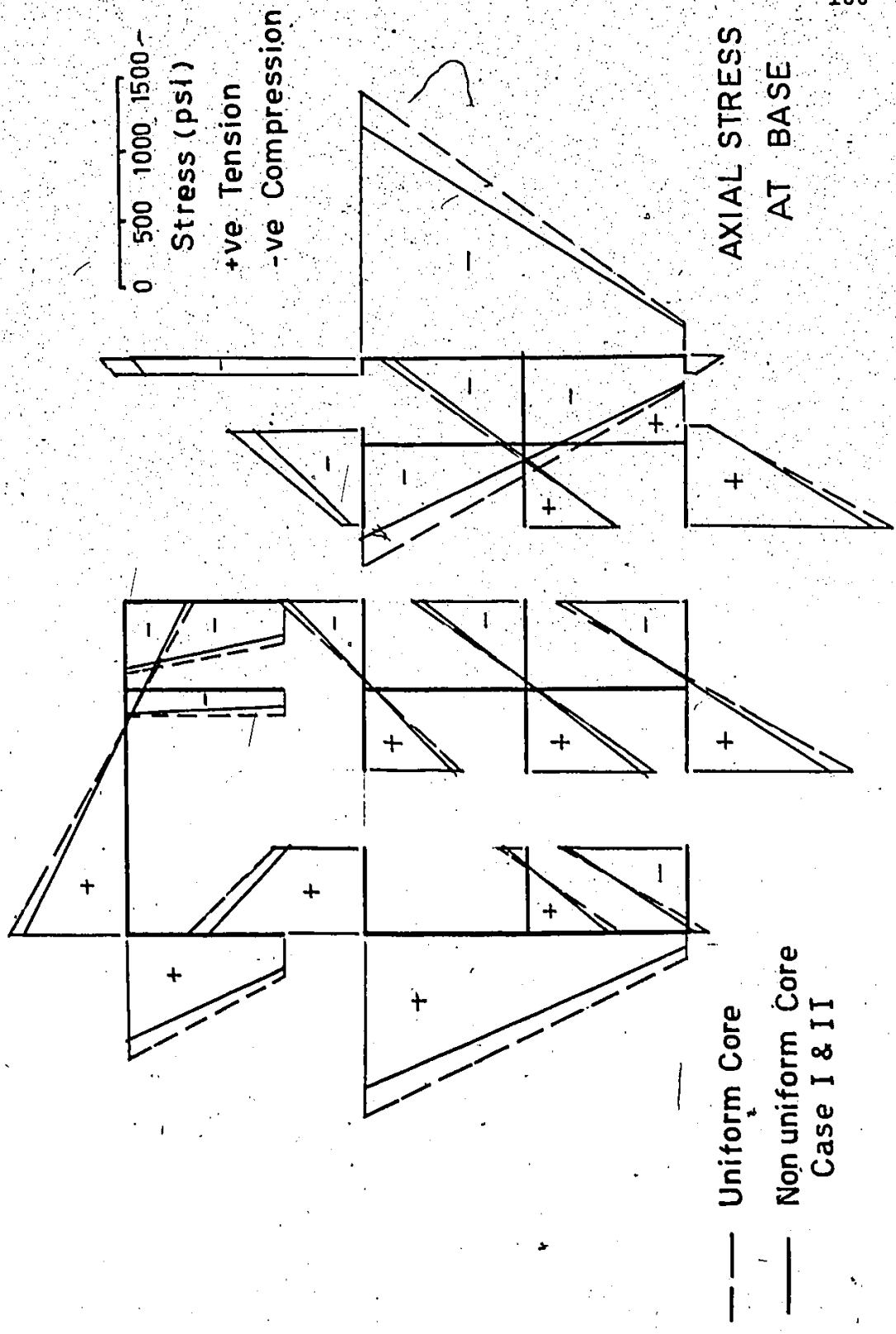


FIG. 4.8 NON-UNIFORM CORE

## CHAPTER V

### DYNAMIC ANALYSIS OF SHEAR WALL BUILDINGS

#### 5.1 Introduction

Buildings located in seismically active areas are subjected to forces due to earthquakes. It is therefore needed to take into account these earthquake forces in design considerations. The National Building Code<sup>(49)</sup> and the recommendations of SEAC<sup>(60)</sup> have provisions of equivalent static lateral forces. The provisions of the above codes are adequate for conventional multi-storey buildings. However, for buildings having irregular or asymmetric layouts, a dynamic analysis becomes necessary. A dynamic analysis consists of two parts. The first part is the determination of the dynamic properties, namely the natural frequencies and the mode shapes. The second part is the prediction of the structural responses for the design earthquakes.

One of the assumptions most commonly made in the dynamic analysis is to lump the mass of the building into a number of chosen levels. Thus, the building is idealised into a multi-degree freedom system which behaves according

to the principles of dynamics<sup>(35, 3)</sup>. With buildings having asymmetric structural plan, the center of mass does not coincide with the center of stiffness. In such cases the dynamic motion of the building consists of coupled translations in two perpendicular directions and rotation about the vertical axis. Medearis<sup>(46)</sup> studied the coupled bending and torsional oscillations of a modern skyscraper the structural system of which consists of an asymmetric arrangement of frames. The floor slab was assumed to be rigid compared to the columns. Thus, a shear building idealization for the individual frames were used in determining their stiffnesses. The natural frequencies and mode shapes were determined. Shepherd and Donald<sup>(62)</sup> studied the response of a torsionally unbalanced building due to a single horizontal component of earthquake motion. The matrix iteration technique was used and the structural response for tower buildings and frame buildings were discussed. Recently, the modal coupling and earthquake response of tall buildings has been studied by Hoerner<sup>(34)</sup>. A continuous idealisation of the building has been used. It was found that significant increase in response may occur in cases where strong modal coupling exists.

The present Chapter deals with the dynamic analysis of high-rise shear wall buildings having asymmetric struc-

tural plan. Lumped mass idealization is used as the mathematical dynamic model. The stiffness matrix of the mathematical model is determined using the static method of analysis presented in Chapter IV. An L-shaped apartment building is taken as an example. The coupled frequencies and mode shapes of the structure are studied. The building is then subjected to earthquake motion in two mutually perpendicular directions at the base. Artificially generated earthquake records are chosen for this purpose. The three-dimensional response of the building due to the earthquake ground motion is then examined in detail to assess the effect of asymmetry. Comparison of the results of the dynamic analysis is made with the provisions in the code of practice.



## 5.2. Notations

The following notations will be used in this Chapter.

$[C]$	= Damping matrix, size $3N \times 3N$ .
$I_m$	= Moment of inertia of mass $m$ about its center of mass.
$\ddot{g}_x, \ddot{g}_y$	= Components of ground acceleration in X and Y direction respectively.
$\ddot{g}_1, \ddot{g}_2$	= Components of ground acceleration acting at an angle $\phi$ with the global axes.
$[K]$	= Stiffness matrix, size $3N \times 3N$ .
$M_m$	= Mass considered at the $m^{\text{th}}$ level.
$[M]$	= Mass matrix, size $3N \times 3N$ .
$N$	= No. of reference levels to be considered.
$\{P\}$	= Loading vector, size $3N$ .
$\ddot{u}_m, \ddot{v}_m$	= Horizontal displacements for the center of mass $m$ in X and Y directions.
$X_m, Y_m$	= Co-ordinates of the center of mass for mass $m$ .
$\alpha, \beta$	= Multiplier for the damping matrix.
$\{\Delta\}$	= Displacement vector, size $3N$ .
$\{\dot{\Delta}\}$	= Velocity vector, size $3N$ .
$\{\ddot{\Delta}\}$	= Acceleration vector, size $3N$ .
$\xi_m, \eta_m, \theta_m$	= Horizontal displacements for point O of mass $m$ in X and Y direction and rotation about OZ axis.

### 5.3. Statement of the Problem

Let us consider a high-rise shear wall building having an asymmetric layout of floor plans. The mass of the building is lumped into  $N$  levels as shown in Figure (5.1).  $OX$  and  $OY$  are orthogonal axes at the base and  $OZ$  is the vertical axis. The displacements of each of the masses is defined by translational displacements in two perpendicular  $OX$  and  $OY$  directions and rotation about the vertical axis. Therefore each mass has three degrees of freedom and the total degree of freedom for the building is  $3N$ . The degrees of freedom for the  $m^{\text{th}}$  mass is illustrated in Figure (5.2).  $\xi_m$  and  $\eta_m$  are the  $X$  and  $Y$  components of the translational displacements of the reference point  $O$  with respect to the base.  $\theta_m$  is the rotation of the mass about  $OZ$  axis.  $C_m$  is the center of mass and its co-ordinates with respect to the reference point  $O$  is taken to be  $(X_m, Y_m)$ . The base of the building is subjected to two mutually perpendicular components of ground acceleration  $\ddot{g}_1$  and  $\ddot{g}_2$  as shown in Figure (5.3). The stiffness of the structure is assumed to be concentrated along the line  $OZ$ . The flexibility matrix of the building is determined by successively applying unit lateral loads and torques at the reference levels and finding the displacements and

rotations at all levels. The static method of analysis as suggested in Chapter IV is used for this purpose. The stiffness matrix can then be obtained by inversion of the flexibility matrix. It is assumed that the material is linearly elastic in the following analysis.

#### 5.4 Equations of Motion

When the structure undergoes dynamic motion, the forces acting to the  $m^{\text{th}}$  mass is shown in Figure (5.4).  $M_m(\ddot{u}_m + \ddot{g}_x)$  and  $M_m(\ddot{v}_m + \ddot{g}_y)$  are the X and Y component of the inertial forces respectively and  $I_m \ddot{\theta}_m$  is the inertial torque.  $M_m$  is the mass at the  $m^{\text{th}}$  level and  $I_m$  is its mass moment of inertia about  $C_m$ .  $\ddot{u}_m$  and  $\ddot{v}_m$  are the X and Y components of the accelerations of the center of mass with respect to the base. They are related to the accelerations of the reference point  $\ddot{\xi}_m$  and  $\ddot{\eta}_m$  by the following relations.

$$\ddot{u}_m = \ddot{\xi}_m - X_m \ddot{\theta}_m \quad (5.1a)$$

$$\ddot{v}_m = \ddot{\eta}_m + Y_m \ddot{\theta}_m \quad (5.1b)$$

$\ddot{g}_x$  and  $\ddot{g}_y$  are the X and Y components of the ground accelera-

tions respectively. They are related to ground accelerations  $\ddot{g}_1$  and  $\ddot{g}_2$  by the following relations.

$$\ddot{g}_x = \ddot{g}_1 \cos\phi - \ddot{g}_2 \sin\phi \quad (5.2a)$$

$$\ddot{g}_y = \ddot{g}_1 \sin\phi + \ddot{g}_2 \cos\phi \quad (5.2b)$$

Where  $\phi$  is the inclination between  $\ddot{g}_1$  and  $\ddot{g}_x$  as shown in Figure (5.3).

The inertial forces developed are resisted by the internal forces of the system. Let  $P_{mx}$  and  $P_{my}$  be the X and Y component of the internal forces and  $P_{m\theta}$  is the internal torque acting at the  $m^{\text{th}}$  mass. These internal forces are related to the displacements of the structure by the following relations.

$$P_{mx} = \sum_{n=1}^N (K_{xx}^{mn} \xi_n + K_{xy}^{mn} \eta_n + K_{x\theta}^{mn} \theta_n) \quad (5.3a)$$

$$P_{my} = \sum_{n=1}^N (K_{yx}^{mn} \xi_n + K_{yy}^{mn} \eta_n + K_{y\theta}^{mn} \theta_n) \quad (5.3b)$$

$$P_{m\theta} = \sum_{n=1}^N (K_{\theta x}^{mn} \xi_n + K_{\theta y}^{mn} \eta_n + K_{\theta\theta}^{mn} \theta_n) \quad (5.3c)$$

where  $K_{xx}^{mn}$ ,  $K_{xy}^{mn}$ ,  $K_{x\theta}^{mn}$  are the elements in the stiffness matrix.  $K_{xx}^{mn}$  means the force acting in the X direction at

level  $m$  due to a unit displacement in the  $X$  direction at level  $n$ ,  $K_{y\theta}^{mn}$  means the force acting in the  $Y$  direction at level  $m$  due to a unit rotation at level  $n$  and so on.

The equilibrium of forces in the  $X$ -direction at the  $m^{\text{th}}$  level leads to:

$$M_m \ddot{\xi}_m - Y_m M_m \ddot{\theta}_m + \sum_{n=1}^N (K_{xx}^{mn} \xi_n + K_{xy}^{mn} \eta_n + K_{x\theta}^{mn} \theta_n) = -M_m \ddot{g}_x \quad (m=1, 2, \dots, N) \quad (5.4)$$

The equilibrium of forces in the  $Y$  direction at the  $m^{\text{th}}$  level leads to :

$$M_m \ddot{\eta}_m + X_m M_m \ddot{\theta}_m + \sum_{n=1}^N (K_{yx}^{mn} \xi_n + K_{yy}^{mn} \eta_n + K_{y\theta}^{mn} \theta_n) = -M_m \ddot{g}_y \quad (m=1, 2, \dots, N) \quad (5.5)$$

The equilibrium of torques about point  $O$  at the  $m^{\text{th}}$  level leads to:

$$\{I_m + M_m (x_m^2 + y_m^2)\} \ddot{\theta}_m - Y_m M_m \ddot{\xi}_m + X_m M_m \ddot{\eta}_m + \sum_{n=1}^N (K_{\theta x}^{mn} \xi_n + K_{\theta y}^{mn} \eta_n + K_{\theta\theta}^{mn} \theta_n) = Y_m M_m \ddot{g}_x - X_m M_m \ddot{g}_y \quad (m=1, 2, \dots, N) \quad (5.6)$$

Equations (5.4, 5.5 and 5.6) can be written in the following matrix form.

$$[M]\{\ddot{\Delta}\} + [K]\{\Delta\} = \{P\} \quad (5.7)$$

Equation (5.7) is the undamped equation of motion. When damping is introduced in the form of equivalent viscous damping, the above equation becomes:

$$[M]\{\ddot{\Delta}\} + [C]\{\dot{\Delta}\} + [K]\{\Delta\} = \{P\} \quad (5.8)$$

Where  $[M]$  and  $[K]$  are the mass matrix and stiffness matrix respectively as explained in Appendix F.  $\{\Delta\}$ ,  $\{\dot{\Delta}\}$ ,  $\{\ddot{\Delta}\}$  and  $\{P\}$  are the displacement, velocity, acceleration and loading vector respectively as explained below.

$$\{\Delta\} = \{\xi_1, \eta_1, \theta_1, \xi_2, \eta_2, \theta_2, \dots, \xi_N, \eta_N, \theta_N\} \text{ col.} \quad (5.8a)$$

$$\{\dot{\Delta}\} = \{\dot{\xi}_1, \dot{\eta}_1, \dot{\theta}_1, \dot{\xi}_2, \dot{\eta}_2, \dot{\theta}_2, \dots, \dot{\xi}_N, \dot{\eta}_N, \dot{\theta}_N\} \text{ col.} \quad (5.8b)$$

$$\{\ddot{\Delta}\} = \{\ddot{\xi}_1, \ddot{\eta}_1, \ddot{\theta}_1, \ddot{\xi}_2, \ddot{\eta}_2, \ddot{\theta}_2, \dots, \ddot{\xi}_N, \ddot{\eta}_N, \ddot{\theta}_N\} \text{ col.} \quad (5.8c)$$

$$\{P\} = \begin{Bmatrix} -M_1 \ddot{g}_x \\ -M_1 \ddot{g}_y \\ Y_1 M_1 \ddot{g}_x - X_1 M_1 \ddot{g}_y \\ \vdots \\ -M_N \ddot{g}_x \\ -M_N \ddot{g}_y \\ Y_N M_N \ddot{g}_x - X_N M_N \ddot{g}_y \end{Bmatrix} \quad (5.8d)$$

[C] is the damping matrix. In the present investigation, it is assumed that the damping matrix is a linear combination of the mass and stiffness matrices as suggested by Clough (15). Thus:

$$[C] = \alpha [M] + \beta [K] \quad (5.9)$$

The percentage critical damping is:

$$\xi_n = \frac{\alpha}{2\omega_n} + \frac{\beta\omega_n}{2} \quad (5.10)$$

Using equation (5.10) it is possible to select the multiplier  $\alpha$  and  $\beta$  so as to provide any desired damping ratio at any two selected modes. In this way a reasonable choice may be

made for the damping matrix  $[C]$ .

#### 5.4 Solution

The undamped natural frequencies of motion can be determined from the solution of the free vibration equation given below.

$$[M]\{\ddot{\Delta}\} + [K]\{\Delta\} = 0 \quad (5.11)$$

Assuming the solution in the form of  $\{\Delta\} = \{\hat{\Delta}\} \sin \omega t$ , the above equation leads to the following eigen-value problem.

$$-\omega^2 [I] + [M]^{-1} [K] \{\hat{\Delta}\} = 0 \quad (5.12)$$

The natural frequencies  $\omega_1, \omega_2, \dots, \omega_N$  and the associated mode shapes  $\{\hat{\Delta}_n\}$  ( $n=1, 2, \dots, N$ ) can be determined from the solution of the eigen-value problem.

To determine the response i.e., the displacement, velocity and acceleration at any instant of time, it is necessary to solve the equation of motion (5.8). The forcing vector  $\{P\}$  depend on the ground acceleration  $\ddot{y}_1$  and  $\ddot{y}_2$  which are complicated functions of time. Therefore,



a step by step procedure is necessary. A procedure suggested by Clough<sup>(15)</sup> is followed in the present study. An incremental form of the equation of motion (5.8) may be written as follows.

$$[M]\{d\ddot{\Delta}\} + [C]\{d\dot{\Delta}\} + [K]\{d\Delta\} = \{dP\} \quad (5.13)$$

where  $\{d\dots\}$  stands for the change of the respective quantities during a small interval of time. Assuming that the acceleration varies linearly during the time increment, the change in acceleration vector can be expressed as:

$$\{d\ddot{\Delta}\} = \frac{6}{dt^2} \{d\Delta\} + \{D(t)\} \quad (5.14)$$

in which

$$\{D(t)\} = -\frac{6}{dt^2} \{\dot{\Delta}(t)\} - 3\{\ddot{\Delta}(t)\} \quad (5.14a)$$

and  $dt$  is the length of the time increment. The time  $t$  in  $\{D(t)\}$  refers to the beginning of the time increment  $dt$ . Similarly, the change in velocity vector can be written as:

$$\{d\dot{\Delta}\} = \frac{3}{dt} \{d\Delta\} + \{F(t)\} \quad (5.15)$$

in which

$$\{F(t)\} = -3\{\dot{\Delta}(t)\} - \frac{dt}{2} \{\ddot{\Delta}(t)\} \quad (5.15a)$$

Substituting equations (5.14 and 5.15) into equation (5.13) leads to the following pseudostatic equation.

$$[\bar{K}]\{d\Delta\} = \{d\bar{P}(t)\} \quad (5.16)$$

in which

$$[\bar{K}] = [K] + \frac{6}{dt^2} [M] + \frac{3}{dt} [C] \quad (5.16a)$$

$$\{d\bar{P}(t)\} = \{dP(t)\} - [M]\{D(t)\} - [C]\{F(t)\} \quad (5.16b)$$

Equation (5.16) can be solved by a standard static analysis procedure for the incremental displacement vector  $\{d\Delta\}$ , and then the total displacement at the end of the time increment is given by:

$$\Delta(t+dt) = \Delta(t) + d\Delta \quad (3.17)$$

Computer programs are prepared to find the natural frequencies, mode shapes, and the structural response due

to applied design earthquake records. The response can be plotted using<sup>a</sup> plotting routine in conjunction with the computer.

### 5.5 Example and Discussion of Results

Let us consider a uniform twenty storey L-shaped apartment building as shown in Figure (5.5). This particular shape is a possible architectural solution for the available space. In the two wings of the building, parallel sets of shear walls are located on both sides of the corridor. The common service core for the two wings houses the elevators and staircase. The shear walls are taken to be 10 inches thick and the floor slab to be six inches thick. The floor height is 9'-6", the modulus of elasticity is  $4.32 \times 10^5$  ksf, and Poisson's ratio is taken to be 0.15. It is assumed that the building is resting on a rigid foundation.

For the dynamic analysis, the mass of the building is lumped into five equally spaced levels. Each level has three degree of freedom. Therefore, the building is idealised into a lumped mass system having 15 degrees of freedom. The stiffness matrix of the structure is determined using the static method of analysis as suggested in Chapter IV. For

that purpose, the floor slab is idealised by 13 connecting beams whose locations are indicated by dotted lines in Figure (5.5). The effective width of the floor slab connecting the cross walls is estimated to be 2.5 feet using the curves given by Quadeer and Stafford Smith<sup>(53)</sup>. This value is used to determine the stiffness of all connecting beams. The shearing deformation of the connecting beams are neglected. The weight of the floor slab and the shear walls are estimated to be 140 lb/ft<sup>2</sup> of floor area per storey. Assuming a uniform distribution of mass on the floor area, the co-ordinates of the center of mass is found to be (52', 58') as shown in Figure (5.6). The location of the center of rigidity as calculated based on a method given by Blume, Newmark and Corning<sup>(5)</sup> is plotted on the same figure.

#### NATURAL PERIODS:

The natural periods of vibration of the building for the first six modes are determined and are presented in Table (5.1). The fundamental period is found to be 1.81 seconds. The fundamental period as given by the formulae in the National Building Code of Canada 1970<sup>(49)</sup> and SEAOC recommendations<sup>(60)</sup> is also shown. It is found that the interpretation of different parameters in the formula is

important. While using the formula  $0.05h_n/\sqrt{D}$ , the parameter  $D$  can be taken either as the total width of the building as 140 feet or the width of the wing as 52 feet. Considering  $D$  as 140 feet leads to a fundamental period of 0.8 seconds which is a gross under estimation of the period. Using  $D$  as 52 feet gives a fundamental period of 1.32 seconds which is lower than the value given by the dynamic analysis by about 25%. The use of the formula  $0.1N$  leads to the fundamental period of 2 seconds which is about 11% higher than the value given by the dynamic analysis.

TABLE 5.1

## NATURAL PERIOD OF VIBRATION (SECS.)

Method Used		M O D E					
		1	2	3	4	5	6
Dynamic Analysis		1.807	1.229	0.905	0.318	0.215	0.160
H. B. C.	$0.05h_n/\sqrt{D}$	0.800*					
		1.320**					
	$0.1N$	2.000					

Notations Used:

$h_n$  = Height of the building in feet above base.

$D$  = Dimension of the building in feet in a direction parallel to the applied forces.

$N$  = Total number of storeys.

\*Fundamental period using  $D$  as the total width of the building in the X direction = 140 feet.

\*\*Fundamental period using  $D$  as the width of the wing = 52 feet.

MODE SHAPES:

The mode shapes associated with the first six modes are plotted in Figure (5.7) and Figure (5.8). Two axes  $\bar{U}$  and  $\bar{V}$  inclined at an angle of  $45^\circ$  to the global X & Y axes, are chosen for plotting the components of translational displacements. It is found that the first mode is predominantly translational in the  $\bar{V}$  direction and the second mode is predominantly translational in the  $\bar{U}$  direction. The third mode exhibit a strong coupling between the torsional and  $\bar{V}$  displacements. The nature of the 4<sup>th</sup>, 5<sup>th</sup> and 6<sup>th</sup> mode is similar to the 1<sup>st</sup>, 2<sup>nd</sup> and 3<sup>rd</sup> mode respectively. However, in these modes, the displacements change direction

in the upper part as compared with the lower part of the building.

#### SEISMIC RESPONSE:

The structural response of the building due to earthquake ground motions is studied next. For this purpose, the artificially simulated earthquake accelerograms type C-1 and C-2 as suggested by Jennings, Housner and Tsai<sup>(40)</sup> are chosen. These accelerograms are scaled so that the maximum value is 8%g. This corresponds to an earthquake of Modified Mercalli intensity VI. These accelerogram records are plotted in Figure (5.9).

The building under study is subjected to four cases of earthquake loading. In the first case the accelerogram C-2 is taken to act in the global X direction. This is the case of a unidirectional earthquake normally used in design considerations. In an actual earthquake there are components of ground motion in two mutually perpendicular directions acting simultaneously. That condition is simulated by applying earthquake motions in two mutually perpendicular directions as in Case II, Case III and Case IV. In Case II the accelerograms C-2 is taken to act in both the X and Y directions. In Case III, the direction of action of earth-

quake in the X direction is reversed as compared with Case II. The earthquakes acting in the two directions are completely correlated in Case II and Case III since the record C-2 is used as ground motions in both directions.

In general, there is no one to one correlation between the ground motions in the two horizontal directions in actual earthquakes. Therefore, another case with two different accelerogram records acting in two directions are used. For that reason Case IV is considered. This case is similar to Case III except the accelerogram record C-2 is replaced by record C-1 acting in the Y direction. The displacements, velocities and accelerations at the reference levels are determined using the step by step procedure as explained in Section (5.4). Using equation (5.9 and 5.10) the damping matrix  $[C]$  is constructed so that the percentage critical damping in the first two modes is 5%. Higher values of damping is used in the higher modes. The percentage critical damping used in the first six modes are tabulated in Table (5.2).

The displacements and accelerations of the reference point O and two corner points A and B are plotted in Figures (5.10 to 5.21).



TABLE 5.2  
DAMPING IN DIFFERENT MODES

MODE	1	2	3	4	5	6
Percentage Critical Damping	5.0	5.0	5.5	12.0	17.4	23.1

In case I where only one component of earthquake is acting in the X direction, the displacements in the Y directions and rotation is caused solely due to the effect of eccentricity. It is noticed from Figures (5.10 to 5.12) that the motions exhibit very strong coupling between translational and torsional modes.

In case II, with a bi-directional earthquake, the building undergoes very little torsional motions as shown in Figures (5.13 to 5.15). The motion in the X and Y directions are completely in phase. It is observed from Figure (5.15) that all points in the cross section of the building are undergoing a rectilinear motion in an angle approximately 45 degrees with the X axis. This behaviour can be explained with the help of Figure (5.22a) where the center of mass and the approximate center of rigidity is plotted. This center of rigidity is obtained by assuming the floor slab to be completely flexible in the out-of-plane direction<sup>(5)</sup>.

It is observed that the center of mass and the approximate center of rigidity lies on a line which is inclined at an angle approximately 45 degrees with the X axis. The resultant inertial force is acting approximately in the same direction as shown in Figure (5.22a). Therefore, a predominantly rectilinear motion is observed in this case.



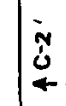

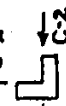
In case III in which the direction of acceleration in the X direction is reversed, the resultant inertial force is acting perpendicular to the line joining the center of mass and the center of rigidity as shown in Figure (5.22b). As observed in Figures (5.16) and (5.17), very high torsional response is present. Consequently the translational displacements and accelerations at points O, A and B are higher than that in the previous cases considered. From Figure (5.18) it is shown that point O undergoes approximately a rectilinear motion in the direction of the resultant inertial force. Point A and B describe two dimensional curves as shown in the figure. The predominant directions of motion of points O, A and B are shown by an arrow in Figure (5.22b). From these directions of motion, the approximate center of rotation of the building for this earthquake case can be determined as shown.

In case IV a different accelerogram record is used in the Y direction. The response of the building is plotted

in Figures (5.19 to 5.21). It is found that the maximum displacements at points O and B are smaller and at A are larger than that obtained in case III. Therefore, uncorrelated ground motion may not necessarily give a reduced response of the structure.

The maximum radial displacements and accelerations at O, A and B for different cases of earthquake are tabulated in Table (5.3). An additional case with a single accelerogram record C-2 acting in the Y direction is included in the table and listed under case I(a). It is found that the bidirectional earthquake oriented in the worst direction leads to an increase of displacement by a factor of 2 and acceleration by 50% as compared with the unidirectional cases. Therefore, the response due to unidirectional earthquake along global directions of an irregularly shaped building multiplied by a factor of  $\sqrt{2}$  is inadequate to cover the worst case of loading. Among all the cases considered, case III and case IV are found to be the critical cases for design. The maximum displacement and acceleration are found to be 0.336 feet and  $12.56 \text{ ft/sec}^2$  respectively and both occurred at point A.

TABLE 5.3  
MAXIMUM RADIAL RESPONSE

Earthquake Input	Maximum Radial Disp. at 0 (ft)	Maximum Radial Accl. at 0 (ft/sec <sup>2</sup> )	Maximum Radial Disp. at A (ft)	Maximum Radial Accl. at A (ft/sec <sup>2</sup> )	Maximum Radial Disp. at B (ft)	Maximum Radial Accl. at B (ft/sec <sup>2</sup> )
Case I 	0.158	6.05	0.178	6.84	0.167	8.80
Case I(a) 	0.150	6.12	0.181	8.51	0.166	7.05
Case II 	0.217	10.86	0.225	11.37	0.214	10.37
Case III 	0.292	8.96	0.286	8.76	0.300	10.88
Case IV 	0.266	8.25	0.336	12.56	0.226	10.13

## 5.6 Conslusions

A method of determining the natural periods, mode shapes and the seismic response of high-rise shear wall buildings has been presented. It can handle uniform or non-uniform buildings with asymmetric layout of shear walls. It is also permissible to apply two components of earthquake motions at two mutually perpendicular directions. As an example to illustrate the power of the technique, the coupled torsional and translational vibration of an L-shaped apartment building was studied in detail.

Based on the structural response of the example building, the following conclusions can be drawn.

- (a) For buildings having asymmetry in plan layout, the ground motions due to earthquake will induce a three-dimensional motion. The motion consists of translational motions in two mutually perpendicular directions and rotation about the vertical axis. A study of the natural frequencies and mode shapes is helpful in understanding the structural behaviour under dynamic loading.
- (b) The structural response of the asymmetric building will depend on the direction of applied ground motion at the base. A single component of the design earth-

quake acting in any axis of the building normally does not cover the worst possible case for design. This is because of two factors. Firstly, in actual earthquakes, there are two components of motion in two mutually perpendicular directions. Secondly, because of the center of mass is eccentrically located with respect to the center of rigidity, the orientation of the earthquake is an important factor which governs the response. When the earthquake is oriented in such a way that the resultant acts in the direction perpendicular to the line joining the center of mass and the center of rigidity, there will be amplification of the response due to the torsional coupling. Therefore, an approximate location of the center of mass and the center of rigidity is very useful in choosing the critical direction for earthquake excitation calculations.

- (c) It is observed that when subjected to earthquake, each point of the building undergoes two-dimensional gyrating motions. Therefore, the vertical resisting elements like columns and walls will be subjected to simultaneous deformations in two perpendicular directions. Most of the laboratory testing to study the behaviour of columns and walls are conducted with deformation in

one direction only. Recommendations on the ductility, joint detailing and other design parameter are made on the basis of these unidirectional test results. The question may arise therefore that how these tests results relate to the situations where there are simultaneous deformations in two perpendicular directions.

- (d) When the two components of ground motion are uncorrelated, it will be more difficult to find the critical orientation of excitation and corresponding maximum response. From the limited study performed it is found that the uncorrelated ground motions may give more severe response as compared with the completely correlated case at certain points of the building. The information about the correlation of the various components of earthquake is scarce<sup>(50)</sup>. It is felt that more research work in this field is necessary to make specific conclusions.

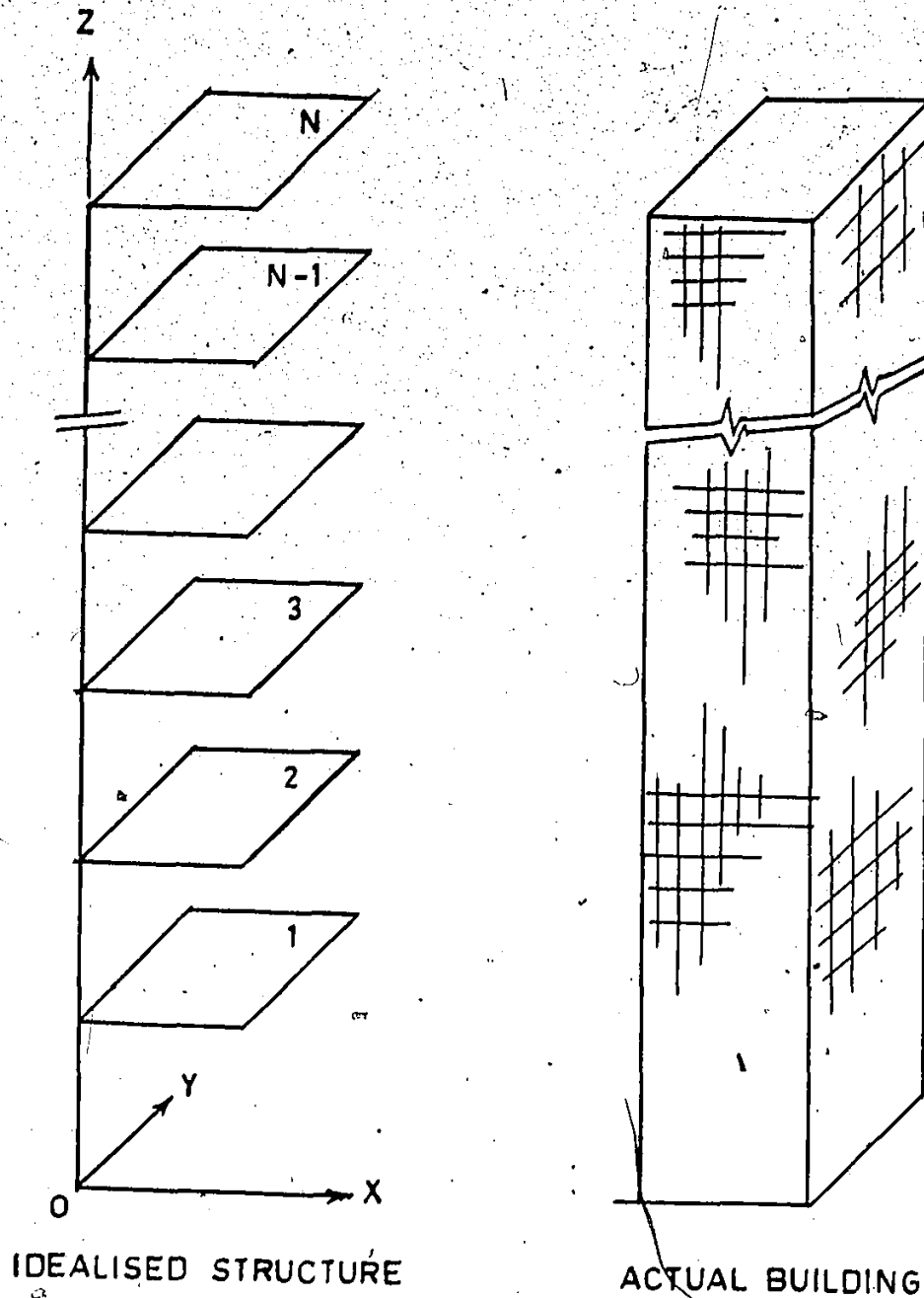


FIG. 5.1 MATHEMATICAL MODEL FOR DYNAMIC ANALYSIS



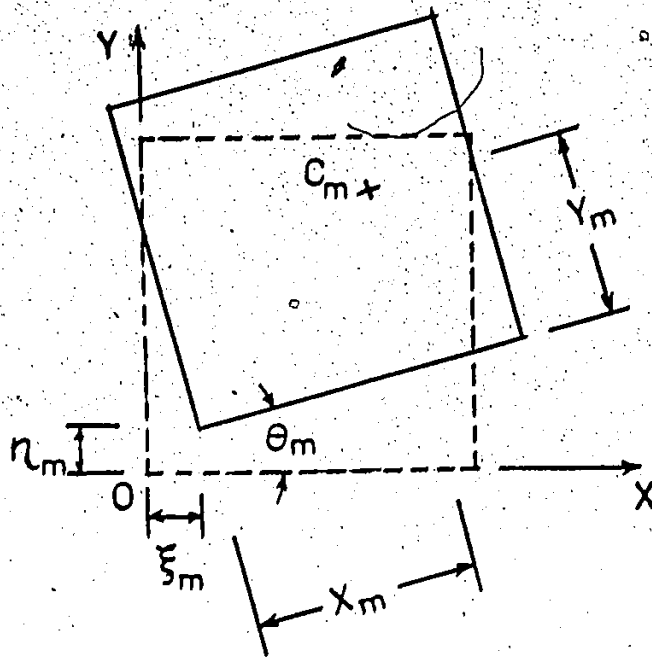


FIG. 5.2 DEGREE OF FREEDOM FOR MASS  $m$

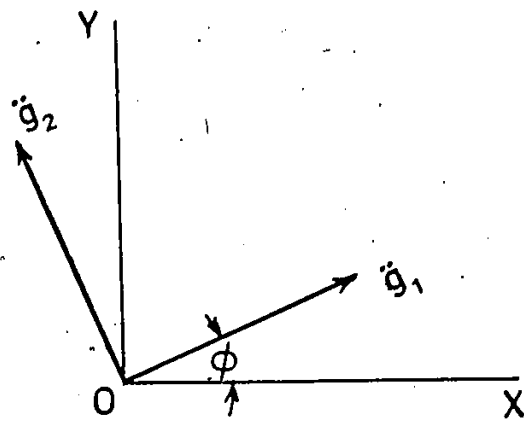


FIG. 5.3 ACCELERATIONS AT THE BASE

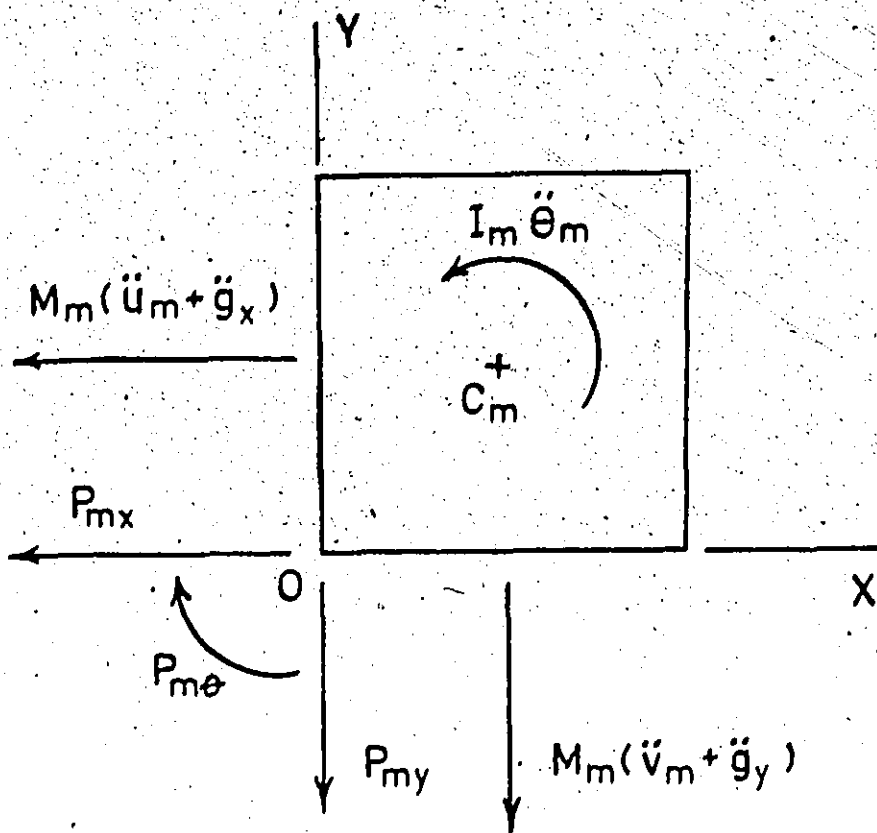


FIG. 5.4 FORCES ACTING ON MASS  $m$

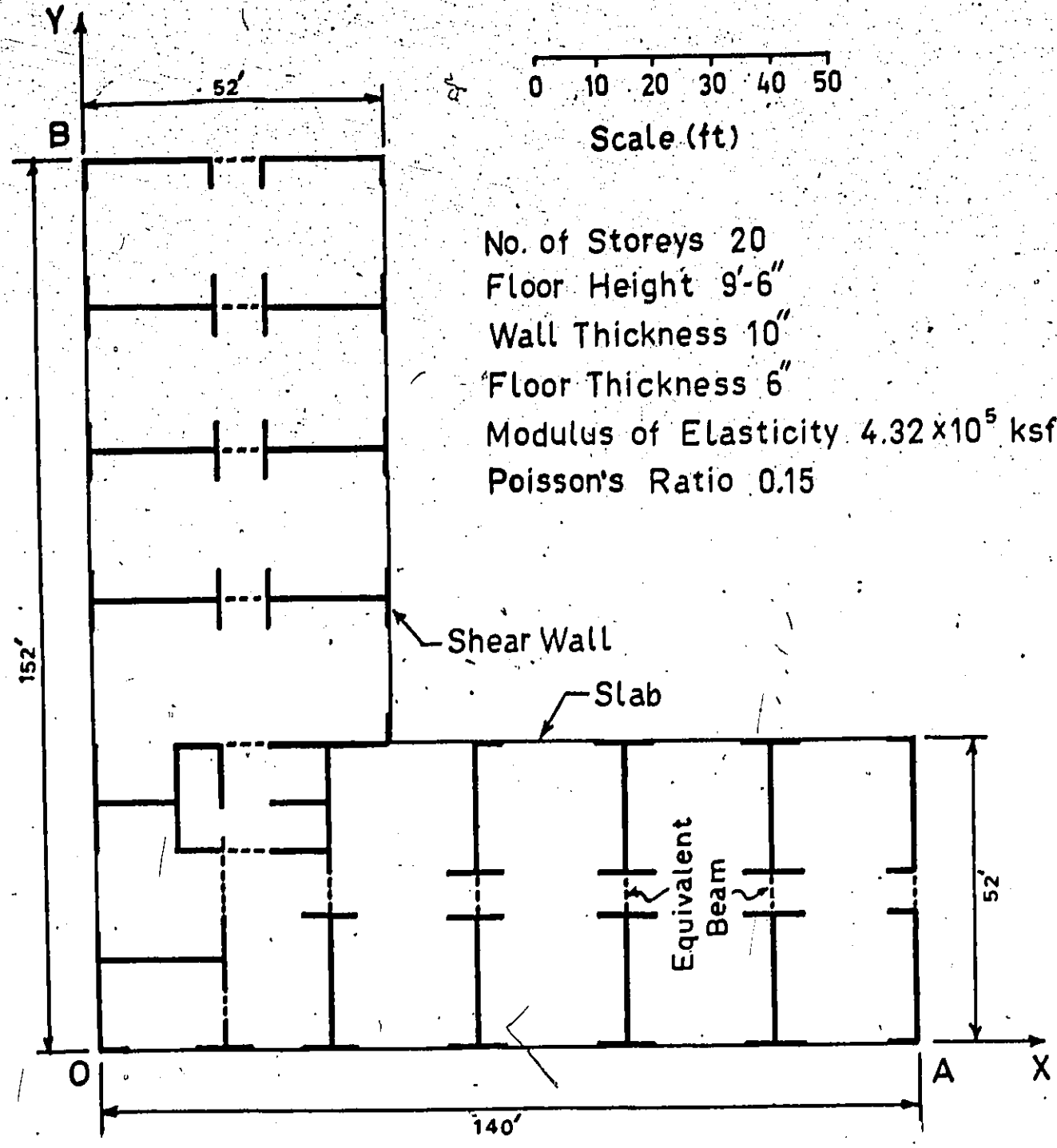
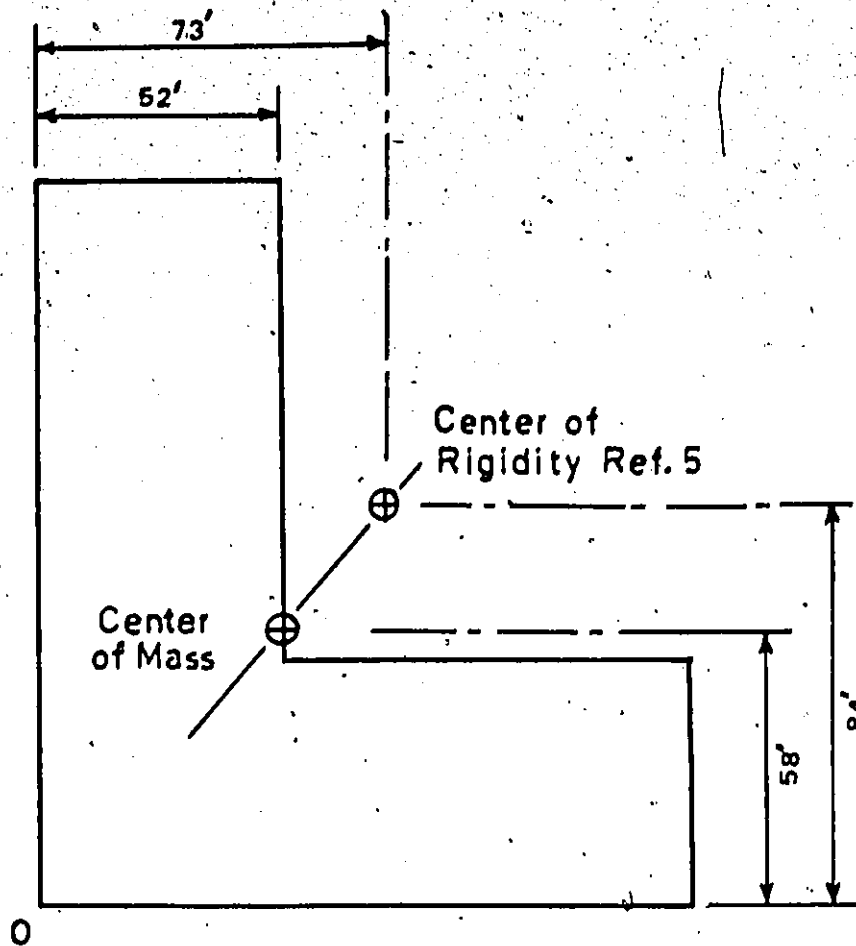


FIG. 5.5 STRUCTURAL PLAN OF A L SHAPED APARTMENT BUILDING

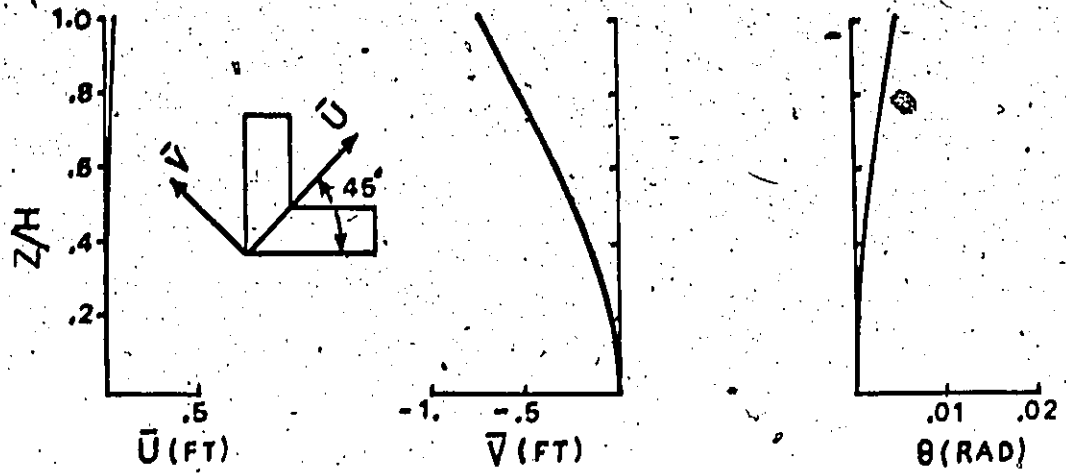


Weight per Storey 1747 k

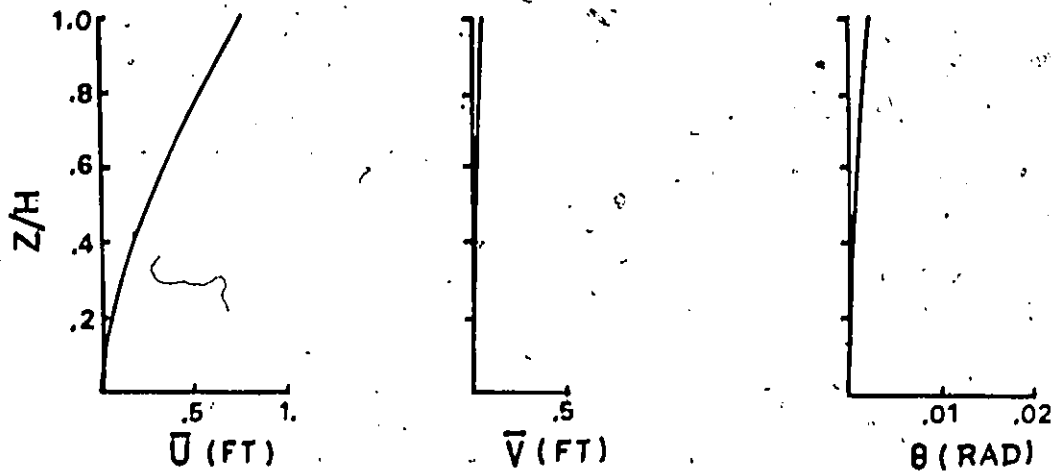
Mass Moment of Inertia per  
Storey About Center of Mass  $5.57 \times 10^6$  k-ft<sup>4</sup>

FIG. 5.6 MASS CHARACTERISTIC OF THE  
L-SHAPED BUILDING

MODE 1



MODE 2



MODE 3

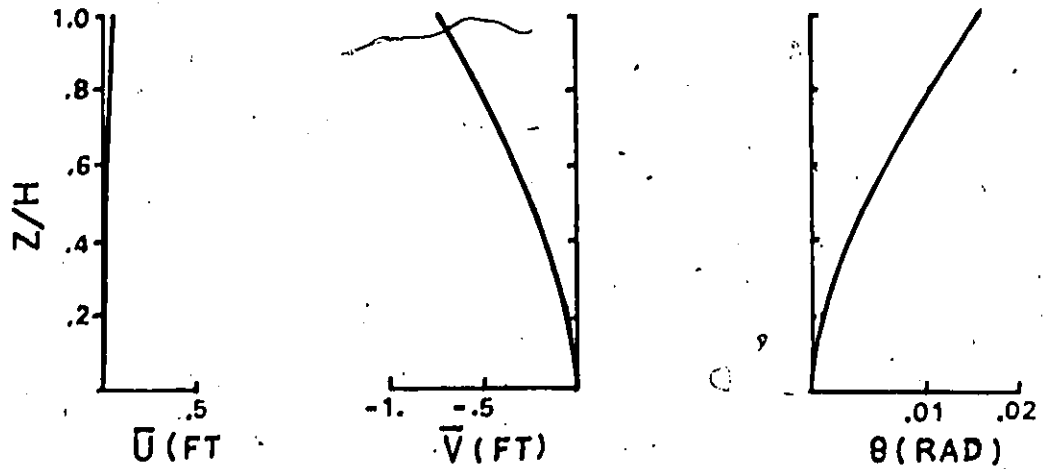
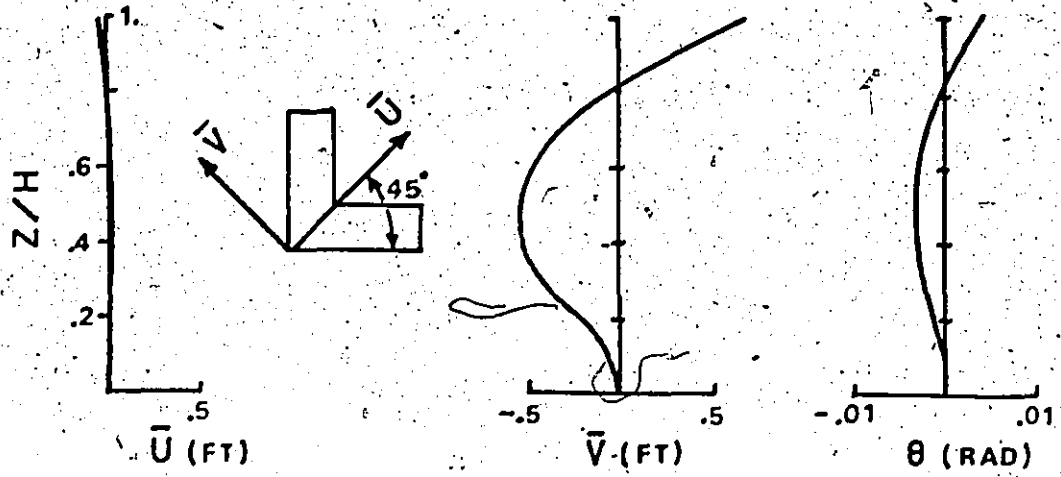
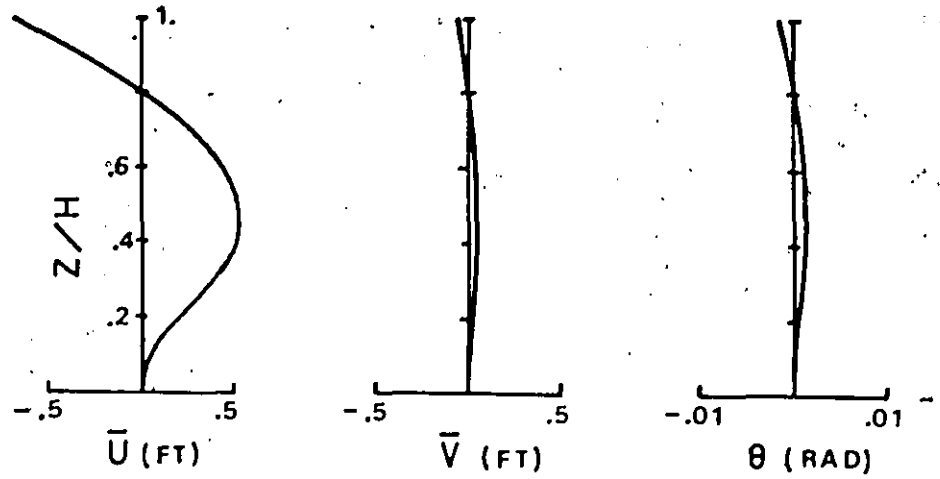


FIG. 5.7 MODE SHAPES

MODE 4



MODE 5



MODE 6

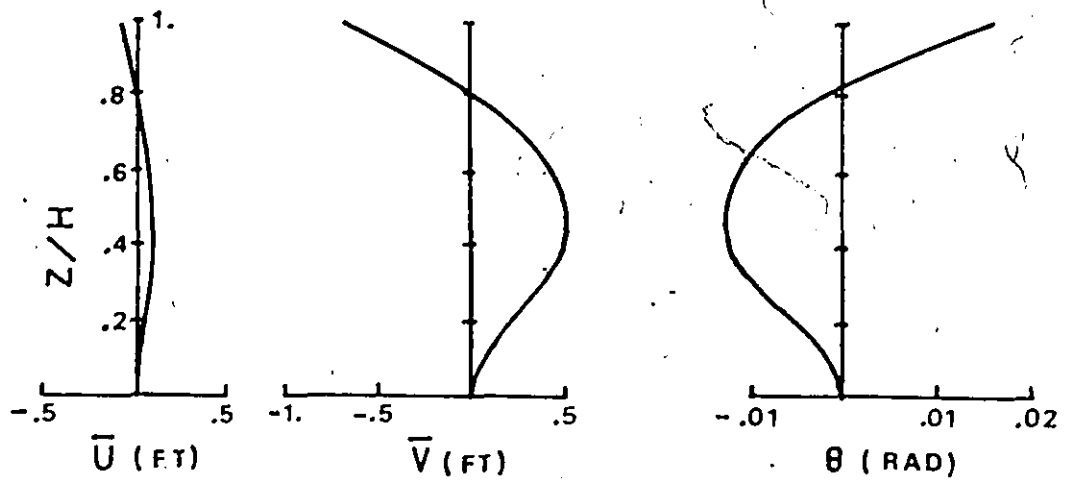


FIG. 5.8 MODE SHAPES

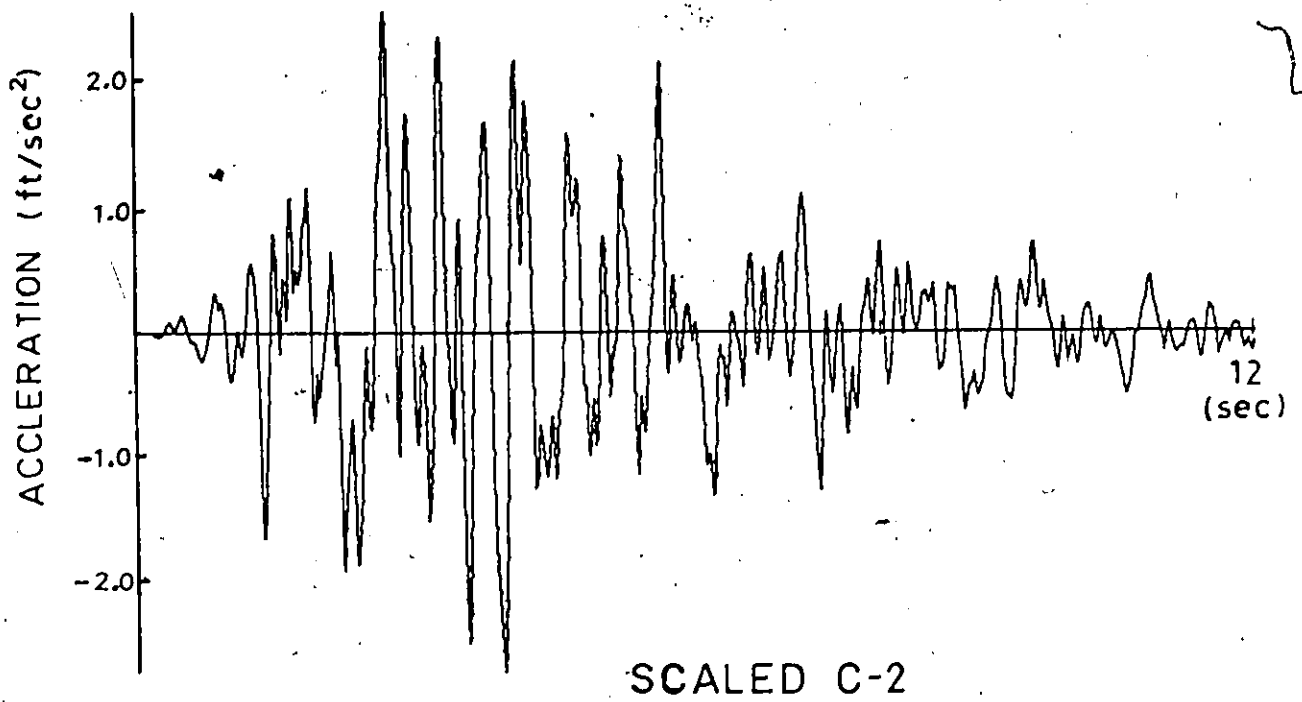
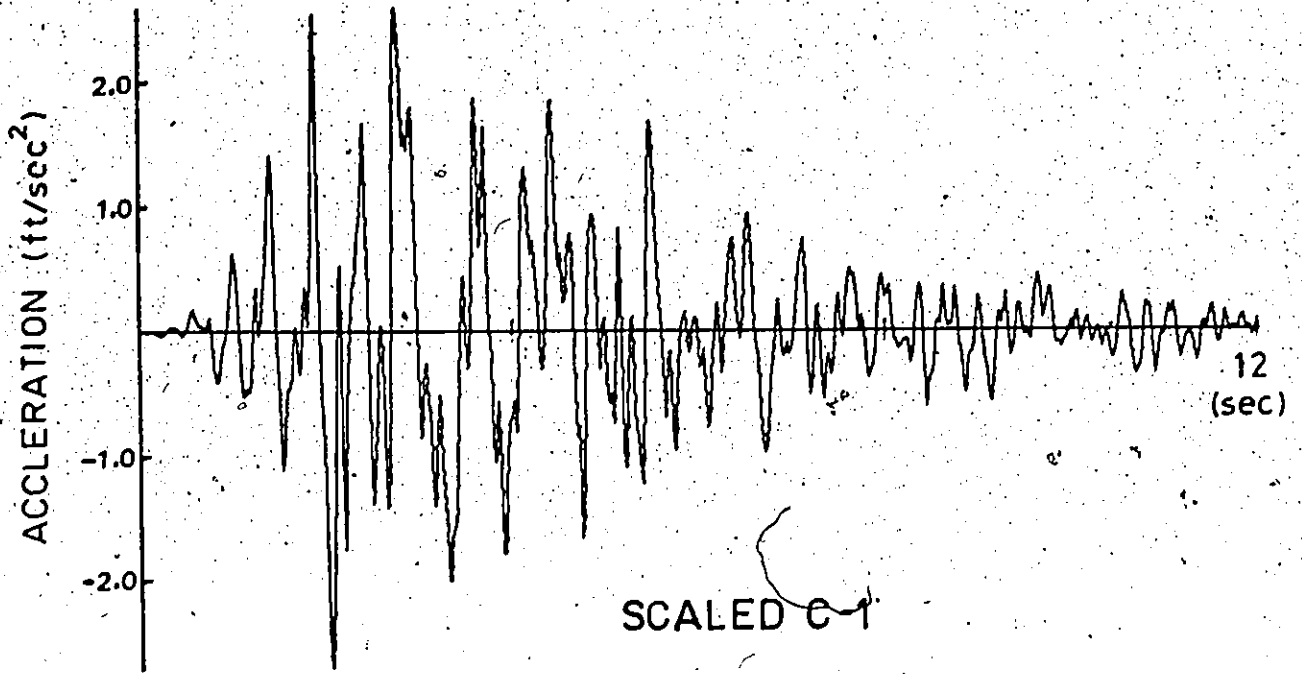
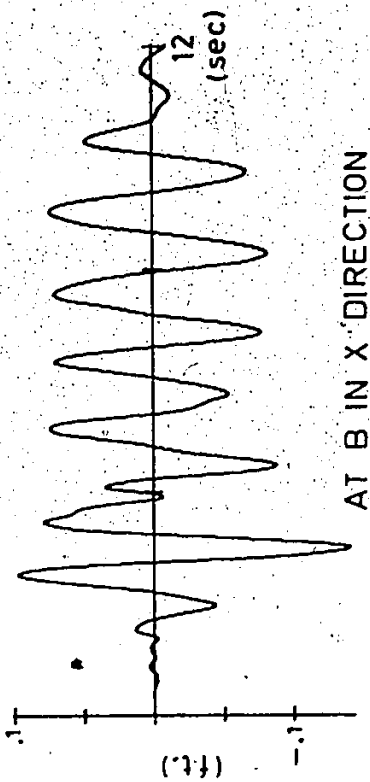
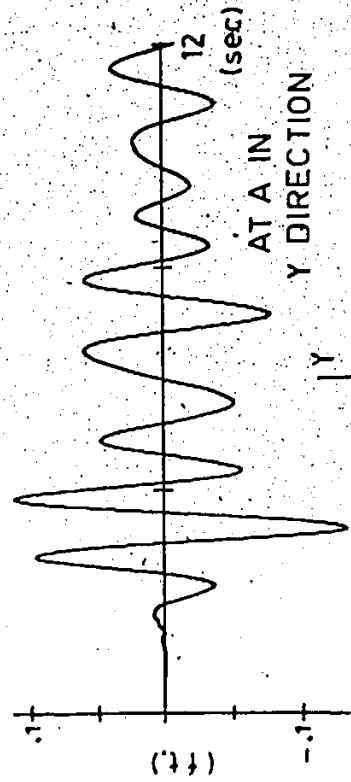


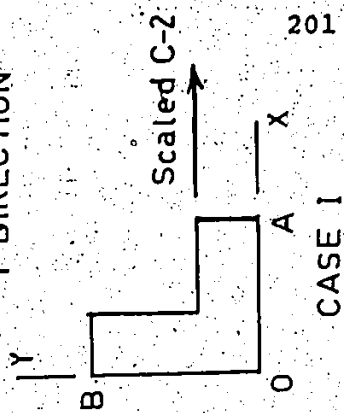
FIG. 5.9 ARTIFICIALLY GENERATED EARTHQUAKES



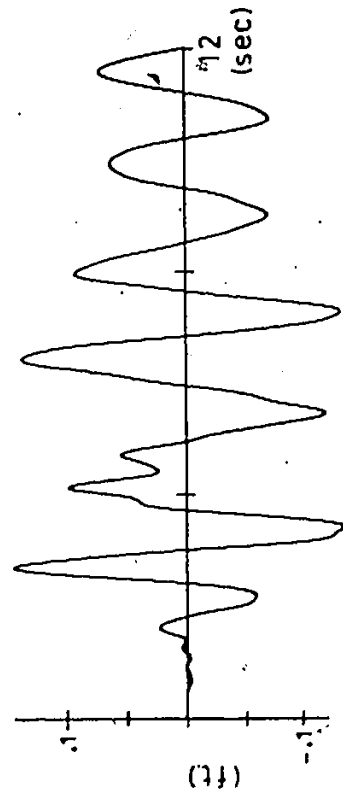
AT B IN X DIRECTION



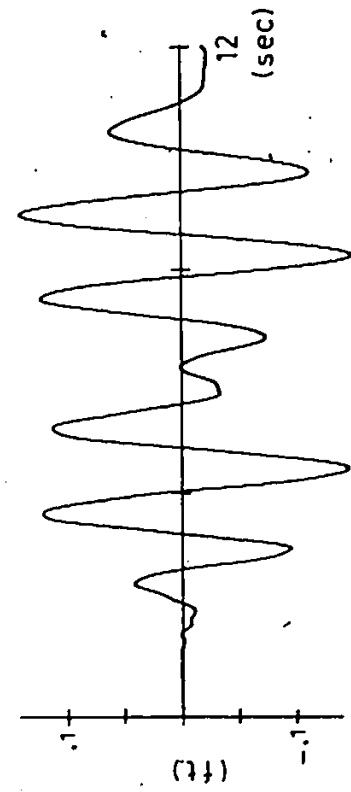
AT A IN Y DIRECTION



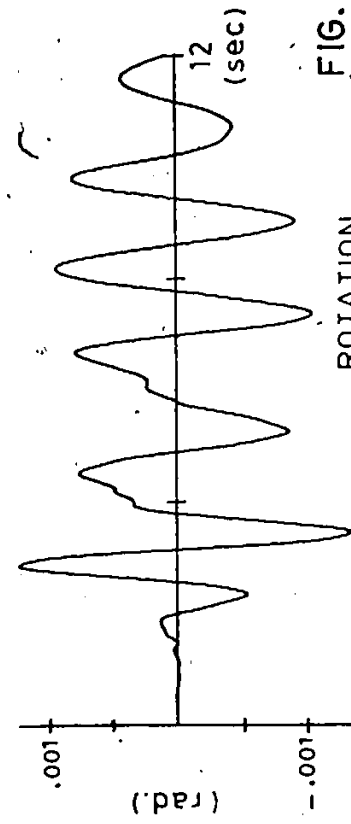
201



AT O IN X DIRECTION



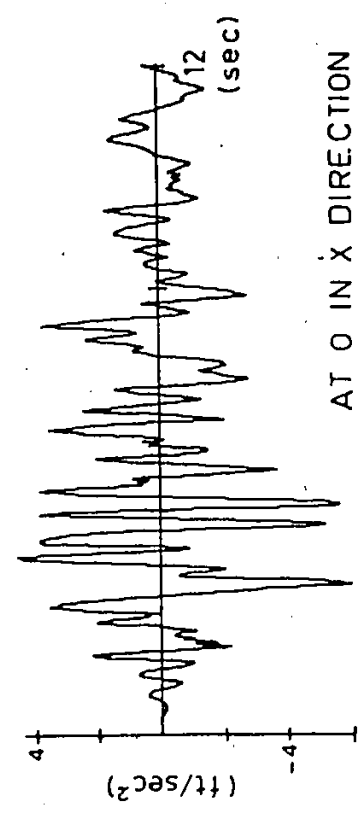
AT O IN Y DIRECTION



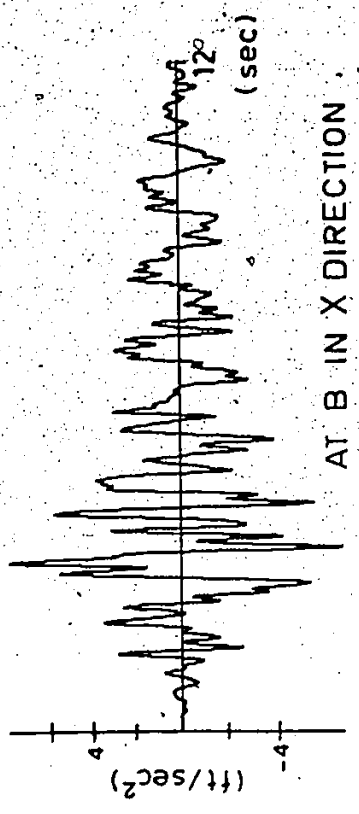
ROTATION

FIG. 5.10 TIME HISTORY OF DISPLACEMENT

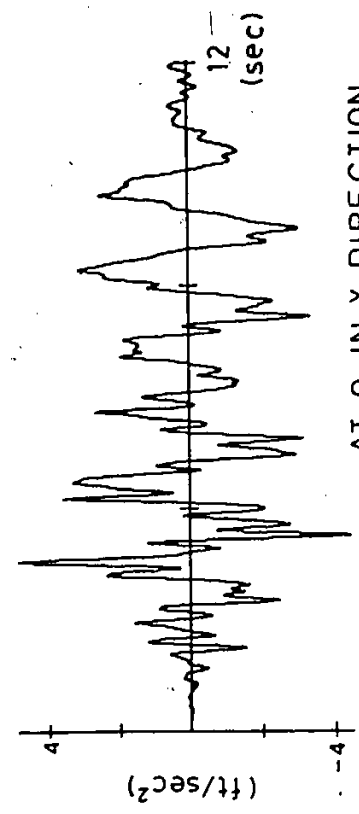




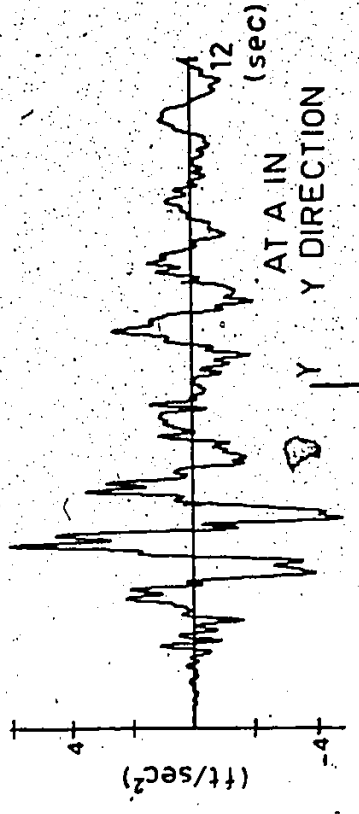
AT O IN X DIRECTION



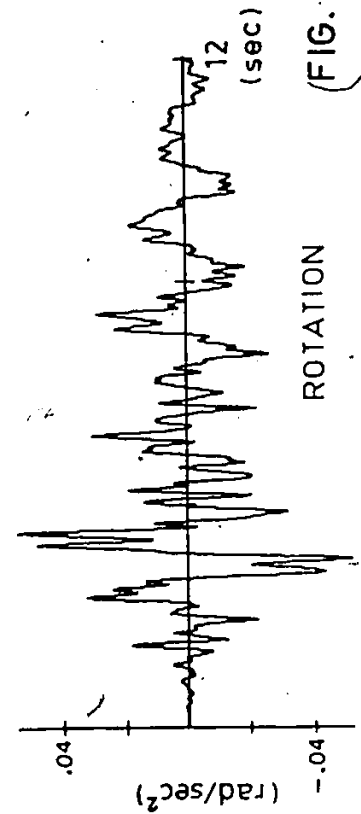
AT B IN X DIRECTION



AT O IN Y DIRECTION



AT A IN Y DIRECTION



ROTATION

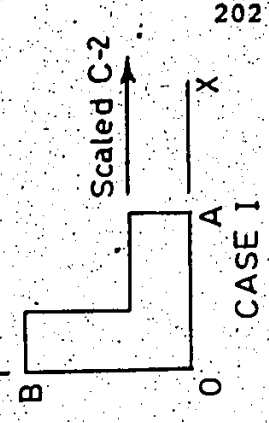
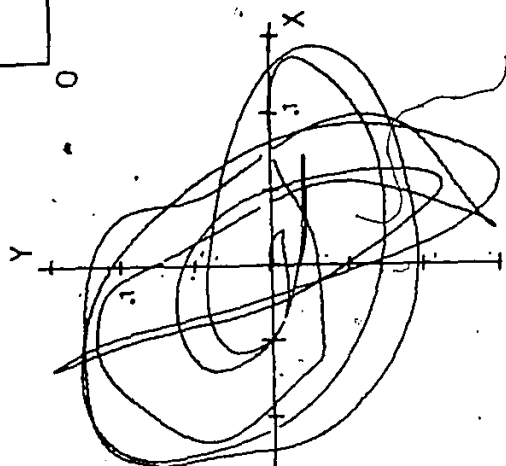
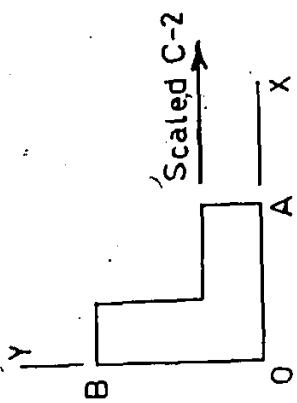
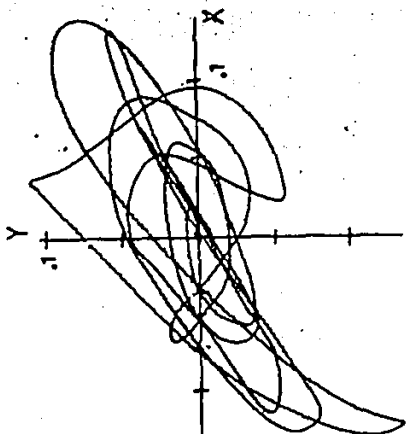


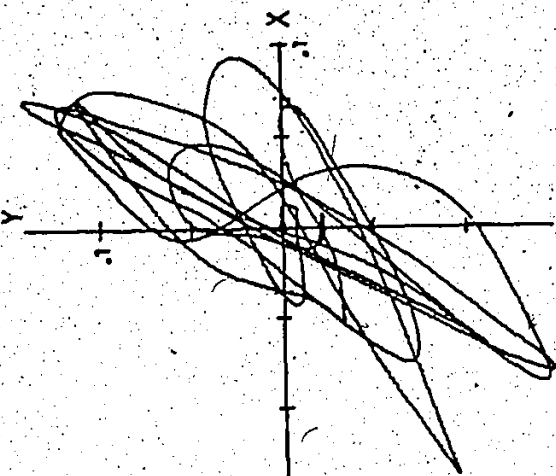
FIG. 5.11 TIME HISTORY OF ACCELERATION



AT O



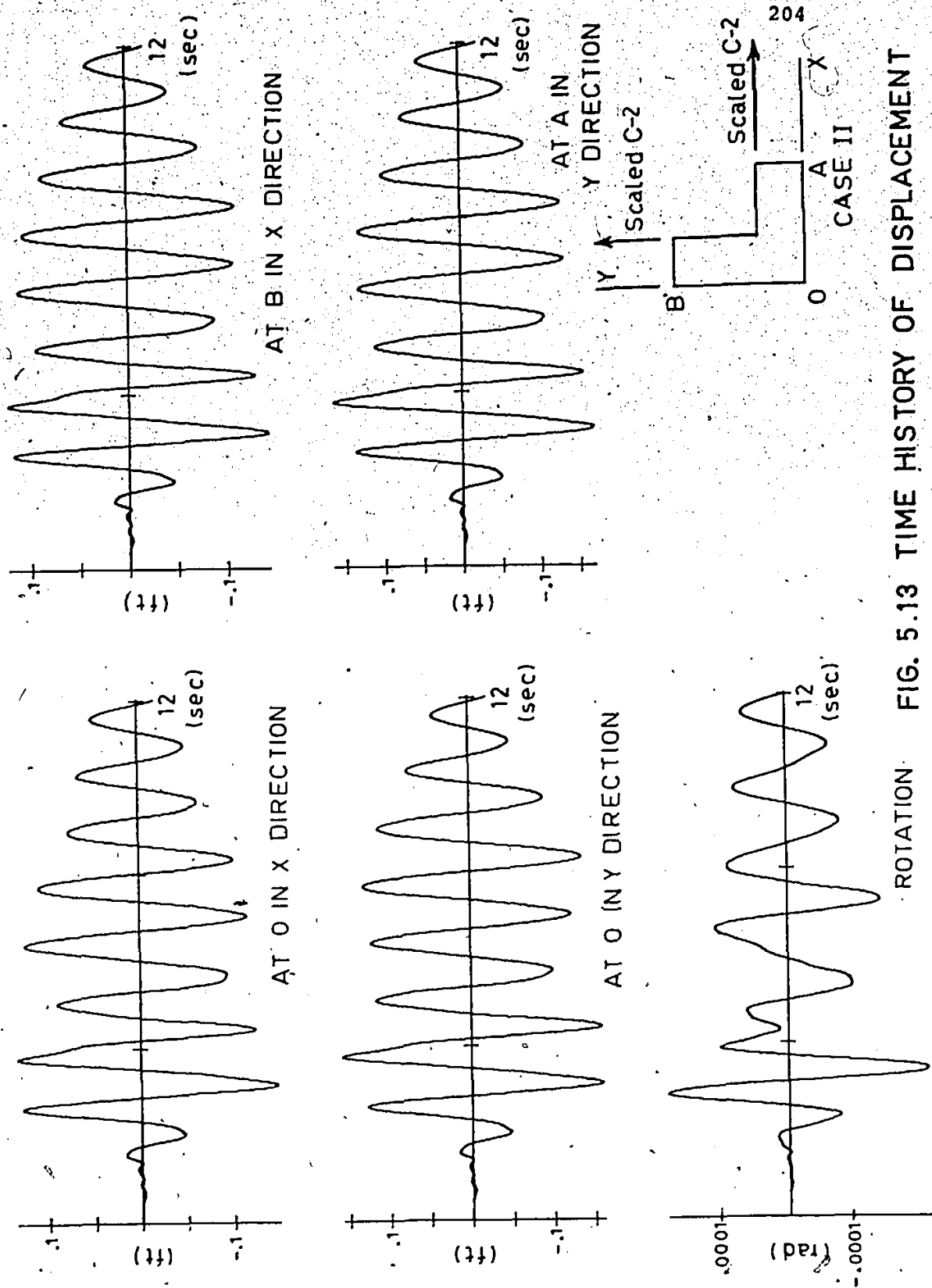
AT A



AT B

(Units are in ft)

FIG. 5.12 GYRATING MOTIONS



ROTATION FIG. 5.13 TIME HISTORY OF DISPLACEMENT

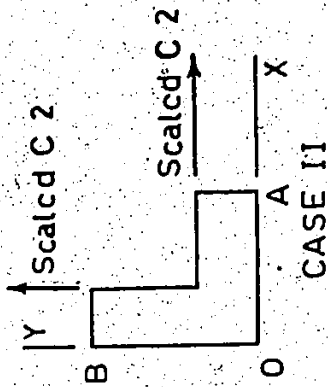
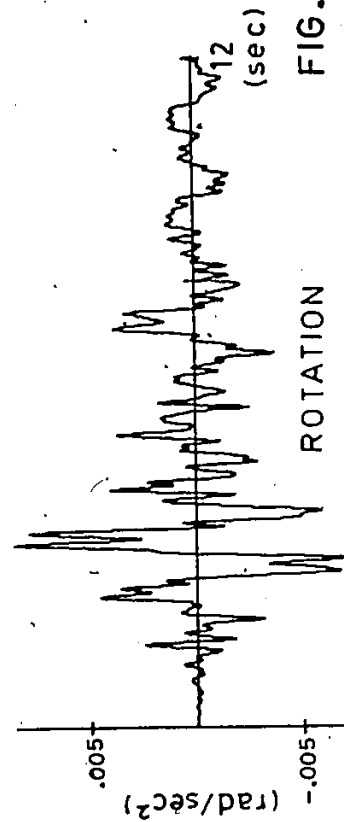
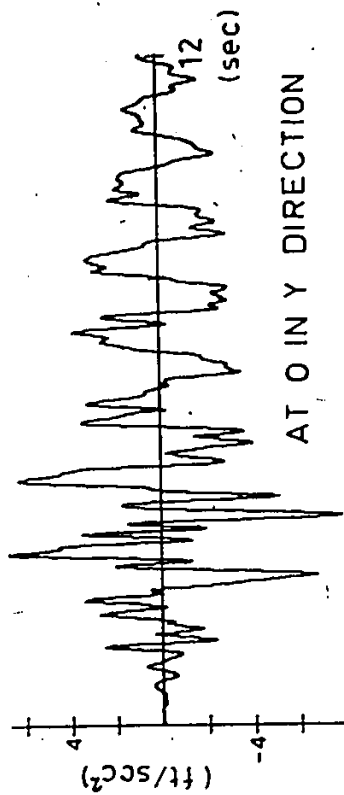
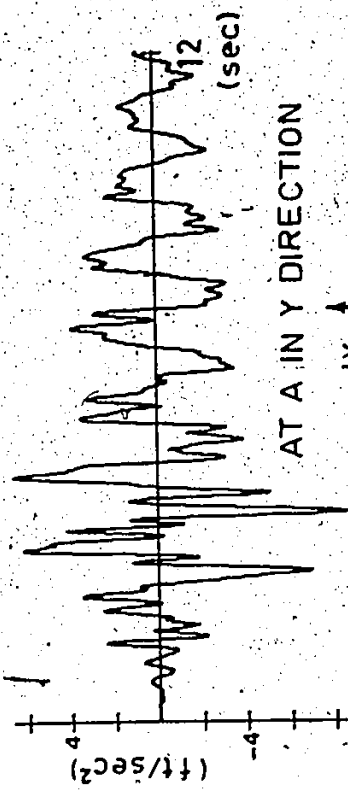
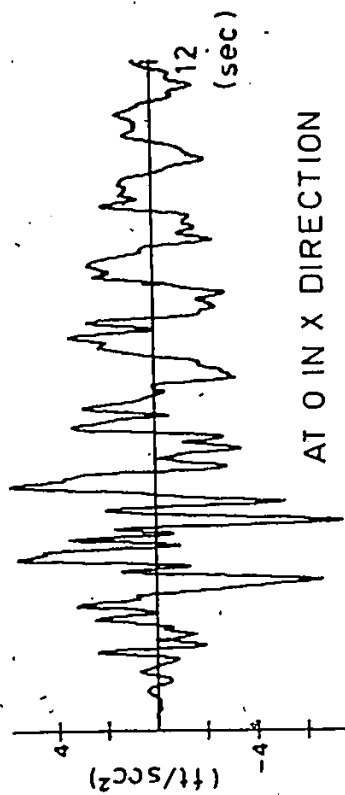
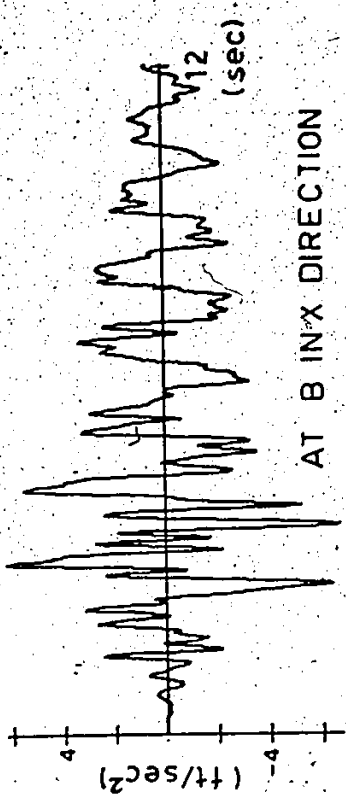
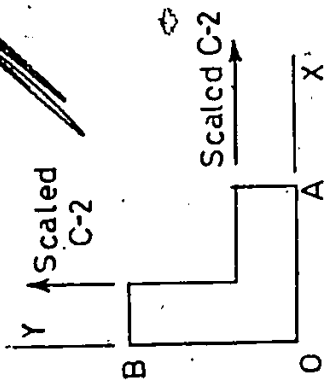
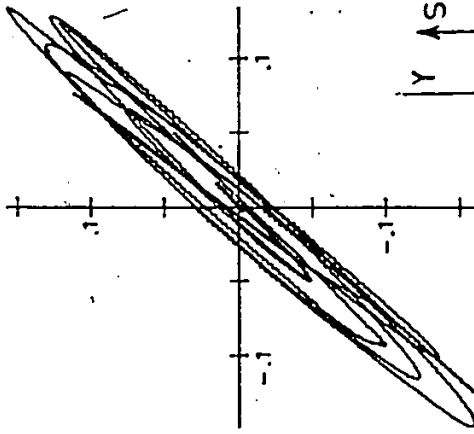
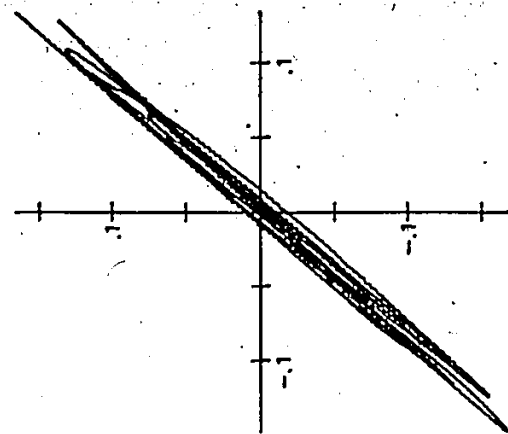
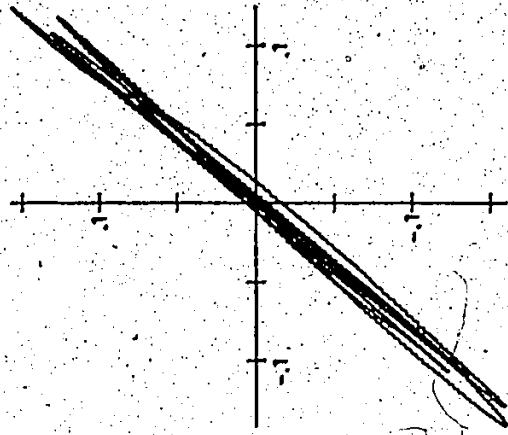


FIG. 5.14 TIME HISTORY OF ACCELERATION



(Units are in ft)

FIG. 5.15 7 GYRATING MOTIONS

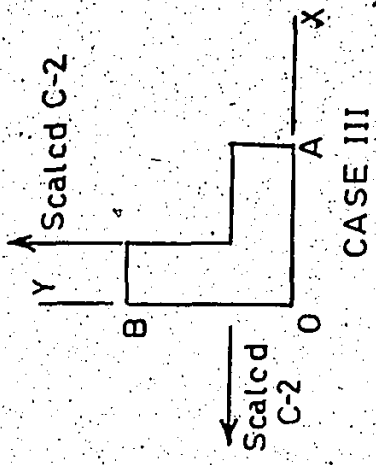
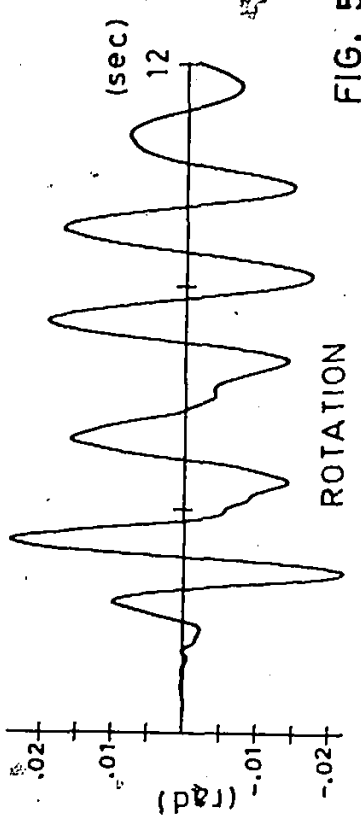
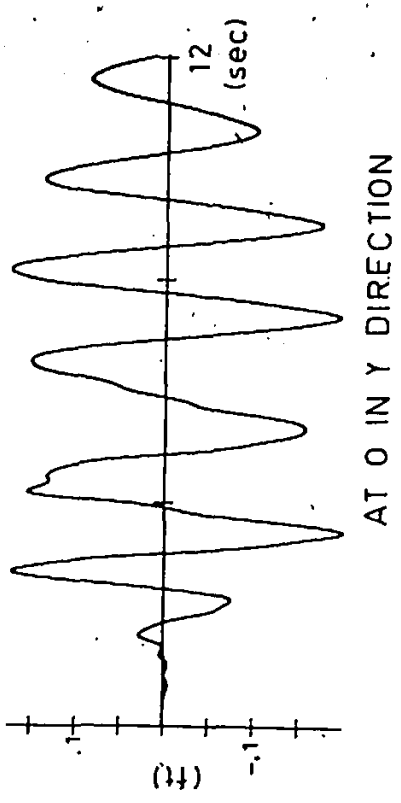
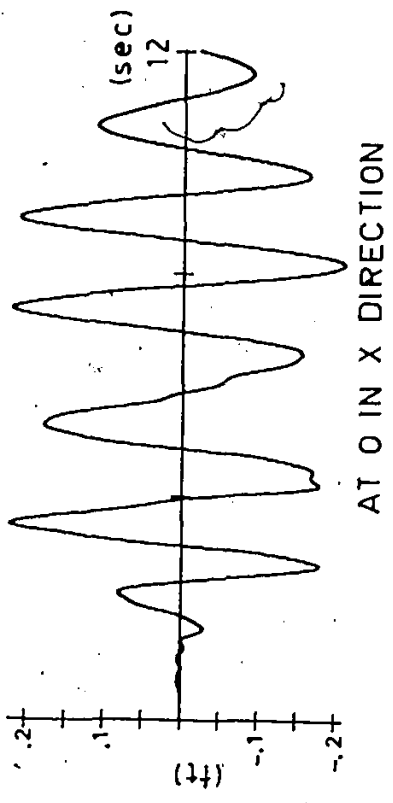
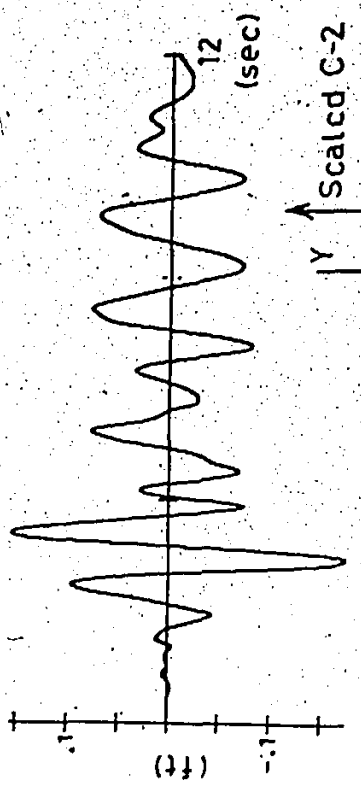
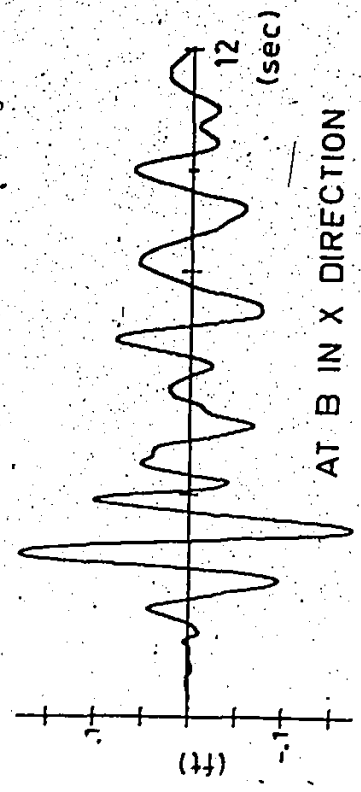
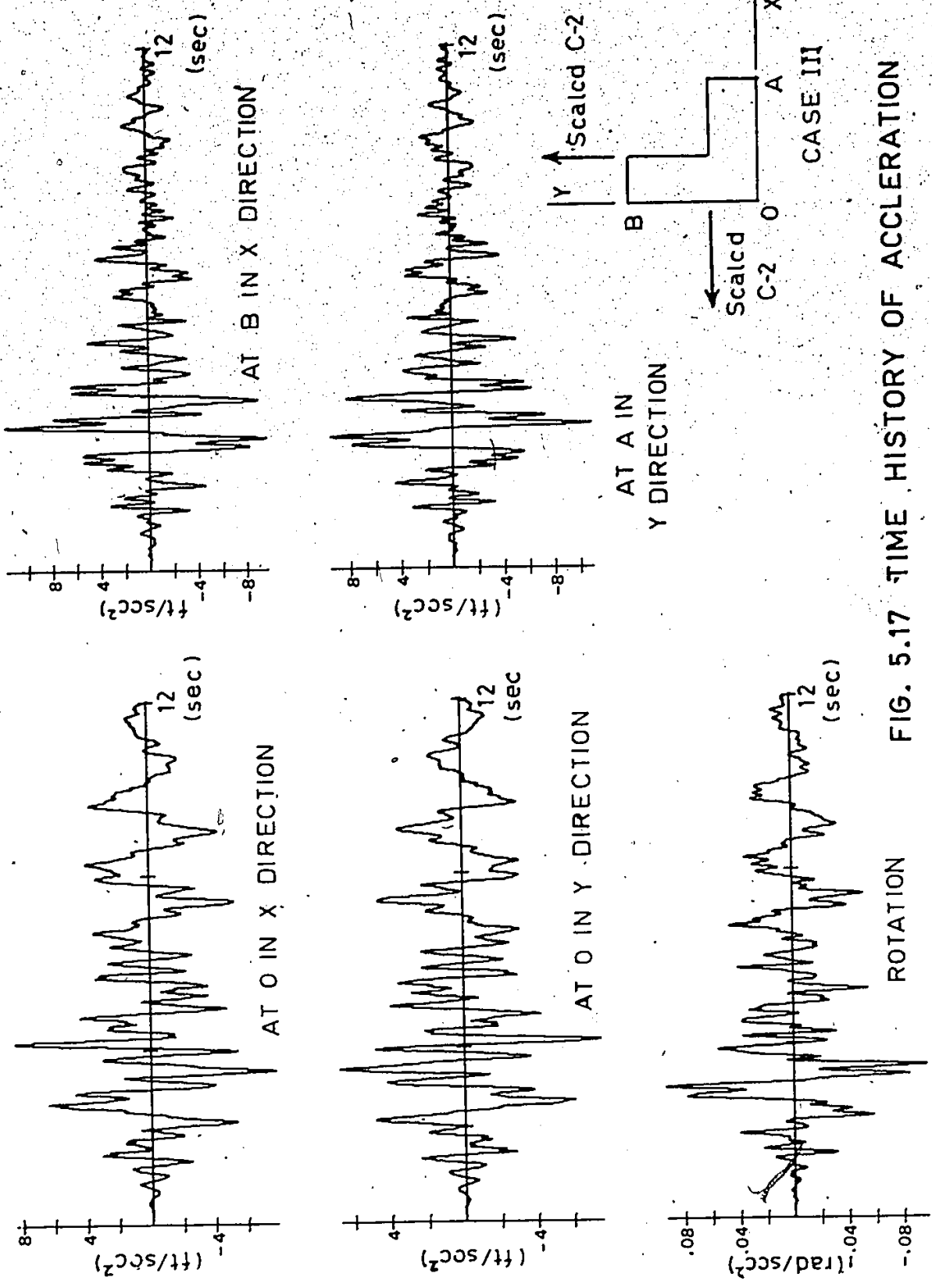
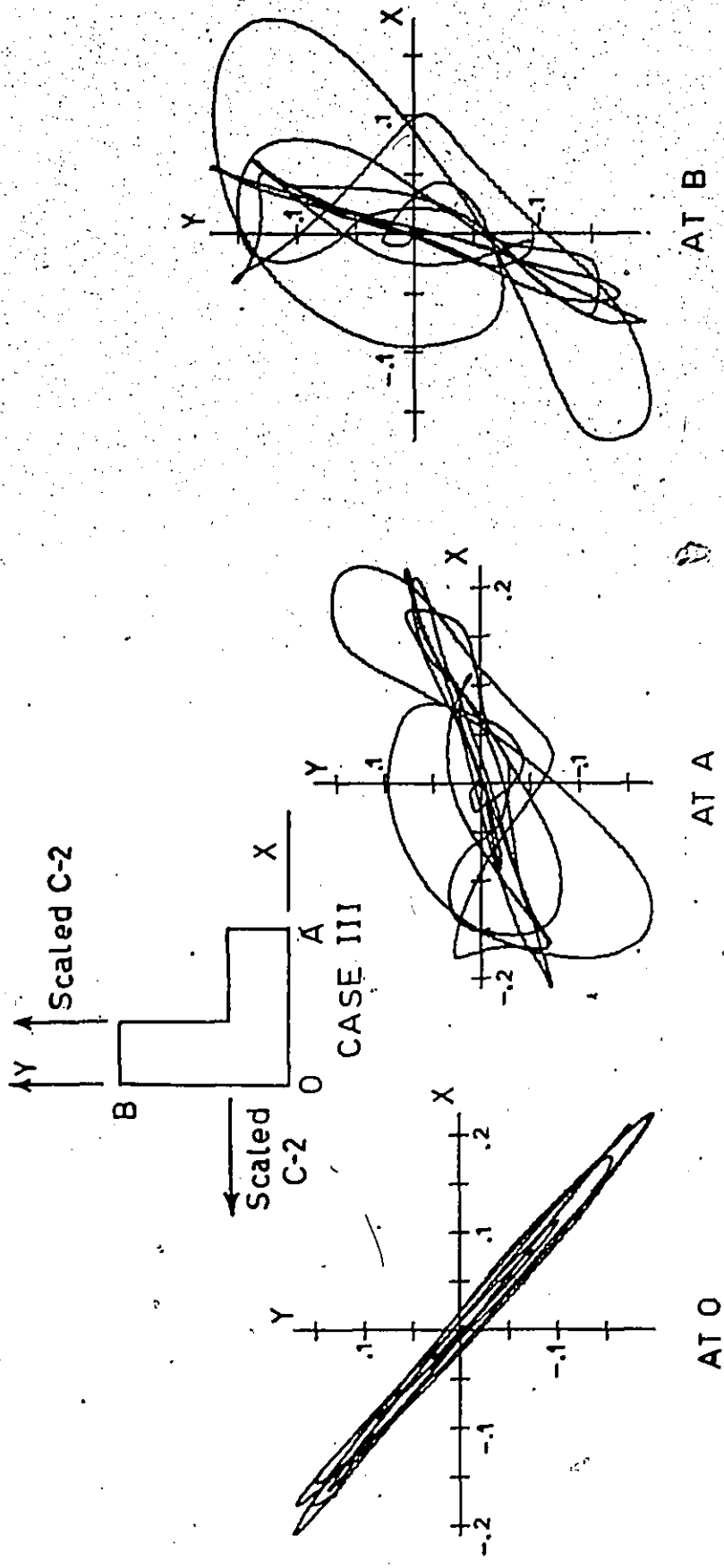


FIG. 5.16 TIME HISTORY OF DISPLACEMENT



ROTATION **FIG. 5.17 TIME HISTORY OF ACCELERATION**



(Units are in ft)

FIG. 5.18 GYRATING MOTIONS



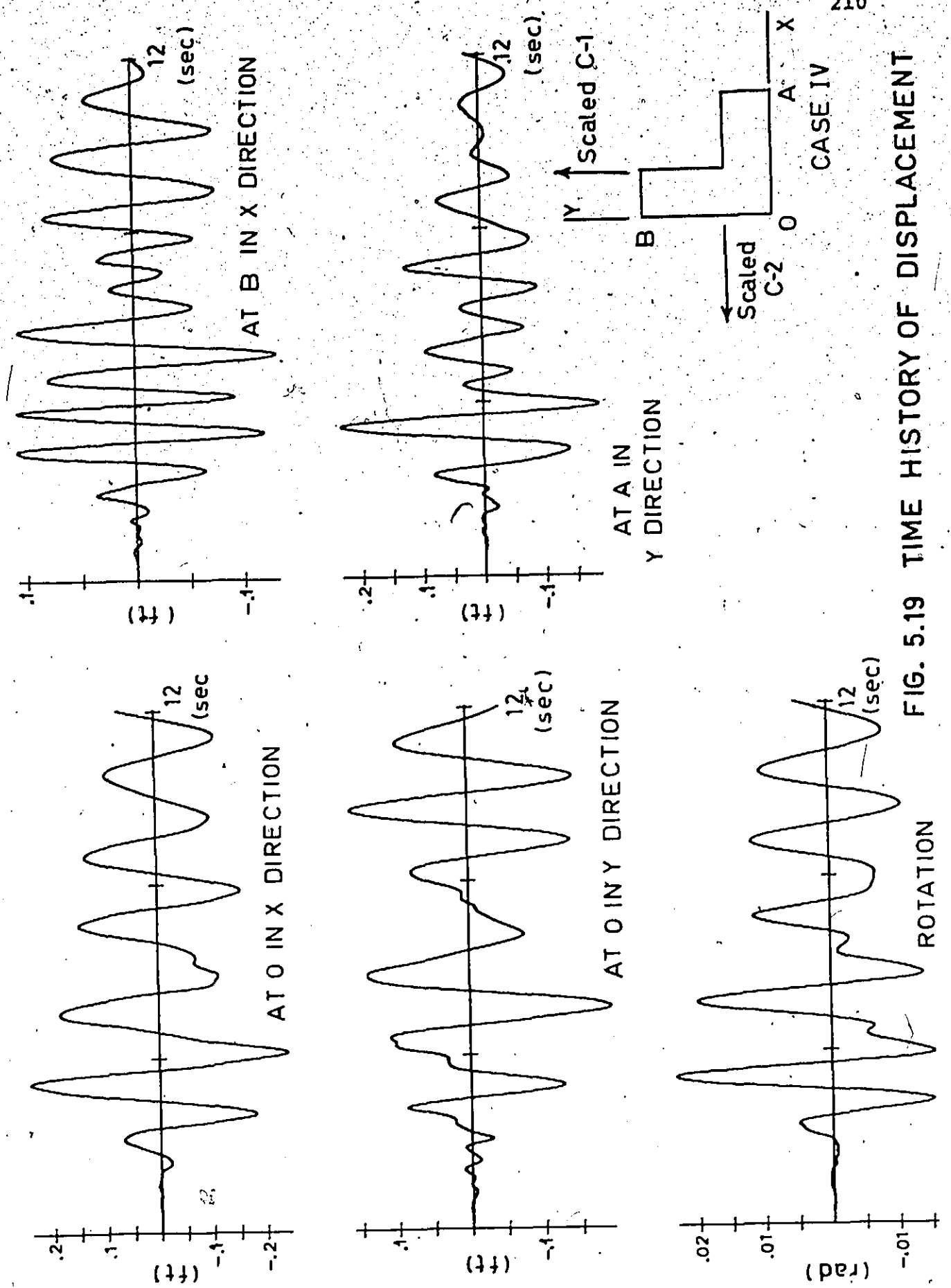
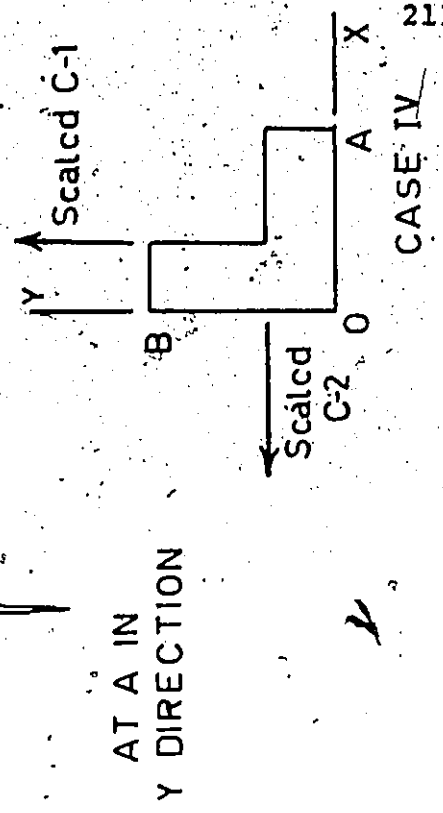
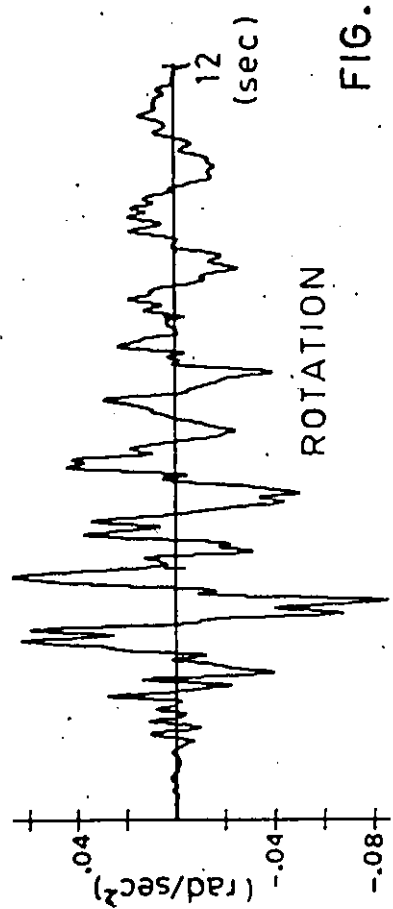
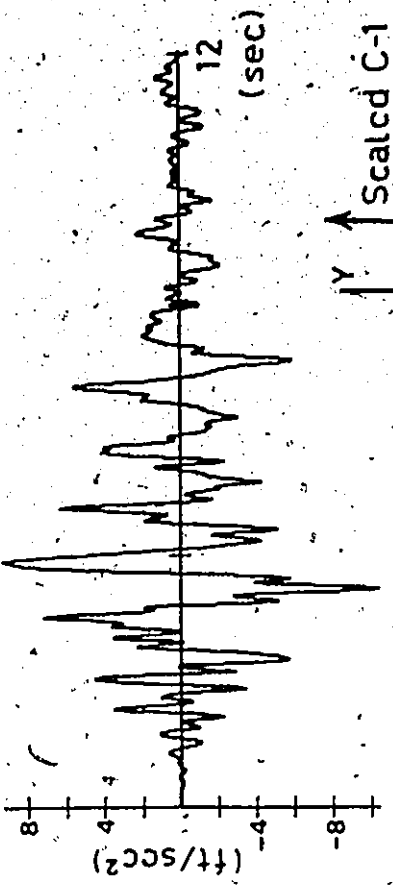
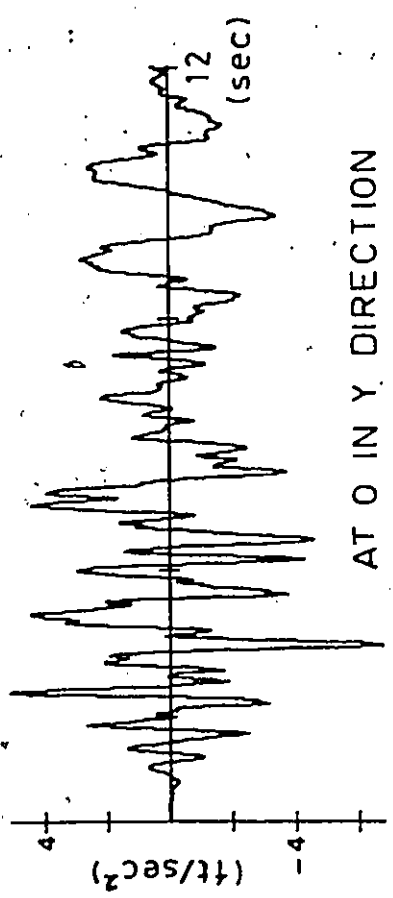
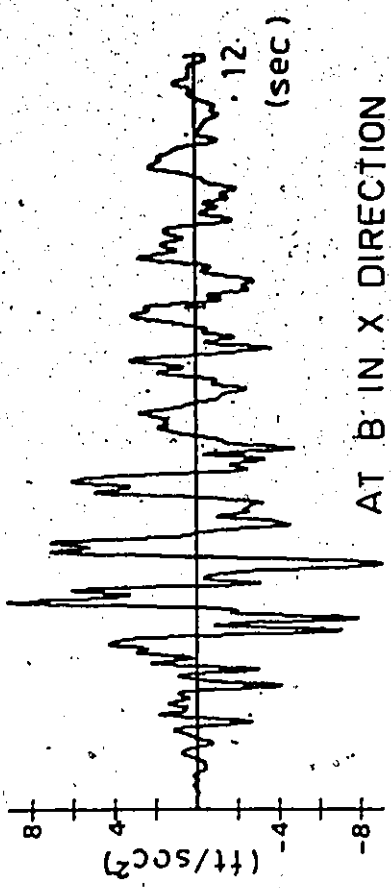
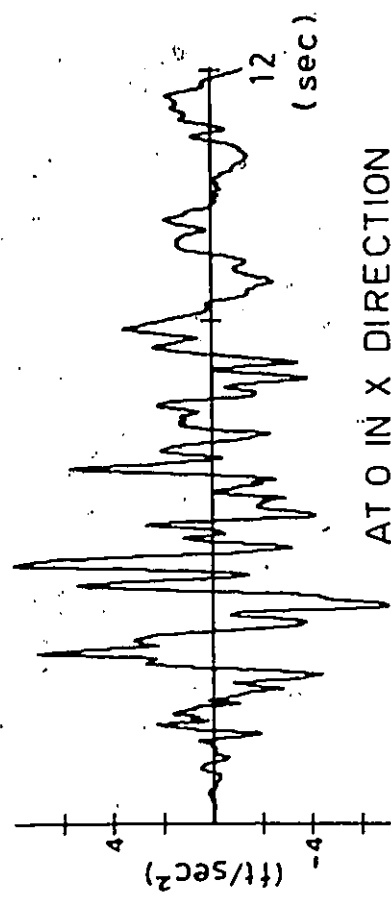
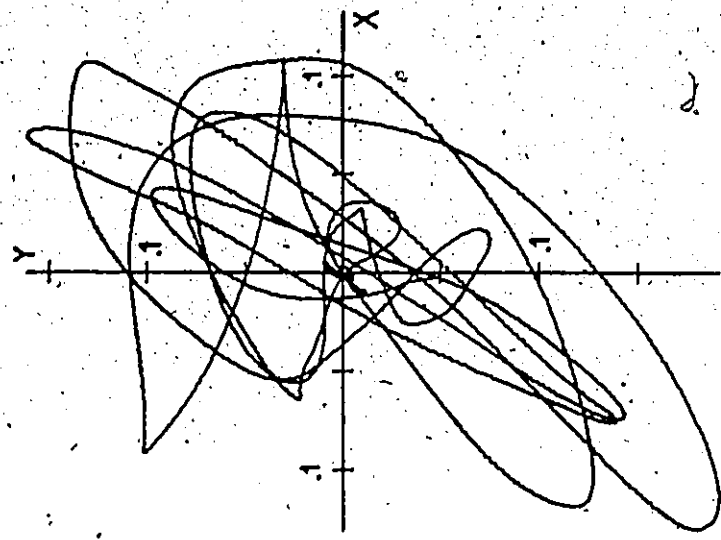


FIG. 5.19 TIME HISTORY OF DISPLACEMENT

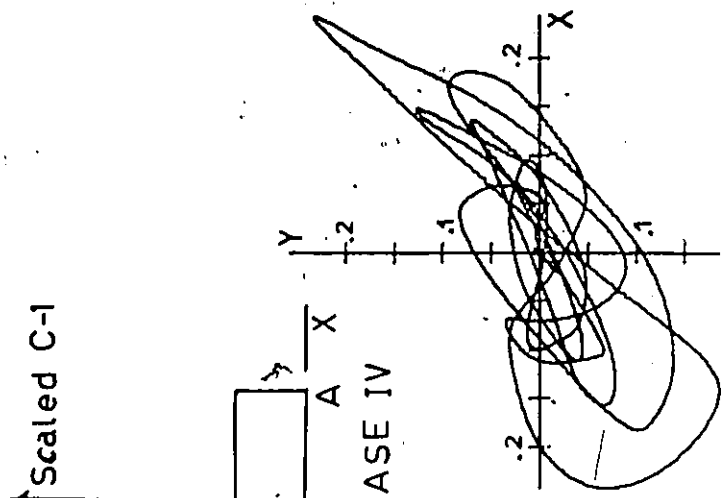


CASE IV 211

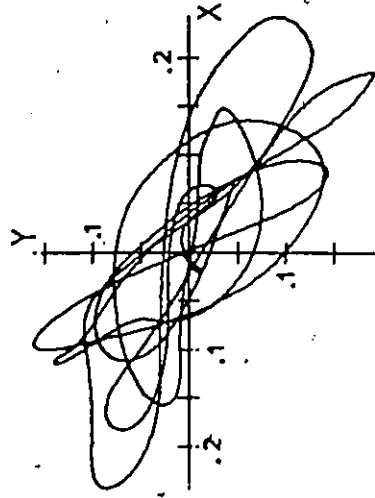
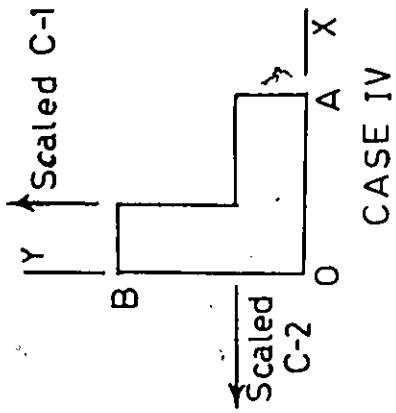
FIG. 5.20 TIME HISTORY OF ACCELERATION



AT B



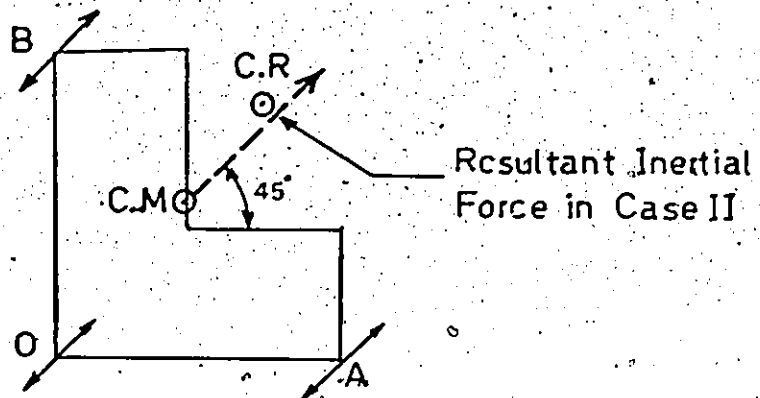
AT A



AT O

(Units are in ft)

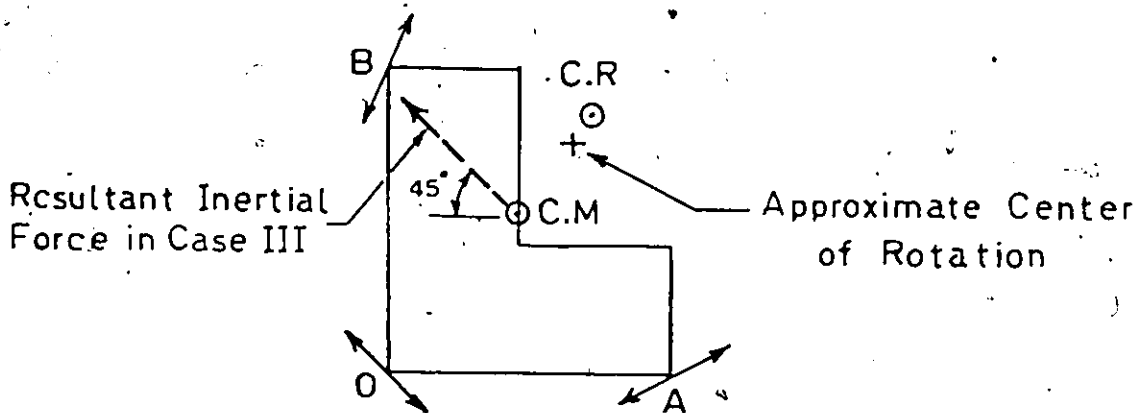
FIG. 5.21 GYRATING MOTIONS



(a)

C.R = Center of Rigidity

C.M = Center of Mass



(b)

FIG. 5.22

## CHAPTER VI

### CONCLUSIONS AND RECOMMENDATIONS

#### 6.1 Conclusions

A method of three-dimensional analysis of shear wall structures subjected to lateral loads has been developed. The coupling action of the shear walls due to the interaction of the floor slabs or floor beams or both has been considered. For simple cases like symmetric two wall cores, computations can be done by hand or by the help of the design curves. A set of such curves has been presented. In cases of complicated asymmetric layout, it is advantageous to use computer programs which have been prepared. The non-uniformity of structural properties can be taken into account if desired. The method can be used for finding the overall stiffness of the structure. The stiffness properties of the structure is necessary to perform a dynamic analysis for finding the response of the structure due to earthquake motions. A number of examples of representative building are worked out in detail. Based on the results of the examples, the following conclusions can be drawn,

1. The effect of the floor slab can be replaced by a

number of connecting beams at appropriate locations.

2. When a non-symmetric shear wall structure is subjected to lateral wind forces, it can suffer considerable twisting in addition to translational displacements. The connecting beams are subjected to shear forces, and the critical beams are located at the lowest third portion of the building.

3. The effect of coupling due to the floor slabs and beams connecting the shear walls is to increase the lateral stiffness of the structure. This factor should be considered in the analysis in general.

4. The effect of neglecting the axial deformation increases the stiffness and decreases the stress levels. This assumption whenever made should be done with caution. This should never be done in the case of slender structures.

5. Making the shear walls thicker at the lower part of the building can be beneficial in resisting lateral loading by reducing the lateral deflection and axial stress levels.

6. For buildings having asymmetric layout, the ground motion due to the earthquake will induce a coupled translational and rotational motion. Two components of ground motion oriented in the worst

direction is a rational way to assess the maximum response due to design earthquake situations.

## 6.2 Recommendations

In view of the present research work, the following recommendations can be made.

1. It has been shown that the most convenient and practical way to include the effect of coupling by the floor slab is to consider a number of connecting beams with equivalent stiffness properties. It is therefore necessary to evaluate the equivalent width of the slabs which acts as beams for a variety of shear wall configurations. Except in cases of regularly spaced cross wall structures, very little work has been done in the area. It is recommended that more theoretical and experimental study should be undertaken to evaluate the equivalent width of the slab for a number of common shear wall configurations. If possible, design curves similar to that given by Quadeer and Stafford Smith<sup>(53)</sup> shall be prepared for all these shear wall configurations.

2. The present analytical method assumes the linear

and elastic behaviour of the structure. The present day practice to design high-rise building structure allows elastic deformation to occur when subjected to lateral forces due to the earthquakes of moderate intensity or wind. The proposed method can therefore be used as a tool for designing the component of the structures. However, when the structure will be hit by earthquakes of high intensity, there will be inelastic deformation in some parts of the structure. In such cases, it is desirable to provide ductility so that energy released by the earthquake will be absorbed in the system without failure. Except in cases of plane coupled shear walls<sup>(52)</sup>, very little study has been done in the elasto-plastic behaviour of shear wall structures. It is therefore recommended to undertake more work in this area to reveal the elasto-plastic behaviour of shear wall structures.

3. The present theory is applicable for buildings having shear walls as the load resisting elements throughout the height. It is not applicable for cases where shear walls are discontinued in a part of the building and replaced by another structural system. A mix use of different structural system can be very desirable when different parts of the building are



used for different purposes. For instance, the lower part of a high-rise building may be used for office spaces using framed construction and the upper part be used as apartment buildings using shear wall construction. Studies in the load resisting behaviour of such structures are recommended.

4. In earthquakes, there are two components of motions acting in two mutually perpendicular directions. There is a scarcity of information regarding the correlation between two components of earthquakes. From the limited study undertaken, it is found that a pair of uncorrelated accelerations may lead to an increased response as compared with the case with completely correlated components. This effect of uncorrelated ground motion on the response should be examined in detail.

## APPENDIX A

VLASOV'S THEORY OF THIN WALLED BEAM

The method of analysis used in the present work is based on the theory presented by Vlasov<sup>(81)</sup>. Vlasov's theory is based on two geometric hypotheses:

(a) a thin walled beam of open section can be considered as a shell of rigid (undeformable) cross section.

(b) the shear deformation of the middle surface (characterising change in the angle between the co-ordinate line) can be neglected.

In shear wall structure, the concrete shear wall can be treated as thin walled beams connected by floor slabs, which are normally located at regular intervals. The action of the floor slab is to prevent any deformation of the section which supports the hypotheses (a). Hypothesis (b) requires shear deformation to be negligible compared with the torsional and flexural deformations. Vlasov states that this is satisfied if for the structure shown in Figure A.1.

$$t/d \leq 0.1 \quad \text{and} \quad d/l \leq 0.1$$

For components of tall building this conditions are satisfied.

The expression of longitudinal stress in Vlasov's theory is:

$$\sigma = \frac{T}{A} - \frac{M_y \cdot x}{I_y} - \frac{M_x \cdot y}{I_x} + \frac{B \cdot \omega}{I_\omega} \quad (\text{A.1})$$

The first three terms coincide with the equation known from elementary theory. The last term of the expression is the longitudinal stress due to warping. The notations of the last terms are explained as:

Bimoment B is a generalised balanced system of forces statically equivalent to zero. Units are force x (length)<sup>2</sup> e.g., lbs. in<sup>2</sup>.

$\omega$  is the sectorial area of the point on the section where the stress is being measured. Units are (length)<sup>2</sup> e.g., in<sup>2</sup>.

$I_\omega$  is sectorial moment of Inertia of the section and is defined as  $\int_A \omega^2 dA$  units are (length)<sup>6</sup> e.g., in<sup>6</sup>.

The distribution of sectorial co-ordinate for some open section is shown in Figure A.2. Right hand co-ordinate system is used in the present work (Figure A.3). The generalised displacement variables are shear center displacements  $\xi$ ,  $\eta$  and  $\theta$  in xy plane and centroidal dis-

placement  $\zeta$  in  $z$  direction (Figure A.4). The sign convention for generalised forces is shown in Figure A.5.

The relation between the generalised forces and displacement variables are:

$$\begin{aligned} T &= EA\zeta'; & M_x &= EI_x\eta''; & M_y &= EI_y\xi''; \\ B &= -EI_\omega\theta''; & Q_t &= -EI_\omega\theta'''; & & + GJ\theta'; \\ V_y &= -EI_x\eta'''; & V_x &= -EI_y\xi''' \end{aligned} \quad (A.2)$$

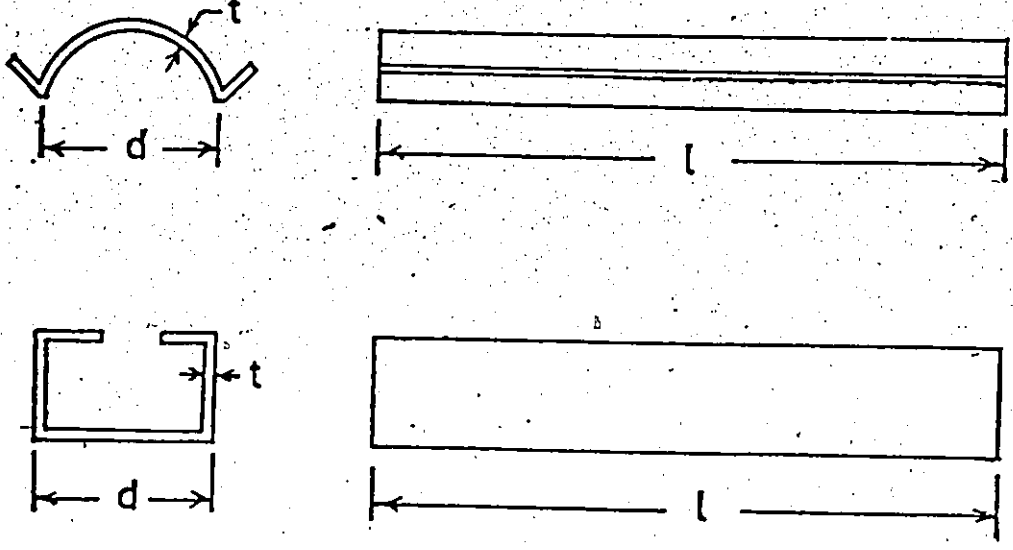
Of these quantities, axial force and bending moments are referred to the centroid and shear forces and torque are referred to the shear center of the section.

The longitudinal stress at any point can be expressed in terms of the displacement variables as:

$$\sigma = E(\zeta' - \xi''x - \eta''y - \theta''\omega) \quad (A.3)$$

Displacement of any point in  $z$  direction is obtained as:

$$\delta = (\zeta - \xi'x - \eta'y - \theta'\omega) \quad (A.4)$$



Dimensional Limitations  
FIG. A 1

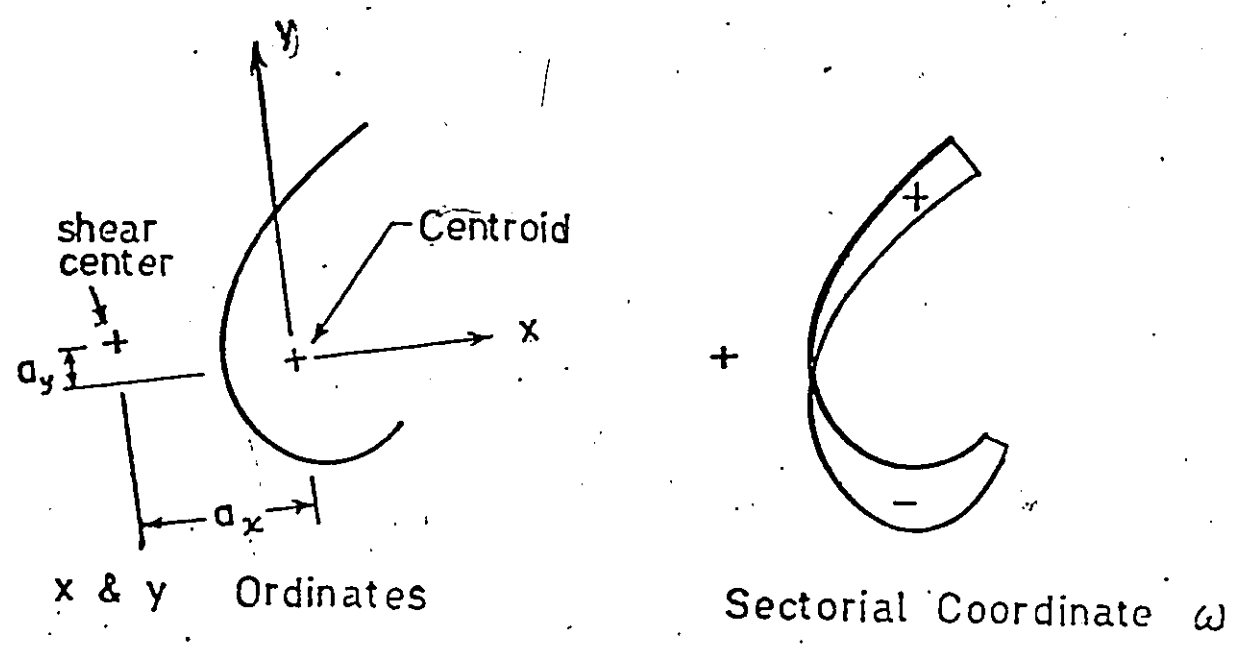
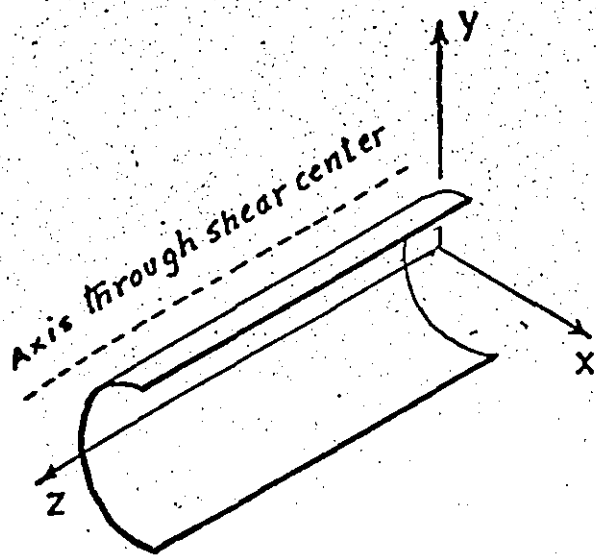
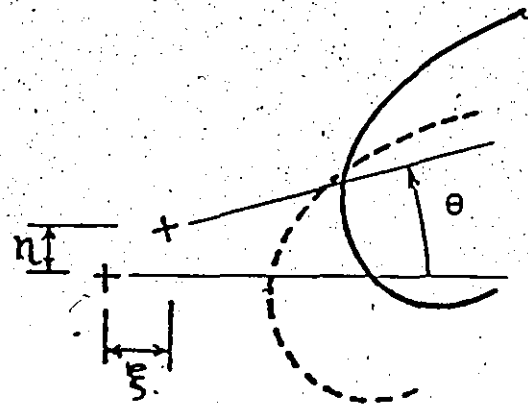


FIG. A 2



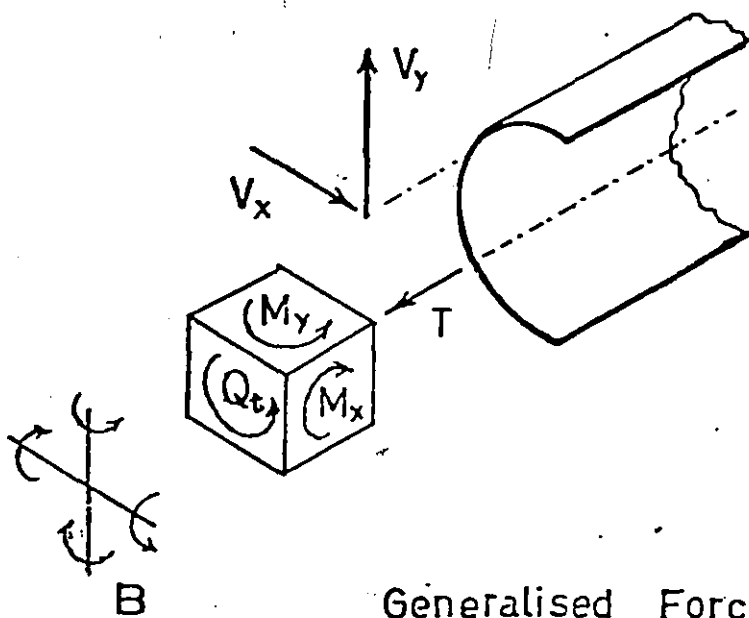
Co-ordinate System

FIG. A 3



Generalised Displacements

FIG. A 4



Generalised Forces

FIG. A 5

## APPENDIX - B

EXPERIMENTAL DATA FOR TWO WALL CORE

TABLE B-1

Strain Gauge No.	Strain in $\mu$ in/in for lateral load at top											
	Loading											
	5 lb.	10 lb.	15 lb.	20 lb.	25 lb.	20 lb.	15 lb.	10 lb.	5 lb.	0		
1 (+)	4	6	16	36	36	26	18	20	14	6		
2	No Strain											
3 (+)	4	6	8	18	18	8	8	4	4	2		
4	No Strain											
5 (-)	28	82	128	180	220	186	140	88	46	8		
6 (-)	44	84	146	202	262	212	158	102	54	10		
7 (-)	22	90	130	194	240	204	148	100	44	12		
8 (-)	42	90	136	200	250	200	150	98	52	2		
9 (-)	42	90	136	190	250	210	160	106	52	2		
10 (-)	34	98	146	208	278	238	172	108	50	6		
11	No Strain											
12	No Strain											
13	No Strain											
14	No Strain											
15 (+)	36	88	136	186	240	194	154	100	48	6		
16 (+)	44	102	172	204	270	210	160	114	58	4		
17 (+)	40	92	144	186	244	198	146	104	52	6		
18 (+)	44	102	146	194	246	202	154	112	52	4		
19 (+)	40	94	140	188	242	208	152	104	54	2		
20 (+)	50	106	158	216	266	226	170	126	68	2		
21 (+)	116	262	412	557	728	602	462	327	162	17		
22 (-)	126	280	444	604	764	646	504	364	186	12		
23 (+)	134	292	458	628	818	688	518	378	198	42		
24 (-)	134	296	466	626	806	686	531	384	198	14		
25 (+)	150	130	510	700	920	760	595	420	220	30		
26 (-)	158	332	518	702	912	768	602	422	214	12		
27 (+)	84	190	302	420	552	460	350	250	125	20		
28 (-)	102	216	336	456	586	506	386	286	146	16		
29	No Strain											
30	No Strain											
31	No Strain											
32 (+)	124	266	422	566	724	614	454	304	164	10		
33 (-)	112	258	410	550	712	592	446	320	167	22		
34 (+)	142	282	454	612	792	652	484	337	178	30		
35 (-)	132	302	458	610	780	650	500	350	190	30		
36 (+)	138	304	466	626	808	664	500	344	184	24		
37 (-)	158	324	488	644	828	686	524	374	206	26		
38 (+)	98	214	338	448	578	476	360	246	133	18		
39 (-)	92	200	302	412	528	434	332	234	122	12		

TABLE B-2

Dial Gauge No.	Deflection in inch for Lateral Load at Top									
	LOADING									
	5 lb.	10 lb.	15 lb.	20 lb.	25 lb.	20 lb.	15 lb.	10 lb.	5 lb.	0
1 (+)	.0024	.0057	.0095	.0129	.0164	.0135	.0103	.0071	.0036	.0011
2 (+)	.0020	.0060	.0100	.0140	.0170	.0150	.0110	.0070	.0040	.0010
3 (+)	.0060	.0150	.0245	.0340	.0430	.0360	.0280	.0180	.0090	.0020
4 (+)	.0070	.0160	.0240	.0350	.0450	.0380	.0280	.0190	.0100	.0030
5 (+)	.0110	.0280	.0440	.0600	.0760	.0640	.0470	.0290	.0170	.0040
6 (+)	.0100	.0290	.0460	.0620	.0780	.0650	.0490	.0340	.0170	.0040
7 (+)	.0180	.0410	.0640	.0860	.1100	.0910	.0710	.0510	.0250	.0040
8 (+)	.0190	.0420	.0640	.0870	.1120	.0920	.0720	.0520	.0260	.0040

TABLE B-3

Strain Gauge No.	Strain in $\mu$ in/in for Torque at Top							
	LOADING							
	50 lb.in	100 lb.in	150 lb.in	200 lb.in	150 lb.in	100 lb.in	50 lb.in	0
1 (-)	10	40	66	90	72	50	14	0
2 (-)	18	58	80	120	100	76	30	2
3 (+)	32	68	102	126	120	82	42	10
4 (+)	40	76	118	158	128	92	50	4
5 (+)	8	28	40	48	38	30	12	0
6 (+)	6	24	40	48	32	26	8	2
7	No Strain							
8	No Strain							
9 (-)	18	28	40	58	52	32	22	6
10 (-)	12	26	34	54	46	34	26	6
11 (-)	22	42	62	102	82	48	8	7
12 (-)	30	62	84	140	102	64	20	8
13 (+)	18	48	92	110	88	62	38	4
14 (+)	38	86	126	156	128	96	48	12



TABLE B-3 (cont'd):

Strain Gauge No.	Strain in in/in for Torque at Top							
	LOADING							
	50 lb.in	100 lb.in	150 lb.in	200 lb.in	150 lb.in	100 lb.in	50 lb.in	0
15 (+)	18	28	48	60	48	38	18	10
16 (+)	24	34	48	60	46	38	26	8
17	No Strain							
18								
19 (-)	10	22	38	46	40	20	10	5
20 (-)	15	26	38	48	40	20	10	2
21 (+)	158	348	540	750	668	418	212	16
22 (-)	160	370	578	800	650	466	248	22
23 (+)	164	380	602	852	670	446	190	30
24 (-)	200	438	686	938	760	540	288	50
25 (+)	220	500	794	1088	878	610	318	18
26 (-)	234	512	804	1104	884	634	344	42
27 (+)	130	290	462	632	510	350	180	6
28 (-)	147	302	480	654	532	382	202	22
29 (+)	18	28	42	60	42	28	13	8
30 (+)	13	10	20	30	22	8	8	7
31	No Strain							
32 (-)	190	410	650	890	728	500	260	20
33 (+)	180	390	610	846	710	472	240	35
34 (-)	212	476	752	1032	852	572	292	22
35 (+)	216	468	734	1006	856	568	286	46
36 (-)	234	512	806	1096	906	622	316	26
37 (+)	230	510	802	1100	920	620	340	30
38 (-)	152	322	502	670	568	390	210	22
39 (+)	152	342	532	738	622	412	204	18

TABLE B-4

Dial Gauge No.	Deflection in inch for Torque at Top							
	LOADING							
	50 lb.in	100 lb.in	150 lb.in	200 lb.in	150 lb.in	100 lb.in	50 lb.in	0
1 (+)	.0006	.0015	.0024	.0033	.0026	.0018	.0009	.0001
2 (-)	.0008	.0020	.0026	.0040	.0032	.0025	.0015	.0002
3 (+)	.0015	.0040	.0075	.0095	.0080	.0055	.0030	.0002
4 (-)	.0021	.0050	.0080	.0110	.0090	.0060	.0027	.0002
5 (+)	.0030	.0070	.0115	.0160	.0120	.0100	.0035	.0002
6 (-)	.0037	.0080	.0125	.0190	.0145	.0100	.0045	.0003
7 (+)	.0060	.0115	.0220	.0260	.0235	.0145	.0080	.0002
8 (-)	.0060	.0110	.0195	.0250	.0220	.0140	.0070	.0001

## APPENDIX - C

ELEMENTS OF MATRIX [A]

The element  $a_{ij}$  in matrix [A] represents the contribution of the distributed shear  $q_j$  to the relative displacement of laminae at band  $i$ . Assuming band  $i$  connects between walls  $m$  and  $n$  ( $m < n$ ). Then, the contribution of  $q_i$  to the relative displacement at band  $i$  is given by:  $\frac{q_i}{E} \left( \frac{1}{A_m} + \frac{1}{A_n} \right)$ . Therefore,  $a_{ii} = \frac{1}{E} \left( \frac{1}{A_m} + \frac{1}{A_n} \right)$ . If band  $j$  does not connect either to wall  $m$  or  $n$ , the contribution is zero. In addition to band  $i$  if band  $j$  connects between walls  $m$  and  $p$  where  $m < p$  and  $m < n$ , then  $a_{ij} = \frac{1}{EA_m}$ . If band  $j$  connects between walls  $m$  and  $l$  where  $m > l$  but  $m < n$ , then  $a_{ij} = \frac{-1}{EA_m}$ . Conversely, if band  $j$  connects between wall  $n$  and  $p$  where  $n > p$  and  $n < m$ ,  $a_{ij} = \frac{-1}{EA_n}$ . Finally, if band  $j$  connects between wall  $n$  and  $l$  where  $n > m$  and  $n > l$ ,  $a_{ij} = \frac{1}{EA_n}$ . As an example, the matrix [A] for the connection pattern shown in Figure C1 is:

$$[A] = \frac{1}{E} \begin{bmatrix} \left( \frac{1}{A_1} + \frac{1}{A_2} \right) & -\frac{1}{A_2} & \frac{1}{A_2} & 0 \\ & \left( \frac{1}{A_2} + \frac{1}{A_3} \right) & -\frac{1}{A_3} & \frac{1}{A_3} \\ \text{Symmetric} & & \left( \frac{1}{A_3} + \frac{1}{A_1} \right) & -\frac{1}{A_3} \\ & & & \left( \frac{1}{A_3} + \frac{1}{A_4} \right) \end{bmatrix}$$

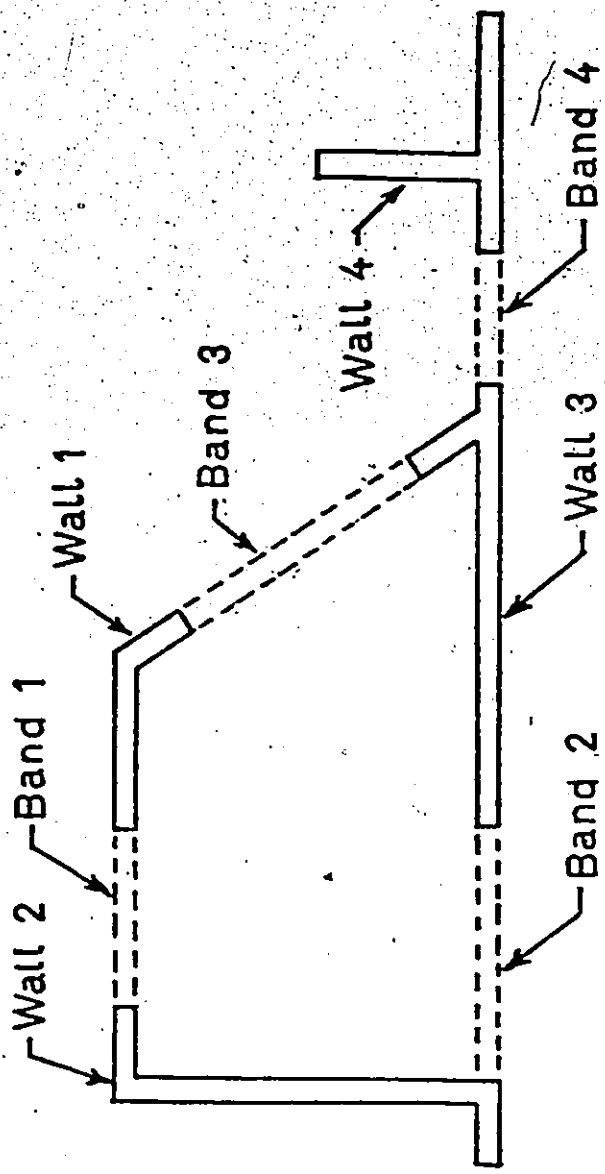


FIG.C1 WALL CONNECTION PATTERN

## APPENDIX - D

SHEAR WALLS CONNECTED BY TWO  
ROWS OF CONNECTING BEAMS

When two shear walls are connected by two rows of connecting beams of type 1, the governing equations are to be eliminated in the following manner.

In this case the number of shear walls  $M = 2$ , the number of type 1 connecting beams  $K = 2$  and there is no type 2 connecting beam. The equilibrium conditions as in equation (3.17, 3.21 and 3.22) can be written as:

$$EI_{YY}^* \xi'''' + EI_{XY}^* \eta'''' - EI_{YC}^* \theta'''' - r_{x1}(q_1 + q_2) = -\dot{V}_x \quad (D-1)$$

$$EI_{XY}^* \xi'''' + EI_{XX}^* \eta'''' + EI_{XC}^* \theta'''' - r_{y1}(q_1 + q_2) = -\dot{V}_y \quad (D-2)$$

$$-EI_{YC}^* \xi'''' + EI_{XC}^* \eta'''' + EI_{\omega}^* \theta'''' - GJ^* \theta' - (r_{\theta 1} q_1 + r_{\theta 2} q_2) = -Q_t \quad (D-3)$$

It is to be noted that in this case

$$r_{x1} \equiv r_{x2} \quad \text{and} \quad r_{y1} \equiv r_{y2}$$

From equation (3.18) the axial force functions are related to the distributed shear forces by the relation

$$T_1 = -T_2 = \int_z^H [q_1(s) + q_2(s)] ds \quad (D-4)$$

Differentiating equation (3.37) twice and eliminating  $T_1$  and  $T_2$  using equation (D-4), the compatibility conditions for the row 1 connecting beam is:

$$r_{x1}\xi'''' + r_{y1}\eta'''' + r_{\theta 1}\theta'''' + \frac{q_1 + q_2}{E\bar{A}} - \frac{q_1''}{E\gamma_1} = 0 \quad (D-5)$$

For the row 2 connecting beam, the compatibility condition is:

$$r_{x1}\xi'''' + r_{y1}\eta'''' + r_{\theta 1}\theta'''' + \frac{q_1 + q_2}{E\bar{A}} - \frac{q_2''}{E\gamma_2} = 0 \quad (D-6)$$

where:  $\bar{A} = \frac{A_1 A_2}{A_1 + A_2}$

The functions  $q_1$ ,  $q_2$  and  $\eta$  can be eliminated between equations (D-1, D-2, D-3, D-5 and D-6) and the resulting equations can be written in the following matrix form.

$$[K_0] \{\bar{\Delta}\}^v - [K_1] \{\bar{\Delta}\}'' = [S_0] \{L\}'' - [S_1] \{L\} \quad (D-6)$$

where:

$$\{\bar{\Delta}\} = \{\xi, \theta\}_{\text{col.}}$$

= Reduced displacement vector.

$$\{L\} = \text{Load vector} = \{-V_x, -V_y, -Q_t\}_{\text{col.}}$$

$[K_0]$ ,  $[K_1]$ ,  $[S_0]$ ,  $[S_1]$  are 2x2 matrices with the element as follows:

$$K_0(1,1) = E(I_{xy}^2 - I_x^* I_y^*) (r_{x1} + r_{y1}) / I_r$$

$$I_r = I_{xy}^* r_{y1} - I_x^* r_{x1}$$

$$K_0(1,2) = E(I_{xy}^* I_{xc}^* + I_x^* I_{yc}^*) (r_{x1} + r_{y1}) / I_r$$

$$K_0(2,1) = E\{-I_{yc}^* + I_{xc}^* (I_{xy}^* r_{x1} - I_y^* r_{y1}) / I_r\}$$

$$K_0(2,2) = E\{I_{xc}^* + I_{yc}^* (I_{xc}^* r_{x1} + I_{yc}^* r_{y1}) / I_r\}$$

$$K_1(1,1) = E(\gamma_1 + \gamma_2) \left[ (r_{x1} + r_{y1}) r_{x1} + (I_{xc}^* - I_{yc}^*) / \bar{A} \right]$$

$$+ \left\{ (r_{x1} + r_{y1}) r_{y1} + (I_x^* + I_{xy}^*) / \bar{A} \right\}$$

$$\left\{ (I_{xy}^* r_{x1} - I_y^* r_{y1}) / I_r \right\}$$

$$K_1(1,2) = E[(r_{x1} + r_{y1})(r_{\theta 1} \gamma_1 + r_{\theta 2} \gamma_2) + (\gamma_1 + \gamma_2)(I_{xc}^* - I_{yc}^*)/\bar{A}] \\ + \{(\gamma_1 + \gamma_2)(r_{x1} + r_{y1})r_{y1} + (\gamma_1 + \gamma_2)(I_x^* + I_{xy}^*)/\bar{A}\} \\ \{(I_{xc}^* r_{x1} + I_{yc}^* r_{y1})/I_r\}]$$

$$K_1(2,1) = E(\gamma_{\theta 1} \gamma_1 + \gamma_{\theta 2} \gamma_2) \left[ r_{x1} + \frac{I_x^* + I_{xy}^*}{(r_{x1} + r_{y1})\bar{A}} \right] \\ + \left\{ r_{y1} + \frac{I_x^* + I_{xy}^*}{(r_{x1} + r_{y1})\bar{A}} \right\} \left\{ (I_{xy}^* r_{x1} - I_{yc}^* r_{y1})/I_r \right\}$$

$$K_1(2,2) = E(r_{\theta 1} \gamma_1 + r_{\theta 2} \gamma_2) \left[ \frac{I_{xc}^* - I_{yc}^*}{(r_{x1} + r_{y1})\bar{A}} + \left\{ r_{y1} + \frac{I_x^* + I_{xy}^*}{(r_{x1} + r_{y1})\bar{A}} \right\} \right. \\ \left. \left\{ \frac{(I_{xc}^* r_{x1} + I_{yc}^* r_{y1})}{I_r} \right\} + E[r_{\theta 1}^2 \gamma_1 + r_{\theta 2}^2 \gamma_2 + GJ^*/E] \right]$$

$$S_0(1,1) = -I_x^*(r_{x1} + r_{y1})/I_r$$

$$S_0(1,2) = I_{xy}^*(r_{x1} + r_{y1})/I_r$$

$$S_0(1,3) = 0$$

$$S_0(2,1) = -I_{xc}^* r_{y1}/I_r$$

$$S_0(2,2) = I_{yc}^* r_{y1}/I_r$$

$$S_0(2,3) = 1$$



$$S_1(1,1) = (\gamma_1 + \gamma_2) \left[ \frac{1}{\bar{A}} - \{(r_{x1} + r_{y1}) r_{y1} + \frac{(I_x^* + I_{xy}^*)}{\bar{A}} \} \frac{r_{y1}}{I_r} \right]$$

$$S_1(1,2) = (\gamma_1 + \gamma_2) \left[ \frac{1}{\bar{A}} + \{(r_{x1} + r_{y1}) r_{y1} + \frac{(I_x^* + I_{xy}^*)}{\bar{A}} \} \frac{r_{x1}}{I_r} \right]$$

$$S_1(1,3) = 0$$

$$S_1(2,1) = (r_{\theta 1} \gamma_1 + r_{\theta 2} \gamma_2) \left[ \frac{1}{(r_{x1} + r_{y1}) \bar{A}} - \left\{ r_{y1} + \frac{I_x^* + I_{xy}^*}{(r_{x1} + r_{y1}) \bar{A}} \right\} \frac{r_{y1}}{I_r} \right]$$

$$S_1(2,2) = (r_{\theta 1} \gamma_1 + r_{\theta 2} \gamma_2) \left[ \frac{1}{(r_{x1} + r_{y1}) \bar{A}} + \left\{ r_{y1} + \frac{I_x^* + I_{xy}^*}{(r_{x1} + r_{y1}) \bar{A}} \right\} \frac{r_{x1}}{I_r} \right]$$

$$S_1(2,3) = 0$$

$$S_2(1,1) = 1$$

$$S_2(1,2) = -I_{xy}^* / I_x^*$$

$$S_2(1,3) = 0$$

$$S_2(2,1) = 0$$

$$S_2(2,2) = -I_{xc}^* / I_x^*$$

$$S_2(2,3) = 1$$

The equation (D-6) is a 2x2 matrix equation with constant coefficients. A similar scheme as in section (3.5) can be used for the solution. The differential equation (D-6) is subjected to the following boundary conditions.

$$\begin{aligned}
 \{\bar{\Delta}\} &= 0 & \text{at } z &= 0 \\
 \{\bar{\Delta}\}' &= 0 & \text{at } z &= 0 \\
 \{\bar{\Delta}\}'' &= 0 & \text{at } z &= H \\
 [K_2] \{\bar{\Delta}\}''' &= [S_2] \{L\} & \text{at } z &= 0 \\
 [K_2] \{\bar{\Delta}\}^{iv} &= [S_2] \{L\}' & \text{at } z &= H
 \end{aligned}
 \tag{D-7}$$

Where  $K_2$  is a 2x2 matrix with the following elements:

$$K_2(1,1) = E(I_y^* - I_{xy}^{*2}/I_x^*)$$

$$K_2(1,2) = K_2(2,1) = -E(I_{yc}^* + I_{xc}^* I_{xy}^*/I_x^*)$$

$$K_2(2,2) = E(I_w^* - I_{xc}^{*2}/I_x^*)$$

The displacement variables  $\xi$  and  $\theta$  are determined from the solution of equation (D-6). The other displacement and force variables  $\eta$ ,  $q_1$  and  $q_2$  are determined from the following relations.

$$\eta'''' = \left\{ \frac{I_{xy}^* r_{x1} - I_{yx}^* r_{y1}}{I_{xy}^* r_{y1} - I_{yx}^* r_{x1}} \right\} \xi'''' + \left\{ \frac{I_{xc}^* r_{x1} + I_{yc}^* r_{y1}}{I_{xy}^* r_{y1} - I_{yx}^* r_{x1}} \right\} \theta''''$$

$$- \frac{r_{y1} V_x}{E(I_{xy}^* r_{y1} - I_{yx}^* r_{x1})} + \frac{r_{x1} V_y}{E(I_{xy}^* r_{y1} - I_{yx}^* r_{x1})} \quad (D-8)$$

$$q_1 = \frac{E}{(r_{\theta 1} - r_{\theta 2})} \left[ \left\{ -I_{yc}^* - \frac{r_{\theta 2} (I_{yx}^* + I_{xy}^*)}{(r_{x1} + r_{y1})} \right\} \xi'''' + \right.$$

$$\left. + \left\{ I_{xc}^* - \frac{r_{\theta 2} (I_{xc}^* + I_{xy}^*)}{(r_{x1} + r_{y1})} \right\} \eta'''' + \left\{ I_{\omega}^* - \frac{r_{\theta 2} (I_{xc}^* - I_{yc}^*)}{r_{x1} + r_{y1}} \right\} \right.$$

$$\left. \theta'''' - \frac{GJ^*}{E} \theta' + \frac{Q_t}{E} - \frac{r_{\theta 2} (V_x + V_y)}{E(r_{x1} + r_{y1})} \right] \quad (D-9)$$

$$q_2 = \frac{E}{(r_{\theta 2} - r_{\theta 1})} \left[ \left\{ -I_{yc}^* - \frac{r_{\theta 1} (I_{yx}^* + I_{xy}^*)}{(r_{x1} + r_{y1})} \right\} \xi'''' + \right.$$

$$\left. + \left\{ I_{xc}^* - \frac{r_{\theta 1} (I_{xc}^* + I_{xy}^*)}{(r_{x1} + r_{y1})} \right\} \eta'''' + \left\{ I_{\omega}^* - \frac{r_{\theta 1} (I_{xc}^* - I_{yc}^*)}{r_{x1} + r_{y1}} \right\} \right.$$

$$\left. \theta'''' - \frac{GJ^*}{E} \theta' + \frac{Q_t}{E} - \frac{r_{\theta 1} (V_x + V_y)}{E(r_{x1} + r_{y1})} \right] \quad (D-10)$$

## APPENDIX - E

## SOLUTION FOR NON-UNIFORM SHEAR

## WALL STRUCTURE

The solution of the differential equation of the  $i^{\text{th}}$  segment (4.12) consists of a homogeneous solution and a particular solution. To determine the homogeneous solution the following characteristic equation is to be solved.

$$| \lambda^2 \mathbf{I} - \mathbf{K}_0^{i-1} \mathbf{K}_1^i | = 0 \quad (\text{E-1})$$

$\lambda_n^2$  ( $n=1,2,3$ ) are the positive definite eigen-values and  $U_{mn}$  ( $m=1,2,3$ ) are the eigen-vectors associated with the  $n^{\text{th}}$  eigen-value. For the particular solution, a 3x3 matrix  $[\mathbf{F}]$  is to be defined as follows:

$$[\mathbf{F}] = [\mathbf{K}_1^i]^{-1} [\mathbf{B}] / 6 \quad (\text{E-2})$$

Following the same procedure as in Chapter 3, the generalised displacement vector  $\{\Delta^i\}$  can be determined. The state vector  $\{\psi^i\}$  at any point within the  $i^{\text{th}}$  segment can be constructed as follows:

$$\{\psi^i(z)\} = [\kappa^i(z)] \{C\} \quad (E-3)$$

where  $\{C\}$  represent a vector of 20 constants. Substituting  $z = H_i$  and  $z = 0$ , the following relations are obtained.

$$\{\psi_B^i\} = [\kappa^i(H_i)] \{C\} \quad (E-4)$$

and

$$\{\psi_A^{i-1}\} = [\kappa^i(0)] \{C\} \quad (D-5)$$

Eliminating  $\{C\}$  between (E-4) and (E-5), there is obtained

$$\{\psi_B^i\} = [\kappa^i(H_i)] [\kappa^i(0)]^{-1} \{\psi_A^{i-1}\} \quad (E-6)$$

$$[\kappa^i(z)] =$$

1	0	0	z	0	0	z <sup>2</sup>	z <sup>2</sup>	z <sup>2</sup>	U <sub>11</sub> sh <sub>1</sub>	U <sub>12</sub> sh <sub>2</sub>	U <sub>13</sub> sh <sub>3</sub>
0	1	0	0	z	0	0	0	0	U <sub>21</sub> sh <sub>1</sub>	U <sub>22</sub> sh <sub>2</sub>	U <sub>23</sub> sh <sub>3</sub>
0	0	1	0	0	z	0	0	0	U <sub>31</sub> sh <sub>1</sub>	U <sub>32</sub> sh <sub>2</sub>	U <sub>33</sub> sh <sub>3</sub>
0	0	0	1	0	0	2z	0	0	U <sub>11</sub> ch <sub>1</sub> λ <sub>1</sub>	U <sub>12</sub> ch <sub>2</sub> λ <sub>2</sub>	U <sub>13</sub> ch <sub>3</sub> λ <sub>3</sub>
0	0	0	0	1	0	0	2z	0	U <sub>21</sub> ch <sub>1</sub> λ <sub>1</sub>	U <sub>22</sub> ch <sub>2</sub> λ <sub>2</sub>	U <sub>23</sub> ch <sub>3</sub> λ <sub>3</sub>
0	0	0	0	0	1	0	0	2z	U <sub>31</sub> ch <sub>1</sub> λ <sub>1</sub>	U <sub>32</sub> ch <sub>2</sub> λ <sub>2</sub>	U <sub>33</sub> ch <sub>3</sub> λ <sub>3</sub>
0	0	0	0	0	0	2	0	0	U <sub>11</sub> sh <sub>1</sub> λ <sub>1</sub> <sup>2</sup>	U <sub>12</sub> sh <sub>2</sub> λ <sub>2</sub> <sup>2</sup>	U <sub>13</sub> sh <sub>3</sub> λ <sub>3</sub> <sup>2</sup>
0	0	0	0	0	0	0	2	0	U <sub>21</sub> sh <sub>1</sub> λ <sub>1</sub> <sup>2</sup>	U <sub>22</sub> sh <sub>2</sub> λ <sub>2</sub> <sup>2</sup>	U <sub>23</sub> sh <sub>3</sub> λ <sub>3</sub> <sup>2</sup>
0	0	0	0	0	0	0	0	2	U <sub>31</sub> sh <sub>1</sub> λ <sub>1</sub> <sup>2</sup>	U <sub>32</sub> sh <sub>2</sub> λ <sub>2</sub> <sup>2</sup>	U <sub>33</sub> sh <sub>3</sub> λ <sub>3</sub> <sup>2</sup>
0	0	0	0	0	0	0	0	0	U <sub>11</sub> ch <sub>1</sub> λ <sub>1</sub> <sup>3</sup>	U <sub>12</sub> ch <sub>2</sub> λ <sub>2</sub> <sup>3</sup>	U <sub>13</sub> ch <sub>3</sub> λ <sub>3</sub> <sup>3</sup>
0	0	0	0	0	0	0	0	0	U <sub>21</sub> ch <sub>1</sub> λ <sub>1</sub> <sup>3</sup>	U <sub>22</sub> ch <sub>2</sub> λ <sub>2</sub> <sup>3</sup>	U <sub>23</sub> ch <sub>3</sub> λ <sub>3</sub> <sup>3</sup>
0	0	0	0	0	0	0	0	0	U <sub>31</sub> ch <sub>1</sub> λ <sub>1</sub> <sup>3</sup>	U <sub>32</sub> ch <sub>2</sub> λ <sub>2</sub> <sup>3</sup>	U <sub>33</sub> ch <sub>3</sub> λ <sub>3</sub> <sup>3</sup>
0	0	0	0	0	0	0	0	0	U <sub>11</sub> sh <sub>1</sub> λ <sub>1</sub> <sup>4</sup>	U <sub>12</sub> sh <sub>2</sub> λ <sub>2</sub> <sup>4</sup>	U <sub>13</sub> sh <sub>3</sub> λ <sub>3</sub> <sup>3</sup>
0	0	0	0	0	0	0	0	0	U <sub>21</sub> sh <sub>1</sub> λ <sub>1</sub> <sup>4</sup>	U <sub>22</sub> sh <sub>2</sub> λ <sub>2</sub> <sup>4</sup>	U <sub>23</sub> sh <sub>3</sub> λ <sub>3</sub> <sup>3</sup>
0	0	0	0	0	0	0	0	0	U <sub>31</sub> sh <sub>1</sub> λ <sub>1</sub> <sup>4</sup>	U <sub>32</sub> sh <sub>2</sub> λ <sub>2</sub> <sup>4</sup>	U <sub>33</sub> sh <sub>3</sub> λ <sub>3</sub> <sup>3</sup>
0	0	0	0	0	0	0	0	0	0	0	0
0	0	0	0	0	0	0	0	0	0	0	0
0	0	0	0	0	0	0	0	0	0	0	0
0	0	0	0	0	0	0	0	0	0	0	0
0	0	0	0	0	0	0	0	0	0	0	0

(continued to next page)

$U_{11}ch_1$	$U_{12}ch_2$	$U_{13}ch_3$	0	0	$f_{11}z^3$	$f_{12}z^3$	$f_{13}z^3$
$U_{21}ch_1$	$U_{22}ch_2$	$U_{23}ch_3$	0	0	$f_{21}z^3$	$f_{22}z^3$	$f_{23}z^3$
$U_{31}ch_1$	$U_{32}ch_2$	$U_{33}ch_3$	0	0	$f_{31}z^3$	$f_{32}z^3$	$f_{33}z^3$
$U_{11}sh_1\lambda_1$	$U_{12}sh_2\lambda_2$	$U_{13}sh_3\lambda_3$	0	0	$3f_{11}z^2$	$3f_{12}z^2$	$3f_{13}z^2$
$U_{21}sh_1\lambda_1$	$U_{22}sh_2\lambda_2$	$U_{23}sh_3\lambda_3$	0	0	$3f_{21}z^2$	$3f_{22}z^2$	$3f_{23}z^2$
$U_{31}sh_1\lambda_1$	$U_{32}sh_2\lambda_2$	$U_{33}sh_3\lambda_3$	0	0	$3f_{31}z^2$	$3f_{32}z^2$	$3f_{33}z^2$
$U_{11}ch_1\lambda_1^2$	$U_{12}ch_2\lambda_2^2$	$U_{13}ch_3\lambda_3^2$	0	0	$6f_{11}z$	$6f_{12}z$	$6f_{13}z$
$U_{21}ch_1\lambda_1^2$	$U_{22}ch_2\lambda_2^2$	$U_{23}ch_3\lambda_3^2$	0	0	$6f_{21}z$	$6f_{22}z$	$6f_{23}z$
$U_{31}ch_1\lambda_1^2$	$U_{32}ch_2\lambda_2^2$	$U_{33}ch_3\lambda_3^2$	0	0	$6f_{31}z$	$6f_{32}z$	$6f_{33}z$
$U_{11}sh_1\lambda_1^3$	$U_{12}sh_2\lambda_2^3$	$U_{13}sh_3\lambda_3^3$	0	0	$6f_{11}$	$6f_{12}$	$6f_{13}$
$U_{21}sh_1\lambda_1^3$	$U_{22}sh_2\lambda_2^3$	$U_{23}sh_3\lambda_3^3$	0	0	$6f_{21}$	$6f_{22}$	$6f_{23}$
$U_{31}sh_1\lambda_1^3$	$U_{32}sh_2\lambda_2^3$	$U_{33}sh_3\lambda_3^3$	0	0	$6f_{31}$	$6f_{32}$	$6f_{33}$
$U_{11}ch_1\lambda_1^4$	$U_{12}ch_2\lambda_2^4$	$U_{13}ch_3\lambda_3^4$	0	0	0	0	0
$U_{21}ch_1\lambda_1^4$	$U_{22}ch_2\lambda_2^4$	$U_{23}ch_3\lambda_3^4$	0	0	0	0	0
$U_{31}ch_1\lambda_1^4$	$U_{32}ch_2\lambda_2^4$	$U_{33}ch_3\lambda_3^4$	0	0	0	0	0
0	0	0	1	0	H-z	0	0
0	0	0	0	1	0	H-z	0
0	0	0	0	0	1	0	0
0	0	0	0	0	0	1	0
0	0	0	0	0	0	0	1

NOTE:  $sh_n = \text{Sinh}(\lambda_n z)$

$ch_n = \text{Cosh}(\lambda_n z)$

(n=1,2,3)





APPENDIX - F  
ELEMENTS OF MATRIX [K] AND [M]

$K_{xx}^{11}$	$K_{xy}^{11}$	$K_{x0}^{11}$	$K_{xx}^{12}$	$K_{xy}^{12}$	$K_{x0}^{12}$	$K_{xx}^{1N}$	$K_{xy}^{1N}$	$K_{x0}^{1N}$
$K_{yx}^{11}$	$K_{yy}^{11}$	$K_{y0}^{11}$	$K_{yx}^{12}$	$K_{yy}^{12}$	$K_{y0}^{12}$	$K_{yx}^{1N}$	$K_{yy}^{1N}$	$K_{y0}^{1N}$
$K_{0x}^{11}$	$K_{0y}^{11}$	$K_{00}^{11}$	$K_{0x}^{12}$	$K_{0y}^{12}$	$K_{00}^{12}$	$K_{0x}^{1N}$	$K_{0y}^{1N}$	$K_{00}^{1N}$
$K_{xx}^{21}$	$K_{xy}^{21}$	$K_{x0}^{21}$	$K_{xx}^{22}$	$K_{xy}^{22}$	$K_{x0}^{22}$	$K_{xx}^{2N}$	$K_{xy}^{2N}$	$K_{x0}^{2N}$
$K_{yx}^{21}$	$K_{yy}^{21}$	$K_{y0}^{21}$	$K_{yx}^{22}$	$K_{yy}^{22}$	$K_{y0}^{22}$	$K_{yx}^{2N}$	$K_{yy}^{2N}$	$K_{y0}^{2N}$
$K_{0x}^{21}$	$K_{0y}^{21}$	$K_{00}^{21}$	$K_{0x}^{22}$	$K_{0y}^{22}$	$K_{00}^{22}$	$K_{0x}^{2N}$	$K_{0y}^{2N}$	$K_{00}^{2N}$
.	.	.	.	.	.	.	.	.
.	.	.	.	.	.	.	.	.
.	.	.	.	.	.	.	.	.
.	.	.	.	.	.	.	.	.
$K_{xx}^{N1}$	$K_{xy}^{N1}$	$K_{x0}^{N1}$	$K_{xx}^{N2}$	$K_{xy}^{N2}$	$K_{x0}^{N2}$	$K_{xx}^{NN}$	$K_{xy}^{NN}$	$K_{x0}^{NN}$
$K_{yx}^{N1}$	$K_{yy}^{N1}$	$K_{y0}^{N1}$	$K_{yx}^{N2}$	$K_{yy}^{N2}$	$K_{y0}^{N2}$	$K_{yx}^{NN}$	$K_{yy}^{NN}$	$K_{y0}^{NN}$
$K_{0x}^{N1}$	$K_{0y}^{N1}$	$K_{00}^{N1}$	$K_{0x}^{N2}$	$K_{0y}^{N2}$	$K_{00}^{N2}$	$K_{0x}^{NN}$	$K_{0y}^{NN}$	$K_{00}^{NN}$

[K] =

$$\begin{bmatrix}
 M_1 & 0 & -Y_1 M_1 \\
 0 & M_1 & X_1 M_1 \\
 -Y_1 M_1 & X_1 M_1 & I_1 + M_1 (X_1^2 + Y_1^2)
 \end{bmatrix}$$

[M] =

$$\begin{bmatrix}
 M_2 & 0 & -Y_2 M_2 \\
 0 & M_2 & X_2 M_2 \\
 -Y_2 M_2 & X_2 M_2 & I_2 + M_2 (X_2^2 + Y_2^2)
 \end{bmatrix}$$

0

$$\begin{bmatrix}
 M_N & 0 & -Y_N M_N \\
 0 & M_N & X_N M_N \\
 -Y_N M_N & X_N M_N & I_n + M_N (X_N^2 + Y_N^2)
 \end{bmatrix}$$

## APPENDIX - G

## LIST OF COMPUTER PROGRAMS

1. Three-dimensional Analysis of Uniform Shear Wall Structures.

---

2. Three-dimensional Analysis of Non-Uniform Shear Wall Structure.

---

3. Generate Flexibility Matrix of Shear Wall Structures.
4. Dynamic Properties of Shear Wall Buildings.
5. Dynamic Response of Shear Wall Buildings.

## BIBLIOGRAPHY

1. ACI Committee 442, "Response of Buildings to Lateral Forces", Journal of the Am. Conc. Inst., Feb. 1971, pp. 81-106.
2. Beck, H., "Contribution to the Analysis of Coupled Shear Walls", Journal of the Am. Conc. Inst., Aug. 1962, pp. 1055-1070.
3. Biggs, J. M., Introduction to Structural Dynamics, McGraw Hill Book Company, New York.
4. Biswas, J. K., "Effect of Floor Slabs and Floor Beams on Static and Dynamic Behaviour of Shear Wall Structures", M. Eng., Thesis, McMaster University, Hamilton, Nov. 1970.
5. Blume, J. A., Newmark, N. M. and Corning, L. H., Design of Multistorey Reinforced Concrete Buildings for Earthquake Motions, Portland Cement Association, Skokie, Illinois, 1961.
6. Burns, R., "An Approximate Method of Analysing Coupled Shear Walls Subjected to Triangular Loading", Proceedings of Third World Conference on Earthquake Engineering, New Zealand, Jan. 1965, pp. IV-123 to IV-143.
7. Butlin, G. A., and McMillan, C. M., "An Improved Finite Element for Analysis of Plane Coupled Shear Walls",

- Civil Engg. and Public Works Review, Dec. 1971,  
pp. 1299-1303.
8. The Canadian Structural Design Manual, 1970, Supplement No. 4 to the N.B.C. of Canada, National Research Council, Ottawa.
  9. Candy, C. F., "Analysis of Shear Wall Frames by Computers", New Zealand Engineering (Wellington). Vol. 19, 1964, pp. 342-347.
  10. Chan, P. C. K., "Static and Dynamic Analysis of Framed Tube Structures", Ph.D. Thesis, McMaster University, Hamilton, 1973.
  11. Chitty, L., "On the Cantilever composed of a Series of Parallel Beams Interconnected by Cross Members", Philosophical Magazine, London, England, Vol. 38, 1947, pp. 685-699.
  12. Choudhury, J. R., "Analysis of Plane Spatial System of Interconnected Shear Walls", Ph.D. Thesis, University of Southampton, Oct. 1968.
  13. Civil Engineer, Proceedings, American Soc. of Civil Engineers, Dec. 1972, pp.25.
  14. Clough, R. W., King, I. P. and Wilson, E. L., "Structural Analysis of Multi-storey Buildings", Journal of Struct. Div. ASCE, Vol. 90, ST3, June 1964, pp. 19-34.
  15. Clough, R. W., "Earthquake Response of Structures",

Earthquake Engineering, edited by Wiegel, R. W.,  
Printice-Hall, Inc., Englewood Cliffs, N.J.

16. Coull, A. and Stafford Smith, B., "Analysis of Shear Walls (A Review of Previous Research)", Tall Building, Pergamon Press, 1967, pp. 139-155.
17. Coull, A. and Choudhurry, J. R., "Stresses and Deflections in Coupled Shear Walls", Journal of Am. Conc. Inst., Feb. 1967, pp. 65-72.
18. Coull, A. and Choudhurry, J. R., "Analysis of Coupled Shear Walls", Journal of Am. Conc. Inst., Sept. 1967, pp. 587-593.
19. Coull, A. and Puri, R. D., "Analysis of Coupled Shear Walls of Variable Thickness", Build. Sci., Vol. 2, 1967, pp. 181-188.
20. Coull, A. and Puri, R. D., "Analysis of Coupled Shear Walls of Variable Cross-section", Build. Sci. Vol. 2, 1968, pp. 313-320.
21. Coull, A. and Irwin, A. W., "Analysis of Load Distribution in Multi-storey Shear Wall Structures", Structural Engineer, Aug. 1970, pp. 301-306.
22. Coull, A., "Interaction of Coupled Shear Walls with Elastic Foundations", Journal of the Am. Conc. Inst., June, 1971, pp. 456-461.

23. Coull, A., "Coupled Shear Walls Subjected to Differential Settlement", *Build. Sci.*, Vol. 6, 1971, pp. 209-212.
24. Coull, A. and Subedi, N. K., "Coupled Shear Walls with Two and Three Bands of Openings", *Build. Sci.* Vol. 7, 1972, pp. 81-86.
25. Elkholy, I. A. S., "Static Analysis of Plane Coupled Shear Walls", M. Eng. Thesis, McMaster University, Hamilton, Ontario, Canada, Dec. 1971.
26. Elkholy, I. A. S. and Robinson, H., "Analysis of Multi-bay Coupled Shear Walls", *Build. Sci.*, Vol. 8, 1973, pp. 153-157.
27. Eriksson, O., "Analysis of Wind Bracing Walls in Multi-storey Housing", *Ingenioren*, International Edition, Vol. 5, Dec. 1961, pp. 115-124.
28. Ghali, A. and Neville, A. M., "Three-dimensional Analysis of Shear Walls", *Proceedings of the Inst. of Civil Engineers*, Vol. 51, Feb. 1972, pp. 347-357.
29. Gluck, J., "Lateral Load Analysis of Asymmetric Multi-storey Structures", *Journal of Struct. Div., ASCE*, Vol. 96, ST2, Feb. 1970, pp. 317-333.
30. Gluck, J. and Gellert, M., "Three Dimensional Lateral Load Analysis of Multi-storey Structures", *International Assoc. of Bridge and Struct. Engg.*, Vol. 32-I, 1972, pp. 77-90.

31. Gluck, J., Gellert, M. and Danay, A., "Dynamics of Asymmetric Multi-storey Structures", International Assoc. of Bridge and Struct. Engg., Vol. 33-III, 1973, pp. 91-106.
32. Heidebrecht, A. C. and Swift, R. D., "Analysis of Asymmetrical Coupled Shear Walls", Journal of Struct. Div., ASCE, Vol. 97, ST5, May 1971, pp. 1407-1422.
33. Heidebrecht, A. C. and Stafford Smith, B., "Approximate Analysis of Open-Section Shear Walls Subject to Torsional Loading", Journal of Struc. Div., ASCE, Vol. 99, ST12, Dec. 1973, pp. 2355-73.
34. Hoerner, J. B., "Modal Coupling and Earthquake Response of Tall Buildings", Ph.D. Thesis, California Institute of Technology, Pasadena, California, 1971.
35. Hurty, W. C. and Rubinstein, M. F., Dynamics of Structures Printice-Hall, Inc., Englewood Cliffs, New Jersey.
36. Hussein, W. A., "Analysis of Multi-Bay Shear Wall Structures by the Shear Connection Method", Build. Sci., Vol. 7, 1972, pp. 69-73.
37. Irwin, A. W., "Static and Dynamic Tests on a Model Shear Wall Structure", Proceedings of the Inst. of Civil Engineers, Vol. 51, Part 2, April 1972, pp. 701-710.
38. Jaeger, L. G., Mufti, A. A. and Mamet, J. C., "The Structural Analysis of Tall Buildings Having Irregularly



- Positioned Shear Walls", Building Science, Vol. 8, 1973, pp. 11-20.
39. Jenkin, W. M. and Harrison, T., "Analysis of Tall Buildings with Shear Walls Under Bending and Torsion", Tall Buildings, Pergamon Press, 1967, pp. 413-439.
  40. Jennings, P. C., Housner, G. W. and Tsai, N. C., "Simulated Earthquake Motions", Earthquake Engineering Research Laboratory, California Institute of Technology, Pasadena, California, April 1968.
  41. Jennings, P. C. and Skattum, K. S., "Dynamic Properties of Planar Coupled Shear Walls", International Journal of Earthquake Engineering and Structural Dynamics, Vol. 1, 1973, pp. 387-405.
  42. Livesley, R. K., Matrix Methods of Structural Analysis, Pergamon Press Ltd., 1964.
  43. Macleod, I. A., "Lateral Stiffness of Shear Walls with Openings", Tall Building, Pergamon Press, 1967, pp. 223-244.
  44. Macleod, I. A., "New Rectangular Finite Element for Shear Wall Analysis", Journal of Struct. Div., ASCE, Vol. 95, ST3, Mar. 1969, pp. 399-409.
  45. Majid, K. I. and Croxton, P. C. L., "Wind Analysis of Complete Building Structures by Influence Co-Efficients", Proceedings of the Inst. of Civil Engineers, Oct. 1970, pp. 169-184.

46. Medearis, K., "Coupled Bending and Torsional Oscillations of a Modern Skyscraper", Bulletin of Seismological Society of America, Vol. 56, No. 4, Aug. 1966, pp. 937-946.
47. Michael, D., "The Effect of Local Wall Deformations of the Elastic Interaction of Cross Walls Coupled by Beams", Tall Buildings, Pergamon Press, 1967, pp. 253-271.
48. Michael, D., "Torsional Coupling of Core Walls in Tall Buildings", Structural Engineer, Feb. 1969, pp. 67-71.
49. National Building Code of Canada, 1970, National Research Council of Canada, Ottawa, Canada.
50. Newmark, N. M. and Rosenblueth, E., Fundamentals of Earthquake Engineering, Prentice-Hall Inc., Englewood Cliffs, N.J., 1971.
51. Osawa, Y., "Seismic Analysis of Core Wall Buildings", Proc. Third World Conference on Earthquake Engineering", Vol. II, 1965, pp. 458-475.
52. Pauley, T., "An Elasto-Plastic Analysis of Coupled Shear Walls", Journal of the Am. Conc. Inst., Nov. 1970, pp. 915-922.
53. Quadeer, A. and Stafford Smith, B., "The Bending Stiffness of Slabs Connecting Shear Walls", Journal of the Am. Conc. Inst. June 1969, pp. 464-473.
54. Rosman, R., "An Approximate Method of Analysis of Walls of Multi-storey Buildings", Civil Engg. and Public

- Works Review, London, Vol. 59, Jan. 1964, pp. 67-69.
55. Rosman, R., "Approximate Analysis of Shear Walls Subject to Lateral Loads", Journal of the Am. Conc. Inst., June 1964, pp. 717-732.
  56. Rosman, R., "Pierced Shear Walls with Stepped Variation in Cross-Section", (in German), Heft 67, Bauingenieur, Praxis Series, W. Ernst and Sohn, Berlin, 1967.
  57. Rosman, R., "Analysis of Pierced Torsion Boxes", Acta Technica Academiae Scientiarum Hungaricae Tomus 65 (3-4), 1969, pp. 365-397.
  58. Rosman, R., "Torsion of Perforated Concrete Shafts", Journal of Struct. Div., ASCE, Vol. 95, ST5, May 1969, pp. 991-1010.
  59. Rosman, R., "Analysis of Spatial Concrete Shear Wall Systems", Proceedings of the Inst. of Civil Engineers, Paper 7266S, 1970, Supplement (vi), pp. 131-151.
  60. SEAOC Recommendations for Lateral Force Requirement and Commentary, Sanfransisco, California, 1968.
  61. Schwaighofer, J. and Microys, H. F., "Analysis of Shear Walls Using Standard Computer Programs", Journal of the Am. Conc. Inst., Dec. 1969, pp. 1005-1007.
  62. Shepherd, R. and Donald, R. A., "Seismic Response of Torsionally Unbalanced Buildings", Journal of Sound and Vibration, Vol. 6, No. I, 1967, pp. 20-37.

63. Stafford Smith, B., "Modified Beam Method for Analyzing Symmetrical Interconnected Shear Walls", Journal of the Am. Conc. Inst. Dec. 1970, pp. 977-980.
64. Stafford Smith, B., "Recent Developments in the Methods of Analysis for Tall Building Structures", Civil Engg. and Public Works Review, Dec. 1970, pp. 1417-1422.
65. Stafford Smith, B. and Taranath, B. C., "The Analysis of Tall Core-Supported Structures Subjected to Torsion", Proceedings of the Inst. of Civil Engineers, Vol. 53, Sept. 1972, pp. 173-187.
66. Stamato, M. C. and Stafford Smith, B., "Approximate Method for the Three-Dimensional Analysis of Tall Buildings", Proceedings of the Inst. of Civil Engineers, July 1969, pp. 361-379.
67. Stamato, M. C., "Three-Dimensional Analysis of Tall Buildings", ASCE-IABSE International Conference Preprints: Reports Vol. III-24, Aug. 1972, pp. 45-61.
68. Swift, R. D., "Analysis of Asymmetrical Coupled Shear Wall Structure", M. Eng. Thesis, McMaster University, Hamilton, 1970.
69. Tani, S., Sakurai, J. and Igudin, M., "An Approximate Method of Static and Dynamic Analysis of Core-Wall Buildings", Proc. Fourth World Conf. on Earthquake Engineering, Vol. II, 1969, pp. B3-53 to B3-68.

70. Taranath, B. S., "The torsional Behaviour of Open Section Shear Wall Structures", Ph.D. Thesis, University of Southampton, 1968.
71. Traum, E. E., "Multi-Storey Pierced Shear Walls of Variable Cross-section", Tall Building, Pergamon Press, 1967, pp. 181-206.
72. Tso, W. K., "Stresses in Coupled Shear Walls Induced by Foundation Deformation", Build. Sci. Vol. 7, 1972, pp. 197-203.
73. Tso, W. K. and Biswas, J. K., "An Approximate Seismic Analysis of Coupled Shear Walls", Building Science, Vol. 7, Dec. 1972, pp. 249-256.
74. Tso, W. K. and Biswas, J. K., "General Analysis of Non-Planar Coupled Shear Walls", Journal of Struct. Div., ASCE, Vol. 99, ST3, Mar. 1973, pp. 365-380.
75. Tso, W. K. and Biswas, J. K., "Seismic Analysis of Multi-storey Shear Wall Buildings", Proceeding of the First Canadian Conference on Earthquake Engineering, Vancouver, B. C., May 1971, pp. 220-235.
76. Tso, W. K. and Biswas, J. K., "Analysis of Core Wall Structures Subjected to Applied Torque", Building Science, Vol. 8, 1973, pp. 251-257.
77. Tso, W. K. and Biswas, J. K., "Torsional Analysis of Core Wall Structures", preprints of the Fifth World

- Conference on Earthquake Engineering, Vol. I, paper No. 17, Rome, Italy, June 1973.
78. Tso, W. K. and Chan, H. B., "Dynamic Analysis of Plane Coupled Shear Walls", Journal of Engg. Mech. Div., ASCE, Vol. 97, EMI, Feb. 1971, pp. 33-48.
  79. Tso, W. K. and Chan, P. C. K., "Flexible Foundation Effect on Coupled Shear Walls", Journal of the Am. Conc. Inst., Nov. 1972, pp. 678-683.
  80. Tso, W. K. and Chan, P. C. K., "Static Analysis of Stepped Coupled Walls by Transfer Matrix Method", Build. Sci. Vol. 8, 1973, pp. 167-177.
  81. Vlasov, V. S., Thin Walled Elastic Beams, English Translation, National Science Foundation, Washington, D.C., 1961.
  82. Weaver, W. and Nelson, M. F., "Three-Dimensional Analysis of Tier Buildings", Journal of Struct. Div., ASCE, Vol. 92, ST6, Dec. 1966, pp. 385-404.
  83. Winokur, A. and Gluck, J., "Lateral Loads in Asymmetric Multi-storey Structures", Journal of Struct. Div., ASCE, Vol. 94, ST3, March 1968, pp. 645-656.
  84. Winokur, A. and Gluck, J., "Ultimate Strength Analysis of Coupled Shear Walls", Journal of the Am. Conc. Inst., Dec. 1968, pp. 1029-1036.
  85. Zbirohowski-Koscia, Thin Walled Beams - from Theory to

Practice, Crosby Lockwood, London, 1969.

86. Zienkiewicz, O. C., The Finite Element Method in Structural and Continuum Mechanics, McGraw Hill, 1967.
87. Zienkiewicz, O. C. Parekh, C. J. and Teply, B., "Three-Dimensional Analysis of Buildings Composed of Floor and Wall Panels", Proceedings of the Inst. of Civil Engineers, Vol. 49, July 1971, pp. 319-332.